Liquid phase catalytic partial oxidation of methane

Williams, Gareth Richard

Award date:
2002

Awarding institution:
University of Bath

LIQUID PHASE CATALYTIC PARTIAL OXIDATION OF METHANE

Submitted by

Gareth Richard Williams

for the degree of PhD of the University of Bath,

2002

ProQuest LLC
789 East Eisenhower Parkway
P.O. Box 1346
Ann Arbor, MI 48106-1346

Dedicated to the memory of my grandfather, James Walter Thomas

SUMMARY

A promising system for the low temperature catalytic partial oxidation of methane to a methanol derivative has been selected for investigation in both a laboratory batch reactor and a semi-continuous porous tube reactor, utilising larger liquid volumes than in the original batch work. The system comprises of a bimetallic catalyst of palladium and copper(II) chloride, in a liquid mixture of trifluoroacetic acid (TFA) and water. Methane, oxygen and the coreductant carbon monoxide constitute the gas phase.

The use of an increased liquid phase volume from 4 to 50 ml in the batch reactor, compared with the original work, and operating at a reduced gas-to-liquid volume ratio of *ca.* 1.6, resulted in a reaction induced pressure drop of more than 10 bar in 3 hours, with the initial reactor pressure being 83 bar at 85 °C. This pressure drop was mainly attributed to the previously postulated *in situ* generation of H_2O_2 and the Wacker oxidation of CO. Yields of the methyl trifluoroacetate product were lower in this study than in previous works with an explanation being the lower gas-to-liquid ratio employed. Furthermore, a "pseudo end" of product formation was observed after *ca.* 2 hours, which was not previously disclosed. Further studies in the batch reactor, focussing on novel changes to the original system, in one case showed the possibility of substituting the relatively expensive TFA solvent with acetic acid, but also highlighted the need of greater understanding of the reaction mechanism.

The semi-continuous reactor employed a ceramic porous tube gas-liquid distributor with a continuous gas supply and re-circulation of the liquid via the "air-lift" effect. The studies carried out in this reactor enabled a time course of reaction to be obtained through liquid sampling of an initial volume of 300 ml. The influence of catalyst concentrations and gaseous reactant partial pressures were investigated with the results comparing favourably with those observed in other corresponding works using batch reactors. However, the drastic reduction in product formation was again observed.

The results obtained from the use of both reactor types together suggested that the cause of the apparent end of product formation was due to instabilities in the catalyst system, possibly linked with the deactivated Wacker chemistry for the palladium and copper catalysts. More work is necessary to fully understand the reaction chemistry and the nature of the species present in the "deactivated" catalyst system. When this has been achieved, studies on ameliorating the productivity can be performed to obtain yields more favourable towards the commercial implementation of the process.

ACKNOWLEDGEMENTS

I would like to extend my gratitude foremost to my supervisors, Dr. Pawel Plucinski and Professor Stan Kolaczkowski for their continued support and encouragement throughout this PhD. Thanks also go to the technical support staff for their help during analysis and rig-construction. Also, I would like to thank Professor Sven Järås at Kungl Tekniska Högskolan (Royal Institute of Technology), Stockholm, Sweden for "accommodating" me for a 3 months study of catalyst preparation techniques. A mention to my two undergraduate project students, Adnan Siddiqui and Sharman Chandran is also worthy. Lastly my appreciation is given to my friends, with a special mention to Sungsoo Kim and also to my family for their everlasting support.

TABLE OF CONTENTS

LIST OF FIGURES

CHAPTER 4

LIST OF PLATES

LIST OF TABLES

CHAPTER 4

CHAPTER 1 - Introduction

The economic conversion of natural gas to liquid fuels represents a favourable alternative to the environmentally detrimental venting and/or flaring of the gas at the well head. In some regions the amount of gas vented or flared constitutes a significant fraction of the gross production *e.g.* Africa. Furthermore, the transport of liquid fuels would be facilitated by the vast distribution infrastructure that is already in operation for crude oil (Taylor *et al.*, 1997). In comparison, the transport of natural gas (mainly methane) either under pressure or liquefied (requires pressure and refrigeration) is a costly process. Methanol is a high-energy liquid fuel, being the primary oxygenate of methane. It is produced on an industrial scale by an energy intensive, two-step process with the generation of a synthesis gas intermediate. A direct one-step process would be highly desirable if the process economics were favourable. Also, a "simpler" process would be more easily fabricated on-site for the natural gas reserves found in remote locations. The direct conversion of methane to methanol represents the theme of this thesis.

Research into methane conversion is well established for the gas phase reaction (detailed in Chapter 2), although the thermodynamics have plagued the radical-based chemistry with the terminal oxidation products (CO_2, H_2O) being more stable and therefore more favoured than the desired methanol product. More recent studies have focussed on the catalytic oxidation of methane to methanol in the liquid phase. These systems generally operate at low temperatures (< 100 °C) by selective non-radical based mechanisms, with the methanol-based product being more stable than the naturally unreactive methane substrate. They often employ "chemical protection" for the methanol product *e.g.* esterification, to provide stability against its overoxidation. At present the methanol yields are in most part very low at *ca.* 1 % which is far removed from that required for an economic industrial process (> 20 %). The majority of this liquid phase research has been carried out in batch reactors using small liquid volumes with the emphasis on developing a catalyst system to effect the desired chemistry, rather than operation at a scale more relevant to commercial assessment.

The work detailed in this thesis selects a promising catalytic system, previously developed at the University of Pennsylvania by Sen and co-workers (Lin *et al.*, 1997),

and applies it employing higher liquid volumes both under laboratory batch operation in an autoclave and semi-continuous operation using a porous tube reactor. This latter reactor utilises a porous ceramic tube as a gas-liquid distributor as well as lending itself as a potential catalyst support. Both the productivity and operational issues from the use of these reactors are discussed and also compared with the original work were relevant.
The catalytic system comprises of a three component gas phase (CH_4, O_2 and CO) and an acidic liquid phase (trifluoroacetic acid and water) containing a main palladium catalyst with a copper(II) chloride cocatalyst. The previously disclosed mechanism (Lin *et al.*, 1997) suggests the intermediate formation of hydrogen peroxide with a by-product generation of carbon dioxide. The hydrogen peroxide subsequently oxidises the methane substrate to a methanol derivative. The use of such *in situ* oxidants is of increasing interest because it is often cheaper to generate the oxidant as required, rather than having to bulk purchase the oxidant with the associated burden of transport and safe storage costs (*e.g.* Clerici and Ingallina, 1998). Furthermore, hydrogen peroxide is a desirable oxidant in that its chemistry is well understood and it has the environmental advantage of being reduced to simply water.

By nature of the chemical protection employed in this system, the methanol-based product is in the form of its ester, methyl trifluoroacetate, which would subsequently require hydrolysing to obtain the desired methanol product, with the recycling of the trifluoroacetic acid. Parallel work at the University of Bath (not by the author) has been focussed on this separation stage, obtaining kinetic parameters for use in the design of a reactive distillation column for the hydrolysis process. The work is detailed in a conference publication by Williams *et al.* (2001), a copy of which is provided in Appendix VIII.
A hypothetical process for the oxidation of methane to methanol in the liquid phase is depicted in Figure 1.1.

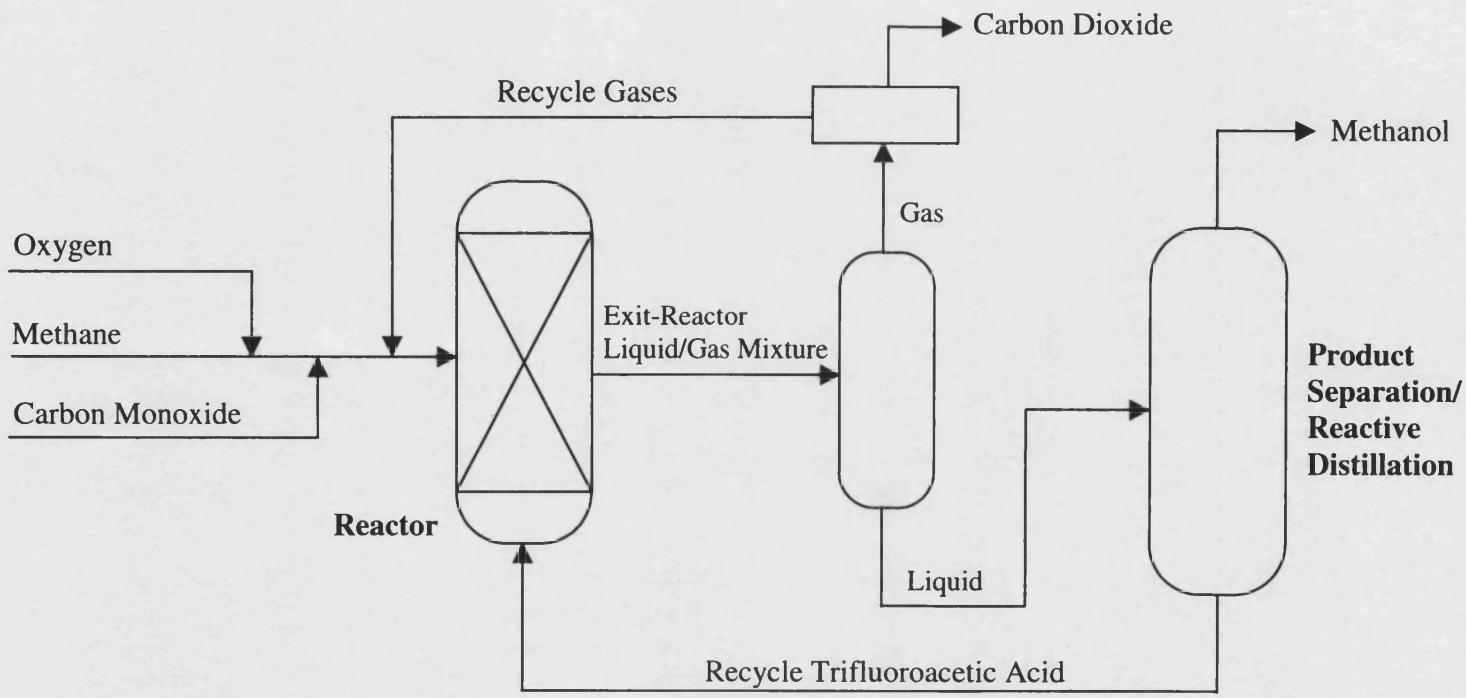

Figure 1.1. Hypothetical Process for the Catalytic Oxidation of Methane to Methanol

1.1 Important Design Parameters for Multiphase Reactors

Although this thesis focuses on obtaining information regarding the initial feasibility of a promising catalytic system, the ultimate outcome of laboratory trials is assessing the validity for further scaled-up testing followed by final industrial reactor design. The fundamental parameter to be obtained at laboratory level is the intrinsic kinetics, as this data is independent of the reactor scale.
When considering multiphase reactor design the following aspects need to be considered, especially with scaled-up studies (listed in Shah, 1979):

- Knowledge of flow regime and flow uniformity
- Pressure drop
- Hold-ups of various phases
- Residence-time distribution and axial mixing
- Gas-liquid mass and heat transfer
- Liquid-solid mass and heat transfer (heterogeneous catalyst)
- Intraparticle mass and heat transfer (heterogeneous catalyst)
- Wall heat transfer
- Intrinsic kinetics

If a solid catalyst is employed then data regarding the long-term stability (both chemically and mechanically) is important.

If the trials in the laboratory reactor prove successful, scale-up is the next step. At this point, selection of the reactor type becomes important. Several commercial reactor designs exist for multiphase reactors including mechanically agitated reactors and bubble columns. For those involving a solid catalyst, as in the system studied in this thesis, Mills *et al.* (1992) lists the main additional reactor types being trickle-bed, ebullated-bed or fluidised-bed reactors and loop reactors. For a more detailed explanation of these multiphase reactors and their design considerations, the reader is invited to consult the works cited in this section together with that by Ramachandran and Chaudhari (1983).

1.2 Structure of Thesis

Chapter 2 focuses on the available literature for natural gas conversion processes, first justifying the requirement then giving several possible routes to achieve the conversion with the selection of methanol as a desirable liquid product. A review of the research studies for the oxidation of methane to methanol is given first for the gas phase works, followed by the liquid phase. Close attention is paid to the liquid phase systems, with a selection of one such system to form the basis of this current study. At the end of the chapter the main aims of the project are highlighted.

The description of the rig design of both the batch reactor and the semi-continuous porous tube reactor are detailed in Chapter 3. The experimental and operating procedures for the aforementioned reactors are also given. With regard to the porous tube reactor, some preliminary experimental studies on liquid re-circulation rate are described, as is a batch experiment to ascertain ideal gas behaviour under operating conditions for use in calculations. Details of the analytical methods used throughout this study are also given.

Chapter 4 contains the results of the experimental work performed in the batch and porous tube reactors. The batch work initial focuses on the validation of the catalyst system for producing a methanol-based product, followed by some experiments on the influence of the gas phase on the reaction. The application of the semi-continuous porous tube reactor then follows as a major part of this chapter. Finally, details are given of batch experiments involving some novel changes to the original catalyst system, in view of obtaining a further understanding of the chemistry involved and to ameliorate the productivity.

The discussion of the experimental results is disclosed in Chapter 5, whilst the conclusions and future work recommendations are detailed in Chapter 6.

A simplified diagram summarising the work described in this thesis is shown in Figure 1.2.

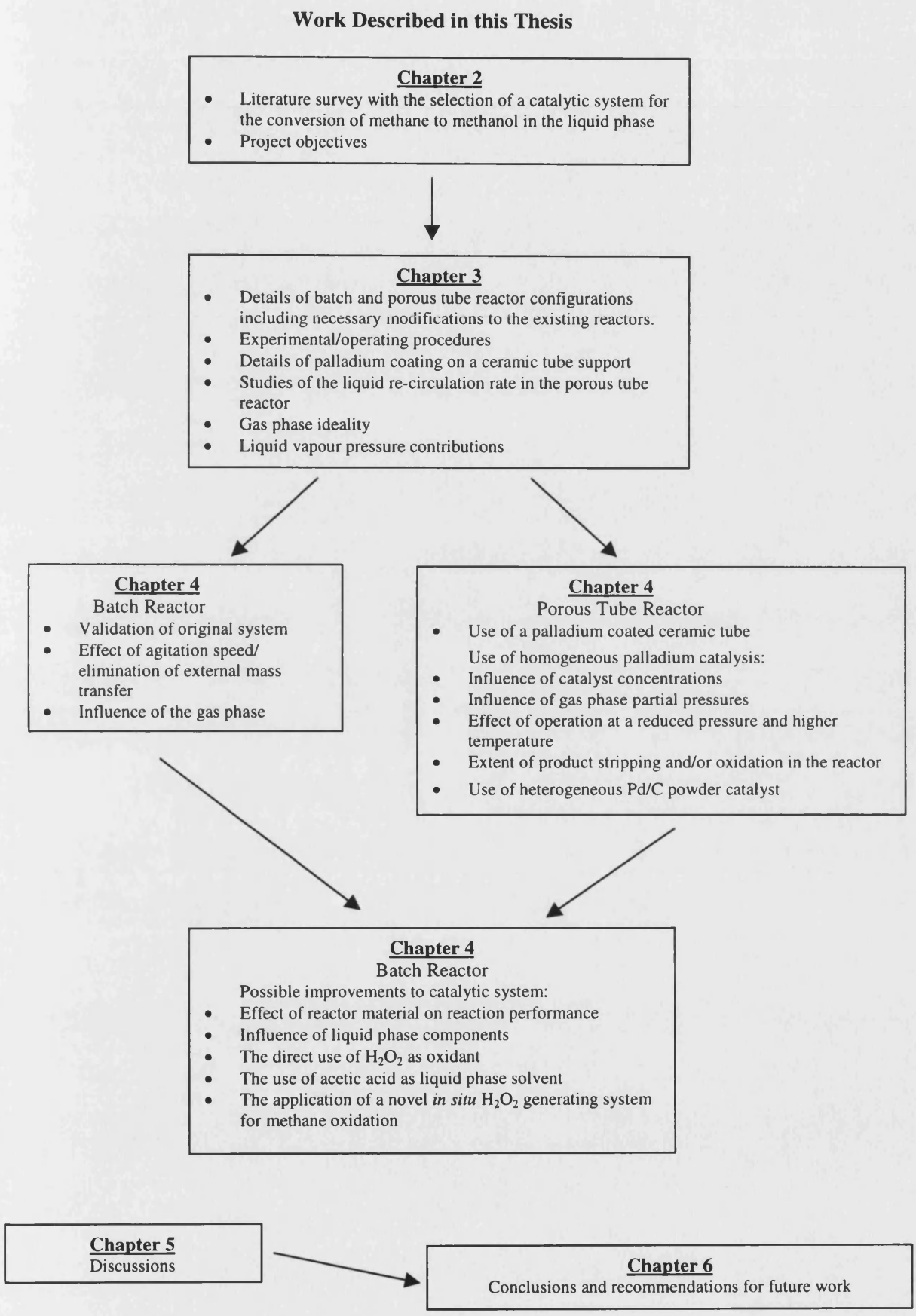

Figure 1.2. A Simplified Representation of the Structure of the Thesis

CHAPTER 2 - Literature Review

This chapter embraces the relevant information available in the literature, identifying and assessing the key developments in natural gas conversion technology. Having first justified the requirement for new methods of gas conversion the current research options available are reviewed with an outcome to support the partial oxidation of methane to methanol. By first summarising the current commercially practised methanol process, the research into direct partial oxidation of methane to methanol is screened. Elements of gas phase oxidation are presented, followed by the corresponding chemistry in the liquid phase process. From this, the catalytic system that forms the basis of this study is selected.

2.1 Natural Gas Conversion

Natural gas, a legacy from the Earth's evolutionary history, is a growing factor in world primary energy production. In 1980 it accounted for 18.4 %, based on calorific value, whilst in 1991 this figure rose to 21.5 % (Crabtree, 1995). Natural gas is found in porous reservoirs located in many regions of the world. Using two broad classifications, that gas found coupled with crude oil is termed associated gas whilst natural gas located independently of oil is "dry" or nonassociated gas.

The main constituent of natural gas is methane, whose fraction varies with global location as illustrated in Table 2.1 below:

Table 2.1. Composition of Natural Gas

Gas	H_2	CO	CH_4	C_2H_6	C_3H_8	C_4H_{10}	CO_2	N_2
Hewitt	0	0	**81.8**	6.0	2.5	0.4	0.1	9.0
West Sole	0	0	**94.1**	3.2	0.6	0.2	0.5	1.2
Algerian LNG	0	0	**87.7**	8.6	2.3	0.9	0	0.4
Lacq	0	0	**82.1**	3.3	1.0	0.7	11.6	0.2
Eurofisk	51.0	14.6	**85.2**	8.6	2.9	0.9	1.7	0.5
Coal Gas	51.0	14.6	**19.1**	1.7	0	0	3.6	6.0

Data in percentage by volume (Adapted from Crabtree, 1995)

With the current production levels at the time, Crabtree (1995) predicted the availability of crude oil for a further 44 years, compared with more than 60 years for natural gas. The known natural gas reserves rival those of crude oil, and furthermore they are increasing more rapidly than for crude oil and it is envisaged that this trend will continue well into the 21st century (Lunsford, 2000). Table 2.2 depicts recent data on both natural gas and crude oil reserves.

The majority of the natural gas reservoirs contain nonassociated gas that is rich in C_1 hydrocarbons. That found coupled with crude oil (associated) contains a much higher C_2 - C_4 hydrocarbon content.

Table 2.2. World Crude Oil and Natural Gas Reserves

Region	Crude Oil (Billion Barrels)	Natural Gas (Trillion Cubic Feet)
North America	55.1	261.3
Central & South America	89.5	222.7
Western Europe	18.8	159.5
Eastern Europe & former U.S.S.R	58.9	1 999.2
Middle East	675.6	1 749.2
Africa	74.9	394.2
Far East & Oceania	44.0	363.5
WORLD TOTAL	1 016.8	5 149.6

(adapted from Oil & Gas Journal (2000), Vol . 97, No. 51 pp. 91-92)

A large proportion of the reserves is found in ex-USSR and the Middle East, with a substantial amount located in remote locations both on land and offshore where there is an inherently low local demand and where it is not economically feasible to transport it to a market. The cost of distribution is also impeded by the unfavourable physical properties of natural gas (methane). Being a permanent gas at normal temperatures (critical temperature = - 102 °C), methane cannot be liquefied by pressure alone. Additional refrigeration is therefore also necessary to produce what is termed liquefied natural gas (LNG). This has been transported by ship since 1959. It is possible to transport natural gas along pipelines, but a pressure of around 8 MPa is required. Natural gas distribution as either LNG or as a pressurised gas is expensive such that the sheer cost generally dictates its consumption within the region of its production. This is in stark contrast with crude oil whereby the cost of transport is only a minor factor. For this reason associated natural gas can have a "negative value" for the crude oil producer who can be under contract to remove the gas as well as the crude oil. Often the gas is reinjected into the reservoir to facilitate oil recovery, but an increasing amount is vented or flared at the well head. Approximately 11 % is reinjected and about 4 % is vented or flared (Lunsford, 2000) which is a waste of a non-renewable energy source. Indeed for some regions the amount of gas vented or flared constitutes a meaningful fraction of the gross production *e.g.* in Africa this fraction represents *ca.* 18 % (see Table 2.3). Furthermore, both methane (venting) and carbon dioxide (the product of combustion/flaring) are greenhouse gases and with the ever increasing environmental legislations this becomes a significant economic burden to the production companies.

Table 2.3. Natural Gas Production

Region	Gross Production	Vented and/or Flared	Reinjected	Marketed Production	Dry Gas Production
North America	32 726	623	3 889	27 603	26 021
Central & South America	5 223	433	1 242	3 548	3 120
Western Europe	11 069	117	1 081	9 872	9 638
Eastern Europe & former U.S.S.R	25 435	253	1	25 182	25 163
Middle East	9 651	546	1 980	7 160	6 596
Africa	8 252	1 465	2 734	4 053	3 699
Far East & Oceania	9 535	288	547	8 700	8 551
WORLD TOTAL	101 891	3 724	11 475	86 117	82 788

(Adapted from Energy Information Administration [WWW] http://www.eia.doe.gov/iea)

Therefore, on consideration of both the energy wastage and the environmental issues associated with the inefficient use of the natural gas resource, it is apparent that alternative methods with utilise the natural gas need to be established.

To ameliorate the problem of natural gas distribution, the on-site conversion to a liquid fuel that is readily transportable, forms a viable option. Indeed this transport would be facilitated by the vast crude oil pipeline, tanker network and distribution infrastructure already in operation (Taylor *et al.*, 1997). Furthermore, natural gas, as itself, only finds limited use as a fuel for domestic and industrial heating and also for electrical power generation. It is mainly used as a feedstock for the manufacture of higher-value products currently produced via the formation of synthesis gas. In view of this, the handling of natural gas is most beneficial via chemical conversion rather than the optimisation of actual natural gas transportation methods.

Current industrial technology for obtaining liquid products from natural gas is often besieged by a two-stage energy intensive process, inherent in the formation of a synthesis gas intermediate. Examples are methane to methanol, methane to higher hydrocarbons and alcohols via Fisher-Tropsch chemistry and more impressively, methane to gasoline. This latter process, operated by New Zealand Synthetic Fuels Corporation, at the time represented an example of a state of the art methane conversion technology (Srivastava *et al.*, 1992).

Clearly, if such technology was to be implemented either off-shore or in the remote locations previously ascribed to a significant number of natural gas reserves, it would need to be efficient in both physical size and operation. All current industrial processes

lack these criteria, mainly because of the inefficiencies associated with the front-end synthesis gas generation step. A one-step direct natural gas conversion process would be a possible solution, although at present, no practical process has been established which obtains product yields and selectivities comparable to the two-step technology. In light of this fact the challenge of obtaining an efficient, direct conversion process has formed the impetus behind almost a century of research. An overview of this research is presented in the next section.

2.2 Potential Direct Methane Conversion Processes

At this stage it is important to point out that research into natural gas conversion has focussed on methane acting as the model substrate. Thus for any real application, natural gas would have to be used as the feedstock in order to fully assess industrial viability.
A large number of direct (one-step) methane conversion processes feasibly exist, although technology is not so advanced as for industrial implementation. Wolf (1992) compiled a methodical list of these processes as follows:

1. Direct partial oxidation (to methanol, methyl halides, or others)
   a) Using oxygen
   b) Using nitrous oxide
   c) Using halogens (*e.g.* oxyhydrochlorination)
   d) Using superacids as catalysts

2. Oxidative coupling (to ethylene)

3. Direct conversion to acetylene and other higher hydrocarbons
   a) To acetylene via thermal pyrolysis
   b) To acetylene using electric arc or plasma
   c) To acetylene via partial oxidation
   d) To other higher hydrocarbons

4. Other direct conversion process
   a) Alkylation with hydrocarbons
   b) Activation using metals, metal oxides, or metal complexes
   c) Conversion using coal or shale

From this list, three main conversion processes have reached a stage where realistic engineering and economic feasibility studies could be performed (Srivastava *et al.*, 1992). These are the gas phase partial oxidation of methane to methanol, oxidative coupling to ethylene and oxyhydrochlorination.
Table 2.4 highlights the main features of these reactions with Table 2.5 showing the results of various feasibility studies found in the literature. It should be duly noted that

these studies are based on conceptional plant designs with the "best" published reaction and process economic data available at the time.

2.2.1 The Choice of Methane Conversion Process

From the previous section's review of the three main contenders, it would be misleading to say that one process stands out from the rest. In fact they are not directly comparable as the one-step products are very different in nature *e.g.* methanol and ethylene. The ultimate goal of this project is to produce a liquid-based fuel from methane and whereas this is possible from all prospective processes, only the partial oxidation achieves this objective in one step. Both the oxidative coupling and the oxyhydrochlorination processes require a second step, involving an oligomerisation reaction to form the aromatic rich hydrocarbons that constitute gasoline. Furthermore, out of the three major liquid products commercially produced from natural gas *i.e.* gasoline, distillate and methanol, it is methanol that stands alone in total quantity of natural gas converted and number of process plants (Gradassi and Green, 1995). Table 2.6 shows the world methanol supply and demand quotas with the consumption data highlighted in Figure 2.1 for the year 1998.

It is the partial oxidation of methane to methanol that will be the theme of this study. Before focussing on the documented research for the partial oxidation of methane to methanol, a brief overview of the current industrial process is given highlighting the limited scope for further research of the process.

Table 2.4. Direct Methane Conversion Processes

Conversion Process	Main Reaction(s)	Catalyst	*T* (°C)	*P* (MPa)
Partial Oxidation: **i) Using Oxygen**	$CH_4 + \frac{1}{2}O_2 \leftrightharpoons CH_3OH$	- None, or *e.g.* MoO_3, SnO_2	300 - 500	5 - 6.5 (high)
ii) Using Nitrous Oxide	$CH_4 + N_2O \leftrightharpoons CH_3OH + N_2$	- *e.g.* MoO_3/Si	500 - 600	0.1+ (low - moderate)
Oxidative Coupling	$CH_4 + \frac{1}{4}O_2 \leftrightharpoons \frac{1}{2}C_2H_6 + \frac{1}{2}H_2O$ $C_2H_6 + \frac{1}{2}O_2 \leftrightharpoons C_2H_4 + H_2O$	- reducible metal oxides *e.g.* $Mn/Na_4P_2O_7/SiO_2$	500 - 900	0.1 - 3 (low - moderate)
Oxyhydrochlorination	$CH_4 + \frac{1}{2}O_2 + HCl \rightarrow CH_3Cl + H_2O$ $CH_4 + O_2 + 2HCl \rightarrow CH_2Cl_2 + 2H_2O$ $CH_3Cl \rightarrow$ -CH_2- (aromatics) + HCl	- $CuCl_2$ (+ promoters) - ZSM-5	300 - 400	1.6 (moderate)

Table 2.5. Feasibility Studies of Direct methane Conversion Processes (Part 1 of 2)

Conversion Process	Reference(s)	Compared Industrial Process	Measured Parameter(s)	Remarks
Partial Oxidation to Methanol using Dioxygen (Gas Phase)	i) Gradassi and Green (1995)	- Conventional Methanol	- Payout time	- Favourable if selectivity > 95 % at 10 % single-pass conversion. Capital costs at lower selectivities contribute a detrimental effect on payout time.
	ii) Wolf (1992)	- Conventional Methanol	- Net thermal efficiency. Heat-transfer duty. Gas compression duty.	- Favourable if selectivity > 90 % at 7.5 % single-pass conversion or > 80 % at 15 % conversion.
	iii) Geerts *et al.* (1990)	- Conventional Methanol	- Investment - Profitability	- Investment comparable, but a selectivity of at least 75 % at complete methane conversion is estimated for the plant to be profitable.
	iv) Edwards and Foster (1986)	- Conventional Methanol	- Investment - Production Cost	- Favourable if selectivity > 77 % at 10 % single-pass conversion.

Table 2.5. Feasibility Studies of Direct Methane Conversion Processes (Part 2 of 2)

Conversion Process	Reference(s)	Compared Industrial Process	Measured Parameter(s)	Remarks
Oxidative Coupling	i) Gradassi and Green (1995)	- Conventional Methanol	- Payout time	- The coupling reactor results in high capital costs and the price could be comparable with the total of the two reactors in the conventional process. Favourable if C_{2+} selectivity > 95 % at a single pass conversion of 30 %.
	ii) Wolf (1992)	- Conventional Methanol	- Net thermal efficiency. Heat-transfer duty. Gas compression duty.	- Due to non-liquid product comparison inexact. Favourable if C_{2+} selectivity > 88 % at a concurrent single pass conversion of 35 %.
Oxyhydrochlorination	Srivastava *et al.* (1992)	- Mobil Methanol to Gasoline - Shell Fischer-Tropsch	- Investment	- Favourable results calling for accelerated research. "Difficult" process engineering associated with the corrosive reactants and intermediates.

Table 2.6. World Methanol Supply/Demand

	1997	1998	1999	2000	2001	2002	2003	2004	2005
SUPPLY									
Capacity Available	31 525	32 747	35 079	36 972	36 972	38 172	38 815	39 422	39 822
Production	25 358	25 872	26 827	28 191	29 189	29 901	30 774	31 671	32 566
Excess Capacity	6 167	6 875	8 252	8 781	7 783	8 271	8 041	7 751	7 256
Operating Rate (%)	80	79	76	76	79	78	79	80	82
DEMAND									
Formaldehyde	9 134	9 120	9 293	9 625	9 918	10 255	10 719	11 076	11 350
MTBE	6 590	6 993	7 204	7 768	7 828	7 906	7 968	8 184	8 195
Acetic acid	2 248	2 274	2 591	2 729	3 090	3 121	3 139	3 155	3 477
DMT	584	584	584	581	588	588	590	591	562
Methyl methacrylate	696	728	769	789	822	840	888	919	974
Gas/Fuels	675	598	623	663	675	695	718	741	763
Solvents	1 032	1 078	1 110	1 164	1 218	1 256	1 297	1 323	1 345
Others	4 399	4 497	4 653	4 872	5 050	5 240	5 455	5 682	5 900
Total Demand	25 358	25 872	26 827	28 191	29 189	29 901	30 774	31 671	32 566

Data in metric tons ($\times 10^3$). Adapted from the American Methanol Institute [WWW]: http://www.methanol.org

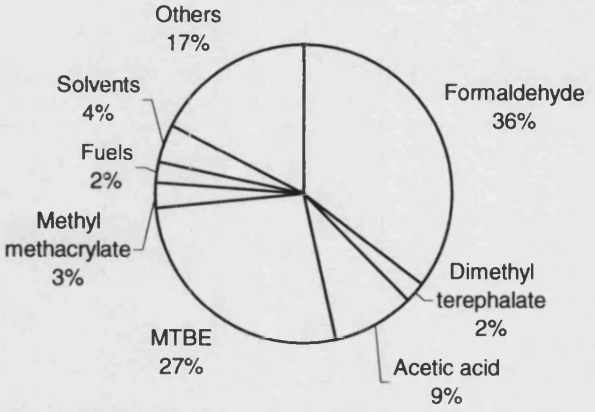

Figure 2.1. World Methanol Demand, 1998

2.3 Industrial Methanol Synthesis

As mentioned earlier, methanol synthesis is an indirect two-step process with the major feedstock being natural gas (mainly methane), although naphtha is also used.
At least 80 % of the world's methanol capacity is derived from the process of steam reforming to produce the synthesis gas (step one) *e.g.* for methane:

$$CH_4 + H_2O \leftrightharpoons CO + 3H_2 \qquad \Delta H^o_{25^oC} = +206.1 \text{ kJ/mol} \qquad (2.0)$$

$$CO + H_2O \leftrightharpoons CO_2 + H_2 \qquad \Delta H^o_{25^oC} = -41.2 \text{ kJ/mol} \qquad (2.1)$$

Noncatalytic partial oxidation or gasification of residual fuel oils or coal accounts for the remainder of methanol production *e.g.* a general fuel of carbon and hydrogen content n and m:

$$C_nH_m + \left(\frac{n}{2}\right)O_2 \rightarrow nCO + \left(\frac{m}{2}\right)H_2 \qquad (2.2)$$

Equation (2.2) represents the overall reaction, but the total combustion reaction ($\rightarrow CO_2 + H_2O$) and equations (2.0) (steam reforming) and (2.1) (water-gas shift) form the main precursors. Reaction temperatures are typically 1250 - 1500 °C with operating pressures between 3 MPa and 8 MPa. The fuel/air ratio is substoichiometric in oxygen (equation (2.2)).
Tennessee Eastman operates an example of a coal gasification methanol plant in the United States. Based on the Texaco coal gasification process, it yields production figures of 195 000 t/yr (Kroschwitz and Howe-Grant, 1995).

Because natural gas constitutes the most common feedstock, the following process description for steam reforming is given in a little more detail than for gasification. Figure 2.2 shows a typical methane to methanol process flowsheet.
The main steam reforming reaction is represented by equation (2.0). This is highly endothermic and thus requires a large heat input to drive the conversion. It is carried out in a steam reformer fire-box comprising of an array of tubes, packed with a nickel-based

catalyst and enclosed in a furnace with direct-fired burners supplying the heat. A temperature profile prevails down the tube axiom, with exit gas temperatures approaching 1000 °C. Thermodynamic considerations of equation (2.0) dictate a high temperature and a low pressure for favourable equilibrium conversions to be achieved. Downstream compressional costs dictate moderate pressures of up to 2 MPa to be used. A stoichiometric molar excess steam to carbon ratio of between 2.5 and 3.0 is usually employed in the feed, with an intention towards minimising the undesirable carbon forming side reactions. The reformer outlet methane conversions can reach up to 95 % with close to equilibrium stream compositions.

After several heat exchange units to cool the synthesis gas stream (210 - 270 °C), followed by compression (5 - 10 MPa), it enters the methanol synthesis reactor.

$$CO + 2H_2 \leftrightharpoons CH_3OH \qquad \Delta H^o_{25°C} = -90.8 \text{ kJ/mol} \qquad (2.3)$$

$$CO_2 + 3H_2 \leftrightharpoons CH_3OH + H_2O \qquad \Delta H^o_{25°C} = -49.4 \text{ kJ/mol} \qquad (2.4)$$

From equations (2.3) and (2.4) a low temperature and high pressure favours methanol formation (compare with steam reforming reactions, equations (2.0 & 2.1)).

By comparing the synthesis gas product of steam reforming (equation 2.0) and that required for methanol synthesis (equation 2.3), it is seen that the synthesis gas composition is rich in hydrogen. According to equations (2.3 & 2.4), the synthesis gas feed should have a stoichiometry given by:

$$\frac{n_{H_2} - n_{CO_2}}{n_{CO} + n_{CO_2}} = 2 \qquad (2.5)$$

However, for synthesis gas arising from methane reforming, this ratio is 3. Due to this reason, by-product carbon dioxide can be added to the reformer feedstock to tune the ratio to a favourable methanol synthesis composition.

The effluent from the methanol synthesis reactor is cooled, with the methanol-water component condensing out. The subsequent disengagement of the unreacted synthesis gas occurs, which is then recycled back to the methanol reactor. The crude methanol

mixture is sent on to the distillation section for final purification, which consists of one to three columns.

The whole process is encompassed by an extensive heat recovery and recycle system. Heat recovery is especially prevalent in the reformer convection section. This is illustrated in Figure 2.2.

Synthetic methanol production from synthesis gas first began in 1923 at BASF's Leuna, Germany, plant, utilising a zinc-chromium oxide catalyst. The activity of this catalyst required an operating temperature of between 320 - 450 °C and pressures of 25 - 35 MPa. The high pressure mandated the uses of reciprocating compressors and limited single-train plant size to about 450 t/d.

The high pressure process was rendered obsolete in the mid-1960s when ICI in the United Kingdom, developed a more active copper/zinc oxide/alumina catalyst facilitating a higher methanol selectivity (> 99.5 %) and possessing a greater stability. In the 1970s, Lurgi developed a similar catalyst. The methanol synthesis process could now operate at 5 - 10 MPa and 210 - 270 °C. Such a decrease in operating conditions permitted a much more energy efficient process and enabled the use of centrifugal compressors, effecting a single train capacity of over 2200 t/d.

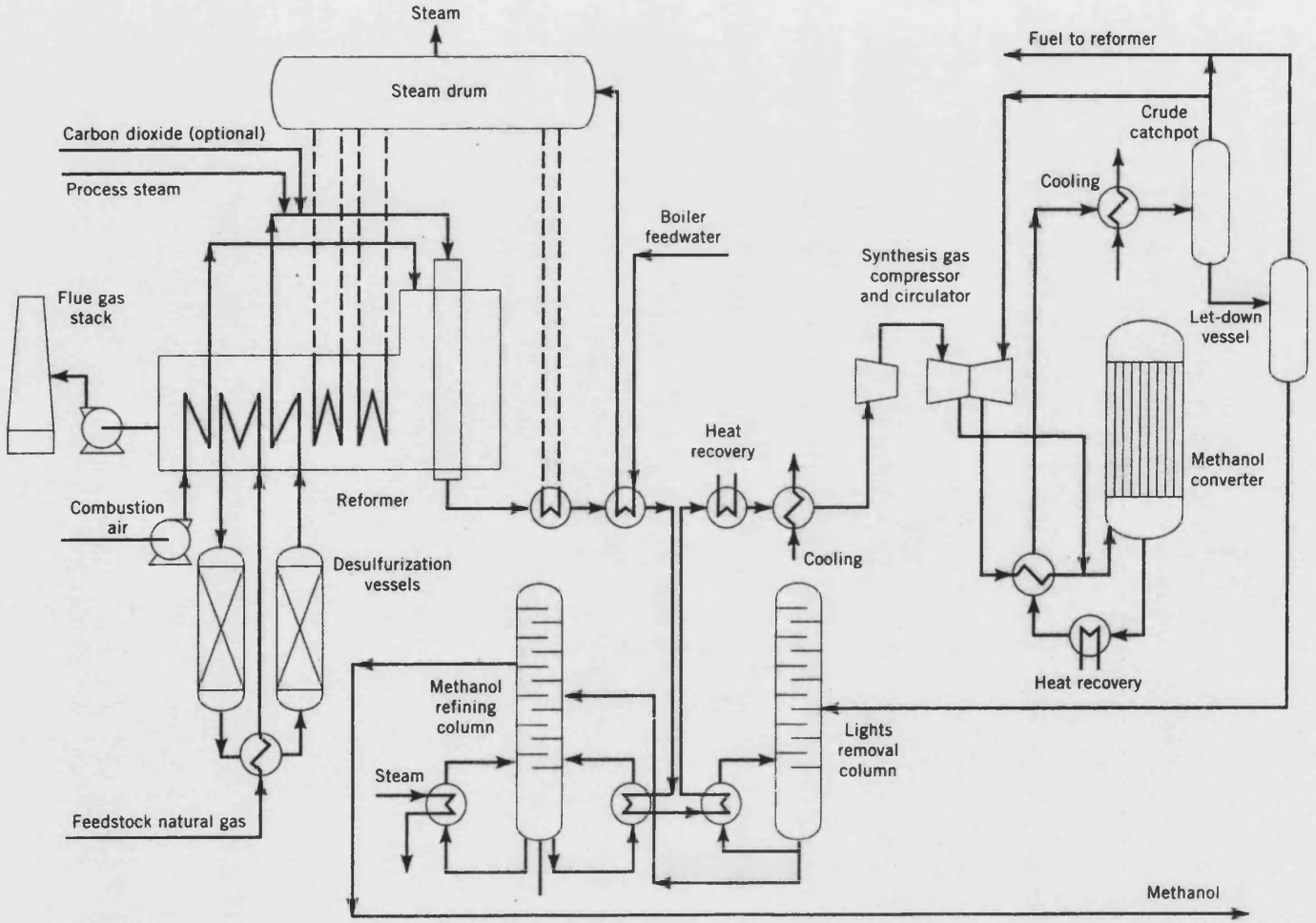

Figure 2.2. Methanol Synthesis Process Flowsheet. (Adapted from Kroschwitz and Howe-Grant, 1995)

Edwards and Foster (1986) reviewed the steam reforming/methanol synthesis technology for methanol production from natural gas and concluded that:

1. Gas feedstock and capital investment form the major components of the overall methanol production cost.

2. The steam reforming section is the highest single capital cost unit of the process and furthermore, it is responsible for more than half of the total process energy inefficiencies.

3. There is only limited scope for reducing the cost of methanol production by the synthesis gas route. Any major research effort in this area should be concentrated on improving the single-pass conversion and the heat recovery in the methanol synthesis reactor.

With respect to the copper/zinc oxide/alumina catalyst, Lunsford (2000) pointed out that there were limited opportunities for further development and attention may turn to supported palladium as the active phase.

2.4 The Gaseous Phase Partial Oxidation of Methane to Methanol

Accepting the high temperatures associated with the industrial methanol synthesis route, a logical progression is to develop a one-step process that remains in the gaseous phase. However, due to the unselective nature of gas phase reactions, a phenomenon that is clarified later in this section, halting the reaction with a desirable yield of methanol poses an inherent challenge. A simple thermodynamic study of the competitive reactions, on the basis of their free energy change, gives an inclination of this difficulty.

$$CH_4 + \frac{1}{2}O_2 \rightarrow CH_3OH \qquad \Delta G^o_{427°C} = -92 \text{ kJ/mol} \qquad (2.6)$$

$$CH_4 + O_2 \rightarrow HCHO + H_2O \qquad \Delta G^o_{427°C} = -293 \text{ kJ/mol} \qquad (2.7)$$

$$CH_4 + \frac{3}{2}O_2 \rightarrow CO + 2H_2O \qquad \Delta G^o_{427°C} = -569 \text{ kJ/mol} \qquad (2.8)$$

$$CH_4 + 2O_2 \rightarrow CO_2 + 2H_2O \qquad \Delta G^o_{427°C} = -791 \text{ kJ/mol} \qquad (2.9)$$

Equations (2.8 & 2.9) result in the formation of "deep oxidation" products, comprising of inorganic carbon oxides. Energetically, these two reactions, together with formaldehyde formation (equation (2.7)), are more favourable than the initial oxidation to methanol (equation (2.6)). Thus at this stage it is already evident that any process which proffers methanol formation would need to overcome the thermodynamic hurdles which incur the greater stability of overoxidation products.

A high pressure favours methanol formation over formaldehyde. Reducing the amount of active oxygen species available (low air/methane ratio; the greater the degree of oxidation, the more oxidant required) together with minimising the contact period between the reactants (low residence time) also serves to promote a methanol-based product.

An important point to make is that the nature of the above reactions, especially from equations (2.8 & 2.9), in effect, describes the combustion of methane. Indeed, similarities of a complex radical-based mechanism and common intermediates do prevail, but in general, to eliminate the safety implications associated with combustion, the partial oxidation reaction is performed outside of the homogeneous flammability limits (lower methane limit = 5.1 vol.%, maximum limit = 61 vol.% at 0.1 MPa) and often (but not

always) below the spontaneous ignition temperature (556 °C at 0.1 MPa). The process is more analogous with the phenomenon known as "cool flame" combustion (Pitchai and Klier, 1986; Glassman, 1987).

As mentioned earlier, the gas phase reaction mechanism is complex consisting of chain-initiation, chain-propagation and chain-termination steps which are characteristic of radical-based chemistry (see *e.g.* Minkoff and Tipper, 1962 for detailed mechanisms). A simplification of this mechanism, which is applicable to the partial oxidation of methane at low temperatures and pressures, is presented below (Pitchai and Klier, 1986):

$$CH_4 + O_2 \rightarrow CH_3\cdot + HO_2\cdot \quad (2.11)$$

$$CH_3 + O_2 \rightarrow CH_3OO\cdot \quad (2.12)$$

$$CH_3OO\cdot \rightarrow HCHO + \cdot OH \quad (2.13)$$

$$CH_4 + HO_2\cdot \rightarrow CH_3\cdot + H_2O_2 \quad (2.14)$$

$$CH_4 + \cdot OH \rightarrow CH_3\cdot + H_2O \quad (2.15)$$

$$HCHO + O_2 \rightarrow CHO\cdot + HO_2 \quad (2.16)$$

$$HCHO + HO_2\cdot \rightarrow CHO\cdot + H_2O_2 \quad (2.17)$$

$$HCHO + \cdot OH \rightarrow CHO\cdot + H_2O \quad (2.18)$$

$$CHO\cdot + O_2 \rightarrow CO + HO_2\cdot \quad (2.19)$$

$$HO_2 + HO_2\cdot \rightarrow H_2O_2 + O_2 \quad (2.20)$$

$$HO_2\cdot \rightarrow \text{inert (at wall)} \quad (2.21)$$

This mechanism can account for a dominance of formaldehyde in the reaction product at low temperatures. The hydroperoxy radicals ($HO_2\cdot$) do not play a major role in the chain propagation reactions except in the initial stages (equation (2.14)). Thus, at low temperatures the propagation reaction (equation (2.17)) is not so significant, preserving the formaldehyde product.

However, at higher temperatures, the hydroperoxy radicals develop a greater affinity towards H abstraction from methane (equation (2.14)) forming hydrogen peroxide which itself is subject to decomposition:

$$H_2O_2 \leftrightarrow 2\cdot OH \quad (2.22)$$

The subsequent increase in hydroxyl radicals (·OH) promotes the conversion of formaldehyde (equation (2.18)) as well as the concurrent oxidation of CO to carbon dioxide:

$$CO + \cdot OH \rightarrow CO_2 + H\cdot \quad (2.23)$$

$$CO + HO_2\cdot \rightarrow CO_2 + \cdot OH \quad (2.24)$$

At the high pressures that favour methanol formation, additional reactions must be added to the mechanism to account for this.

$$CH_3OO\cdot + CH_4 \rightarrow CH_3OOH + CH_3\cdot \quad (2.25)$$

$$CH_3OOH \rightarrow CH_3O\cdot + \cdot OH \quad (2.26)$$

$$CH_3O\cdot + CH_4 \rightarrow CH_3OH + CH_3\cdot \quad (2.27)$$

$$CH_3\cdot + \cdot OH \rightarrow CH_3OH \quad (2.28)$$

$$HCO\cdot + \cdot OH \rightarrow HCOOH \quad (2.29)$$

$$HCO\cdot + \cdot OCH_3 \rightarrow HCOOCH_3 \quad (2.30)$$

$$CH_3OO\cdot \rightarrow \text{termination} \quad (2.31)$$

The main differences between the mechanisms at low and high pressures are that the methyl peroxy radical ($CH_3OO\cdot$) is involved in the formation of methyl hydroperoxide (equation (2.25)) and the methoxyl radical ($CH_3O\cdot$) in the formation of methanol by hydrogen abstraction from methane (equation (2.27)). The high pressure favours the bimolecular step of equation (2.25) over the unimolecular step of equation (2.13) which involves the formation of formaldehyde. Thus, the formation of products from equation (2.25) followed by equation (2.26), favour methanol formation (equations (2.27 & 2.28)).

With unfavourable thermodynamics and complex reaction chemistry, the concept of the partial oxidation to methanol presents a challenge. Nevertheless, research into this field has been ongoing for almost a century *e.g.* Lance and Elworthy (1906). The three main possibilities of oxidant are molecular oxygen, air and nitrous oxide. The use of air in a conceptional plant design would require extensive recycle and compression, due to the inert nitrogen content. Nitrous oxide is produced from ammonium nitrate which itself is derived from nitric acid. The result is an oxidant more expensive than the methanol

product (Srivista *et al.*, 1992). In view of this, practicality and economics dictate the use of molecular oxygen as the preferred oxidant (Sen, 1998; Stahl *et al.*, 1998; Clerici and Ingallina, 1998).

Literature works can be divided into two main classes; those involving the homogeneous gas phase and those investigating the heterogeneous catalytic reaction. By definition, the use of a catalyst alters the reaction pathway or mechanism and by affecting the competing reactions to different extents, the selectivity can be altered. Also, by lowering the activation energies, the process reaction temperature can be lowered which has obvious benefits for production costs. Thus, it is easy to see why there is so much interest in the heterogeneous reaction. In fact, the catalytic route forms the bulk of the research documented to date.

The homogeneous partial oxidation is illustrated by the extensive work carried out by Professors Gesser and Hunter at the University of Manitoba (*e.g.* Gesser *et al.*, 1985; Gesser *et al.*, 1986; Yarlaggadda *et al.*, 1988; Hunter *et al.*, 1990). Their work is summarised in Table 2.7 below:

Table 2.7. Highlights of Direct Partial Oxidation Data from the University of Manitoba.

1. Noncatalytic system ("cool flame" combustion)
2. 300 - 500 °C and 50 - 65 atm (5 - 6 MPa)
3. 10.5 mm inside diameter glass-lined reactor (microreactor)
4. Reaction temperatures decreasing by 100 °C with higher methanol selectivity due to the presence of C_{2+} paraffins in feed
5. Methanol selectivities of 80 % at methane conversions up to 10 %
6. Increasing selectivity with decreasing conversion
7. Only patent showing negligible formaldehyde formation in noncatalytic system

(Adapted from Wolf, 1992).

The claimed methanol selectivity and methane conversion is very promising. However, duplication of their work by Burch *et al.* (1989), only produced a selectivity of around 40 % and so the results are somewhat controversial. Burch and co-workers concluded that the discrepancies could be attributed to the intricate design of the employed reactors.

They also looked at the effect of the reactor wall material on methanol production. By comparing 316 stainless steel with Pyrex glass, they clearly showed a marked increase in the selectivity and yield of methanol upon using the latter material. Furthermore, the first signs of methanol were observed at much lower pressures using the Pyrex-lined reactor. Interestingly, the presence of C_{2+} hydrocarbons in the feed was said to increase the methanol selectivity and also decreases the required reaction temperature for comparable activity (Table 2.7). This increase in methanol selectivity was also observed by Foral (1992), albeit at the expense of a reduced methane conversion, and the lowering of the activity temperature by Burch *et al.* (1989) without any change in methanol selectivity. Although non-conclusive, these findings have significant implications for a natural gas feedstock (see Table 2.1).
Gesser and co-workers also studied the catalytic oxidation of methane using tin(IV) oxide (Gesser *et al.*, 1986) but the general conclusion was that no real advantage was gained over the homogeneous counterpart.

A comprehensive review of the catalytic partial oxidation of methane was given by Hall *et al.* (1995). Table 2.8 is adapted from this work and presents the wide range of catalysts employed for the reaction. The majority of them are oxide based - notably molybdenum trioxide. It should also be observed that many of the products comprise of formaldehyde and although this constitutes a useful outcome, it highlights the difficulty thus far, in obtaining methanol-based products.

A schematic representation of the mechanism for methane oxidation over a silica supported molybdenum oxide catalyst was given by Spencer *et al.* (1990) (Figures 2.3 & 2.4). They proposed that the initial CH_4 activation took place on a Mo-O· species, thermally generated at the temperatures of reaction, with the subsequent formation of adsorbed transitions with +5 and +4 molybdenum oxidation states.
Significant research into the catalytic mechanism of oxide catalysts has also been performed by Parmaliana and co-workers *e.g.* Parmaliana and Arena (1997); Arena *et al.* (1997).

Table 2.8. Performance of Catalysts used for the Partial Oxidation of Methane

Catalyst	Temperature (°C)	Oxidant	CH_4 Conversion (%)	Product	Selectivity (%)	Space-Time Yield (STY) ($g/kg_{cat}.h$)
Nafion-H/teflon/C	120	H_2O_2	N/A	CH_3OH	100	0.4
ZrP	700	O_2	2.0	HCHO	32.1	10.3
SiO_2	520	O_2	N/A	HCHO	53	17.9
$MoO_3/Fe_2O_3/SiO_2$	600	N_2O	0.65	HCHO	20	20.9
V_2O_5/SiO_2	600	N_2O	0.56	HCHO	26	22.8
$BeO/B_2O_3/SiO_2$	600	O_2	*ca.* 2.8	HCHO	*ca.* 32	24
Cu/Fe/ZnO	750	O_2	2.5	HCHO	10	76
SiO_2	680	O_2	1.53	HCHO	40.2	77.7
Mo-Sn/SiO_2	700	O_2	20	HCHO	80	80
SiO_2	600	O_2	0.036	HCHO	75	116
$Sr/La_2O_3/MoO_3/SiO_2$	630	O_2	8.2	HCHO	3.3	129
Fe Sodalite	435	O_2	5.8	CH_3OH	25	186[a]
$Sr/La_2O_3/MoO_3/SO_2$	630	O_2	6.7	HCHO	4.1	186.7
MgO	750	O_2	0.7	HCHO	60	270
SiO_2	650	O_2	0.11	HCHO	63	304
V_2O_5/SiO_2	600	O_2	0.151	HCHO	48	318
Cu-Fe ZSM-5	342	N_2O	1.12	CH_3OH + (HCHO)	50 (6.2)	347[b] (40)[b]
Mo/2Su/P	675	O_2	7.2	HCHO	64.8	400
$CuO.MoO_3$	485	O_2	1.4	Oxygenates	79	490
V_2O_5/SiO_2	650	O_2	13.5	HCHO	35	760
V_2O_5/SiO_2	650	O_2	0.521-0.0078	HCHO	35-48	793-819
SiO_2	780	O_2	0.68	HCHO	28	812.8
$(MoO_3)_3.Fe_2O_3$	439	O_2	2.1	CH_3OH + (HCHO)	65 (8)	869 (100)
FeNbO	870	O_2	2.15	HCHO	61.6	1 210

[a]Calculated assuming a packing density of 1 g cm^{-3} and a 3:1 methane:air reaction mixture

[b]Calculated using a gas hourly space velocity (GHSV) of 43100 h^{-1}

(Adapted from Hall *et al.*, 1995)

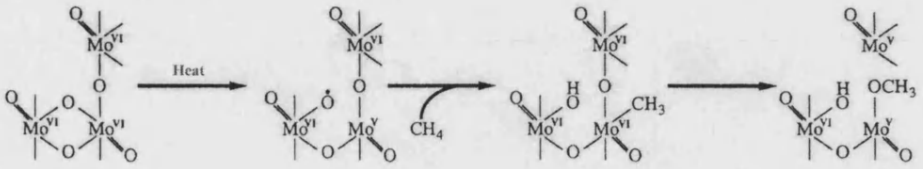

Figure 2.3. Reaction Pathway Schematic for Initial Attack on Methane.
(Adapted from Spencer *et al.*, 1990).

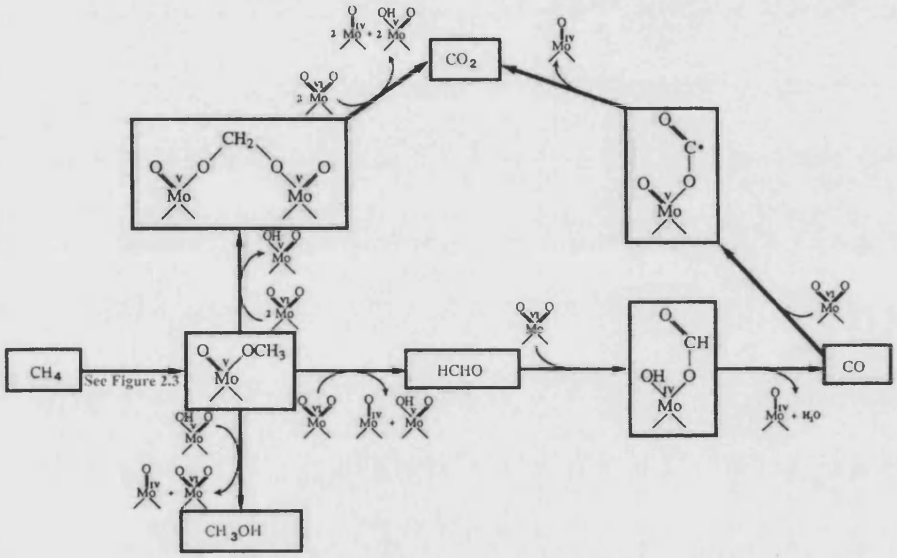

Figure 2.4. Main Reaction Pathway Schematic for Methane Oxidation Reactions.
(Adapted from Spencer *et al.*, 1990).

Because of the number of catalytic systems investigated for this methane partial oxidation reaction, it would seem prudent to develop a generic mechanism that would aid future catalyst development.

A general approach to catalyst design was first developed by Dowden *et al.* (1968) and labelled the 'virtual mechanism'. The selective oxidation of methane to formaldehyde was used as the case study. The suggested catalyst surface scheme is shown in Figure 2.5.

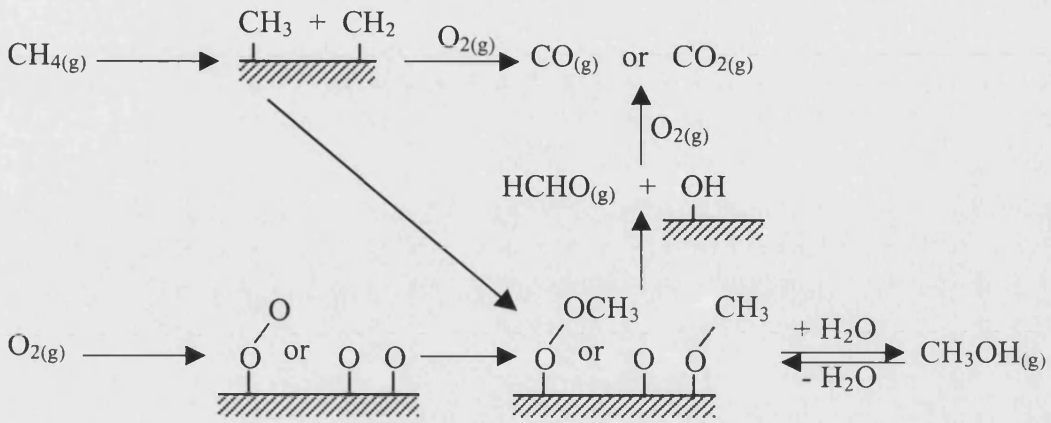

Figure 2.5. Surface Scheme for the Design of Oxidation Catalysts
(Adapted from Hall *et al.*, 1995)

Based on the two main fundamentals of the mechanism, dehydrogenation and oxygen insertion, the author suggested certain ions as suitable candidates for the selective reaction; for dehydrogenation, V^{5+}, Fe^{3+} and Cu^{2+} and for oxygen insertion, V^{5+}, Fe^{3+}, Zn^{2+}, Mo^{6+} and Ti^{4+}.

More recently, Hutchings and Taylor (1999) presented a simplified design approach for oxidation catalysts. They proposed three criteria for catalyst selection.

A desirable catalyst would:

1. not catalyse the oxidation of the required product under the reaction conditions.
2. activate the oxidant.
3. activate the substrate.

From experimental work based on this methodology, they concluded that Ga_2O_3/MoO_3 was a suitable catalyst in the oxidation of methane to methanol. However, they stated that on comparison with the homogeneous reaction, the use of any catalyst was deleterious.

Hall *et al.* (1995) noted that the vast majority of research into the catalytic partial oxidation of methane has been unable to avoid conditions where there may be contributions from homogeneous reactions. Such approaches are undesirable, as both the reactor design and control become complex and the products, in particular methanol, are susceptible to further oxidation.

For reasons such as those mentioned above, parallel research has been directed towards the oxidation of methane at lower temperatures, in particular in a liquid phase medium. In this case, oxidations utilising transition metal ions are usually characterised by an electrophilic mechanism. The avoidance of the unselective radical-based pathway forms a possibility of harnessing the primary oxidation products in commercially viable yields, not yet attainable in the gas phase.

The liquid phase partial oxidation of methane to methanol forms the basis of the next section.

2.5 The Liquid Phase Partial Oxidation of Methane to Methanol

The exothermicity of oxidation reactions provides the incentive to carry out the reactions in a liquid based medium. The high heat capacity of a liquid can help facilitate the removal of heat allowing the reactor to operate at higher levels of conversion and selectivity (Lee and Foster, 1996). Before focussing on the major research achievements to date, it useful to acknowledge that there are several liquid phase oxidation processes currently carried out in industry *e.g.* ethylene oxidation to form acetaldehyde. Table 2.9 highlights the fundamental features of some of these commercial processes. It should be noted that the liquid phase oxidations are characterised by relatively low to moderate temperatures, are catalytic in nature and often employ pure oxygen rather than air as the stoichiometric oxidant. Unfortunately, the substrates used for the aforementioned industrial oxidations are much more reactive than methane is at the low temperatures used. Indeed, the activation and subsequent functionalisation of methane at low temperatures has been described as a "Holy Grail" in chemistry (Sen, 1998).

Despite being the most abundant and least expensive hydrocarbon, methane is the most unreactive. This chemical inertness is attributed to methane possessing a high ionisation energy and a low electron affinity, but mainly towards its unusually high C-H bond energy (CH_3-H) of 435.4 kJ/mol (Lide, 1991). Table 2.10 below depicts some key physical properties of methane that indicate its reluctance to react.

Table 2.10. Some Physical Properties of Methane

Property	**Value**	**Property**	**Value**
Melting Point	- 182.6 °C	**Viscosity (at 35 °C)**	1.12×10^{-4} g/cm.s
Boiling Point	- 161.6 °C	**1st Bond Energy**	435.4 kJ/mol
Density (liquid at bp)	0.4240 kg/m^3	**Proton Affinity**	546 kJ/mol
Critical Temperature	- 82 °C	pK_a **(estimated)**	*ca.* 40
Critical Pressure	4.641 MPa	$\Delta H°_f$	- 74.898 kJ/mol
1st Ionisation Potential	13.16 eV	**C-H Bond Length**	0.11068(10) nm
2nd Ionisation Potential	19.42 eV	**H-H Distance**	0.18118(70) nm

(Adapted from Crabtree, 1995)

Thus, many reactions involving methane require high temperatures and/or photolytic conditions *e.g.* chlorination. For this reason, the partial oxidation of methane in the gaseous phase would be an obvious choice. However, as shown in the last section, the initial formation of methyl radicals from the homolysis of the methane C-H bond, results

Table 2.9. Key Features of Several Industrial Liquid Phase Processes

Industrial Process	Operating Conditions		Catalyst	Reaction(s)
	T (°C)	*P* (MPa)		
Ethylene oxidation to acetaldehyde (one-step process)	130	0.3	$PdCl_2$ and $CuCl_2$	$C_2H_4 + PdCl_2 + H_2O \rightarrow CH_3CHO + Pd + 2HCl$ $Pd + 2CuCl_2 \leftrightharpoons PdCl_2 + 2CuCl$ $2CuCl + 0.5O_2 + 2HCl \rightarrow 2CuCl_2 + H_2O$
Propylene oxide formation via the ethylbenzene hydroperoxide process (two-step process)	140 - 150 (step one) 95 - 130 (step two)	0.206 - 0.275 2.5 - 4	No catalyst for step one Either homogeneous Mo, W or Ti or heterogeneous TiO_2/SiO_2	$(C_6H_5)\text{-}C_2H_5 + O_2 \rightarrow (C_6H_5)\text{-}HC(OOH)CH_3 + (C_6H_5)\text{-}C(O)CH_3$ $(C_6H_5)\text{-}HC(OOH)CH_3 + C_2H_6 \rightarrow H_2C(O)CHCH_3 + (C_6H_5)\text{-}HC(OH)CH_3$
Acetaldehyde oxidation to acetic acid	60 - 80	0.3 - 1	Co or Mn salt	$CH_3COH + 0.5O_2 \rightarrow CH_3COOH$
Butane oxidation to acetic acid	152	5.6	Co, Cr and Mn acetates	$2C_4H_{10} + 5O_2 \rightarrow 4CH_3COOH + 2H_2O$
* Methanol carbonylation to acetic acid (Monsanto Process)	150 - 200	3.3 - 6.6	Rh with I^- promoter	Well documented reaction mechanism *e.g.* Campbell *et al.*, 1985. Overall: $CH_3OH + CO \rightarrow CH_3COOH$

* This process is strictly a carbonylation incorporating CO insertion, but is included in the table as an example of an important reaction for homogeneous catalysis and furthermore, it uses methanol as the substrate

in a very unselective mechanism. Considering the C-H bond energy in methanol ($HOCH_2$-H) is 393.6 kJ/mol (Lide, 1991), the mechanism involving H-atom abstraction, favours the overoxidation of methanol over the primary oxidation of methane (which forms the methanol product).

Labinger (1995) considered a homogeneous series reaction in which reactant A gives product B which reacts further to give the co-product C. The results of simple calculations were presented in the form of a graph (Figure 2.6). This shows the dependence of product yield B on the ratio of the specific reaction rates of the two reaction steps.

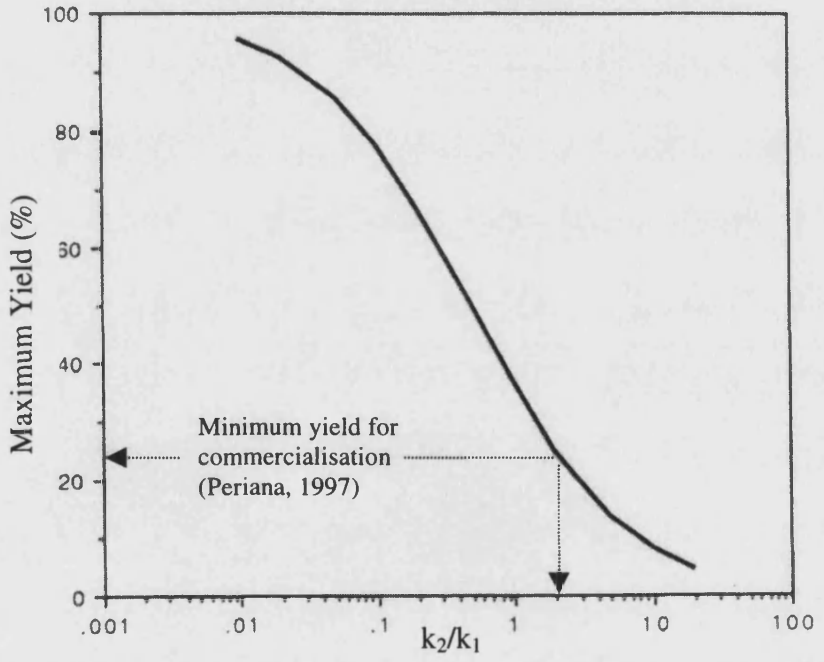

Figure 2.6. Maximum Possible Yield of Desired Product B in the Reaction Sequence: $A \xrightarrow{k_1} B \xrightarrow{k_2} C$ as a Function of k_2/k_1. (Adapted from Labinger, 1995)

It is therefore desirable to facilitate a mechanism in which the substrate (methane) is more reactive than the product (methanol) and at the same time effecting reaction rates and product yields of industrial significance. Engineers at Catalytica, Inc. (California, USA) estimated that for a one-step methane to methanol process to be competitive with the current industrial process, single-pass conversions in excess of 30 % at greater than 80 % selectivity are required (Periana, 1997). Considering the low methane conversions achieved to date in the gaseous phase partial oxidations, these figures present a daunting challenge for the liquid phase chemistry.

In the 1970s, new reactions of methane at relatively low temperatures and without the intervention of free radicals, were reported. Broadly classified, these reactions all involved two-electron redox changes that could be divided into reactions of methane with protons/carbonium ions and those with metal complexes. A general example of each of these reaction-types is shown below (Periana, 1997):

- Superacid: $CH_4 + H^+ \rightarrow CH_5^+$ (2.32)
- Carbonium ion: $CH_4 + CH_3^+ \rightarrow CH_3\text{-}CH_3 + H^+$ (2.33)
- Transition metal: $L_nM + CH_4 \rightarrow L_nM(CH_3)(H)$ (2.34)

  $MX_n + CH_4 \rightarrow MX_{n-2} + CH_3X + HX$ (2.35)
- Rare earth: $MR + CH_4 \rightarrow MCH_3 + RH$ (2.36)
- Metal-oxo: $L_nM{=}O + CH_4 \rightarrow L_nM(CH_3)(OH)$ (2.37)

(Here "L" represents a ligand, "M" a metal and "X" a halide, hydroxide, carboxylate *etc.*)

The essential characteristics of these reactions are that:

1. the reactions occurred at low temperature (< 100 °C).
2. electrophilic processes are important.
3. the reactions are homogeneous.
4. efficient catalysis is lacking.

It is the reaction of methane with the metal complexes (organometallic) which generated most interest for methane oxidation research. In this field two fundamental terms are widely used. "Activation" is used to describe a process in which substitution of a stronger C-H bond (375 - 440 kJ/mol) occurs to produce a weaker metal-carbon bond (210 - 335 kJ/mol). "Functionalisation" refers to a process in which the metal-carbon bond is replaced by any bond other than a C-H bond (*e.g.* C-OH) (Periana, 1997; Shilov and Shul'pin, 1997).

Many researchers have proposed that the intermediate leading to methane activation is a sigma complex. Possessing no lone pair electrons, methane must engage its σ-electrons for bonding in this complex. The subsequent fate of this species depends on the metal

centre, but generally one of five possibilities arises namely, oxidative addition, electrophilic activation (see Figure 2.7), sigma-bond metathesis, 1,2-Addition and metalloradical activation. For further details on the aformentioned pathways, the reader is invited to consult the reviews of Labinger (1995) and Shilov and Shul'pin (1997). In terms of the actual functionalisation of methane rather than just organometallic compound formation, it is the electrophilic pathway that has yielded the most success.

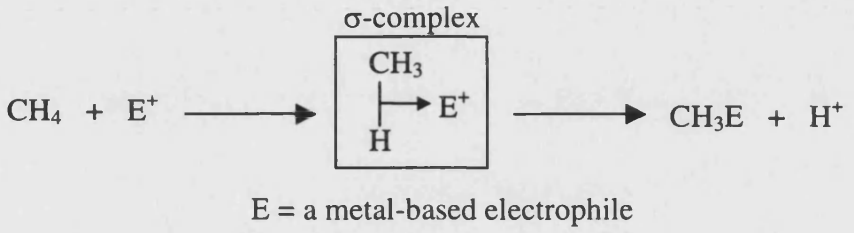

Figure 2.7. Electrophilic methane activation with the formation of a sigma complex

Despite being able to effect methane activation, few of the organometallic systems were capable of subsequent substrate functionalisation and regeneration of the metal fragment as required for catalytic turnover. In most cases, the reactive metal species used would be incompatible (*i.e.* deactivated) with stoichiometric oxidants that might be used for a catalytic reaction (*e.g.* O_2, H_2O_2) (Labinger *et al.*, 1990; Stahl *et al.*, 1998).

An important and even pioneering example to this limitation is the reaction of methane with chloroplatinum salts in aqueous solution. The work which started in 1969, was carried out by Alexander Shilov and co-workers (see Shilov, 1984). They started with the incorporation of deuterium into the methane substrate in solutions of $K_2[PtCl_4]$ in D_2O/[D_1]acetic acid. Three years later they reported that addition of $H_2[PtCl_6]$ to the reaction mixture generated oxidised products:

$$CH_4 + [PtCl_6]^{2-} + H_2O\ (Cl^-) \xrightarrow[H_2O,\ 120\ °C]{[PtCl_4]^{2-}} CH_3OH\ (CH_3Cl) + [PtCl_4]^{2-} + 2HCl \quad (2.38)$$

Additionally, the platinum complexes were shown to be unaffected by the presence of oxygen (Rostovtsev *et al.*, 1998). A significant amount of work to characterise this

reaction has been undertaken by several researchers other than the founders (*e.g.* Labinger *et al.*, 1993; Luinstra *et al.*, 1995; Stahl *et al.*, 1995; Stahl *et al.*, 1996; Holtcamp *et al.*, 1997). Figure 2.8 illustrates the proposed mechanism that is generally accepted by the different research groups.

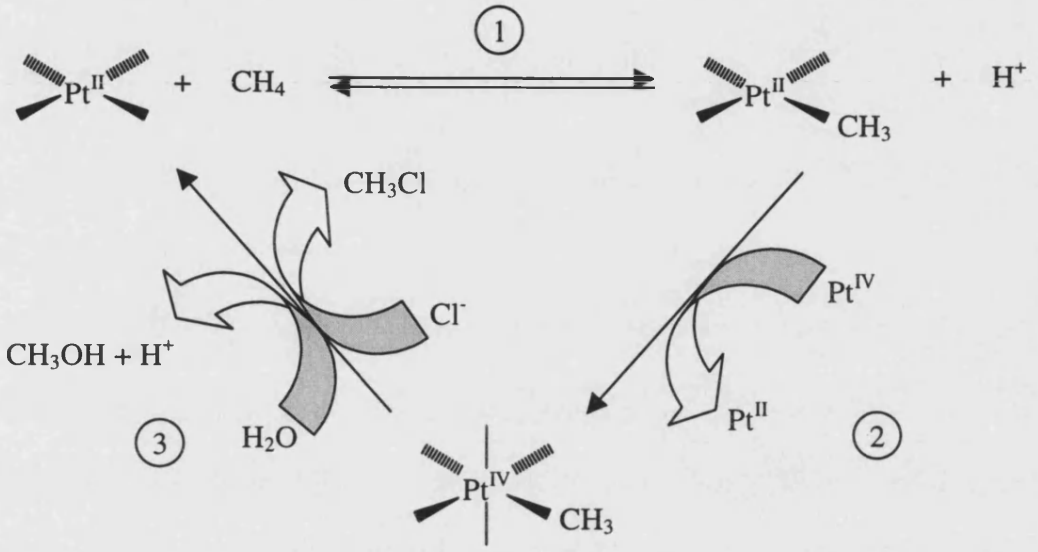

Figure 2.8. Proposed Catalytic Cycle for the Homogeneous Platinum Catalysed Oxidation of Methane in an Aqueous Solution. (Adapted from Stahl *et al.*, 1998)

Relating to Figure 2.8, Step 1 represents methane activation by Pt^{II} to generate an alkylplatinum(II) intermediate, Step 2 the two-electron oxidation of the alkylplatinum(II) intermediate to generate an alkylplatinum(IV) species and Step 3 the reductive elimination of either methyl chloride or methanol to liberate the oxidation product and the Pt^{II} catalyst. It has recently been established that although the presented mechanism is accepted, each of the three steps can proceed in a least two different pathways (see review, Stahl *et al.*, 1998).

The "Shilov" system is attractive because of the unique selectivity patterns observed. Although not relevant to a methane substrate, its regioselectivity for alkanes is completely opposite to that achieved in a radical-based mechanism. In this case, the order of attack is dictated by the homolytic C-H bond energy whereby $3^o < 2^o < 1^o$ and so preferential activation is in the order $3^o > 2^o > 1^o$. With the organometallic electrophilic

system, the order is completely reversed. This point is illustrated by the possible oxidation of ethane to ethylene glycol. Here the order of oxidation with the organometallic system is $H\text{-}CH_2CH_3$ > $H\text{-}CH_2CH_2OH$ > $H\text{-}CH(OH)CH_3$. Indeed, the preferential oxidation of the methyl group in ethanol to form ethylene glycol was demonstrated first by Labinger *et al.* (1993), followed by Sen *et al.* (1994) who obtained ethylene glycol as the sole product.

In light of this observation, methanol should be less susceptible to oxidation than its precursor methane. Results published by Sen *et al.* (1994) indicated that methane and methanol exhibit similar reactivity towards oxidation using the platinum system. Although the rates are similar, which is in contrast with the gas phase reaction in which methanol can react up to six orders of magnitude faster, the fact that methanol is much more soluble in the aqueous phase means that ultimately, the methanol will be oxidised. For an economic process, it is mandatory that the expensive Pt^{4+} is replaced with oxygen as the stoichiometric oxidant. Unfortunately, success in this area remains elusive. For these reasons, the system has limited practical application.

The use of an aqueous solvent for these reaction-types is generally limiting. Although the O-H bond energy in water is considerably higher than the C-H bond in methane, water has a greater affinity as a ligand to compete for the co-ordination sites of the metal ion, which are necessary for the substrate activation. Furthermore, any methane-metal ion complex formed would be subject to hydrolytic attack. Nevertheless, success in the aqueous phase is apparent, as shown in the previous example.

Considerable attention has recently been directed towards the oxidation of alkanes by electrophilic metal ions in strong acid media. For two reasons, a strongly acidic solvent is beneficial. First, the conjugate bases of strong acids are poorly co-ordinating, thereby enhancing the electrophilicity of the metal ion. Second, the subsequent esterification of the alcohol (methanol) acts as a chemical protectant, suppressing its overoxidation.

The importance of the choice of solvent was demonstrated by the catalytic system developed by Lin *et al.* (1996). Using rhodium trichloride and halide promoters, the low temperature hydroxylation and hydroxycarbonylation of methane with molecular oxygen and carbon monoxide occurred. A change in the solvent system from water to a mixture of water and perfluorobutyric acid, dramatically changed the product composition from virtually all acetic acid to one in which the methanol ester dominated.

The second point can be illustrated by comparing the C-H bond energy of methanol to that of a representative ester *i.e.* $HOCH_2$-H = 393.6 kJ/mol, (C_6H_5)-$COOCH_2$-H = 419.5 kJ/mol (Lide, 1991), although the chemical selectivity in the electrophilic reaction is not explicitly dictated by homolytic bond energies.

Periana (1997) gave a pictorial representation of this "protection" mechanism in the form of a free-energy reaction co-ordinate plot. An adapted form for the strong acid, trifluoroacetic acid (TFA), is shown in Figure 2.9.

$$CH_4 + 2O_2 + CF_3COOH \xrightarrow{\text{Main Reaction}} CF_3COOCH_3 + H_2O + \frac{3}{2}O_2$$

$$CF_3COOCH_3 + H_2O + \frac{3}{2}O_2 \xrightarrow{\text{Overoxidation}} CO_2 + 2H_2O + CF_3COOH$$

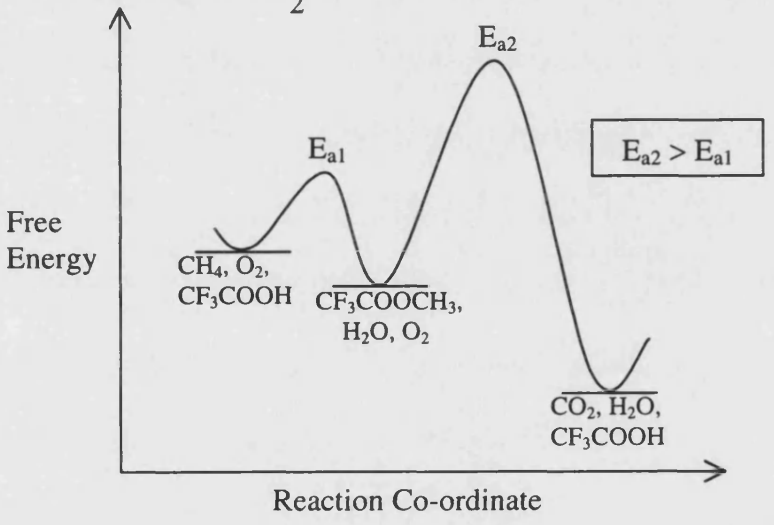

Figure 2.9. Chemical Protection Strategy to Prevent Overoxidation

Periana *et al.* (1993), used concentrated sulphuric acid as both the stoichiometric oxidant and the protection medium to form the methane product methyl bisulphate. Although, the product would need subsequent hydrolysis to obtain methanol, in this system the yields were unprecedented and will be described later.

A key characteristic of many of the recent systems is that they employ oxygen as the oxidant and true catalysis is evident. (*e.g.* Lin *et al.*, 1996; Yamanaka *et al.*, 1995; Vargaftik *et al.*, 1990).

As well as the electrophilic-based mechanism, some systems are effected by other reaction pathways. The use of hydrogen peroxide often facilitates a radical-based mechanism with H-abstraction of methane, but it is much more controlled than in the gaseous phase, as shown by Nizova *et al.* (1997)[a]. Lin *et al.* (1997) developed a catalytic system that is analogous to the biological reactions of monooxygenase enzymes in that a coreductant is required (this system is discussed later).

Table 2.11 highlights the key features of several liquid phase methane oxidations to a methanol-based product. Attention is drawn for the reader not to view this as an exhaustive list of works, but as a compilation of the more promising catalytic systems published to date. Many of the systems proffer from very high selectivities (approaching 100 %) of the methanol-based product, although, with one exception (Periana *et al.*, 1993), are often plagued by product yields of only a few percent and correspondingly low methane conversions. In light of this, research into the liquid phase oxidation is less mature than in the gas phase for which steady interest has been apparent for almost a century. The immediate advantages evident of liquid phase methane oxidations are exemplified by the low temperatures employed and the highly selective chemical mechanism which results with significantly higher product selectivities than in the gaseous phase.

Table 2.11. Methane Oxidation from Selected Liquid Phase Works (Part 1 of 4)

Author	Base Reactants (oxidising agent in **bold-type**, catalyst in *italics*)	Reactor Type (Batch or Continuous)		*T* (°C)	*P* (MPa)	Reaction Time (h)	Observed Products	(A)dvantages/ (D)isadvantages
		Reactor Volume (ml)	Liquid Volume (ml)					
Lin *et al.* (1996) (see also Chepaikin *et al.*, 2001)	*$RhCl_3.3H_2O$ (5.0 mg)* KI (10.0 mg) NaCl (15 mg) D_2O (0.5 ml) C_3F_7COOH (3 ml) CO (200 psi) CH_4 (1000 psi) **O_2 (100 psi)**	Batch N/A	3.5	80	9.65	80	$C_3F_7COOCH_3$ CH_3COOH HCO_2H CO_2	(A) Low temperature (A) O_2 oxidant (A) Good selectivity (A) C-C cleavage (D) High pressure (D) Requirement of coreductant CO (D) Low conversions and yields (D) High batch time
Lin *et al.* (1997) (see also Park *et al.*, 2000[a])	*5 % Pd/C (1.0 mg)* $CuCl_2$ (13.5 mg) CF_3COOH (3 ml) H_2O (1.0 ml) CO (200 psi) CH_4 (900 psi) **O_2 (100 psi)**	Batch 125	4	85	8.3	20	CF_3COOCH_3 CH_3OH CH_3COOH HCO_2H CO_2	(A) Heterogeneous catalysis (separation) (A) Low temperature (A) O_2 oxidant (A) Highly selective (A) C-C cleavage (D) High pressure (D) Requirement of coreductant CO (D) Low conversions and yields
Periana (1993)	*100 mol/m^3 solution of $Hg(OSO_3H)_2$ in* **100% H_2SO_4 (300 ml)** 97/3 % CH_4/Ne (34.5 bar)	Batch 1000	300	180	3.45	3	CH_3OSO_3H SO_2 H_2O CO_2	(A) Highly selective (A) High conversions and yields (A) Low batch time (D) High temperature (D) H_2SO_4 oxidant

Table 2.11. Methane Oxidation from Selected Liquid Phase Works (Part 2 of 4)

Author	Base Reactants (oxidising agent in bold-type, catalyst in *italics*)	Reactor Type (Batch or Continuous)		*T* (°C)	*P* (MPa)	Reaction Time (h)	Observed Products	(A)dvantages/ (D)isadvantages
		Reactor Volume (ml)	Liquid Volume (ml)					
Periana *et al.* (1998)	*(bpym)$PtCl_2$ (50 mol/m^3)* **102% H_2SO_4 (80 ml)** 97/3 % CH_4/Ne (500 psi(g))	Batch 300	80	220	3.55	2.5	CH_3OSO_3H CH_3OH CO_2	(A) Highly selective (A) Very high conversions and yields (A) Low batch time (D) High temperature (D) H_2SO_4 oxidant (D) Expensive catalyst
Yamanaka *et al.* (1995) Yamanaka *et al.* (1996)	*$EuCl_3.6H_2O$ (0.03 mmol)* CF_3COOH (4 ml) Zn powder (1 g) Optional catalyst promoter either bis(2,4,-pentanedionato)TiO or TiO_2 **O_2 (4 atm)** CH_4 (10 atm)	Batch 47 As above	4 As above	40 As above	1.4 As above	1 As above	CF_3COOCH_3 CO_2 (derived from CF_3COOH)	(A) Very low temperature (A) O_2 oxidant (A) Highly selective (A) Low pressure (A) Low batch time (D) Low conversions and yields (D) Expensive catalyst (D) Loss of solvent → CO_2
Yamanaka *et al.* (1998)	Either *bis(2,4-pentanedionate)VO* or *NH_4VO_3 (0.03 mmol)* CF_3COOH (4 ml) Zn powder (1 g) **O_2 (4 atm)** CH_4 (10 atm)	Batch 47	4	40	1.4	1	CF_3COOCH_3 CO_2 (derived from CF_3COOH)	(A) Very low temperature (A) O_2 oxidant (A) Highly selective (A) Low pressure (A) Low batch time (D) Low conversions and yields (D) Loss of solvent

Table 2.11. Methane Oxidation from Selected Liquid Phase Works (Part 3 of 4)

Author	Base Reactants (oxidising agent in bold-type, catalyst in *italics*)	Reactor Type (Batch or Continuous)		*T* (°C)	*P* (MPa)	Reaction Time (h)	Observed Products	(A)dvantages/ (D)isadvantages
		Reactor Volume (ml)	Liquid Volume (ml)					
Vargaftik *et al.* (1990)	*$Co(O_2CCF_3)_3$ (0.09 mol/m^3)* in CF_3COOH CH_4 (20 atm) **O_2 (3 atm)**	N/A	N/A	180	≈ 2.3	4	CF_3COOCH_3 CO_2	(A) O_2 oxidant (A) Highly selective (A) Low pressure (A) Low batch time (D) High temperature
Nizova *et al.* (1997)[a]	*$(NBu_4)VO_3$ (0.1 mol/m^3)* Pyrazine-2-carboxylic acid (0.4 mol/m^3) H_2O_2 (35% aq) (200 mol/m^3) All above in acetonitrile solution **Air (10 bar)** CH_4 (75 bar)	Batch 100	 10	40	8.5	1	CH_3OOH (reduced to CH_3OH using added PPH_3) HCHO HCOOH	(A) Very low temperature (A) Air/O_2 oxidant (A) Low batch time (D) High pressure (D) Low selectivity (D) Unstable products (D) Low conversions and yields
Nizova *et al.* (1997)[b] (See also Süss-Fink *et al*, 1998)	*$(NBu_4)VO_3$ (1 mol/m^3)* Pyrazine-2-carboxylic acid (4 mol/m^3) H_2O_2 (30% aq) (2000 mol/m^3) All above in acetonitrile solution **O_2 (10 bar)** CH_4 (75 bar)	300	100	40	8.5	12	CH_3OH HCOOH (no methyl hydro peroxide or formaldehye observed when using this higher concentration of catalyst and/or steel walls)	

Table 2.11. Methane Oxidation from Selected Liquid Phase Works (Part 4 of 4)

Author	Base Reactants (oxidising agent in bold-type, catalyst in *italics*)	Reactor Type (Batch or Continuous)		*T* (°C)	*P* (MPa)	Reaction Time (h)	Observed Products	(A)dvantages/ (D)isadvantages
		Reactor Volume (ml)	Liquid Volume (ml)					
Gretz *et al.* (1987)	**$Pd(O_2CCH_3)_2$** (0.15 g) CF_3COOH (5.00 g) CH_4 (800 psi)	Batch N/A	N/A	80	5.52	150	CF_3COOCH_3 Pd CH_3COH CH_3COOH CO_2	(A) Low temperature (D) Expensive Pd salt oxidising agent reduced to metallic Pd residue (D) High batch time (D) Non-catalytic (D) High pressure (D) Low conversions and yields
Kao *et al.* (1991)	*$Pd(O_2CC_2H_5)_2$ (0.15 mmol)* **H_2O_2 (30 % aq) (2 mmol)** $(CF_3CO)_2O$ (1.8 ml) CH_4 (900 psi)	Batch N/A	1.8	90	6.21	≈ 25 (Longer times lead to the decomposition of Me(ester)	CF_3COOCH_3 CF_3COOH CO_2	(A) Highly selective (D) Low Yields (D) H_2O_2 oxidising agent (more expensive than O_2)
Piao *et al.* (1999)	*$H_5PV_2Mo_{10}O_{40}$ (0.022 mmol)* **$K_2S_2O_8$ (5.00 mmol)** TFA (5.0 ml) TFAA (10 mmol) CH_4 (20 atm)	Batch 100	5	80	2	20	CF_3COOCH_3 CH_3COOCH_3	(A) Low temperature (A) Low Pressure (A) High product selectivity (A) Very high product yields possible if small gas volume is used (D) $K_2S_2O_8$ oxidant
Parmaliana *et al.* (1992) (see also Frusteri *et al.*, 1999 and Frusteri *et al.*, 1991)	*Nafion-H membrane (perfluororesinsulfonic acid) 1.4-1.8 g (0.06 cm thick)* **H_2O_2 (440 mol/m^3)** CH_4 (17 mmol)	Semi-Continuous N/A	N/A	120	0.14	3	CH_3OH	(A) Very Low Pressure (A) Stable Catalyst (A) Very high product selectivities (A) Novel use of a 3-phase catalytic membrane reactor (D) H_2O_2 oxidant

From the systems detailed in Table 2.11, three are selected for further discussion. These are the works of Yamanaka *et al.* (1995) because of the very low temperature (< 40 °C) reaction and O_2 as the oxidant, Periana *et al.* (1993) because of the unprecedented high conversion, selectivity and product yield, and lastly Lin *et al.* (1997) which uses a relatively inexpensive heterogeneous system with O_2 oxidant, somewhat of a novelty in this field.

1) Yamanaka *et al.* (1995)

Using a europium trichloride catalyst with a zinc promoter in a trifluoroacetic acid (TFA) medium, the selective partial oxidation of methane to a methanol derivative was achieved using oxygen. The reaction was carried out in a 47 ml glass-lined autoclave.

$$CH_4 + \frac{1}{2}O_2 \ (+ \ CF_3COOH) \rightarrow CH_3OH \ \ (CF_3COOCH_3 + H_2O) \qquad (2.39)$$

This was said to have occurred even at room temperature. The pressures used were relatively low; typically oxygen at 0.44 MPa and methane at 1 MPa.

The methanol was in the form of its ester, but selectivities in the liquid phase were typically 100 %. Subsequent hydrolysis of the ester would be required to yield the methanol product and regenerate the TFA solvent:

$$CF_3COOCH_3 + H_2O \rightleftharpoons CH_3OH + CF_3COOH \qquad (2.40)$$

Carbon dioxide was produced in the gaseous phase and was said to be attributed to the catalytic oxidation of the TFA solvent.

Increasing the methane partial pressure resulted in higher methanol selectivities when considering the products in both phases, not just the liquid phase. Also, increasing the reaction temperature caused an increase in the turnover number (TON) of methanol *(e.g.* TON = 4 in 1 h at 40 °C and 5.3 at 50 °C).

Other rare earth salts and transition metal salts were tested as catalysts for the methane oxidation. The authors concluded that the europium cation had a special activity for the catalytic oxidation of methane to methanol. Out of the rare earth elements, only europium has a standard electrode potential above zinc and thus is reducible, although not as far as its elemental state as is feasible with some transition metals.

It was later shown that titanium(II) enhanced the catalytic system (*e.g.* TON = *ca.* 10 in 1 h at 40 °C) (Yamanaka *et al.*, 1996).

The proposed reaction mechanism is shown in Figure 2.10 below

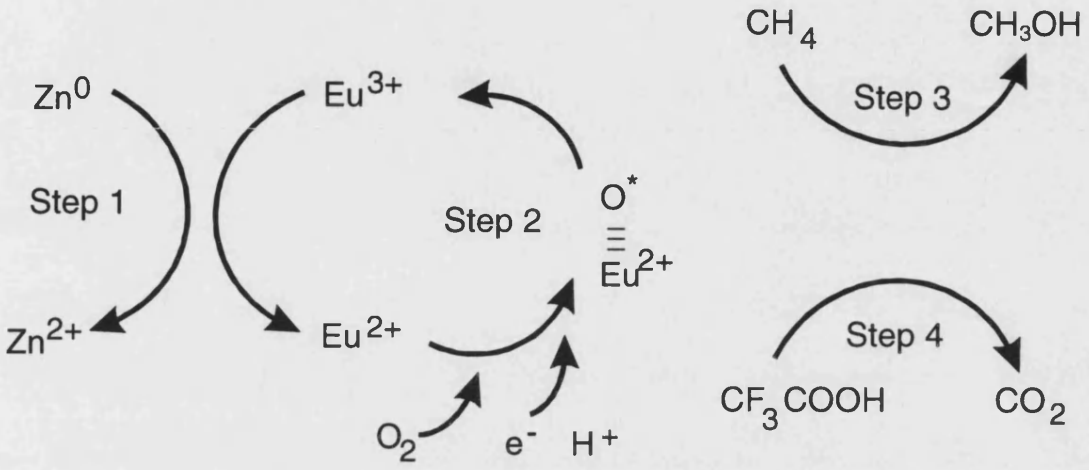

Figure 2.10. Model of the Reaction Mechanism for the Methane Oxidation in $EuCl_3$-Catalytic System at Room Temperature (Adapted from Yamanaka *et al.*, 1996).

Steps 1-4 can be summarised as follows:

Step 1: reduction of Eu^{3+} to Eu^{2+} with Zn^0

Step 2: reductive activation of O_2 with e^- (from Eu^{2+} or Zn^0) and H^+ from CF_3COOH

Step 3: oxidation of CH_4 to CH_3OH by the activated oxygen on Eu-catalyst

Step 4: formation of CO_2 from CF_3COOH with the activated oxygen

It was proposed that the titanium(II) promoter accelerates the electron transfer reactions (steps 1 and 2) or the activation of CH_4 to CH_3OH (step 3)

More recently (Yamanaka *et al.*, 1998), the europium-based catalyst was replaced with a vanadium species *e.g.* bis(2,4-pentanedionate)VO, with a higher catalyst activity being reported (*e.g.* TON > 10 in 1 h at 40 °C).

Despite the low temperature and pressures used, the deleterious effect of solvent degradation and the resultant low yield and conversion with the expensive europium catalyst, make it appear unfavourable for any scaled-up operation.

2) Periana *et al.* (1993)

Using a medium of 100 % sulphuric acid and mercury(II) ions, methane was converted to methyl bisulphate in a 43 % yield at 85 % selectivity and 50 % conversion. The work was carried out at Catalytica, Inc. (California, USA) where the engineers had stated that for an economically competitive direct methane to methanol process, it would have to be carried out at high one-pass methane conversion and selectivity. In fact evaluations indicated that for such an idealised process, single-pass conversions in excess of 30 % at greater than 80 % selectivity are required for an economical process. Thus from the start, this catalytic system seems very promising indeed.

The overall reaction is:

$$CH_4 + 2H_2SO_4 \xrightarrow[3.5\ MPa]{180\ ^\circ C} CH_3OSO_3H + 2H_2O + SO_2 \qquad (2.41)$$

Based on a series of observations by the original developers, the postulated mechanism is depicted in Fig. 2.11.

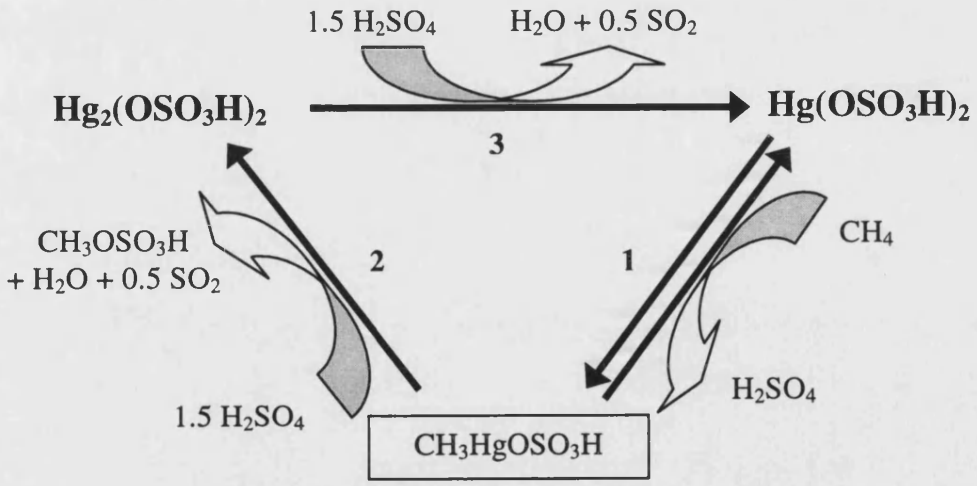

Figure 2.11. Proposed Mechanism for the Oxidation of Methane to Methyl Bisulphate by the $Hg(II)/H_2SO_4$ System. (Adapted from Stahl *et al.*, 1998).

Referring to Figure 2.11:

Step 1: electrophilic activation of methane to generate a methylmercury(II) intermediate (activation)

Step 2: reductive elimination of methyl bisulphate (functionalisation)

Step 3: oxidation of mercurous bisulphate to regenerate the catalyst (regeneration of catalyst)

The precise mechanism of C-H activation by Hg(II) remains the subject of some debate (Stahl *et al.*, 1998). While many features of this reaction are consistent with a simple electrophilic substitution mechanism, Sen *et al.* (1994) have suggested that an outer-sphere electron transfer pathway may also account for many of the observations. Periana (1997) did not consider a radical-based activation because of the high product selectivities encountered.

Through this mechanism and the resultant observed selectivities, it was concluded that the methane was 100-fold more reactive than the product, mercury bisulphate.

Gang *et al.* (2000) studied this homogeneous system in more detail, emphasising the observed methane pressure drop relating to reaction performance. They concluded that the reaction was first order with the rate constant being proportional to the concentration (and hence solubility) of the mercury(II) sulphate catalyst in the sulphuric acid solvent. One query arises from their limited data given for obtained methanol concentrations. They are *ca.* 94 mol/m^3 and based on their reactor volumes (200 ml total volume, 50 ml liquid volume) and a methane initial pressure of 5.0 MPa at 180 °C, an estimated methanol yield of only a few percent is calculated. This is significantly different from the quoted 43 % obtained by the original workers. This was not commented on in Gang *et al.* (2000), but they hydrolysed the methane bisulphate prior to analysis which could have caused this discrepancy. Furthermore, the reactor dimensions differed, with Gang and co-workers using a 200 ml autoclave whilst Periana employed a 1000 ml autoclave, although similar gas:liquid ratios were used. Although inconclusive, this point raises the question regarding the incompatibilities with scale-up - an important aspect that needs to be assessed before commercial implementation.

In a more recent publication (Periana *et al.*, 1998) the reaction in equation (2.41) was catalysed even more efficiently by a bipyrimidine complex of platinum(II):

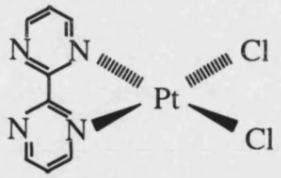

At 200 °C, methyl bisulphate can be obtained at 81 % selectivity and 72 % yield with 90 % methane conversion.

One problem associated with these systems is the use of sulphuric acid as the stoichiometric oxidant. Although the acid can be regenerated from the hydrolysis of methyl bisulphate, evident loses in the form of sulphur dioxide are present. A practical process based on oxygen as the overall oxidant was proposed, but not verified. The reaction scheme for such a process was as follows:

$$CH_4 + 2H_2SO_4 \rightarrow CH_3OSO_3H + 2H_2O + SO_2 \qquad ((2.41))$$

$$CH_3OSO_3H + H_2O \rightarrow CH_3OH + H_2SO_4 \qquad (2.42)$$

$$SO_2 + \frac{1}{2}O_2 + H_2O \rightarrow H_2SO_4 \qquad (2.43)$$

OVERALL:

$$CH_4 + \frac{1}{2}O_2 \rightarrow CH_3OH \qquad (2.44)$$

Thus, the sulphuric acid merely acts as an oxygen transfer reagent, with molecular oxygen being the net oxidant.

The use of concentrated (100 %) sulphuric acid also has significant implications on the cost of construction materials and safety. The authors employed a 1000 ml Hastaloy-C autoclave in which to carry out the reaction. Wolf (1998), questioned the long term stability of the more recent platinum(II) estimating that the catalyst remains deactivated for a timespan of 14 h based on the turnover numbers and frequencies given (Periana, 1993). He also pointed out that when evaluating the process efficiency, the necessary post-separation steps namely, hydrolysis of the ester, distillation of the methanol, and the oxidation of the formed SO_2 to SO_3 for regeneration of the sulphuric acid oxidising agent, all need to be accounted for.

3) Lin *et al.* (1997)

The selective partial oxidation of methane to a methanol derivative was achieved in a 3:1 (v/v) medium of trifluoroacetic acid:water with a heterogeneous palladium and copper(II) chloride catalytic system. Molecular oxygen was used as the stoichiometric oxidant with carbon monoxide as a co-reagent. Although the fundamentals of the system were reported in the work of Lin and Sen (1992), impetus for improvement came from the more favourable system comprising the rhodium trichloride catalysed oxidation of methane (Lin *et al.*, 1996). A criticism of this latter system, however, was that the rhodium was relatively expensive and the efficient post-separation posed a problem with homogeneous catalysis. Furthermore, although the reaction was selective to the methanol ester, there was always a significant amount of acetic acid in the product. Thus, this new system effected a very high selectivity using the cheaper 5 wt.% palladium on carbon heterogeneous catalyst.

At 85 °C and 8.3 MPa total pressure, approximately 100 % selectivity to methanol trifluoroacetate was achieved in the liquid phase (albeit at a low yield of only a few percent). Carbon dioxide was observed in the gaseous phase. It was concluded that the copper(II) chloride cocatalyst was crucial for product selectivity; in its absence formic acid became the preferred product. Unlike the previous system (Lin *et al.*, 1996), a change in the solvent composition had little effect on product distribution, although no reaction was observed in the absence of water.

The elucidated reaction scheme, based on a methanol product, is shown in Figure 2.12.

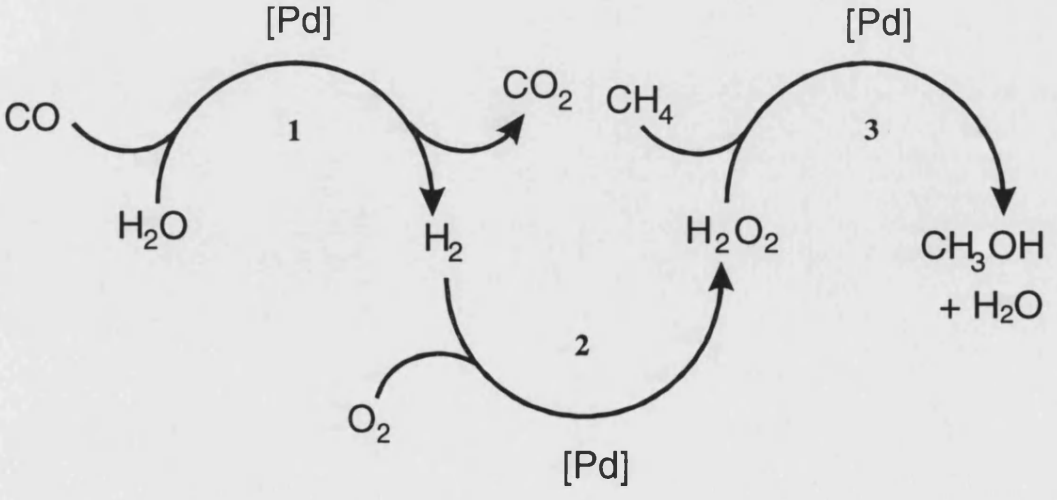

Figure 2.12. Overall Reaction Scheme for Bimetallic System (Adapted from Lin *et al.*, 1997).

Relating to Figure 2.12:

Step 1: The metal catalysed water gas shift reaction involving the oxidation of carbon monoxide to carbon dioxide and hydrogen.

Step 2: The catalytic combination of hydrogen with oxygen to yield *in situ* hydrogen peroxide.

Step 3: The metal-catalysed oxidation of methane to methanol by hydrogen peroxide.

The overall reaction can be represented by the following equation:

$$CH_4 + CO + O_2 \rightarrow CH_3OH + CO_2 \qquad \Delta H^{o}_{25^{o}C} = -447 \text{ kJ/mol} \qquad (2.45)$$

With the subsequent ester formation represented by:

$$CH_3OH + CF_3COOH \rightleftharpoons CF_3COOCH_3 + H_2O \qquad (2.46)$$

The presence of both the copper(II) ions and the chloride ions of the cocatalyst was necessary for the reaction. An alternative way of adding both the chloride ions and metallic palladium was by starting with the compound K_2PdCl_4. On contact with carbon monoxide, this compound was reduced to elemental palladium with the simultaneous release of chloride ions.

During the course of the reaction, the copper(II) chloride was observed to have been reduced to copper(I) chloride by the carbon monoxide. Thus a white precipitate was seen, with the initially blue solution having turned colourless by the end of the reaction.

The synergy of palladium and copper is well established in commercial Wacker oxidation chemistry *e.g.* ethylene oxidation to acetaldehyde and also in novel research for methane carboxylations (*e.g.* Kurioka *et al.*, 1995) to afford acetic acid. Park *et al.* (2000)[a] attributed similar Wacker-characteristics to this system after carrying out extensive studies using X-ray diffraction (XRD) and X-ray absorption fine structure (XAFS) techniques. They concluded that the metallic palladium is oxidised by copper(II) to form a palladium(II) species stabilised with chloride ions as part of the cyclic Wacker oxidation of carbon monoxide:

$$Pd(bulk) + 2CuCl_2 \rightarrow PdCl_2 + 2CuCl \quad (2.47)$$

$$2CuCl + \frac{1}{2}O_2 + 2HCl \rightarrow 2CuCl_2 + H_2O \quad (2.48)$$

$$PdCl_2 + CO + H_2O \rightarrow Pd(0) + CO_2 + 2HCl \quad (2.49)$$

During this process CO is consumed, with the liberation of CO_2.

The reaction then proceeds according to Steps 1, 2 and 3 in Figure 2.12 as described by the original founders. It was found that the palladium(II) species, generated by the Wacker oxidation of CO, was necessary for the functionalisation of CH_4 to form the methanol-based product (CF_3COOCH_3) using the *in situ* formed hydrogen peroxide. The Pd(0) species was used for the generation of *in situ* H_2O_2, whilst Pd(II) is active for the subsequent methane oxidation. Further evidence supporting the Wacker-based initial mechanism is from comparable product yields being obtained from starting the reaction with homogenous Pd(II). The mechanistic findings of Park and co-workers are shown diagrammatically in Figure 2.13.

Relating to reaction performance the effect of methane partial pressure on the reaction rate was measured and saturation kinetics observed by Lin and co-workers. A first-order dependence on methane was obtained. The dependence of carbon monoxide partial pressure was noted at two different methane pressures. In both cases, a first order relationship was observed. The activation parameters for the overall reaction were obtained under the reaction conditions when the rate was first order in both methane and carbon monoxide. The values obtained where $A = 2 \times 10^4$ s^{-1} and $E_a = 64.1$ kJ/mol. The authors compared their best data set with the rate of formation of acetic acid from methanol in the benchmark 'Monsanto process'. Here the rate is approximately 38 mol/m^3.min at 180 °C. Their system yielded a rate of 6.5 mol/m^3.min at 145 - 150 °C. This value is comparable with the more favourable conditions of increased temperature and substrate concentration (methanol compared with low solubility methane) inherent in the industrial process.

A novel and unprecedented feature of this catalytic system and the rhodium trichloride system (Lin *et al.*, 1996) is an ability to effect C-C cleavage as well as C-H cleavage. The authors observed dominant C_1 products from C_{2+} alkanes *e.g.* methanol from ethane. The ability to achieve both cracking and oxidation of higher hydrocarbons in a "one-pot" system has obvious implications for a natural gas feedstock. The generation of an *in situ*

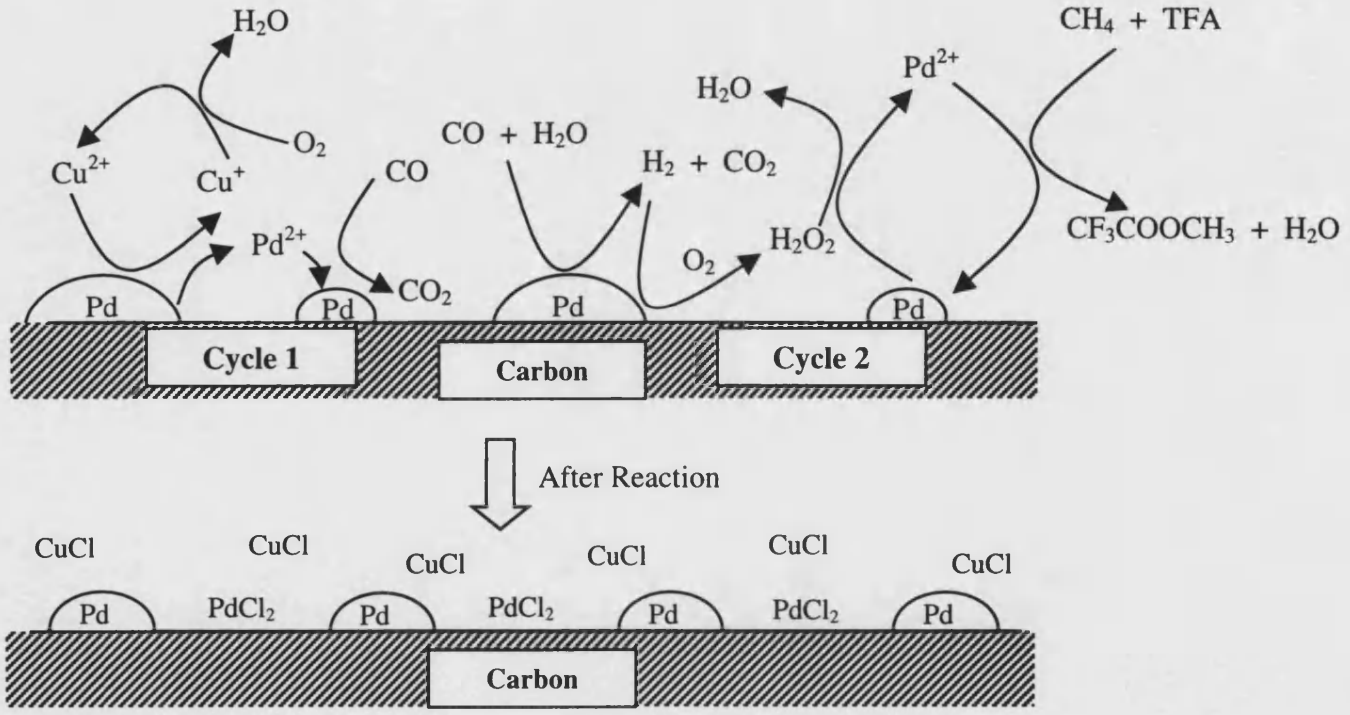

Figure 2.13. The Bimetallic Catalytic System for the Oxidation of Methane (adapted from Park *et al.*, 2000[b])

oxidant for substrate funtionalisation has yielded recent interest (*e.g.* Clerici and Ingallina, 1998). A problem with the direct use of molecular oxygen is the incompatibility of many potential catalysts and that associated with any monooxygen donor *e.g.* peroxide, arises from the cost of its shipping and market supply constraints. Therefore generating a monooxygen species from oxygen and a reducing agent goes some way in circumventing these obstacles. Significant research into propylene expoxidation to propylene oxide with titanium-based catalysis has incorporated the *in situ* generation of hydrogen peroxide from oxygen and hydrogen (both inexpensive and readily available feedstocks) (*e.g.* Mantegazza *et al.*, 1999; Laufer and Hoelderich, 2001; Jenzer *et al.*, 2001). Hydrogen peroxide has an environmental advantage as an *in situ* oxidant because its reduced form is simply water.

An interesting aspect of the system of Lin *et al.* (1997) is that there is the requirement of a coreductant, in this case carbon monoxide. No reaction is evident in its absence. Thus, there is a remarkable anologue with monooxygenases. In nature it is the dioxygenases which utilise the (di)oxygen molecule most efficiently, but for the "difficult" alkane oxidations the prescence of monooxygenases is necessary to catalyse these reactions *e.g.* methane monooxygenase. With Nature's system, one of the two oxygen atoms of molecular oxygen is reduced to water in a highly thermodynamically favourable reaction and the free energy gained thereby is employed to generate a high-energy oxygen species, such as a metal-oxo complex, from the second oxygen atom (Sen, 1998).

$$O_2 + 2H^+ + 2e^- \rightarrow H_2O + [O] \qquad (2.50)$$

or

$$O_2 + H_2 \rightarrow H_2O + [O] \qquad (2.51)$$

With the palladium-based system, the coreductant carbon monoxide generates hydrogen in the water gas shift reaction.

$$CO + H_2O \rightarrow CO_2 + H_2 \qquad ((2.1))$$

Another example of an alkane oxidation system with a natural analogue are the Gif systems developed by Barton and co-workers (*e.g.* Barton and Doller, 1992; Barton *et*

al., 1996) which comprise of a metal salt (*e.g.* Fe^{2+}), a peroxidic oxidant or the combination of molecular oxygen and a reductant (*e.g.* metallic Fe or Zn), pyridine and acetic acid. Unfortunately, the systems are not active for methane and the products are often ketones with no alcohol-based intermediates.

In conclusion of this bimetallic catalytic system, although at present the yields and conversions are not industrially viable, the heterogeneous system coupled with the ability to handle a natural gas feedstock for methanol production makes this process one of the forerunners in novel liquid phase methanol production chemistry.

2.5.1 Alternative Liquid Phase Oxidation Systems

The previous section dealt with the low temperature methane oxidation in the liquid phase and encompassed the majority of research in this field. A number of systems exist which are classed outside the bounds of the main process characteristics of the systems described earlier. Two examples of these are briefly summarised, together with an insight into biological methane conversion leading onto biomimetric studies.

1) Direct partial oxidation of methane to methanol in supercritical water

The work carried out by Lee and Foster (1996) exemplifies this process. The impetus for this system was two-fold. Firstly, as mentioned earlier, the exothermicity ($\Delta H^{o}_{25^{\circ}C}$ = - 126.4 kJ/mol) of the overall partial oxidation reaction (equation 2.6) provides the incentive to carry out the reaction in a fluid medium such as supercritical water which would facilitate the removal of heat, thus enabling the reactor to operate at a high level of conversion and selectivity. Secondly, since methane, oxygen and methanol are miscible with supercritical water, the oxidation reaction can proceed in a single phase without the complications of diffusion controlled kinetics.

Experiments were carried out in an isothermal laminar reactor at 400 - 450 °C and 25 MPa. Methane was mainly oxidised to carbon monoxide, carbon dioxide, methanol and hydrogen. The highest selectivity to methanol obtained was approximately 35 % with methane conversions of 1 - 3 % at 400 - 410 °C. Thus the results are not as favourable as the conventional gas and liquid phase partial oxidations. Similar supercritical studies had also been carried out by Savage *et al.* (1994).

2) The photochemical conversion of methane to methanol

Noceti *et al.* (1997) (see also Taylor and Noceti, 2000), demonstrated this process using three main reactants, light, water and methane, all of which are abundant and inexpensive. In the absence of a photocatalyst, ultraviolet light was required. The proposed reaction scheme is as follows:

$$H_2O \xrightarrow[\lambda \geq 185\ nm]{U.V\ Light} H_2 + \frac{1}{2}O_2 \qquad (2.52)$$

$$H_2O \xrightarrow[\lambda \geq 185\ nm]{U.V\ Light} \frac{1}{2}H_2 + OH\cdot \qquad (2.53)$$

$$CH_4 + OH\cdot \longrightarrow CH_3\cdot + H_2O \qquad (2.54)$$

$$CH_3\cdot + H_2O \longrightarrow CH_3OH + \frac{1}{2}H_2 \qquad (2.55)$$

The use of a doped semiconductor photocatalyst *e.g.* lanthanum on tungsten oxide, together with an electron transfer reagent, methyl viologen dichloride hydrate, resulted in methane conversions of ~ 4 % to the main products methanol and hydrogen and some acetic acid. The reactions were carried out in a commercially supplied quartz photochemical reaction vessel at less than 100 °C and atmospheric pressure. Addition of hydrogen peroxide augmented the reaction, consistent with the mechanism proposing hydroxyl radicals as the intermediate.

3) Biological methane conversion

Enzymatic hydroxylation of alkane C-H bonds is well known. A group of enzmes called methane monooxygenases (MMO) are found in a variety of methanotrophic bacteria. They can catalyse methane hydroxylation according to the following equation:

$$CH_4 + O_2 + NAD(P)H + H^+ \xrightarrow{MMO} CH_3OH + NAD(P) + H_2O \qquad (2.56)$$

The precise mechanism is still an uncertainty but it appears to involve free-radicals, similar to that associated with cytochrome P-450 which is the catalyst for higher alkanes. However, the observed high selectivities and the fact that methane behaves up to 1000 times more reactive than methanol, seems to contradict a radical-based mechanism.

In view of this fact, one questions the possibility of exploiting this intricate chemistry for a practical methane conversion process. The direct use of intact cells or cell extracts to produce methanol has been investigated, but both present severe difficulties. Firstly, other enzymes present in the intact cell can catalyse the overoxidation of methanol (Corder *et al.*, 1988). Secondly, the reaction rate is very slow. Furthermore, the use of either intact cells or cell extracts will at best only produce low methanol concentrations that would require an expensive bio-separation step (*e.g.* Mehta *et al.*, 1991).

One methology, based on the natural enzymes, is to design a synthetic catalyst that uses the same principles. This class of catalyst design is termed "biomimetric". Unfortunately, the exact mechanism for MMO is poorly understood. If it is related with the detailed enzyme structure and conditionally restricted substrate access, it is unlikely that someone will be able to come anywhere close to reproducing that in the foreseeable future. Incorporation of catalysts into organised media that might lead to enzyme-like behaviour, such as zeolites and membranes is another avenue of research that has been pursued, although the results so far offer only very limited grounds for encouragement (Labinger, 1995).

2.6 CONCLUSIONS

The requirement for natural gas conversion is two-fold. Although there is a plentiful supply of this resource, the geographical location does not often permit an economic distribution to a market in the form of LNG or by using gas transport. Also, from an environmental viewpoint, the flaring and/or venting of natural gas at production sites contributes a pollutant in the form of greenhouse gases as well as wasting a non-renewable energy source.

With regard to the selection of a natural gas conversion process, one that converts the feedstock to a readily transportable liquid fuel in a single step is the most desirable. The direct partial oxidation of methane to methanol is one such example and thus merits further investigation.

From consulting the available literature, it is evident that the direct partial oxidation of methane to methanol is a daunting challenge. Research into the gas phase oxidation has been ongoing since the turn of this century. Similarly, liquid phase oxidations span over three decades. The chemical inertness of methane, mainly attributed to its unusually high homolytic bond energy, plagues both reaction systems. The gas phase overcomes this initial hurdle by employing relatively high temperatures, but is subsequently confronted by an unselective radical-based mechanism. The organometallic chemistry, dominant in the liquid phase systems, facilitates a non-radical pathway, often electrophilic, and coupled with chemical protection methods *e.g.* esterification, can result with very high selectivities.

The plethora of research into the gas phase has only concluded with industrially non-viable conversions and selectivities. Less documented investigations have been carried out in the liquid phase, allowing more scope for future research. Furthermore, many of the liquid phase processes have only been studied at a small scale in that often only a few millilitres of liquid phase were used, and generally only under batch operation. Clearly, to assess the feasibility of such a process, tests employing larger reactant volumes are needed in order to obtain meaningful data for industrial validity. This work is selected for further research as the focus of this PhD study. On screening the liquid phase catalytic systems for effecting methane to methanol conversions, the bimetallic system of Lin *et al.* (1997) is chosen; firstly because of the use of inexpensive molecular oxygen as the stoichiometric oxidant and secondly because of its unprecedented advantage of obtaining methanol-based products from higher alkanes because of C-C cleavage. As the project

impetus is for the discovery of new technology for the conversion of a natural gas feedstock, obtaining methanol from the C_{2+} alkanes in natural gas would be of great benefit as a "one pot" system.

2.7 Project Objectives

- To verify that the bimetallic catalyst system developed by Lin *et al.* (1997) can be used to produce a methanol-based product from methane via *in situ* produced H_2O_2, using an increased liquid phase volume in a batch reactor.
- To explore any observed phenomena resulting from the "scale-up" in the batch reactor.
- The application of the system for semi-continuous operation, using a porous tube reactor with liquid sampling facilities.
- Investigation of possible improvements to the catalytic system, via novel changes to the original system, using a batch reactor.
- By assessing the data obtained from both the batch and semi-continuous operation, it is intended to ascertain industrial feasibility and to identify any bottlenecks that may need further investigation.

CHAPTER 3 - The Design and Use of Experimental Apparatus

This chapter details the reactors used for the methane oxidation experiments, focussing on both reactor design and operating procedures. For the investigations under batch operation, a commercially available autoclave was used, whilst for semi-continuous studies a porous tube reactor, previously built "in-house", was employed after several modifications had been made. Relating to the latter reactor, details of a palladium catalytic tube preparation are given together with an insight into some of the characterisation techniques. A simple analysis for the model behaviour of both the gas and liquid phases is provided for use in product yield calculations and liquid vapour pressure estimation. Finally, information regarding the chemicals used and the reaction sample preparation and analysis procedure is given.

3.1 The Batch Reactor

The reactor was supplied by Baskerville (Reactors & Autoclaves) Ltd. (Manchester, UK) and rated at a working pressure of 30 MPa at a temperature of 300 °C. The main body was constructed from 316 stainless steel. The internal stirrer and thermocouple pocket was coated with PTFE (Teflon). A 175 ml detachable reaction vessel equipped with a Pyrex glass-liner was used for the experiments. The stirrer, thermocouple pocket and glass-liner together accrued a volume of 45 ml, providing an effective reactor volume of 130 ml. Agitation of the reaction mixture was effected by a direct drive variable speed stirrer with paddle attachment. For heating the reaction mixture, a removable electric heater which "houses" the main reaction vessel was used. Regulation of stirring, heater control and temperature readout was via a separate control panel. For temperature measurement, a type K (chromel/alumel) thermocouple was employed. Indication of the reactor pressure was given by a Bourdon gauge (0 - 100 bar) supplied by S.M Gauge Co. (Bristol, UK) with a factory calibrated accuracy of ±0.5 bar. A proportional pressure relief valve (Swagelok, UK) set at 15 MPa was also fitted to the reactor.

Figure 3.1 shows a diagram of the reactor with actual photographs depicted in Plate 3.1 and Plate 3.2 below:

Plate 3.1. Batch Reactor and Control Panel

Plate 3.2. Reaction Vessel and Stirrer

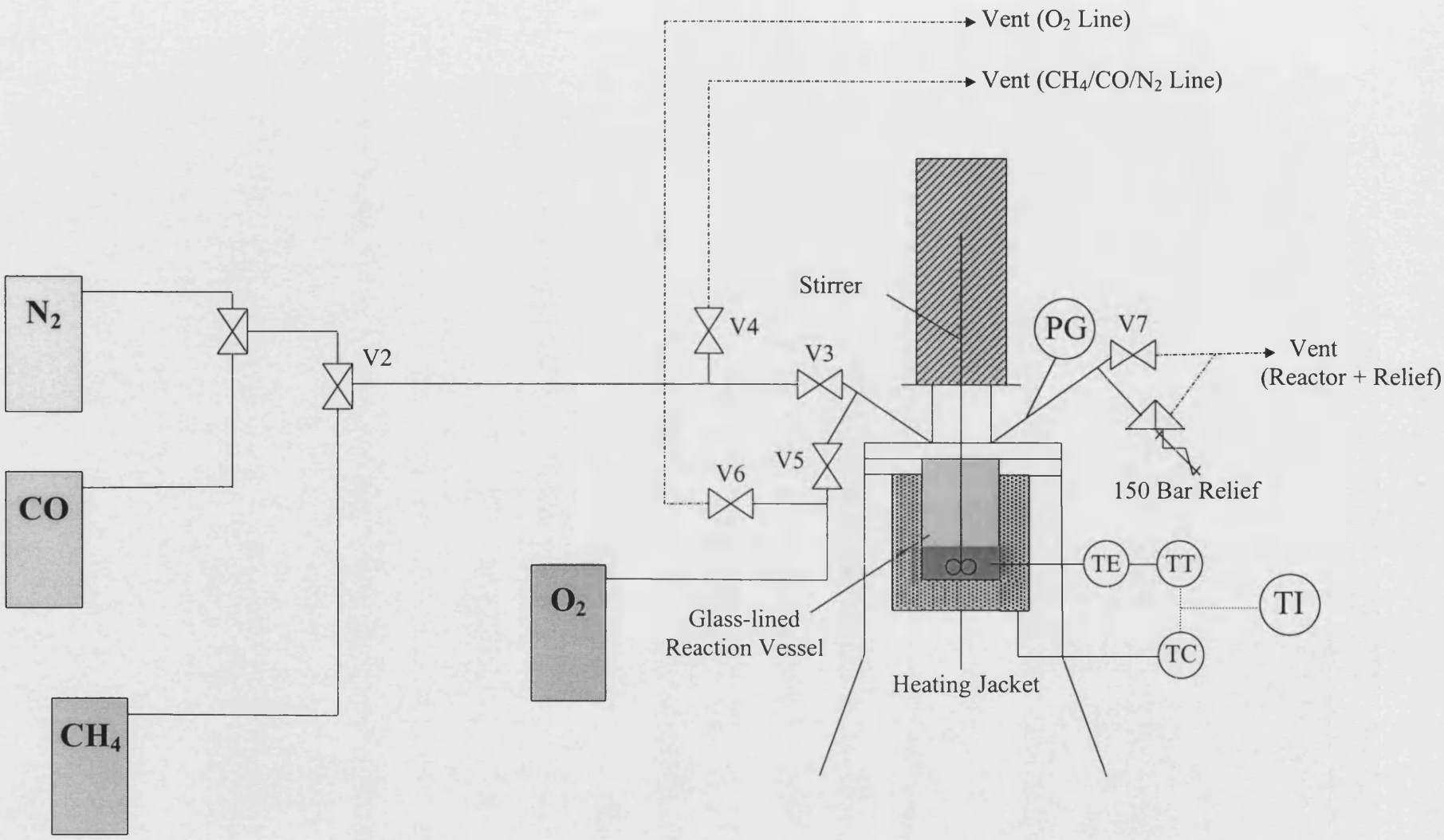

Figure 3.1. Batch Reactor Set-up

The feed lines to the reactor where constructed "in house" to accommodate the safe, high pressure delivery of the three main reactant gases. The pipe-work was constructed from 1/4" (6.3 mm) o.d annealed copper tubing (Swagelok, UK). The gas cylinders were all equipped with high pressure regulators (BOC gases, Bristol, UK).

3.1.1 Batch Reactant Mixture

The experimental base-case inventory followed the standard composition as used by Lin *et al.* (1997), albeit scaled-up from the original 4 ml to a 50 ml liquid phase. A value of 50 ml of liquid was chosen because for the 175 ml reaction vessel, this was the recommended amount to accommodate efficient mixing. All the chemicals used are detailed in Section 3.7.
The quantities of the substances used for the base-case mixture were as follows:

Liquid Phase

i) Water = 12.5 ml
ii) Copper(II) chloride = 0.1345 g (20 mol/m^3)
iii) 5 wt.% palladium on activated carbon = 0.0125 g (catalyst loading = 0.25 kg/m^3)
iv) Trifluoroacetic acid = 37.5 ml

Gas Phase

i) Methane = 62 bar(a) (6.2 MPa) at reaction temperature
ii) Carbon monoxide = 14 bar(a) (1.4 MPa)
iii) Oxygen = 7 bar(a) (0.7 MPa)

Variation from the above reactant mixture was generally referenced to this base-case. Changes and/or additions of chemicals to this recipe are detailed, where relevant, in the experimental results section (Chapter 4) *e.g.* the replacement of TFA with an acetic acid solvent (Section 4.3.4) or the use of a novel two-phase system (Section 4.3.5). The pre-reaction liquid mixture was blue in colour with a suspension of black Pd/C particles, settling under gravity in the absence of any agitation. Plate 3.3 shows an example of this reactant mixture contained in the glass-liner.

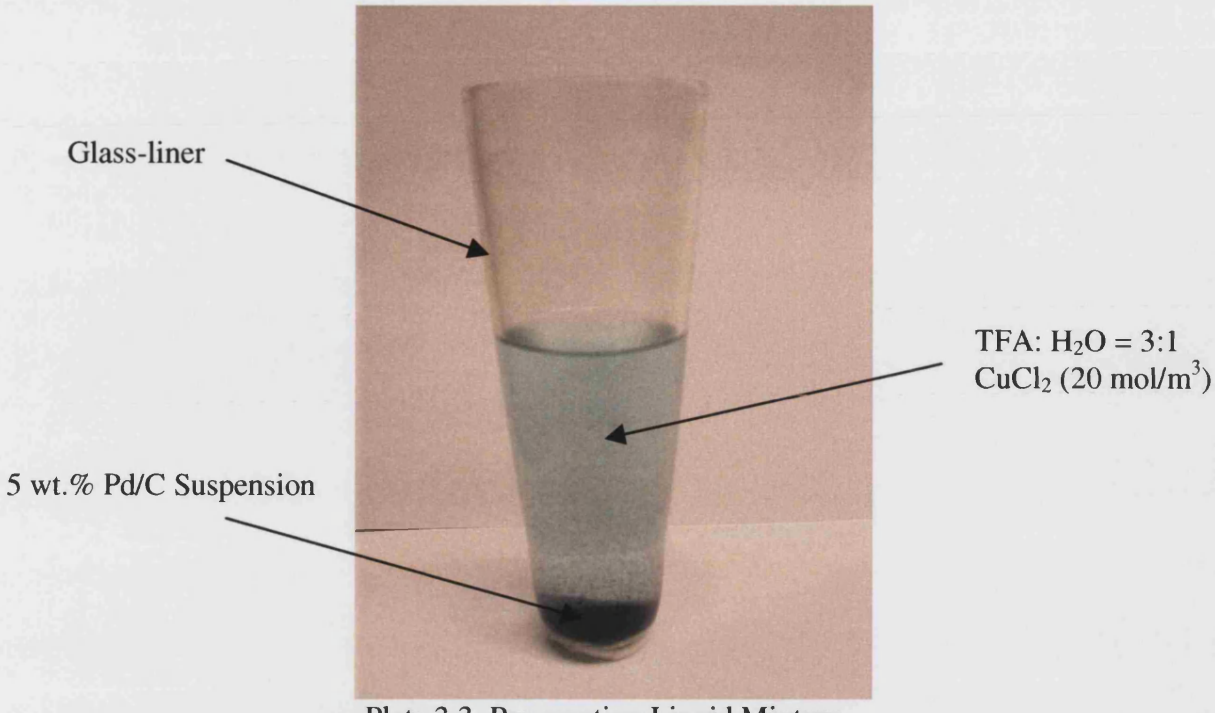

Plate 3.3. Pre-reaction Liquid Mixture

The commercial Pd/C catalyst (Sigma-Aldrich Chemical Co. Ltd., Gillingham, UK) was analysed using a scanning electron microscope, model JEOL 6310 (JOEL UK Ltd., Welwyn Garden City, UK). The result is shown in Plate 3.4 below:

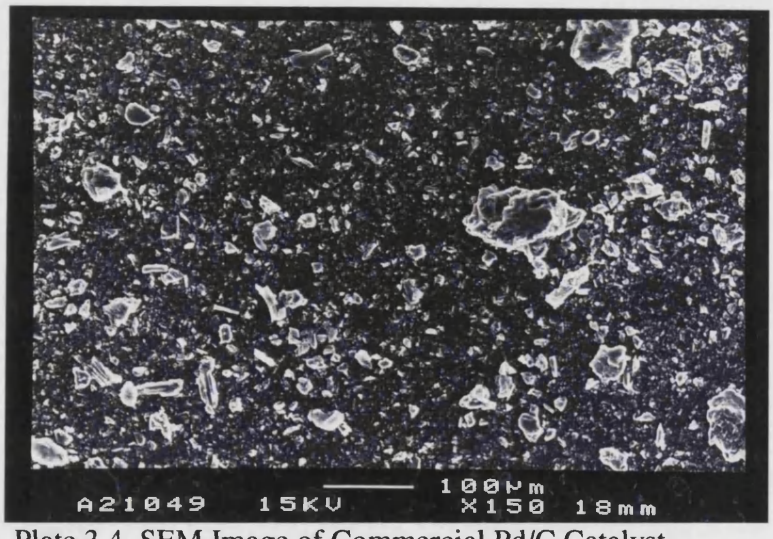

Plate 3.4. SEM Image of Commercial Pd/C Catalyst

According to Pham-Huu *et al.* (2000) the range of grain size for this catalyst was *ca.* 50 - 100 µm. A BET surface area of 889 m^2/g was also obtained for the catalyst powder using nitrogen adsorption experiments (ASAP 2010, Micrometrics Instrument Co., USA).

3.1.2 Batch Operating Procedure

(Refer to Figure 3.1)

GENERAL START-UP

1) Close all valves (V1 - V7) and gas cylinder regulators (for no flow conditions)
2) Add the liquid reactant mixture to the glass-liner
3) Place the glass-liner containing the liquid mixture inside the stainless steel reaction vessel and seal the vessel to the main autoclave body using the designated nuts
4) Adjust V1 and V2 to allow nitrogen flow and open V7
5) Carefully adjust the nitrogen gas regulator, to purge the reaction vessel, then close the nitrogen cylinder
6) Select methane gas flow with V2 and adjust the regulator to purge the reaction vessel
7) Close V7 and V3
8) Using the methane regulator set the delivery line pressure at approximately equal to the final partial pressure of methane required in the reaction vessel. A slightly lower pressure than the final value is advised to allow for the increase that will occur during the preheat
9) Open V3 to pressurise the reaction vessel with methane, then close V3
10) Close the methane cylinder
11) Slowly open V4 to vent the delivery line to atmosphere
12) Switch on the stirrer and set to the desired speed using the control panel
13) Attach the heating unit to the reaction vessel and heat the reaction mixture to the desired stable temperature (~2 h)
14) If necessary adjust the methane pressure in the reactor (+ liquid vapour pressure) to the selected value using V7 as the initial charge pressure will change due to the pre-heating
15) Adjust V1 and V2 to allow carbon monoxide flow
16) Adjust the carbon monoxide gas cylinder regulator to purge the delivery line
17) Close V4
18) Set the delivery line pressure at least equal to the final pressure of carbon monoxide + methane (+ liquid vapour pressure) required in the reaction vessel
19) Open V3 to pressurise the reaction vessel with carbon monoxide, then close V3
20) Close the carbon monoxide cylinder

21) Slowly open V4 to vent the delivery line to atmosphere

22) Using the oxygen regulator set the oxygen delivery line pressure at least equal to the final pressure of oxygen + carbon monoxide + methane (+ liquid vapour pressure) required in the reaction vessel

23) Open V5 to pressurise the reaction vessel with oxygen, then close V5

24) Start timing the batch run

25) Close the oxygen cylinder

26) Slowly open V6 to vent the oxygen delivery line to atmosphere

27) Wait for batch time to elapse with periodic monitoring of pressure and temperature

If only two gases are required *e.g.* methane and oxygen or carbon monoxide and oxygen, the procedure is similar to that detailed, but omitting one of the "gas-charging" stages

SHUT-DOWN

1) Switch off electric heater and remove it to allow reaction vessel to cool to approximately ambient temperature. The use of iced-water facilitates this process

2) Slowly open V7 to vent reactor gaseous contents to atmosphere

3) Switch off the stirrer at the control panel

4) Remove reaction vessel from main autoclave body

5) Remove glass-liner for analysis of liquid contents

6) Thoroughly wash reactor internals ready for next run

EMERGENCY SHUT-DOWN

1) Switch off power supply to control box

2) Close all gas cylinders if open

3) Slowly open V7 to vent reactor if appropriate

3.2 The Semi-continuous Porous Tube Reactor

3.2.1 Ameliorations of a Porous Reactor for Methane Oxidation Experiments

A lack in the number of reported methane to methanol liquid phase oxidation studies at a larger scale has been concluded from consulting the available literature (Chapter 2). The previously described batch reactor represents a scale-up of liquid phase volume by a factor of 12.5 from the original work of Lin *et al.* (1997). The porous tube reactor not only allows for the use of an even greater liquid phase volume (300 ml), but also for the continuous supply of the gaseous reactants. Furthermore, the facility of liquid sampling enables the time course of reaction to be ascertained. This was not possible, or at least not detailed, in the original work and indeed in many other works, probably because the low liquid volumes employed did not accommodate liquid sampling.

The porous tube itself has two main functions. Firstly it facilitates effective gas-liquid contacting producing small bubbles of high interfacial area (McLurgh, 1997), and secondly, it lends itself as a catalyst support.

3.2.2 Modifications

The original design of this rig was constructed as part of a PhD study for the wet air oxidation (WAO) of phenol and other wastewater pollutants (McLurgh, 1997). The WAO experiments were carried out at lower pressure (*ca.* 4 MPa) than the methane oxidation experiments in the present work. Also, only one gas (air or oxygen) was used and so the original rig configuration did not accommodate the safe, continuous delivery of up to 3 gases required for this current investigation. Therefore, several modifications had to be made before the apparatus was suitable for the methane oxidation experiments. These are summarised in Table 3.1.

Table 3.1. Details of Modifications to the Porous Tube Reactor

Practical Difference Between Original WAO Work and the Requirement for the Present Methane Oxidation Experiments	**Modifications Necessary to Existing Porous Tube Reactor**
Number of feed gases	i) Addition of 3 new gas feed-lines ii) Addition of a static mixing vessel iii) Inclusion of a feed vent-line iv) Incorporation of electronic mass flow controllers for the 3 gases
Operating pressure	Replacement to a higher pressure Bourdon Gauge (0 - 100 bar)
Nature of liquid mixture	i) Due to the volatility of TFA, incorporation of a spiral condenser with an ice-pack/freezeable gel-pack cooling medium ii) Replacement of 316 stainless steel thermocouples with either Hastelloy or Inconel 600
General safety	i) Addition of extra vent-line on gas exit ii) New Start-up/Shut-down procedure

3.2.3 Rig Description

The porous tube reactor was operated in semi-continuous mode. Here, the gaseous reactants enter the main reactor where they contact the liquid phase via the porous tube, disengage in a hold-up vessel and subsequently vent through the exit-line. The liquid phase is continuously re-circulated. This is achieved passively via the "air-lift" effect eliminating the need for an expensive high pressure liquid pump. Because the effective density of the gas/liquid (two-phase) mixture is less than that of the liquid alone, a natural circulation is induced. A simplified schematic of the reactor, highlighting the basic principles, is shown in Figure 3.2.

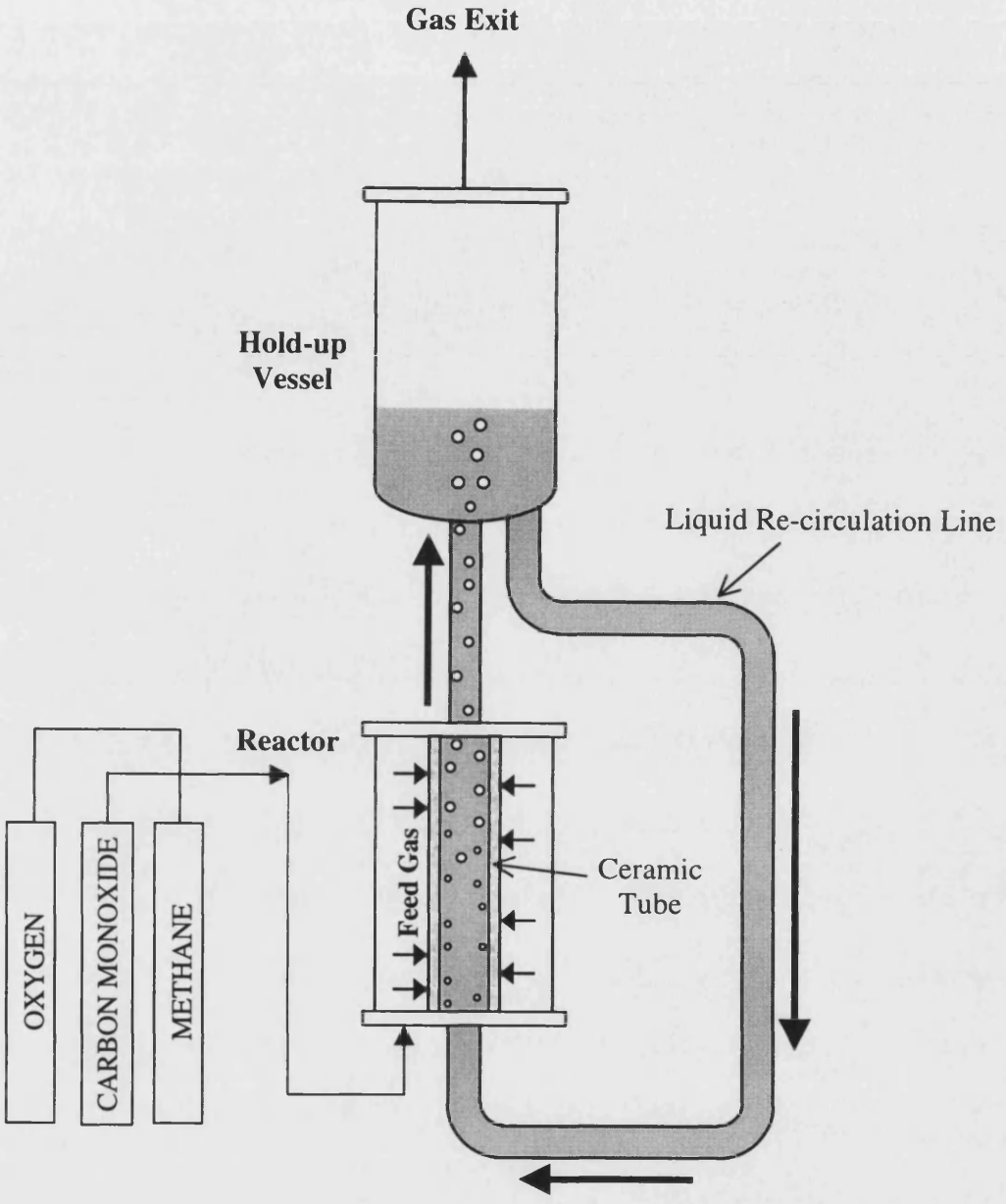

Figure 3.2. Porous Tube Reactor Simplified Schematic

The main body of the experimental apparatus was constructed from 316 stainless steel. It comprised of two main pressure vessels that were fabricated by Baskerville (Reactors & Autoclaves) Ltd. (Manchester, UK). One of these vessels, the main reactor (400 ml), "housed" the porous tube, whilst the other acted as a liquid hold-up vessel (600 ml) facilitating the efficient disengagement of the gases from the liquid. These vessels were rated at a maximum working pressure of 20 MPa at 300 °C, depending on the nature of the O-ring seal. Both the vessels were protected from over pressurisation by a nickel

bursting disc rated at 22 MPa. The vessels were connected together via a re-circulation line made from 1/2" (12.7 mm) o.d stainless steel tubing (Swagelok, UK). The porous tube was installed in the main reactor vessel via a double O-ring seal, enabling the relative ease of tube replacement. The O-rings, together with those used for the pressure vessel sealings, were made from the fluoroelastomer material viton, with a maximum operating temperature of 200 °C. They were supplied by James Walker & Co. Ltd. (Cockermouth , UK). Plate 3.5 depicts one of the two reaction vessel flanges with incorporated O-rings, whilst actual instalment of the porous tube is shown in Plate 3.6

The gas feed-lines were constructed from 1/4" (6.3 mm) o.d 316 stainless steel tubing and to facilitate the mixing of the 3 gaseous reactants, a pressure vessel (Swagelok, UK) was installed prior to the main reaction vessel entry. This increased gas hold-up and also due to the rapid expansion from a 1/4" (6.3 mm) line to approximately 1" diameter of the pressure vessel, mixing was encouraged.

Measurement of reactor pressure was via a Bourdon Gauge (0 - 100 bar) supplied pre-calibrated by S.M Gauge Co. (Bristol, UK) with an accuracy of ±0.5 bar. The incurred pressure difference between the gas inlet and the gas exit was measured by an Ashdown Process Control Ltd. differential pressure transmitter with read-out via a Newport Electronics Ltd. indicator, both supplied by Transinstruments (Basingstoke, UK). The device was capable of measuring a differential pressure from 0 - 32 psi (0 to 0.22 MPa) at a line pressure of up to 10 MPa. Inferred from the measurement of differential pressure was an indication of any fouling on the wall of the porous tube, during the course of the reaction run.

The temperature was measured at several key locations in the reactor *e.g.* main reactor outlet, liquid re-circulation line, hold-up vessel liquid. Measurement was carried out by either Hastelloy or Inconel 600 type K thermocouples supplied by T.C. Direct (Uxbridge, UK), and connected to a digital temperature indicator supplied by Digitron Instrumentation Ltd. (Hertford, UK). Accuracy of the thermocouples was ±1 °C. To attain a desired reactor temperature, jacket-style heaters (Elmatic Ltd., Cardiff, UK) were installed around the walls of both the hold-up vessel and the main reactor vessel. Feedback control of the hold-up vessel heater was effected by an RS Components Ltd. (Corby, UK) controller, based on the measurement of the hold-up liquid temperature. A Pye Ether (Pye Ether Ltd., UK) mini controller was used for the main reactor heating jacket, using the reactor wall temperature as a set-point.

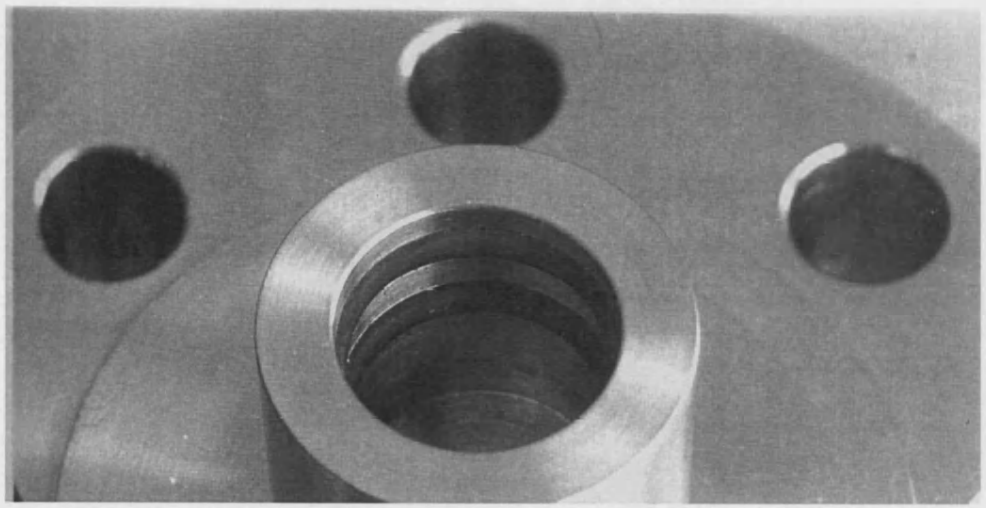

Plate 3.5. Reactor Flange Showing Double O-ring Seal

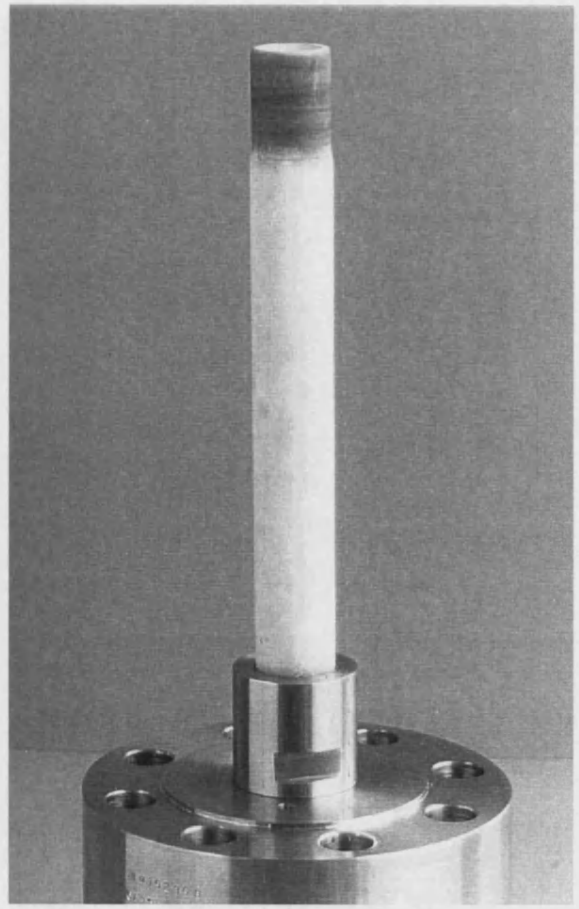

Plate 3.6. Ceramic Tube Installed

Accurate flow measurement was obtained from thermal mass flow controllers (Brooks 5850S) with control and read-out via a Brooks 0154 controller, all supplied by Flotech Solutions Ltd. (Stockport, UK). The mass flow controllers were factory calibrated to provide a flow range of 0 – 2 l/min (0 °C, 0.10 MPa) with an accuracy of ±0.75 %, and installed on the gas feed-lines for methane, carbon monoxide and oxygen. The outlet gas flow was monitored via a 0 – 2 l/min (15 °C, 0.10 MPa) glass rotameter (Fisher Controls Ltd., Croydon, UK) after pressure let-down by manual control of two high pressure needle valves (Swagelok, UK).

To help prevent any stripping of the liquid phase, a concentric tube condenser with mains cooling water was connected to the exit of the hold-up vessel. As a precautionary measure, a "spiralled-tube" condenser, chilled by ice-packs containing freezeable gels, was coupled to the main condenser. For sampling the liquid phase, a high pressure needle valve (Swagelok, UK) was installed, with the sample being cooled by a concentric tube heat exchanger using mains cooling water, prior to discharge. All heat exchangers were fabricated "in-house" using tubes and fittings supplied by Swagelok (UK).

A flow diagram showing the line connections and temperature and pressure indications is shown in Figure 3.3. Plate 3.7 Plate 3.8 and Plate 3.9 are photographs of the apparatus.

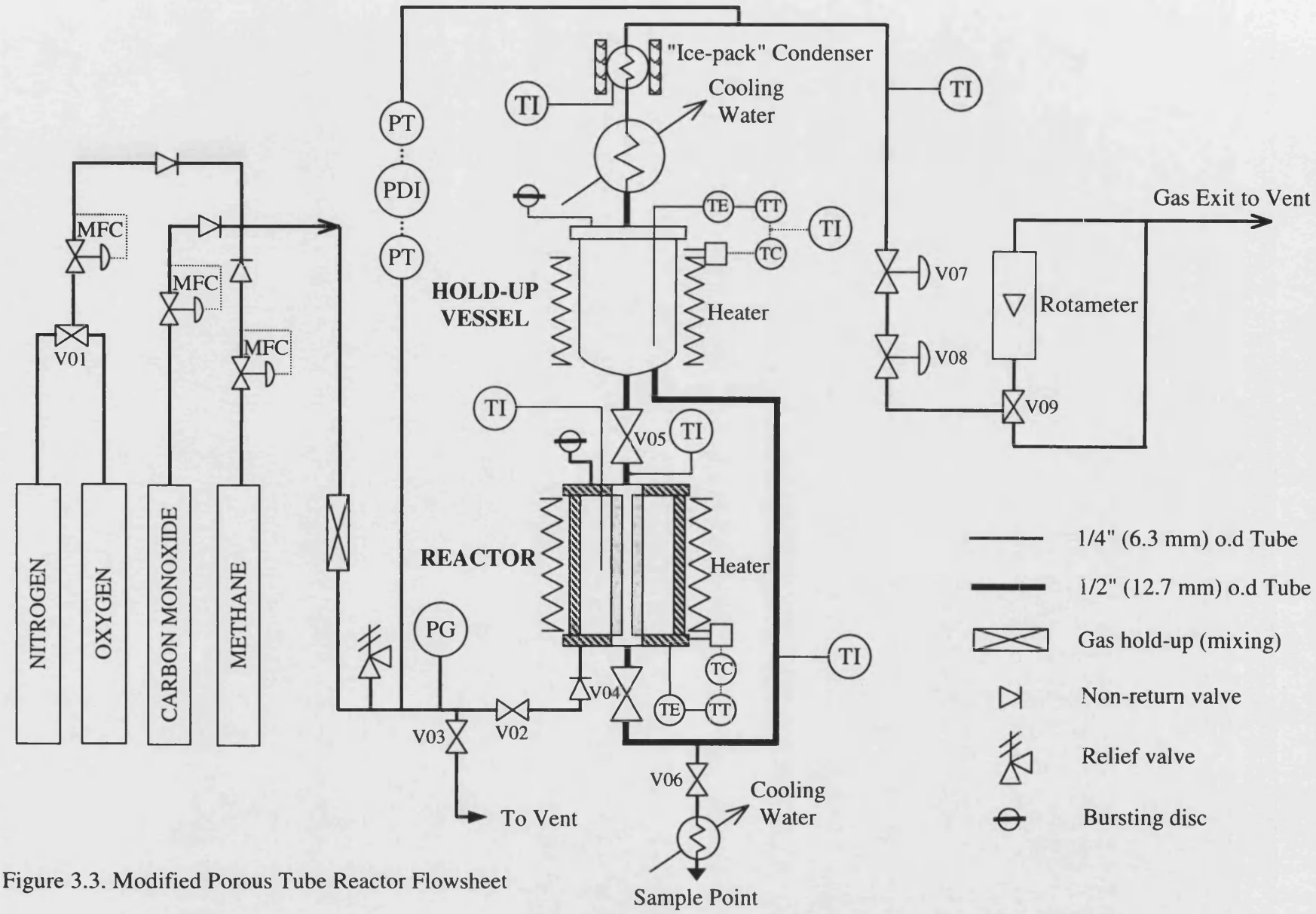

Figure 3.3. Modified Porous Tube Reactor Flowsheet

Plate 3.7. Porous Tube Reactor

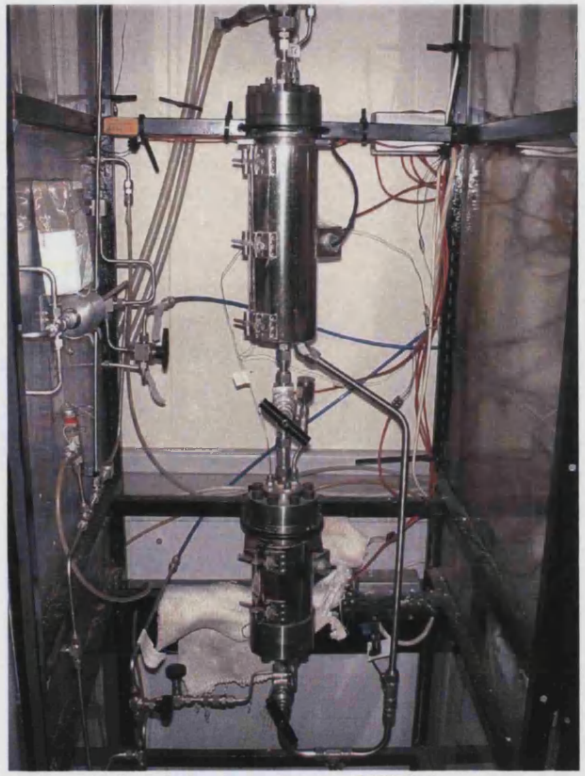

Plate 3.8. Main Reactor and Hold-up Vessel

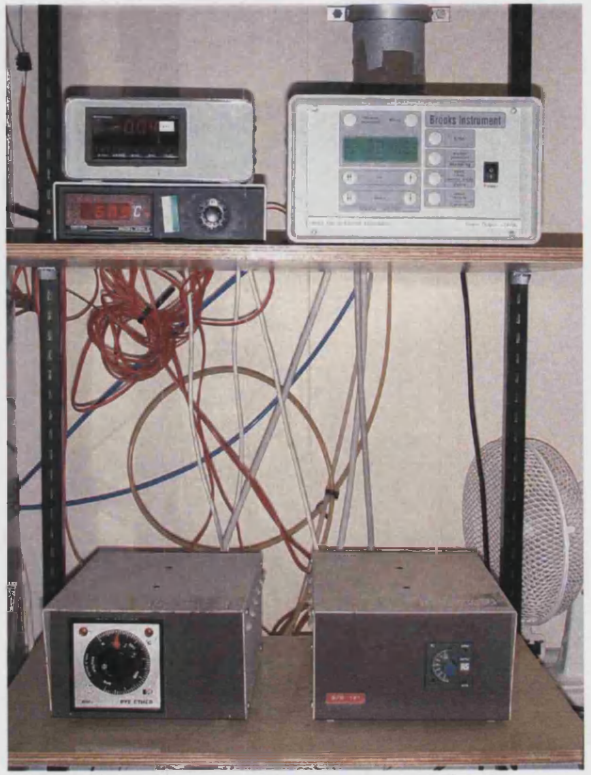

Plate 3.9. Control and Read-out Displays

3.2.4 Porous Tube Characteristics

An alumina-based porous ceramic tube was used as the gas/liquid contacter and also as a catalyst support. Desirable properties of the tube include mechanical strength, chemical resistance and low cost. Two types of ceramic tube were used for the experiments; those used as a catalyst support had the trade name "Alsint porous" whilst those for the blank tube runs were "Sillimantin 65". The tubes were all supplied by Multilab Ltd. (Newcastle, UK). Their selected physical properties are depicted in Table 3.2.

Table 3.2. Ceramic Tube Physical Properties

Property	AlSint Porous	Sillimantin 65
Al_2O_3 content (%)	99.5	78 - 80
Water Absorption (%)	3	5
Density (g/cm^3)	3.30	2.60
Flexural Strength (MPa)	80	45
Thermal Expansion ($\times 10^{-6}$ /grd)	8.6	6.1
Max. Working Temperature (°C)	1700	1400
Thermal Shock Resistance	Good	Very Good
Diameter of Pores approx. (μm)	1.5	1

(Data supplied by MultiLab Ltd.)

The tubes were supplied in 1 m lengths with an outside diameter of 20 mm and wall thickness of 2.5 mm. Before installation into the main reactor, the tubes were machined to the dimensions depicted in Figure 3.4.

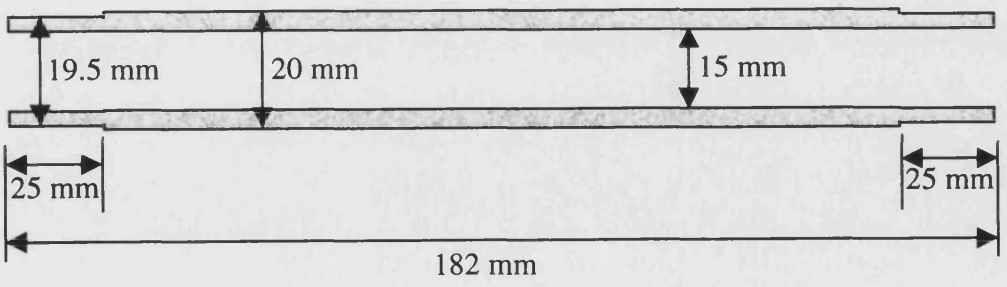

Figure 3.4. Ceramic Tube Dimensions

3.2.4.1 Catalytic Tube Preparation

The coating of metallic palladium on the inner surface of the porous tube, if successful, would have the advantage over a liquid suspension (*i.e.* Pd/C) in the final product separation process. Palladium coated alumina tubes have been used successfully for several other reactions *e.g.* the hydrogenation of α-methylstyrene (AMS) (Cini and Harold, 1991) and the partial hydrogenation of acetylene and 1,3-butadiene (Lambert and Gonzalez, 1999).
In light of the aforementioned successes in using a palladium coated alumina tube, it was decided to attempt the same for the methane oxidation reaction.

Analysis of the surface area of the unmodified "Alsint porous" tube using nitrogen adsorption studies (ASAP 2010, Micrometrics Instrument Co., USA) revealed a BET surface area of only 0.20 m^2/g. One method of increasing this surface area is to apply a thin washcoat of high surface area material to the tube wall. A commonly used washcoat material is γ-alumina (*e.g.* Kim, 2000) which can be formed from the calcination of an alumina precursor *e.g.* AlOOH sol-gel, at moderate temperatures of approximately 500 °C for several hours (Cini *et al.*, 1991). Several methods exist for applying the washcoat, including the simple "dipping" of the tube in a γ-alumina slurry. Over the last decade, the "sol-gel" technique has been widely used (Kim, 2000). In the use of palladium for both membrane based hydrogen gas separation (Konno *et al.*, 1988; Lee *et al.*, 1994) and catalytic membrane application (Lambert and Gonzalez, 1999; Shu *et al.*, 1997), the sol-gel method was the preferred technique of washcoat deposition. According to Lambert and Gonzalez (1999), a greater control of the final catalyst properties can be obtained from the sol-gel method compared to other techniques. Stated advantages include well-defined pore size distributions, superior homogeneity, and improved thermal stability of the supported metal.
The formation of a stable alumina sol from alkoxides for coating purposes is detailed in an authoritative article by Yoldas (1975). For the current study, a commercially available alumina sol (DISPAL 23N4-20) was used as supplied by CONDEA Vista Co. (Texas, USA). The decision not to prepare the sol "in-house" was augmented by the recommendation of this commercial sol by Cini *et al.* (1991). They stated that the Vista sols possessed the desirable properties of both a high alumina content (thicker coatings)

and a low viscosity (stable coatings). The key properties of the sol are shown in Table 3.3.

Table 3.3. Selected Properties of DISPAL 23N4-20

Chemical / Physical Property		DISPAL 23N4-20
Al_2O_3 Content	(%)	20
NO_3^- Content	(%)	0.380
pH of Dispersion		4
Density	(g/ml)	1.2
Dispersed Particle Size	(nm)	100
Particle Charge	(C/g)	+ 30
Viscosity	(mPa.s)	< 50
Surface Area (BET)	(m^2/g)	185
(after thermal treatment at 550 °C, 3h)		(Verified "in-house" to be 194)

(Data supplied by CONDEA Vista Co.)

The procedure for washcoating the tube inside wall was adapted from the method used in Cini *et al.* (1991). The method involved repeated cycles of pouring the alumina sol through the tube, drying at room temperature for 12 h, followed by calcination at 550 °C for 3 h. At the end of each cycle, the tube mass was noted. The cycle was stopped after a negligible gain in mass was observed compared to the previous cycle or film instability (peeling) was evident. A final calcination at 550 °C for 12 h was then carried out to help stabilise the γ-alumina film.

Having added the washcoat, the palladium active phase was administered. Commonly, this is achieved via contacting the tube with a solution of a palladium precursor (*e.g.* ammonium tetrachloropalladium(II)), calcination at moderate temperates *ca.* 400 °C followed by reduction of the palladium compound to metallic palladium using hydrogen. The method used for the current work was adapted from a patent granted for Retallick (1988) because of the relative ease of application. This technique replaces hydrogen as the reducing agent, with a hydrazine solution. The selected palladium precursor was ammonium hexachloropalladate(IV) with the reduction chemistry as in equation (3.1).

$$(NH_4)_2PdCl_6 + NH_2NH_2 \xrightarrow{Al_2O_3} Pd + N_2 + 2NH_3 + 6HCl \qquad (3.1)$$

A 1 wt.% solution of the palladium salt was carefully poured into the tube and allowed to stand for several minutes. Having drained away the excess solution, the now red-brown coloured tube was then dried at room temperature for 2 h. It was then submersed in a

hydrazine solution (1 wt.%) for several minutes, observing the colour change of reduction from red-brown to grey-black, associated with the formation of metallic palladium. The tube was then thoroughly washed in water to remove excess reagents, dried at 80 °C and weighed. The whole cycle was then repeated, if necessary, to obtain a palladium mass representing approximately 5 wt.% of the washcoat. To finish, the tube was washed thoroughly in hot water to remove any "loose" palladium particles with the final dry mass noted.

The weighings for the washcoating and the active phase (Pd) deposition for a typical tube are shown in Table 3.4 and Table 3.5 respectively, with a photograph of the inside of a coated tube depicted in Plate 3.10.

Table 3.4. Tube Mass Gain during Washcoating Process

Washcoat Cycle	**Total Tube + Washcoat Mass (g)**	**Total Washcoat Mass (g)**	**Washcoat Equivalent of Uncoated Tube Mass (wt.%)**
0 (uncoated tube)	81.70	-	-
1	81.96	0.26	0.32
2	82.01	0.31	0.38
3	82.11	0.41	0.50
Final Calcination	82.10	0.40	0.49

Table 3.5. Tube Mass Gain during Active Phase Deposition

Active Phase Cycle	**Total Tube + Washcoat + Pd Mass (g)**	**Total Pd Mass (g)**	**Pd Equivalent of Washcoat Mass (wt.%)**
0 (washcoated tube)	82.10	-	-
1	82.11	0.01	2.5
2	82.13	0.03	7.5
Final Washing	82.12	0.02	5.0

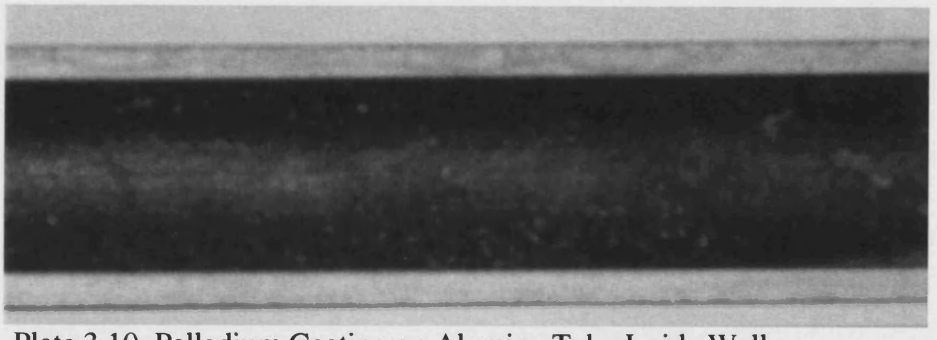

Plate 3.10. Palladium Coating on Alumina Tube Inside Wall

At this stage in the thesis, it is pointed out that the palladium coated tube was not successful for the experimental runs using the semi-continuous reactor. As will be discussed in Chapter 4, leaching of the palladium was observed during early experimentation with the reactor. Although problems were apparent with tube coating instabilities (*e.g.* peeling), which were also experienced by Cini *et al.* (1991), this was not considered the main cause leading to the removal of palladium from the tube wall. It was thought that the nature of the catalytic cycle for methane oxidation, as proposed by Park *et al.* (2000)[a] (*i.e.* $Pd \rightarrow Pd^{2+}$), was the reason behind the palladium leaching, accelerated by a strongly acidic liquid phase. Indeed, on submersion of a palladium coated tube in a TFA-based solvent mixture containing copper(II) chloride, evidence of palladium going into solution was apparent (not shown here), even at room temperature.
Therefore, due to the incompatibility for the studied reaction chemistry, further optimisation and actual characterisation of the coated tubes were not performed.

3.2.5 Liquid Natural Re-circulation and Gas-Liquid Mass Transfer

As mentioned in Section 3.2.3, the liquid phase in the porous tube reactor is re-circulated, allowing renewed contact with the continuously flowing gaseous reactants. The circulation process is due to the passive "air-lift" effect, which relies on the difference in density between the gas/liquid mixture and that of the liquid alone. The actual rate of liquid circulation is mainly dependent on gas flowrate and reactor geometry. Increasing gas flowrate induces a greater effective density difference driving force and thus increases the liquid flow (Choi and Lee, 1993). The occurrence of a high pressure drop due to restricted flow *e.g.* the narrowing in the pipe diameter or the closure of a valve, would result in a lower liquid circulation rate (Kaštánek *et al.*, 1993). The degree of liquid circulation itself can influence reactor performance in terms of the gas hold-up and the mass transfer with respect to the extent of the liquid film boundary development on the porous tube wall and the gaseous bubble size. An increase in circulation rate would have a positive effect on the mass transfer, reducing both the bubble size (suppression of bubble coalescence) and liquid boundary layers, although gas hold-up is decreased.
The mixing properties, phase hold-up, interfacial area and mass and heat transfer coefficients are dependent on the flow regime in the reactor (Shah *et al.*, 1982). The main

flow regimes are homogeneous bubble flow, churn turbulent, and slug flow. Unfortunately, the conditions leading to the occurrence of each regime is not well established (Kaštánek *et al.*, 1993).

With respect to the gas-liquid mass transfer, for sparingly soluble gases (*e.g.* O_2, CH_4) it is the resistance in the liquid film surrounding the bubble that is important (McLurgh, 1997). This mass transfer is conveniently represented by a lumped-parameter designated the volumetric mass transfer coefficient, k_La, whereby:

$$k_La = \frac{6\varepsilon_G}{d_{bm}} k_L \tag{3.2}$$

Here, k_L represents the liquid-side mass transfer coefficient, ε_G the gas hold-up and d_{bm} the mean bubble diameter.

This quantity depends primarily on the size of bubbles in the system. For bubbles of large diameter, several correlations exist for the prediction of k_La in bubble-columns (see *e.g.* Shah *et al.*, 1982). However for small bubbles (< 2 mm), scarcely any, if none, quantitative relations are available. Furthermore, an exact correlation of k_La in air-lift reactors represents a complex and uncertain task (Kaštánek *et al.*, 1993). Because both a predicted small bubble size (see Appendix VII) and an air-lift type reactor is employed in this study, the mass transfer coefficient would need to be evaluated experimentally. The difficulty with the porous tube reactor used in this study is that it is not a formal air-lift reactor design so data existing for these type of reactors cannot be explicitly used. For more information, the reader is encouraged to read the PhD thesis of McLurgh (1997) which describes the original design of the porous tube reactor.

Relating back to the re-circulation rate in the porous tube reactor, this value is not directly measured due to the requirement of an expensive high pressure liquid flowmeter. However, an indication of the flowrate would represent a useful measure. Furthermore, this information would help in the selection of both the amount of liquid phase to use and the total gas flowrate; both these are important values because of the relatively expensive cost of the laboratory liquid and gaseous reactants for the methane oxidation experiments.

Therefore, as part of this study, a simple experiment was performed to obtain a ballpark liquid circulation rate. The porous tube reactor was modified in that a glass-rotameter, calibrated for water (Fisher Controls Ltd., Croydon, UK), was installed in the re-circulation line. The use of this mandated the use of near atmospheric pressure operation and a non-corrosive liquid phase. For this reason, water was used with the gas phase being nitrogen with a reactor pressure of *ca.* 0.1 MPa. The nitrogen flowrate was measured via the rotameter on the gas exit-line of the reactor. The results are shown in Figure 3.5 for two different liquid volumes (350 ml being the amount used in the work of McLurgh, 1997). It can clearly be seen that for nitrogen flowrates above *ca.* 1 l/min (15 °C, 0.1 MPa), the water circulation rate was effectively the same for the two liquid volumes used. Furthermore, increasing the gas flowrate above this value had only a limited effect on the water circulation rate. This trend was also observed by Choi and Lee (1993) in their external-loop air-lift reactor, with an explanation that at higher liquid circulation rates, bubbles are carried over into the downcomer (equivalent to the re-circulation line) with the gas hold-up increasing in this part of the reactor. However, the increase in gas hold-up in the riser section (equivalent to the path from reactor to hold-up vessel) due to increased gas flowrate is suppressed by the water circulation and the net effect is a reduced density difference between the fluids in the riser and the downcomer, hence limiting the achievable liquid circulation rate. As a guide to the extent of this phenomena occurring in the porous tube reactor, an estimate of the bubble rise velocity, together with the superficial liquid velocity, is detailed in Appendix VII.

Although the reactants and experimental conditions used in the actual experiments are considerably different from those employed here, these results are viewed as indicative towards the selection of process parameters. The use of an increased reactor pressure would serve to decrease the circulation rate by increasing the gaseous density significantly more than that of the liquid (incompressible), thus reducing the "buoyancy effect". However, it would have a positive effect on bubble mass transfer due to creating smaller bubble sizes.

Therefore, in conclusion to this data and in light of economic considerations for the reactants used (not detailed here), a total gas flow rate (methane, oxygen and carbon monoxide) of 2 l/min (0 °C, 0.1 MPa) and a liquid volume of 300 ml were chosen for the main experiments. The higher liquid volume was selected on the basis that less error would be induced by the volume decrease due to sampling.

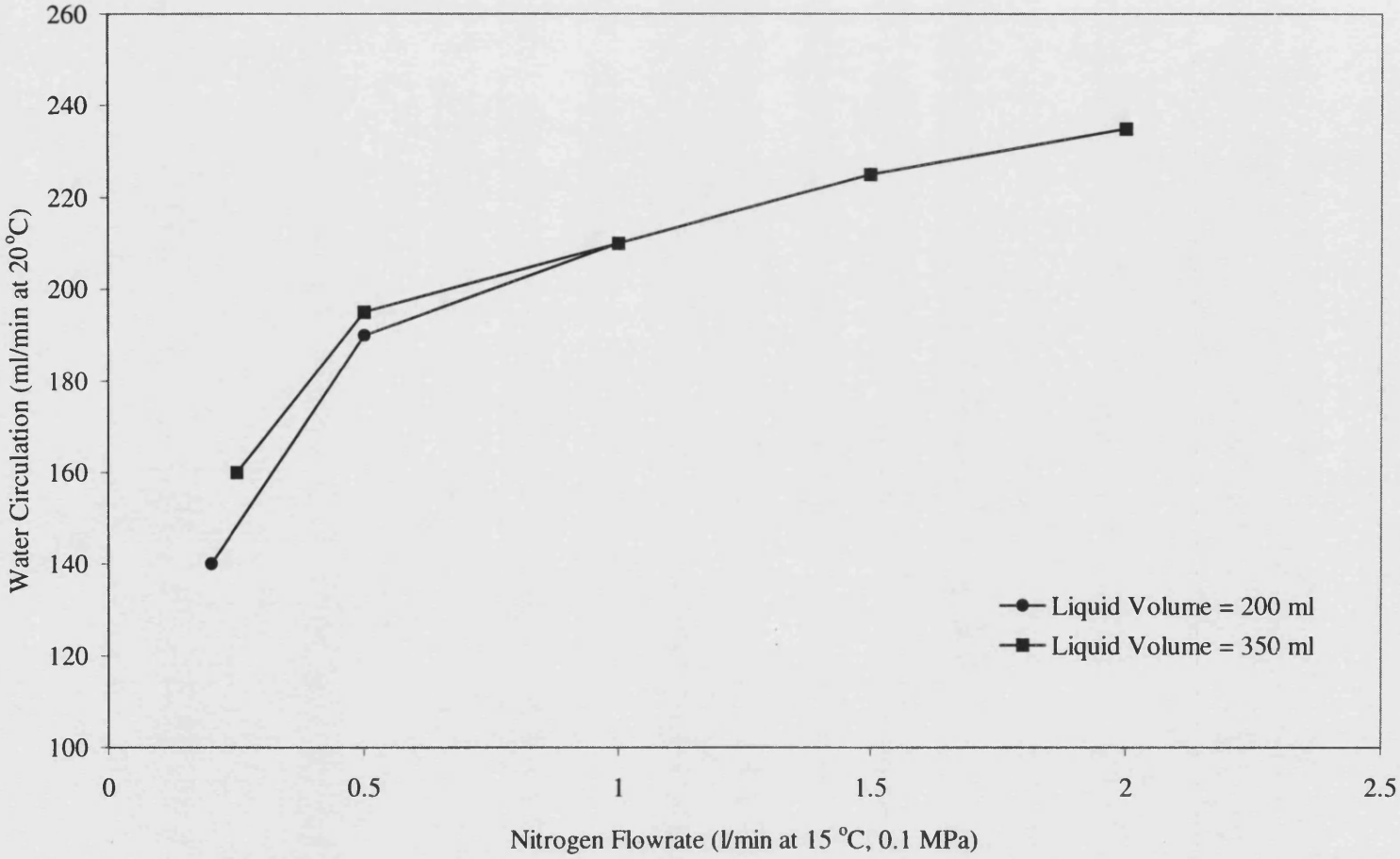

Figure 3.5. Liquid Circulation Rates in the Porous Tube Reactor

3.2.6 Reactant Mixture

The reaction mixture used for experiments in the porous tube reactor consisted of a similar solvent phase of TFA and water in a ratio of 3:1, but with different catalyst concentrations compared with the base-case used in the batch reactions. This was mainly because of the necessary use of homogeneous palladium due to the incompatibility of the palladium coated porous tube. Furthermore, the absence of a glass-liner in the porous tube reactor suggested possible problems with chloride corrosion of the 316 stainless steel. According to Oettinger and Fontana (1976) 316 stainless steel shows excellent resistance to chloride concentrations of up to 350 mg/l (9.86 mol/m^3). Therefore, the concentration of copper(II) chloride used reflected this value.

Partial pressures in the gaseous phase were generally similar to those in the batch, although they were continuously supplied to the reactor. The gas flowrates were calculated according to their "batch equivalent" partial pressures with a total flowrate of 2 l/min (0 °C, 0.1MPa).

The individual chemical amounts/concentration ranges used for the semi-continuous work are shown below:

Liquid Phase

i) Water = 75 ml

ii) Copper(II) chloride = 0.199 - 0.796 g (5 - 20 mol/m^3)

iii) Palladium(II) acetate = 0.0079 - 0.0443 g (0.12 - 0.66 mol/m^3)

iv) Trifluoroacetic acid = 225 ml

Gas Phase

i) Methane = 28 - 62 bar(a) (2.8 - 6.2 MPa) at reaction temperature
Flow = 1.14 - 1.80 l/min (0 °C, 0.1 MPa)

ii) Carbon monoxide = 7 - 14 bar(a) (0.7 - 1.4 MPa)
Flow = 0.17 - 0.34 (0 °C, 0.1 MPa)

iii) Oxygen = 7 bar(a) (0.7 MPa)
Flow = 0.17 (0 °C, 0.1 MPa)

Where relevant, further details regarding the reactants used are give in their corresponding results section (Chapter 4).

3.2.7 Operating Procedure

(Refer to Figure 3.3)

GENERAL START-UP

1) Close all valves (V01 - V09) and gas cylinder regulators
2) Switch on all instrumentation and allow *ca.* 40 minutes for the thermal mass flow controllers (MFC) to stabilise. Reset differential pressure meter
3) Open the top flange of the hold-up vessel and carefully pour liquid reactant mixture into the reactor
4) Close reactor flange
5) Switch on water to the main condenser
6) Remove "ice-pack" condenser from freezer and attach to rig
7) Open V02
8) Open methane cylinder regulator and adjust mass flow controller (at control box unit) to allow 1 l/min (at 0°C, 0.1 MPa) methane flow
9) When the reactor pressure reaches approximately 10 bar, open V04 and V05 to allow the porous tube to fill with liquid
10) Adjust V07 and V08 to obtain a flow as indicated by the rotameter (make sure that V09 is adjusted to allow flow through the rotameter). Keep the reactor pressure at a value of at least 10 bar of methane
11) Switch on the two electric heaters and adjust desired set-point liquid temperature on control box
12) Wait for the temperature to stabilise at the desired value, monitoring all the thermocouple readings, in particular those for the hold-up liquid and the re-circulation line liquid
13) When desired temperature is reached close V08 to stop flow through the reactor
14) Add the required experimental partial pressure of methane, making sure the cylinder regulator is set to a value greater than the desired total pressure in the reactor (use the mass flow controller fully open with manual override function)
15) Close the methane mass flow controller at the control box unit
16) Open V03 to vent the methane feed-line, then close V03
17) Open carbon monoxide cylinder regulator and allow full flow through the mass flow controller to desired pressure of methane + carbon monoxide

18) Close the carbon monoxide mass flow controller and open V03 to vent the feed-line then close V03
19) Open the oxygen cylinder regulator and allow full flow through mass flow controller until the desired total pressure of methane + carbon monoxide + oxygen is reached
20) Close the oxygen mass flow controller and open V03 to vent the feed-line then close V03
21) Close V02
22) Fill the feed-line with the required gas composition at the reactor total pressure value and set the individual gas flowrates for the mass flow controllers and allow some purging of the feed line via V03
23) Open V02 and V08 to allow a gas flow through the reactor to the exit vent
24) Start timing the reaction run
25) Adjust V08 and/or V09 to keep reactor pressure constant
26) Periodically monitor the temperatures at the various points in the reactor. Good agreement of the hold-up liquid temperature and that in the re-circulation line indicates liquid flow. Also watch the differential pressure value

LIQUID SAMPLING

1) About 2 minutes before sampling, allow cooling water to flow through the sample-point condenser
2) Carefully open V06 and allow 2 ml of sample to flow in a suitable container. This volume represents the dead-volume in the sampling line. Close V06
3) Open V06 and carefully allow 4 ml of liquid to flow into a sample jar. Close V06 and place sample jar in ice
4) Switch off water to the sample-point condenser
5) Repeat steps 1) - 4) for further samples

SHUT-DOWN

1) Switch off electric heaters and close all mass flow controllers and gas cylinders
2) Allow the reactor gases to slowly vent through the rotameter as it cools down
3) When liquid temperature approaches a close to ambient value, switch on sample condenser and allow liquid contents to empty into a designated vessel. Take a final sample from this mixture

4) Open the top flange of the reactor vessel and thoroughly wash the reactor with water. Use of a nitrogen flow prevents liquid percolating through the porous tube
5) Switch off all instrumentation

EMERGENCY SHUT-DOWN

1) Switch off all electrics
2) Close all gas cylinders
3) If reactor is pressurised adjust V09 to by-pass rotameter and fully open V07 and V08. Open V03 to vent the feed-line
4) Empty liquid contents only when reactor has cooled

3.3 Calculated Measures of Reactor Performance

To ascertain the reaction performance, key parameters need to be established allowing some form of comparison with other similar reaction systems. Common measures are the substrate conversion, product yield and product selectivity *(e.g.* Wolf, 1992; Periana, 1997). Relating to catalyst performance, the turnover number (TON) has also been widely used (*e.g.* Yamanaka *et al.*, 1995; Kitamura *et al.*, 1998; Süss-Fink *et al.*, 1998) and on a rate basis, the space-time yield (STY). The use of the STY has been encouraged by several authors (*e.g.* Hall *et al.*, 1995; Parmaliana *et al.*, 1993) as a more reliable index for comparing reaction performance for non-identical reaction systems.
The equations used to calculate these parameters, as applied to a methanol-based product and a methane substrate, are shown below:

$$CH_4 \text{ Conversion } (\%) = \left(\frac{n_{CH_4(i)} - n_{CH_4(f)}}{n_{CH_4(i)}} \right) \times 100 \qquad (3.3)$$

$$CH_3OH \text{ Selectivity } (\%) = \left(\frac{n_{CH_3OH}}{n_{CH_4(i)} - n_{CH_4(f)}} \right) \times 100 \qquad (3.4)$$

$$CH_3OH \text{ Yield } (\%) = \left(\frac{n_{CH_3OH}}{n_{CH_4(i)}} \right) \times 100 \qquad (3.5)$$

$$CH_3OH \text{ TON } = \frac{n_{CH_3OH}}{n_{Catalyst}} \qquad (3.6)$$

$$CH_3OH \text{ STY } = \frac{w_{CH_3OH}}{w_{Catalyst} \times t} \qquad (3.7)$$

For this current study, because on-line gaseous analysis was not available, it was not possible to accurately compute the methane conversion or the overall product selectivity. Therefore, the parameters used in this work are the product yield (equation (3.5)), the TON (equation (3.6)) and the STY (equation (3.7)). The values for methanol (ester)

yields obtained in the original work of Lin (Lin *et al.*, 1997) and in other studies (Park *et al.*, 2000[a]) using the same catalytic system have been very low and so the emphasis of this current work was on trying to increase the methanol-based yield in the liquid phase as that was the desired product.

3.4 Ideality of Gas and Liquid Phase Behaviour

In order to calculate the product yield under batch conditions, the amount of methane used is required. In the absence of any formal measuring device, this value must be obtained theoretically. Furthermore, the use of gas partial pressures inherently assumes ideality and the validity of this at the employed reaction pressures and temperatures needs to be established. At the operating temperatures used, knowledge of the liquid vapour pressure is also required. These two aspects form the content of this section.

3.4.1 Gas Phase

Theoretical predictions of the pressure-volume-temperature (*PVT*) behaviour of a gas can be obtained by either the application of the ideal gas equation of state or another more rigorous expression or correlation to model real-gas attributes.

In this work, typical reaction conditions were pressures approaching 8.5 MPa and temperatures up to 120 °C. A deviation from ideal gas behaviour is most prominent at high pressures and low temperatures. One measure of ideality is the compressibility factor, Z, which for a high pressure of 10 MPa and a low temperature of 27 °C, explicit values can be found in Perry and Green (1984). Table 3.6 shows these values:

Table 3.6. Values of the Compressibility Factor for the Reactant Gases

Component	Z (10 MPa, 27 °C)
Methane	0.8556
Carbon monoxide	0.9935
Oxygen	0.9542
Nitrogen	1.0052

For ideal gas behaviour, $Z = 1$, and it is seen that under the disclosed *P-T* conditions the greatest deviation occurs for methane. In the experiments carried out, methane was the

main constituent (up to ~ 75 vol.%). A simple test to gather some data for calculation of the *PVT* behaviour of methane was carried out in the batch reactor. An amount of methane was introduced to the reactor at a fixed temperature and pressure (this defines the number of moles of methane, which is assumed a constant). The reactor was then slowly heated, with the recording of the pressure change with temperature.

The results were compared with the ideal gas equation of state as well as two real gas expressions, the Redlich/Kwong cubic equation and the Benedict/Webb/Rubin equation. This latter equation is widely used in the natural gas and petroleum industries for light hydrocarbons (Smith and Van Ness, 1987). The equations are shown below:

Ideal Gas

$$P = \frac{RT}{V_m} \tag{3.8}$$

Redlich/Kwong (RK)

$$P = \frac{RT}{V_m - b} - \frac{a}{T^{1/2} V_m (V_m + b)} \tag{3.9}$$

Where:
$$a = \frac{0.42748 R^2 T_c^{2.5}}{P_c} \tag{3.10}$$

$$b = \frac{0.08664 RT_c}{P_c} \tag{3.11}$$

Benedict/Webb/Rubin (BWR)

$$P = \frac{RT}{V_m} + \frac{B_0 RT - A_0 - C_0/T^2}{V_m^2} + \frac{bRT - a}{V_m^3} + \frac{a\acute{a}}{V_m^6} + \frac{c}{V^3 T^2}\left(1 + \frac{\tilde{a}}{V^2}\right) exp\frac{-\tilde{a}}{V_m^2} \tag{3.12}$$

The relevant methane constants for use in equation (3.9) and equation (3.12) are shown in Table 3.7. The values are taken from Felder and Rousseau (1986) with the constants

for the BWR equation applicable for P in atm., T in K, V_m in litres/mol and R in litres.atm/mol.K.

Table 3.7. Various Methane Gas Constants for Use in Equation (3.9) and Equation (3.12)

Constant		Value
P_c	(Pa)	46×10^5
	(atm)	45.4
T_c	(K)	190.7
R	(J/mol.K)	8.314
	(litres.atm/mol.K)	0.08206
A_0		1.85500
B_0		0.042600
C_0	($\times 10^{-6}$)	0.0257
a	(BWR only)	0.049400
b	(BWR only)	0.00338004
c	($\times 10^{-6}$)	0.002545
α	($\times 10^3$)	0.124359
γ	($\times 10^2$)	0.6000

Using the initial temperature and pressure experimental readings, the molar volume, V_m, was calculated using the three equations (3.8, 3.9 and 3.12). For equation (3.9) and equation (3.12) this required a trial-and-error solution. Having obtained V_m, this value is assumed constant and values of pressure are calculated using temperature values over the experimental range. The results are displayed in Figure 3.6. It can be seen that the ideal gas equation is the most successful in predicting the experimental methane pressures, with an error margin of within 2 %. Although the limited data does not warrant definite conclusions, the result suggests that the use of the ideal assumption is appropriate for the conditions used in the methane oxidation experiments.

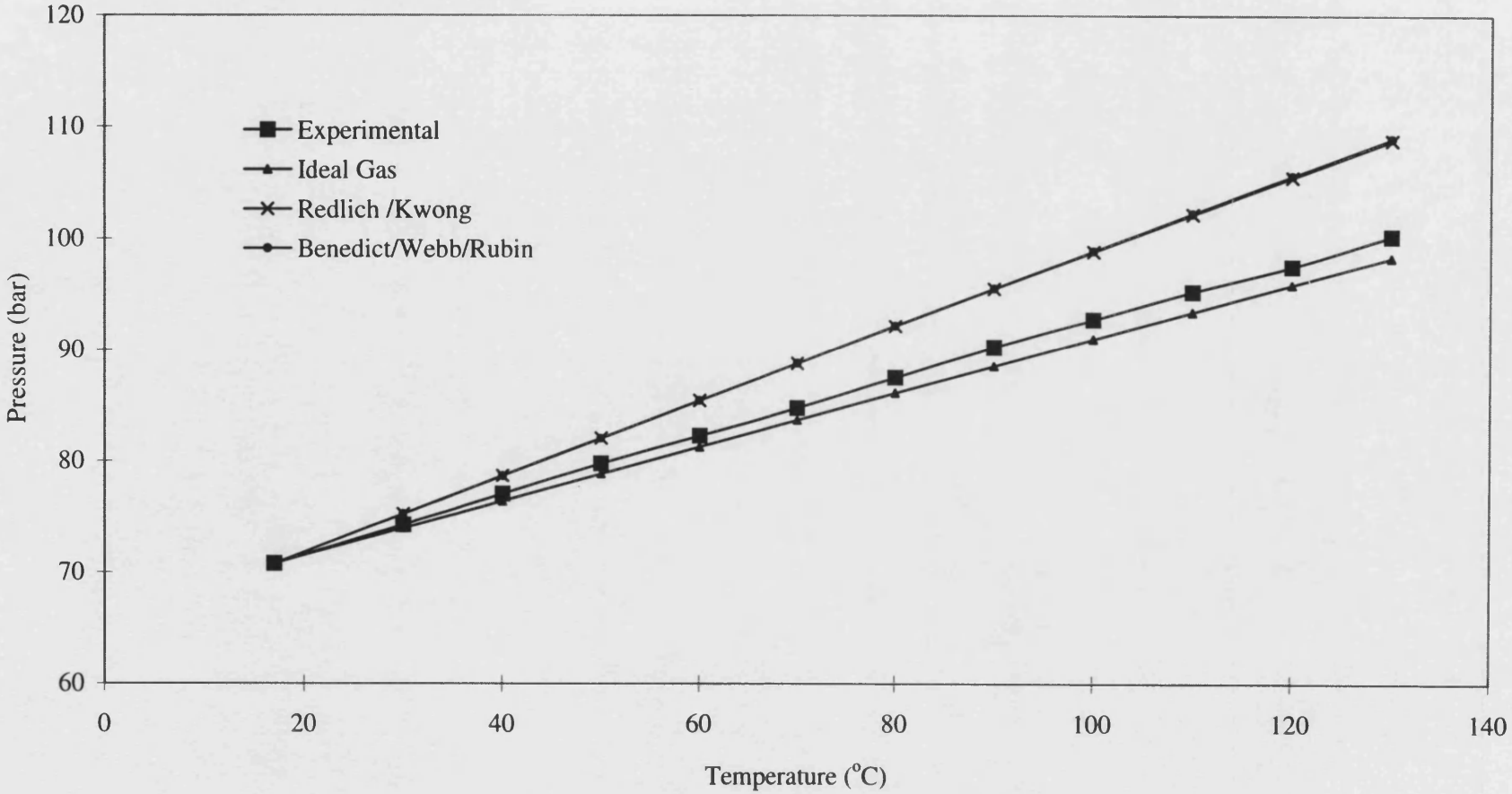

Figure 3.6. Prediction of Experimental Methane *P-T* Behaviour

3.4.2 Liquid Phase

Knowledge of the liquid phase vapour pressure is useful because it contributes to the total pressure inside the reactor. Although the temperatures used in the experiments are relatively low (≤ 120 °C), the TFA is a volatile component so its presence in the gas phase needs to be established.

The vapour pressure of the individual liquid components, TFA and water, are well represented by the Wagner equation and the Antoine equation respectively. These equations are shown below with their relevant "constant" values inserted:

Wagner (for TFA) (taken from Engineering Sciences Data Unit Item No. 80029, 1980)

$$\ln(P^o) = 8.08887 + \frac{T}{491.3}\left[-9.02105q + 2.23341\,q^{\frac{3}{2}} - 4.16182q^3 - 4.16182q^6\right] \qquad (3.13)$$

$$\text{Where:} \qquad q = 1 - \frac{T}{491.3} \quad , P^o \text{ is in kPa, } T \text{ in Kelvin;} \quad 185 < T < 490 \text{ K} \qquad (3.14)$$

Antoine (for water) (taken from Sinnott, 1993)

$$\ln(P^o) = 18.3036 - \frac{3816.44}{T - 46.13} \qquad (3.15)$$

Where P^o is in mmHg and T in K; $284 < T < 441$ K

Figure 3.7 shows a graphical plot of vapour pressure-temperature for TFA and water using values calculated from their respective equations.

Because a 3:1 (v/v) TFA:water liquid mixture was used in the experiments, the resultant pressure is significantly different from that of the individual vapour pressures. The simplest way to model the behaviour of the liquid mixture is to assume ideality. However, due to the electronegative CF_3 group in TFA, this assumption is not wholly valid. Indeed, observation of heat of mixing on contact of the two liquids was apparent

during the preparation of the reactant mixture. What it does give though, is an indication as to the order of magnitude of vapour induced pressure that one can expect.
For a binary mixture, Raoult's law is given for a general component "*A*" as:

$$P_A = P_A^o x_A \tag{3.16}$$

For a 3:1 (v/v) mixture of TFA and water, the total equilibrium pressure, at a particular temperature, can be obtained by the direct addition of the individual partial pressures for each component that are given by equation (3.16), thus:

$$P_{Total} = P_{TFA}^o x_{TFA} + P_{water}^o x_{water} \tag{3.17}$$

The results of applying this expression to a 3:1 (v/v) TFA:water liquid mixture are shown in Figure 3.8. From this estimation, values of the pressure for the experimental temperatures used (85 - 120 °C) are in the range of *ca.* 1 - 3 bar (0.1 - 0.3 MPa). Considering that the total reactor pressure was around 85 bar (8.5 MPa), the contribution of the liquid vapour pressure was not deemed to be significant, especially as the majority of the experiments were carried out at 85 °C. Furthermore, the addition of the homogeneous copper chloride to the liquid phase would serve to suppress the observed vapour pressure. Therefore, more rigorous modelling *e.g.* application of the NRTL (Non-Random-Two-Liquid) or the UNIFAC group contribution models was not thought necessary, especially with only limited thermodynamic data currently available for TFA. However, for higher temperature applications, accurate vapour pressure prediction would be a necessary requirement.

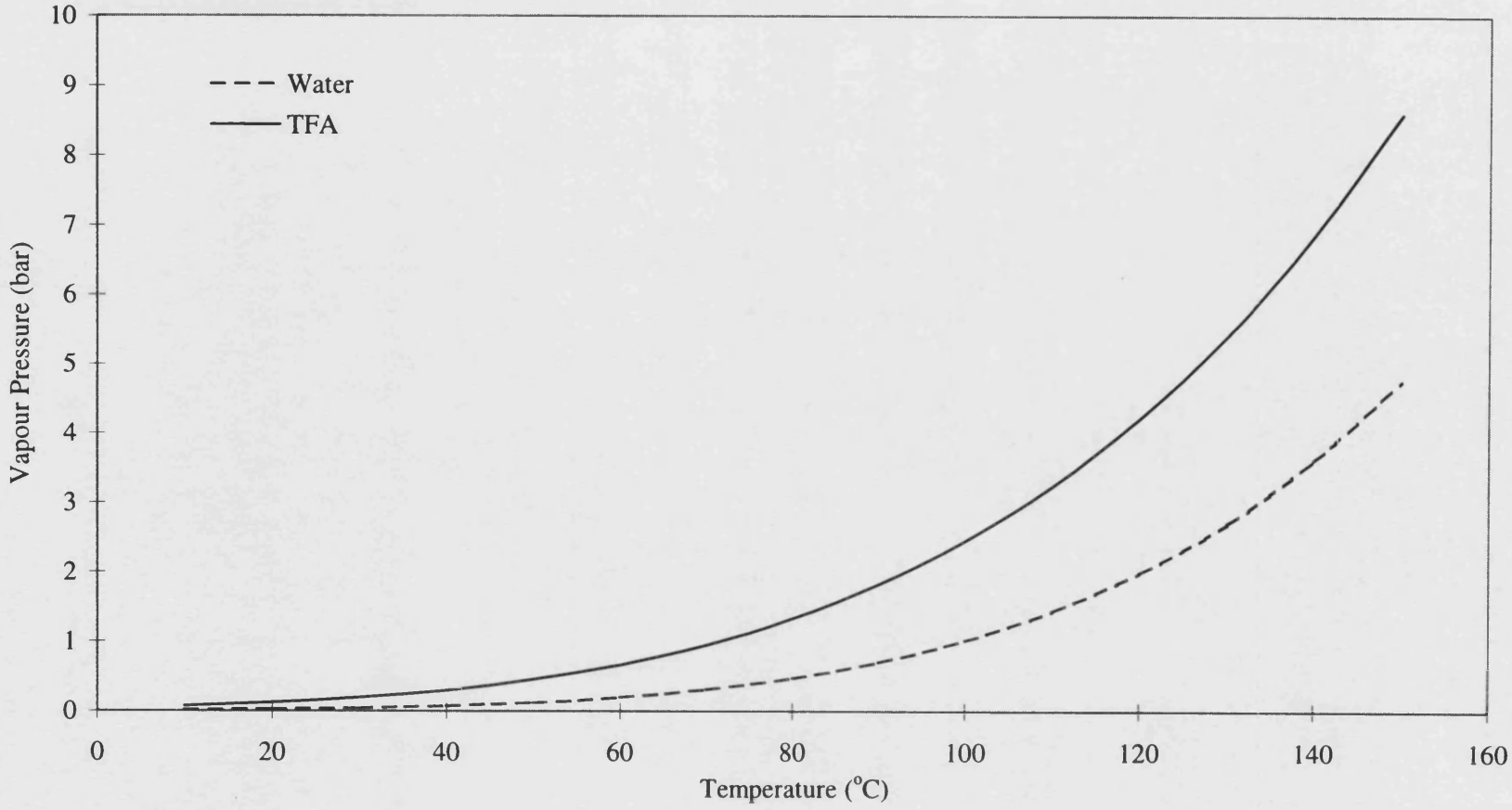

Figure 3.7. Vapour Pressure Predictions for TFA and Water

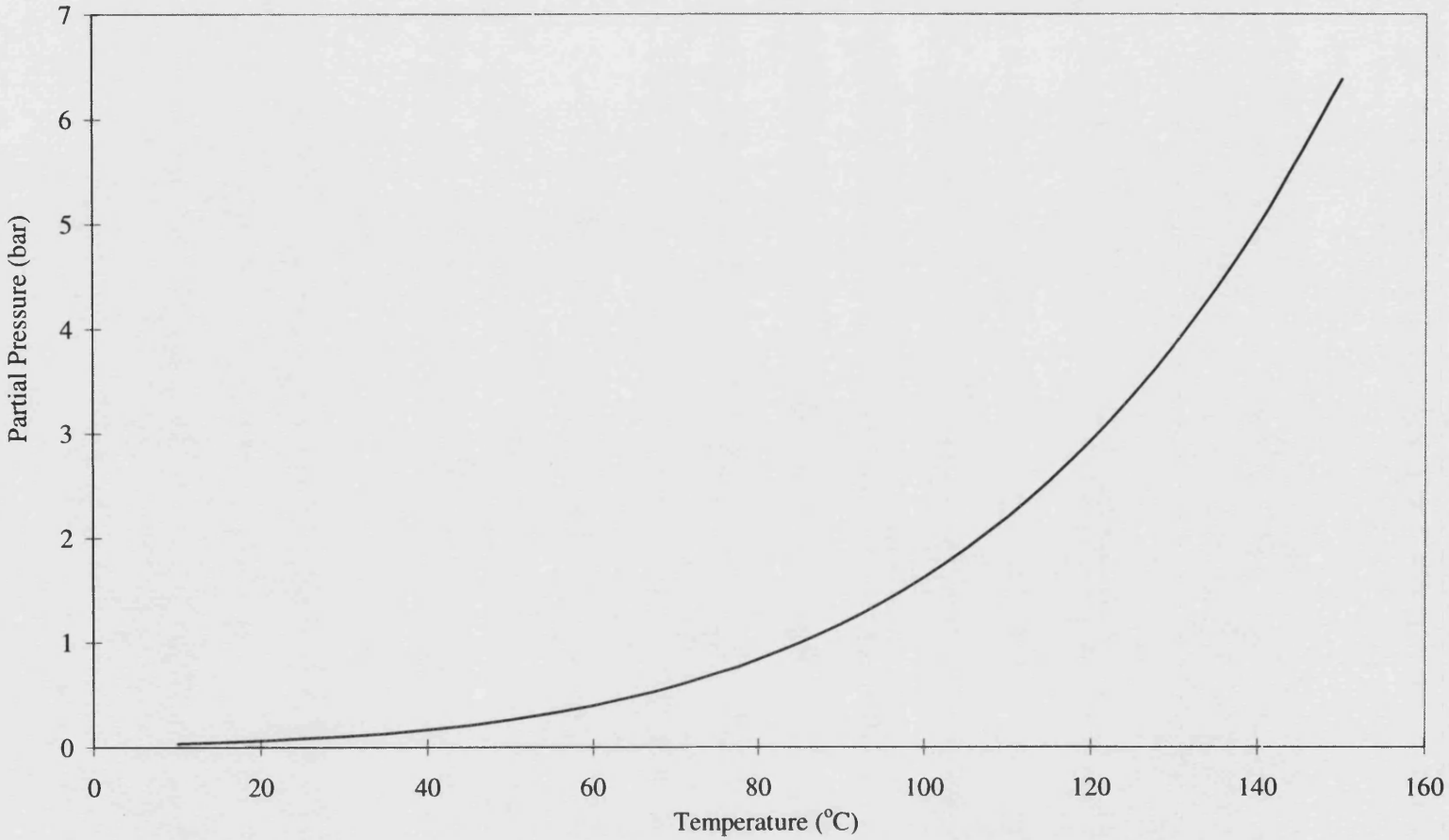

Figure 3.8. Application of Raoult's Law to a 3:1 (v/v) mixture of TFA:Water

3.5 Sample Analysis

3.5.1 Gas Chromatography

The liquid samples from both the batch and semi-continous reactors were analysed for the methanol-based product, methyl trifluoroacetate, using a gas chromatograph (GC). A HP 5890 Series II GC was used, equipped with a HP7673 automatic sampler and a HP 3396 Series II integrator (Agilent Technologies (UK), Queensferry, UK). Because of the low product concentrations obtained in the original work for this catalytic system, a capillary column was selected which would effect a greater peak resolution compared with a packed column. A BP20 (polyethylene glycol polar stationary phase) supplied by SGE Europe Ltd. (Milton Keynes, UK) was used. The compounds were detected via a flame ionisation detector (FID) which used hydrogen and air. Helium was employed as the carrier gas. The main GC settings and temperature profile are displayed in Table 3.8.

Table 3.8. Programmed GC Settings

GC Setting		Value
Carrier Gas Flowrate	(ml/min)	1.5
Injection Temperature	(°C)	130
Initial Temperature	(°C)	35
Initial Time	(min)	2
Temperature Ramp	(°C/min)	30
Final Temperature	(°C)	170
Final Time	(min)	23.5
Total Run Time	(min)	30

In the case of experiments involving a change in reaction solvent from TFA to acetic acid or the two-phase catalytic system, details of the temperature programming are given in Appendix II.

Prior to analysis, the GC was calibrated with standard solutions of methyl trifluoroacetate in the 3:1 (v/v) TFA:water solvent mixture. The data obtained from the GC for the samples and standards was reproducible to within ±5 %. The ester product was identified via its retention time and further by analysis with a gas chromatograph mass spectrometer (GCMS) (Q-Mass 910, Perkin Elmer, Beaconsfield, UK).

Because the raw reaction samples contained particulates (*e.g.* Pd/C) and dissolved copper compounds, it was not possible to inject them without preparation, else the capillary column would become "blocked". This process involved the simple vacuum distillation of the sample using a liquid nitrogen cold-trap. Approximately 4 ml of sample was distilled at a temperature between 45 - 50 °C for about 10 minutes. The distillation was stopped when dryness was observed (as seen by flaking residue in the distillation flask). Figure 3.9 shows a diagram of the distillation apparatus.

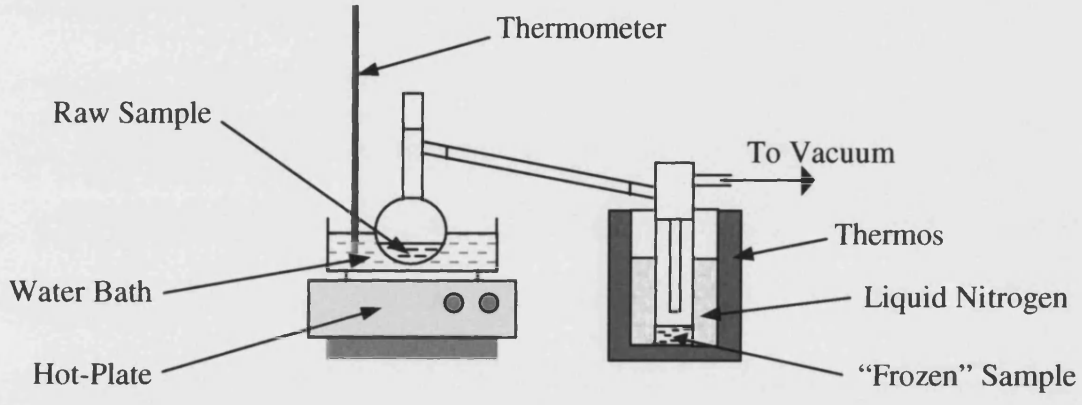

Figure 3.9. Sample Preparation Apparatus

To ascertain the efficiency of this process in terms of "losing" ester product, a number of samples containing known amounts of methyl trifluoroacetate in the solvent mixture, were made up and analysed with the GC before and after being distilled. The results are shown in Table 3.9. Although there was a variation in distillation performance between samples, as a ballpark figure one can say that approximately 20 % of the ester product was "lost". Because the ester product concentrations from the reactions were generally low (see Chapters 4), this value was not thought significant. If higher, more industrially meaningful product concentrations were obtained, then a more efficient sample preparation would have to be established or indeed the direct analysis of the untreated sample.

Table 3.9. Efficiency of the Sample Preparation Procedure

Sample Ester Concentration BEFORE Distillation (mol/m^3)	Sample Ester Concentration AFTER Distillation (mol/m^3)			Apparent Sample Ester "Loss" (%)					Maximum Ester "Loss" (%)	Minimum Ester "Loss" (%)
	1	2	3	1	2	3	Mean	Standard Deviation		
13.19	9.49	10.68	9.88	28.04	19.04	25.06	24.04	4.58	28.62	19.46
28.02	22.13	22.80	24.39	21.04	18.63	12.97	17.55	4.14	21.69	13.41
49.10	40.53	39.80	34.22	17.45	18.95	30.31	22.23	7.03	29.26	15.20
72.90	54.55	62.07	63.83	25.17	14.86	12.45	17.49	6.76	24.25	10.73
183.05	153.78	144.99	151.80	15.99	20.79	17.07	17.95	2.52	20.47	15.43
Overall Estimate for Ester "Loss" = 19.9 ±5.3%										

3.5.2 Atomic Absorption Spectrometry

Selected liquid samples were analysed for palladium content using atomic absorption spectrometry (AAS). The equipment used was a Varian AA-275 Series (Varian Ltd., Walton-on-Thames, UK) using a palladium lamp at an absorption wavelength of 244.8 nm. Acetylene and air were used for the oxidising flame. Before analysis, the machine was calibrated with authentic standards (derived from a palladium AAS standard solution supplied by Sigma-Aldrich Chemical Co. Ltd., Gillingham, UK).

3.5.3 X-ray Diffraction

To identify the crystalline form of palladium from an exemplary product sample, a Philips X-ray power diffraction (Philips, the Netherlands) unit was used. The radiation emitted was Cu K_{α}, which has a wavelength of 0.1542 nm and was generated via a PW 1730/10, 4kW unit with a PW 1710 control system.

3.5.4 Scanning Electron Microscopy

For obtaining information about the commercially available (Sigma-Aldrich Chemical Company Ltd., Gillingham, UK) Pd/C catalyst particle sizes, scanning electron microscopy (SEM) was used. The equipment employed was a JEOL 6310 (JOEL UK Ltd., Welwyn Garden City, UK) operating at 15 kV.

3.5.5 Nitrogen Adsorption

To ascertain the Brunauer-Emmett-Teller (BET) surface areas of the uncoated ceramic tube and the Pd/C catalyst, nitrogen adsorption experiments were performed. These were carried out using an ASAP 2010 unit, supplied by Micrometrics Instrument Co., USA.

3.6 Safety

The use of corrosive liquids (*e.g.* TFA) and high pressures mandates the application of prudent safety measures for both the experimentalist and any neighbouring workers. All reactant liquid mixtures were prepared in a chemical fume hood, wearing appropriate personal protective equipment. Reaction samples were withdrawn whilst wearing a protective face-shield. The use of carbon monoxide necessitated the instalment of a carbon monoxide detector (domestic-type).

Inherent in the experimental make-up is the use of flammable gases (methane and carbon monoxide) in the presence of oxygen. This imposed a limitation on the gas phase composition that was used for the experiments. Unfortunately, this experimental boundary is faced in the majority of experiments involving methane oxidation. Table 3.10 highlights the flammability limits and the spontaneous ignition temperatures of the concerned gases.

Table 3.10. Flammability Limits

Component	**Lower Flammability Limit in O_2 (vol.%, 25 °C, 0.1 MPa)**	**Upper Flammability Limit in O_2 (vol.%, 25 °C, 0.1 MPa)**	**Ignition Temperature in O_2 (0.1 MPa)**
Methane	5.1	61	556
Carbon Monoxide	15.5	94	588

(Adapted from Glassman, 1987)

The effect of increased pressure tends to increase the upper flammability limit whilst hardly affecting the lower limit (Glassman, 1987). The presence of two combustible gases and a low oxygen concentration (*ca.* 8 vol.%) at elevated pressures, makes prediction of the flammability limits very difficult. Therefore, the gas phase compositions, which were used in the experiments, were based on already documented work (*e.g.* Lin *et al.*, 1997; Park *et al.*, 2000[a]).

3.7 Chemicals

The majority of the non-gaseous chemicals used in this study were purchased from Sigma-Aldrich Chemical Co. Ltd. (Gillingham, UK), with the TFA solvent bought from Apollo Scientific (Whaley Bridge, UK). Gaseous components were supplied by BOC Gases Ltd. (Bristol, UK). All chemicals were used as delivered, without the need for any further purification.

Table 3.11 shows details of the chemicals used.

Table 3.11. Chemicals Used for Methane Oxidation Experiments (Part 1: Solids)

Solid Substance	Formula	Purity (%)	Supplier
5 wt.% Palladium on activated carbon	Pd/C	-	Aldrich
Copper(II) chloride	$CuCl_2$	99.999	Aldrich
Palladium(II) acetate	$Pd(CH_3CO_2)_2$	98	Aldrich
Copper(II) sulphate hydrate	$CuSO_4.xH_2O$	98	Aldrich
Sodium chloride	NaCl	99.5	Sigma
Copper(II) trifluoroacetate	$Cu(CF_3CO_2)_2.xH_2O$	-	Aldrich
Tol-4-sulfonic acid monohydrate	$C_7H_8O_3S.H_2O$	99	Sigma
2,9-dimethyl-4,7-diphenyl-1,10-phenanthroline	$C_{26}H_{20}N_2$	98	Aldrich
Ammonium hexachloropalladate (IV)	$(NH_4)_2PdCl_6$	99.99	Aldrich

Table 3.11. Chemicals Used for Methane Oxidation Experiments (Part 2: Liquids)

Liquid Substance	Formula	Purity (%)	Supplier
Trifluoroacetic acid	CF_3COOH	99.9	Apollo Scientific
Water	H_2O	Distilled	"On-site"
Acetic acid	CH_3COOH	99.8	Aldrich
Methyl trifluoroacetate	CF_3COOCH_3	99	Fluka Chemika
Methyl acetate	CH_3COOCH_3	99.5	Aldrich
Hydrogen peroxide	H_2O_2	27 wt.% in water	Aldrich
Toluene	$(C_6H_5)CH_3$	99.9	Sigma
2-methyl-2-butanol	$C_2H_5C(CH_3)_2OH$	99	Aldrich
Hydrazine hydrate	$N_2H_4.H_2O$	64 % hydrazine equivalent in water	Sigma
Hydrochloric acid	HCl	1 M	Aldrich
Sulphuric aid	H_2SO_4	97.5	Aldrich
Potassium Permanganate	$KMnO_4$	0.1 M	Aldrich
Alumina sol (23N4-20)	-	No contaminants	CONDEA Vista Co.

Table 3.11. Chemicals Used for Methane Oxidation Experiments (Part 3: Gases)

Gaseous Substance	Formula	Purity (%)
Methane	CH_4	99.5
Carbon monoxide	CO	99.9
Oxygen	O_2	99.5
Nitrogen	N_2	99.998
Helium	He	99.96
Hydrogen	H_2	99.992
Air	-	-

CHAPTER 4 - Experimental Results

This chapter details the results obtained from the reaction studies of the selected catalytic methane oxidation system (Lin *et al.*, 1997). First the focus is on initial work performed in the batch reactor, in attempt to validate the catalytic system and also to observe any phenomena attributed to the increased liquid volume. Then the attention of the chapter turns to the use of the semi-continuous porous tube reactor. Finally, based on the performance of the two aforementioned reactors, some novel changes are made to the original system and also the use of a novel biphasic system for *in situ* H_2O_2 production is explored, in attempt to ameliorate the reaction performance.

In this chapter, the key observations are briefly explained were relevant with the main discussion of results being the focus of Chapter 5.

4.1 Batch Operation

The original work of Lin *et al.* (1997) was carried out in a 125 ml batch reactor, with 4 ml of liquid phase (gas-to-liquid ratio *ca.* 31). In this current work, a 175 ml reactor was employed with 50 ml of liquid phase. Thus the liquid volume ratio to the original work was 12.5, and with an effective gaseous volume of 80 ml, the gas-to-liquid ratio was *ca.* 1.6. The base parameters used were those found in the original work and detailed in Chapter 3 (Section 3.1.1).

At this point it is worthwhile presenting Figure 2.12 again, which shows the proposed mechanism for methane oxidation using the bimetallic catalyst system:

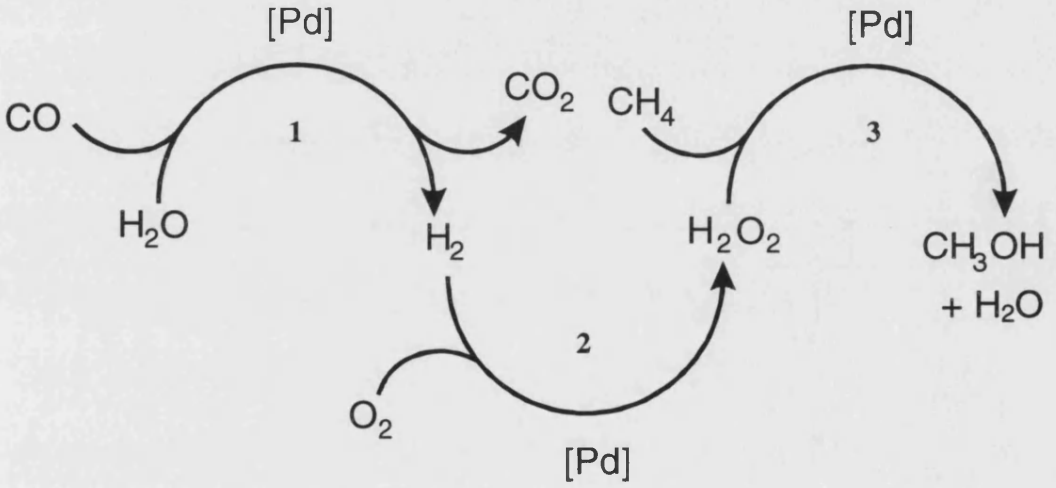

(Figure 2.12. Overall Reaction Scheme for Bimetallic System (Adapted from Lin *et al.*, 1997).

4.1.1 Validation of Catalytic System

The purpose of these experiments was to verify that the system actually produces the methanol-based product (methyl trifluoroacetate), according to equation (4.1):

$$CH_4 + CO + O_2 + CF_3COOH \rightarrow CF_3COOCH_3 + CO_2 + H_2O \qquad (4.1)$$

Experimental runs with batch times of 1, 2, 3 and 20 hours were performed with monitoring of both the liquid temperature and the reactor pressure. The results are

displayed in Table 4.1, with a graphical plot of the product concentration shown in Figure 4.1. The temperature and pressure profiles are shown in Figure 4.2 and Figure 4.3 respectively. The pressures are reported in the pressure gauge equipment units (bar).

Table 4.1. Verification of the Catalytic System

Batch Time (h)	Reaction ΔP (bar)	[Methyl trifluoroacetate] (mol/m^3)	Methyl trifluoroacetate Yield (%)	TON (based on Pd catalyst)	STY (kg/kg$_{Pd}$.h)
1	7	40	1.2	342	412
2	9.5	50	1.5	430	259
3	11	50	1.5	430	172
20	11	51	1.5	438	26

Conditions: $P_{CH4(i)}$ = 62 bar; $P_{CO(i)}$ = 14 bar; $P_{O2(i)}$ = 7 bar; 5 wt.% Pd/C = 12.5 mg; [$CuCl_2$] = 20 mol/m^3; TFA:H_2O = 3:1 (50 ml); T = 85 °C; N = 500 rpm

From this data it seems that the methyl trifluoroacetate product was formed mainly during the first 2 hours. Figure 4.2 indicates that the observed reaction pressure drop also occurred chiefly during the first 2 hours. This latter phenomenon was not reported in the original work, possibly because their large gas-to-liquid volume ratio of *ca.* 31 did not facilitate an observable reaction pressure drop. In this current work, the gas-to-liquid ratio used was *ca.* 1.6. The temperature profiles (Figure 4.3) remained fairly constant at the set value of 85 °C throughout the experiments. The initial rise of 1 - 2 °C could indicate the presence of a reaction exotherm.

Regarding the product concentrations of methyl trifluoroacetate obtained, these appeared lower than those derived using similar reactant concentrations in the original work of Lin *et al.* (1997) even after compensating for product "loss" during pre-analysis sample preparation (*e.g.* in 20 h at 85 °C, a concentration of 51 mol/m^3 was obtained for this work compared with 120 mol/m^3 at 85 - 95 °C).

In conclusion, this preliminary data has shown the validity of the catalytic system in that a methanol-based product was formed, thus providing the foundation for a continued investigation. However, one noticeable observation, not explicitly reported in the original work of Lin *et al.* (1997), was the pseudo-end of product formation after *ca.* 2 h. As this corresponded to the apparent end of the pressure drop, one possible explanation of this decay in product formation rate is that it was due to the depletion of gaseous reactants.

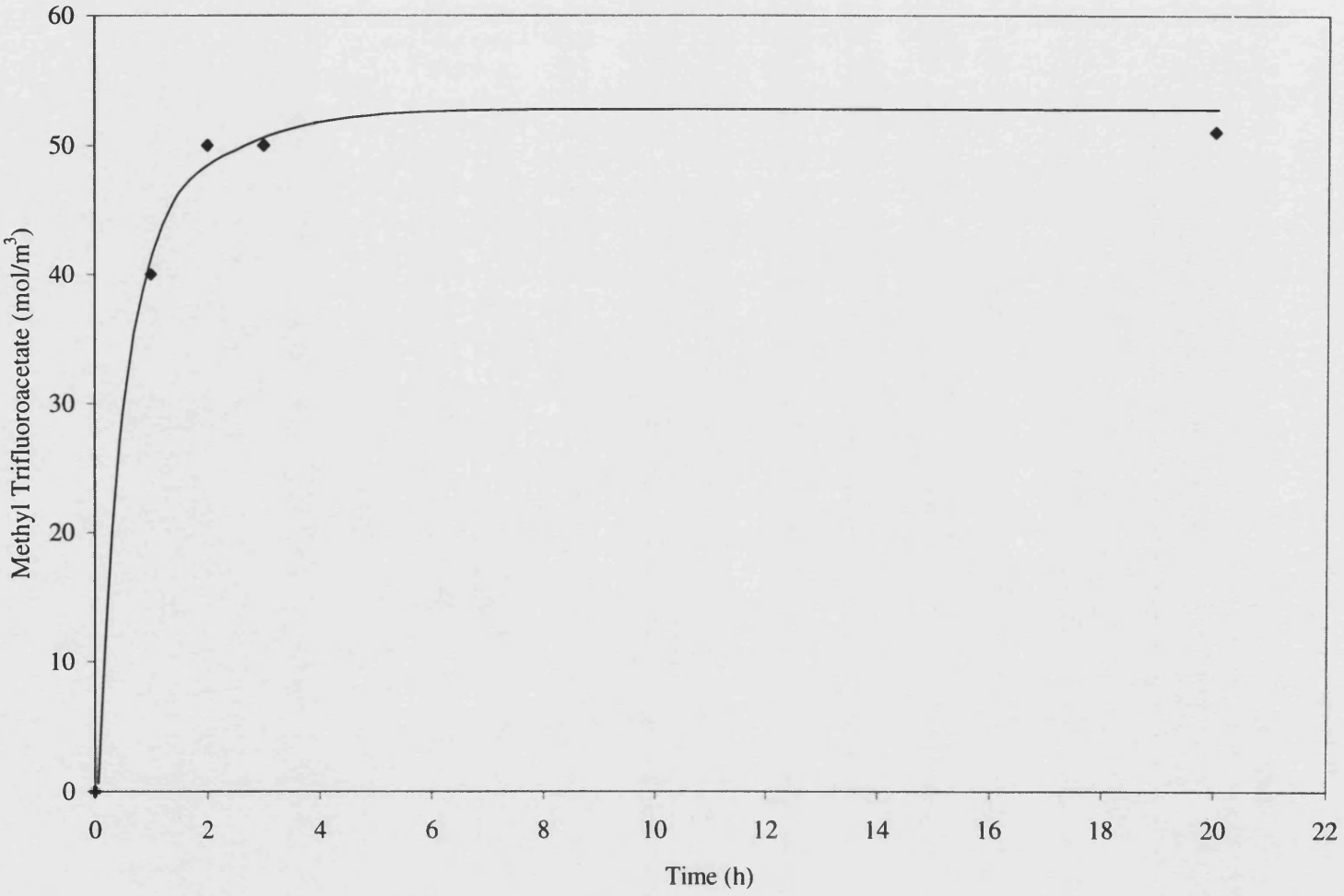

Figure 4.1. Time Course of Methanol-based Product

Conditions: $P_{CH4(i)}$ = 62 bar; $P_{CO(i)}$ = 14 bar; $P_{O2(i)}$ = 7 bar; 5 wt.% Pd/C = 12.5 mg; [$CuCl_2$] = 20 mol/m^3; TFA:H_2O = 3:1 (50 ml); T = 85 °C; N = 500 rpm

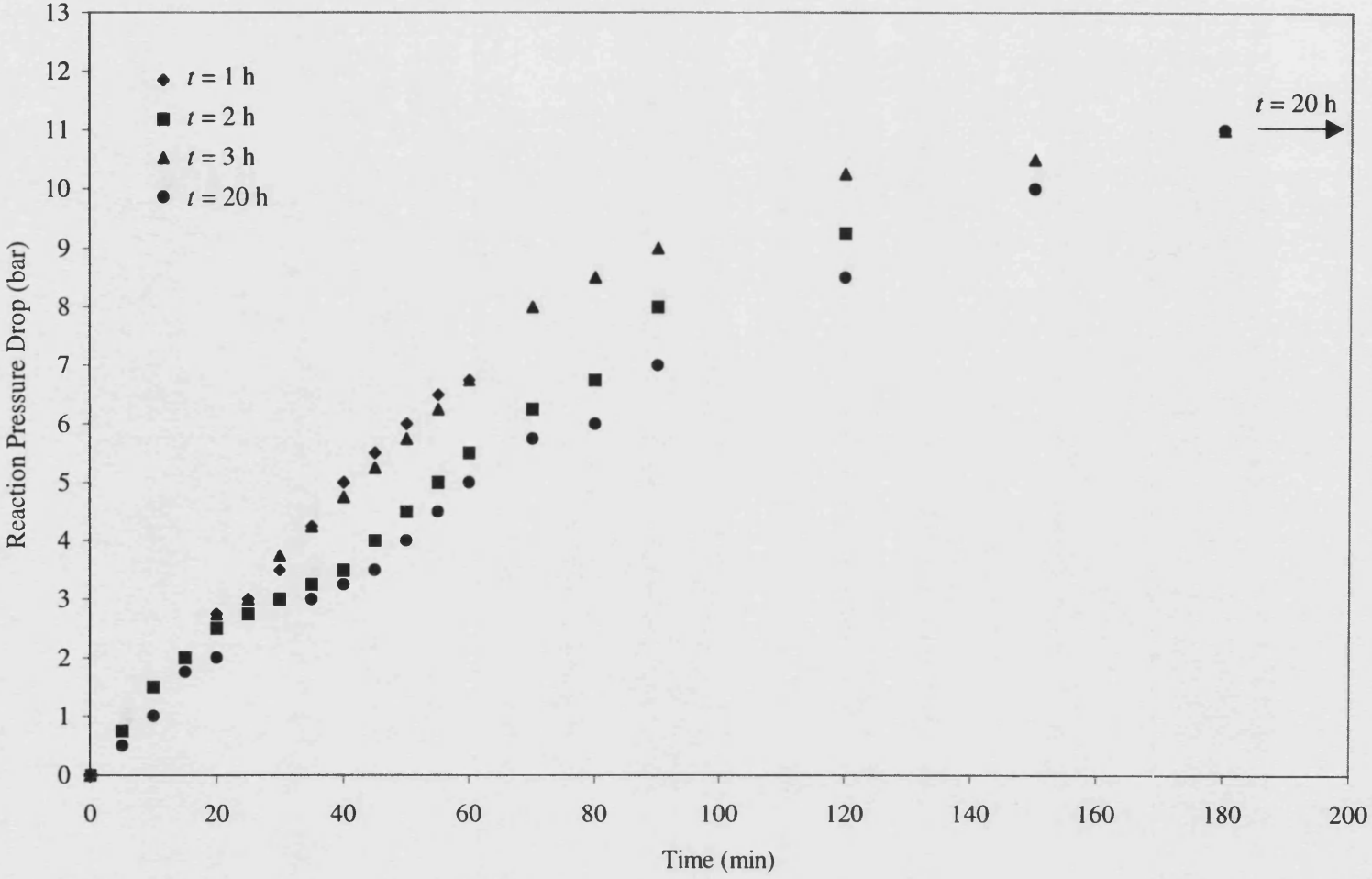

Figure 4.2. Batch Reaction Pressure Drop Profile

Conditions: $P_{CH4(i)}$ = 62 bar; $P_{CO(i)}$ = 14 bar; $P_{O2(i)}$ = 7 bar; 5 wt.% Pd/C = 12.5 mg; [$CuCl_2$] = 20 mol/m^3; TFA:H_2O = 3:1 (50 ml); T = 85 °C; N = 500 rpm

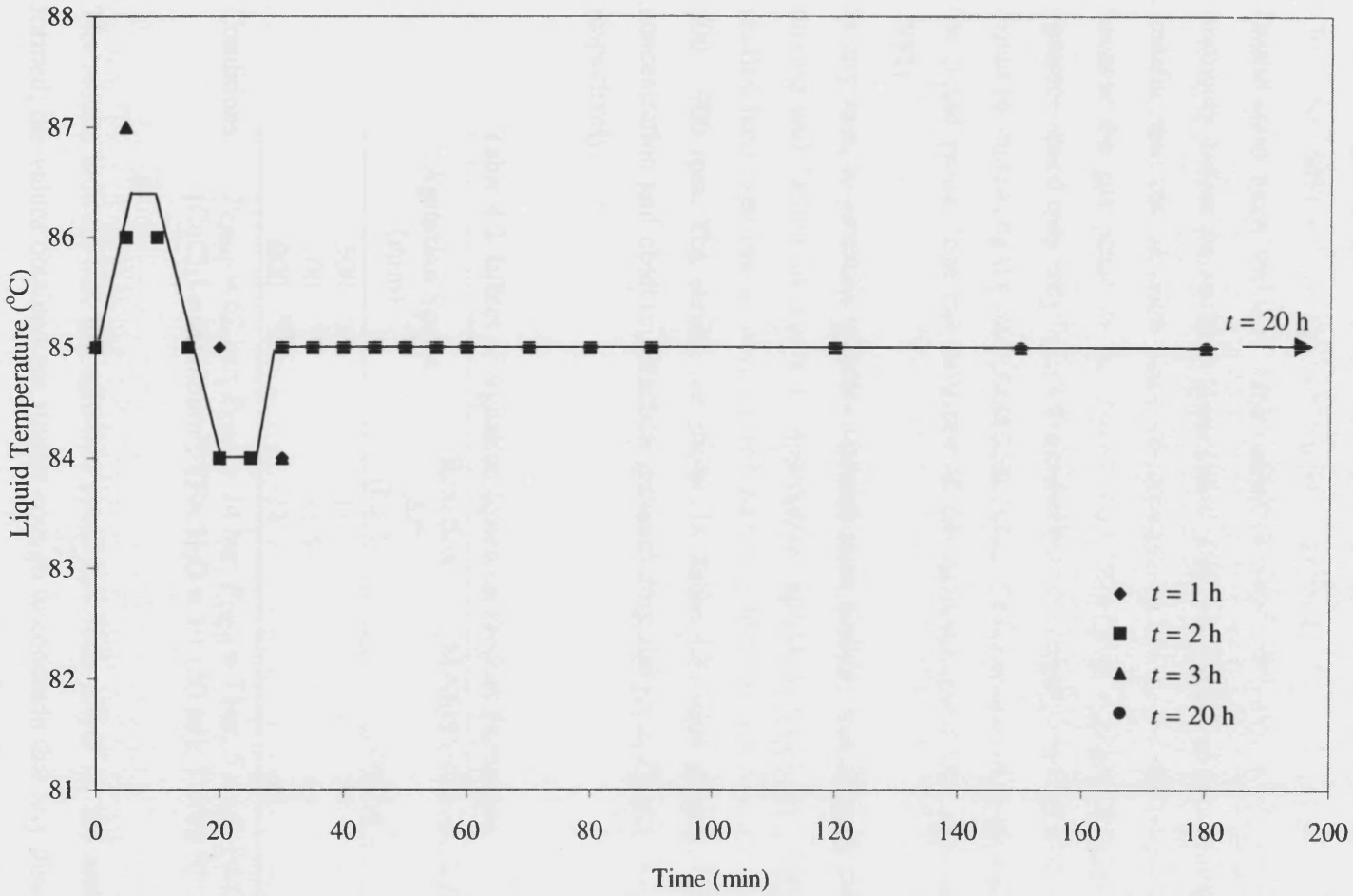

Figure 4.3. Batch Liquid Temperature Profile

Conditions: $P_{CH4(i)}$ = 62 bar; $P_{CO(i)}$ = 14 bar; $P_{O2(i)}$ = 7 bar; 5 wt.% Pd/C = 12.5 mg; [$CuCl_2$] = 20 mol/m^3; TFA:H_2O = 3:1 (50 ml); T = 85 °C; N = 500 rpm

4.1.2 Effect of Agitation Speed

For the methane oxidation reaction to occur, the gaseous reactants must first dissolve into the bulk liquid phase. This mass transfer is affected by the gas-liquid interfacial area. Then they diffuse from the bulk liquid to the heterogeneous palladium catalyst surface (liquid-solid mass transfer) after which internal diffusion to the active site may be necessary before the reaction takes place. The gas-liquid and liquid-solid external mass transfer rates can, in some cases, be enhanced by increasing the stirrer speed. However, because the gas phase in the reactor was effectively a stagnant layer, increasing the agitation speed may only have a limited effect on bringing more gas into contact with the liquid by increasing the interfacial area. Also, if the catalyst particles are non-shearing in the liquid phase, then the influence of the agitation speed may also be small (Fogler, 1992).

In any case, to ascertain whether external mass transfer was limiting due to the general mixing and further to select an appropriate agitation speed for further experimental studies, base experiments were carried out using different agitation speeds in the range of 500 - 900 rpm. The results are shown in Table 4.2, with graphical plots of product concentration and observed reaction pressure drop shown in Figures 4.4 and Figure 4.5 respectively.

Table 4.2. Effect of Agitation Speed on Product Formation

Agitation Speed (rpm)	**Reaction ΔP (bar)**	**[Methyl trifluoroacetate] (mol/m^3)**
500	11	50
700	11.5	46
900	11	45

Conditions: $P_{CH4(i)}$ = 62 bar; $P_{CO(i)}$ = 14 bar; $P_{O2(i)}$ = 7 bar; 5 wt.% Pd/C = 12.5 mg; $[CuCl_2]$ = 20 mol/m^3; TFA:H_2O = 3:1 (50 ml); T = 85 °C; t = 3 h

The results indicate that the agitation speed had little effect on the amount of product formed; the values obtained are similar enough to conclude that any discrepancies could be due to the variability in the sample preparation before GC analysis whereby it was estimated that 19.9 ±5.3 % of product was "lost". The rate of pressure drop (inferred from Figure 4.5) tended to increase with a rise in agitation speed indicating a possible mass transfer limitation, although above 700 rpm the variation was close to the nominal

accuracy of the pressure gauge. In light of this information, the extent of any external mass transfer limitation amenable to the mixing was not thought to be significant at the low temperature employed and an agitation speed of 700 rpm was selected for subsequent experiments.

Regarding internal resistance, for an intermediate Pd/C particle diameter of 75 μm an approximate calculation based on the Weisz-Prater parameter (*e.g.* Fogler, 1992) suggested an insignificant intra-particle resistance (see Appendix VII for calculation).

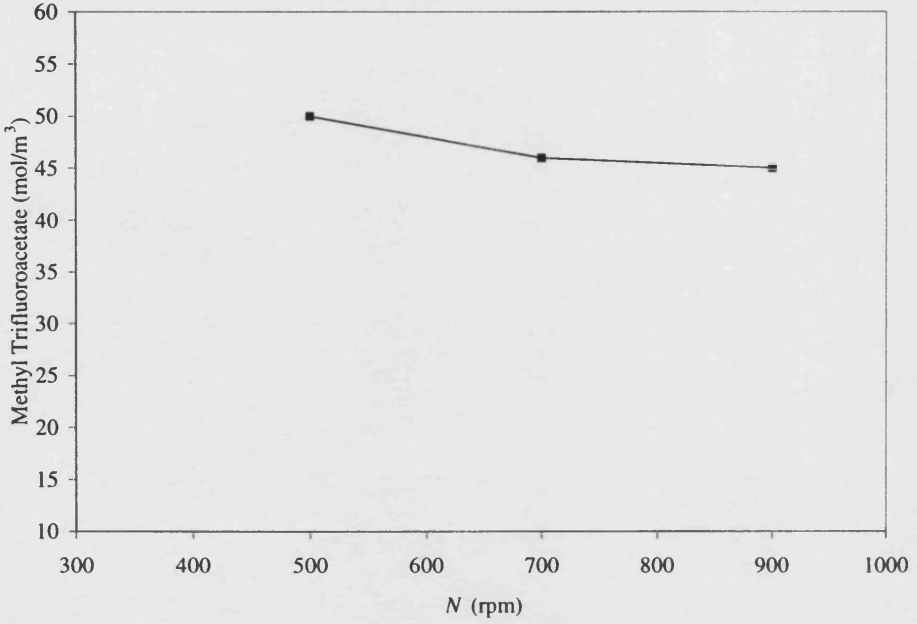

Figure 4.4. Effect of Agitation Speed on Product Formation

Conditions: $P_{CH4(i)}$ = 62 bar; $P_{CO(i)}$ = 14 bar; $P_{O2(i)}$ = 7 bar;
5 wt.% Pd/C = 12.5 mg; [$CuCl_2$] = 20 mol/m^3;
TFA:H_2O = 3:1 (50 ml); T = 85 °C; t = 3 h

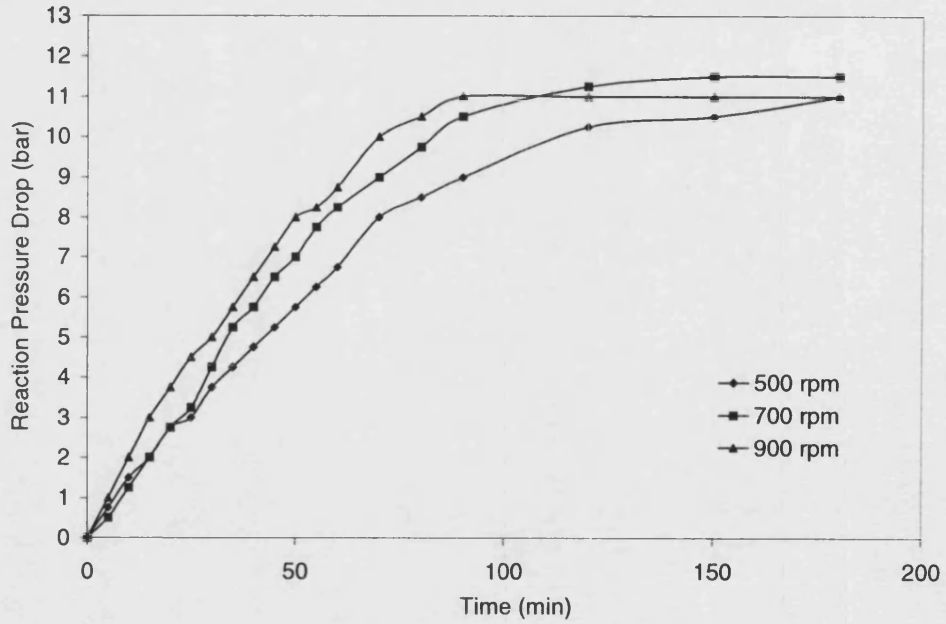

Figure 4.5. Effect of Agitation Speed on Reaction Pressure Drop

Conditions: $P_{CH4(i)}$ = 62 bar; $P_{CO(i)}$ = 14 bar; $P_{O2(i)}$ = 7 bar;
5 wt.% Pd/C = 12.5 mg; [$CuCl_2$] = 20 mol/m^3;
TFA:H_2O = 3:1 (50 ml); T = 85 °C; t = 3 h

4.1.3 Relevance of the Gas Phase Constitution to Reaction Performance

The gaseous components present in the base mixture were methane, carbon monoxide and oxygen. The observation of a reaction pressure drop gives an indication of gas consumption and by performing experiments in the absence of a gaseous component one can ascertain the importance of that component to the reaction.

The results are shown in Table 4.3

Table 4.3. Relevance of Gas Phase Species to Reaction Performance

Gaseous Species Omitted	Reaction ΔP (bar)	[Methyl trifluoroacetate] (mol/m^3)	Methyl trifluoroacetate Yield (%)	TON (based on Pd catalyst)	STY (kg/kg$_{Pd}$.h)
None (base)	11	50	1.5	430	259
CO	2.5	7	0.2	61	24.4
CH_4 (replace with N_2)	9	N/A	-	-	-
O_2	0	N/A	-	-	-

Conditions: Where included $P_{CH4(i)}/P_{N2}$ = 62 bar; $P_{CO(i)}$ = 14 bar; $P_{O2(i)}$ = 7 bar; 5 wt.% Pd/C = 12.5 mg; [$CuCl_2$] = 20 mol/m^3; TFA:H_2O = 3:1 (50 ml); T = 85 °C; t = 3 h; N = 700 rpm

Of initial interest is methane oxidation in the absence of the coreductant, CO. There was some evidence of product formation with a reaction pressure drop of 2.5 bar, although this was much less than that obtained from using CO. Although not shown, this experiment was also carried out for 20 h with a resulting methyl trifluoroacetate concentration of 20 mol/m^3. It is possible that CO was formed from either methane "deep" oxidation (equation 2.8) or methane steam reforming (equation 2.0) with the reaction then proceeding in the normal way (see Figure 2.12). However, these CO forming reactions are unlikely, mainly because of the low temperatures involved, with the steam reforming reaction being very endothermic. Nonetheless, the reaction performance is significantly impaired without the inclusion of carbon monoxide and further investigation was not warranted.

With regard to the reaction pressure drop, it appears that this was mainly due to the consumption of carbon monoxide and oxygen (no pressure drop was observed in the absence of O_2). Figure 4.6 compares the pressure drops obtained from experiments

involving the complete system (CH_4, CO and O_2) and using CO and O_2 only. It can be seen that the reaction pressure drop time course of the complete reaction system was very similar to that observed in the absence of CH_4 during the first hour, which was when the main part of the pressure drop occurred. By considering the main reactions proposed in the mechanism (Lin *et al.*, 1997; Park *et al.*, 2000[a]), the pressure drop inducing reactions can be established.

1) Wacker oxidation of CO (Park *et al.*, 2000[a]):

$$CO + \frac{1}{2}O_2 \rightarrow CO_2 \qquad (4.2)$$

2) Water gas shift reaction

$$CO + H_2O \rightarrow CO_2 + H_2 \qquad ((2.1))$$

3) *In situ* hydrogen peroxide formation

$$H_2 + O_2 \rightarrow H_2O_2 \qquad (4.3)$$

4) Methane oxidation

$$CH_4 + H_2O_2 + CF_3COOH \rightarrow CF_3COOCH_3 + 2H_2O \qquad (4.4)$$

Thus a pressure drop due to gaseous reaction stoichiometry arises from equation (4.2), equation (4.3) and equation (4.4). The observed pressure drop is facilitated further by a limited solubility of the gaseous products in the liquid phase. Because the pressure drop incurred from using CO and O_2 in the absence of CH_4, represented *ca.* 80 % of that observed with the complete system, it is suggested that the formation of H_2O_2 and the Wacker oxidation of CO both induced the major part of the reaction pressure drop. From equation (2.1) it appears that CO was not explicitly involved in the pressure drop due to H_2O_2 formation and indeed in the absence of O_2 no pressure drop was observed. However, CO consumption was apparent because a pressure drop of *ca.* 9 bar was observed and only 7 bar O_2 was used in experiments omitting CH_4. This further supports the (Wacker) oxidation of CO (equation (4.2)), as proposed by Park *et al.* (2000)[a], which consumes both CO and O_2.

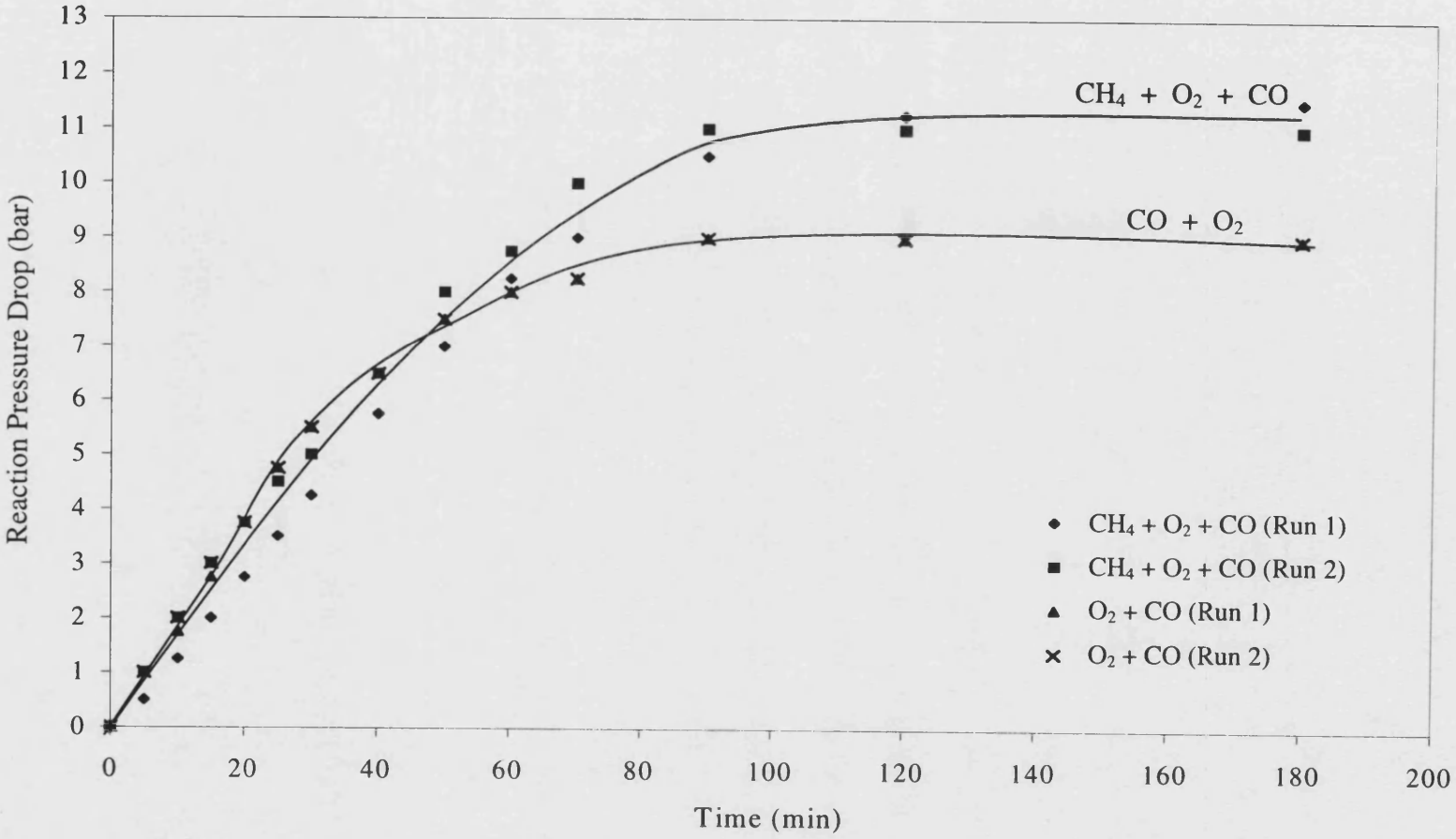

Figure 4.6. Influence of Methane Presence on Reaction Pressure Drop

Conditions: $P_{CH4(i)}/P_{N2}$ = 0 or 62 bar; $P_{CO(i)}$ = 14 bar; $P_{O2(i)}$ = 7 bar; 5 wt.% Pd/C = 12.5 mg; [$CuCl_2$] = 20 mol/m^3; TFA:H_2O = 3:1 (50 ml); T = 85 °C; N = 700 rpm

4.2 Semi-continuous Operation

The application of an increased liquid volume of 50 ml in the batch reactor (gas-to-liquid ratio *ca.* 1.6) revealed some interesting observations, some of which were not noted by the original workers who employed a liquid volume of only 4 ml (gas-to-liquid ratio *ca.* 31). The pseudo-end of the methyl trifluoroacetate formation after around 2 h, coupled with a similar observation for the pressure drop, signified the depletion of gaseous reactants being a possible cause.

The use of the porous tube reactor provides a continuous feed of gaseous reactants ameliorating the aforementioned problem. The liquid sampling facilities enable a true time course behaviour to be established, seldom reported in other similar works. This last factor would also provide more scope for studying the impact of catalyst concentration and gas partial pressures, not explored with the batch reactor. Lastly, the reactor uses a further increased liquid phase volume of 300 ml, representing a 75 times increase from the original work, providing a more relevant scale for this feasibility study.

This section details the general application of the porous tube reactor for the methane oxidation reaction, with the intention of limiting the problems that arose from the batch reactor, together with investigations of variation in catalyst concentrations and gas partial pressures.

4.2.1 Use of the Palladium Coated Porous Tube

It was decided to first attempt methane oxidation in the absence of the coreductant, carbon monoxide. Under these conditions, there was evidence of product formation using the batch reactor, although significantly less than that obtained using the complete reaction system.

Preliminary experiments using a palladium coated ceramic tube, obtained from methods detailed in Chapter 3 (Section 3.2.4.1), revealed that the palladium was leaching during the course of the reaction. The same tube was used for 3 similar experiments, with effectively no or very little product being formed. Observation of the porous tube showed that the palladium been removed during the experimentation (see Plate 4.1). Atomic absorption spectroscopy (AAS) of the liquid samples revealed that the majority of the palladium was removed during the first experiment (see Appendix I). Consideration of the postulated reaction mechanism, in particular the proposed Wacker chemistry synergy between Pd and Cu components, could explain the observed leaching of metallic palladium from the tube with the formation of palladium(II) ions in solution. Thus, the cause of the palladium removal from the tube was attributed as much to the inherent consequence of the reaction chemistry as to the physical instability of the palladium film. Therefore, the use of the catalytic porous tube was deemed not applicable for this system.

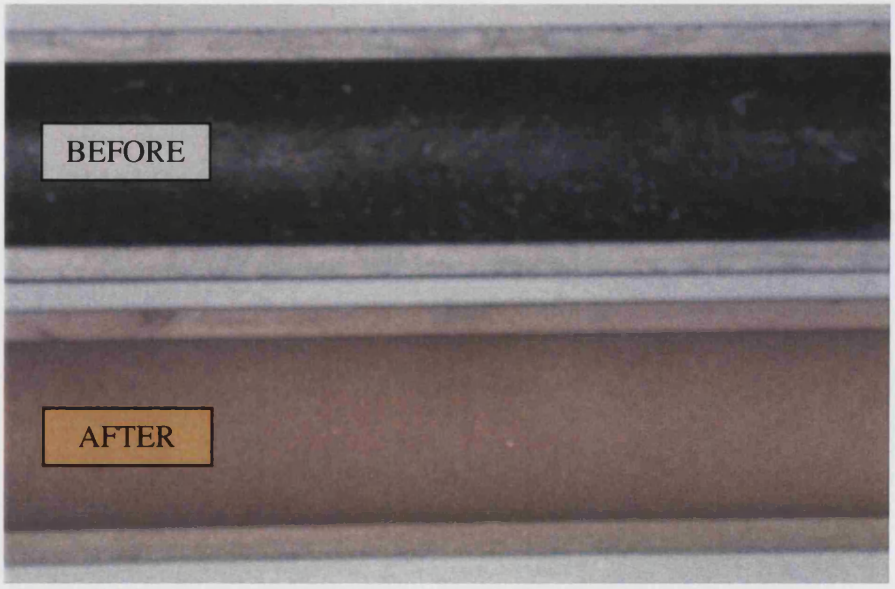

Plate 4.1. Evidence of Palladium Removal from the Porous Tube

4.2.2 Homogeneous Palladium Catalysis

The incompatibility of the catalytic porous tube for the methane oxidation reaction made necessary the use of an alternative source of palladium catalyst. Although a suspension of the commercial Pd/C catalyst, as used in the batch experiments, was a possible option it was thought that the design of the reactor would not properly accommodate the efficient use of a slurry system *e.g.* efficient mixing capabilities. Furthermore, particulate blockages in the valve systems was also a possibility. However, the use of this catalyst was later tried and is detailed elsewhere in this chapter. The majority of the work, using the porous tube reactor, employed a homogeneous palladium catalyst in the form of palladium(II) acetate. This catalyst had already been tested in another work (Park *et al.*, 2000[a]) giving product yields comparable to that of the heterogeneous Pd/C catalyst.

4.2.2.1 Validation of the Catalytic System under Semi-continuous Operation

To demonstrate the feasibility of using the porous tube reactor for the catalytic system, an experiment was performed, employing reactant conditions mimicking those of the base composition as used in the batch experiments. Liquid samples were withdrawn at the beginning of the experiment ($t = 0$) and then at 30 minutes intervals, for a total run time of 180 minutes (3 hours). A time course profile of the methyl trifluoroacetate product is shown in Figure 4.7. It can be seen that the majority of the product was formed during the first *ca.* 60 minutes (1 hour) with evidence of product "loss" towards the end of the run time. Comparing with the batch experiments, the product concentrations obtained here were lower, although the nature of the palladium catalysts were different in the two systems. At this stage it is too early to speculate on the data, although the results verified that a methanol-based product was formed and shows the worth of the porous tube reactor as a tool for reaction studies.

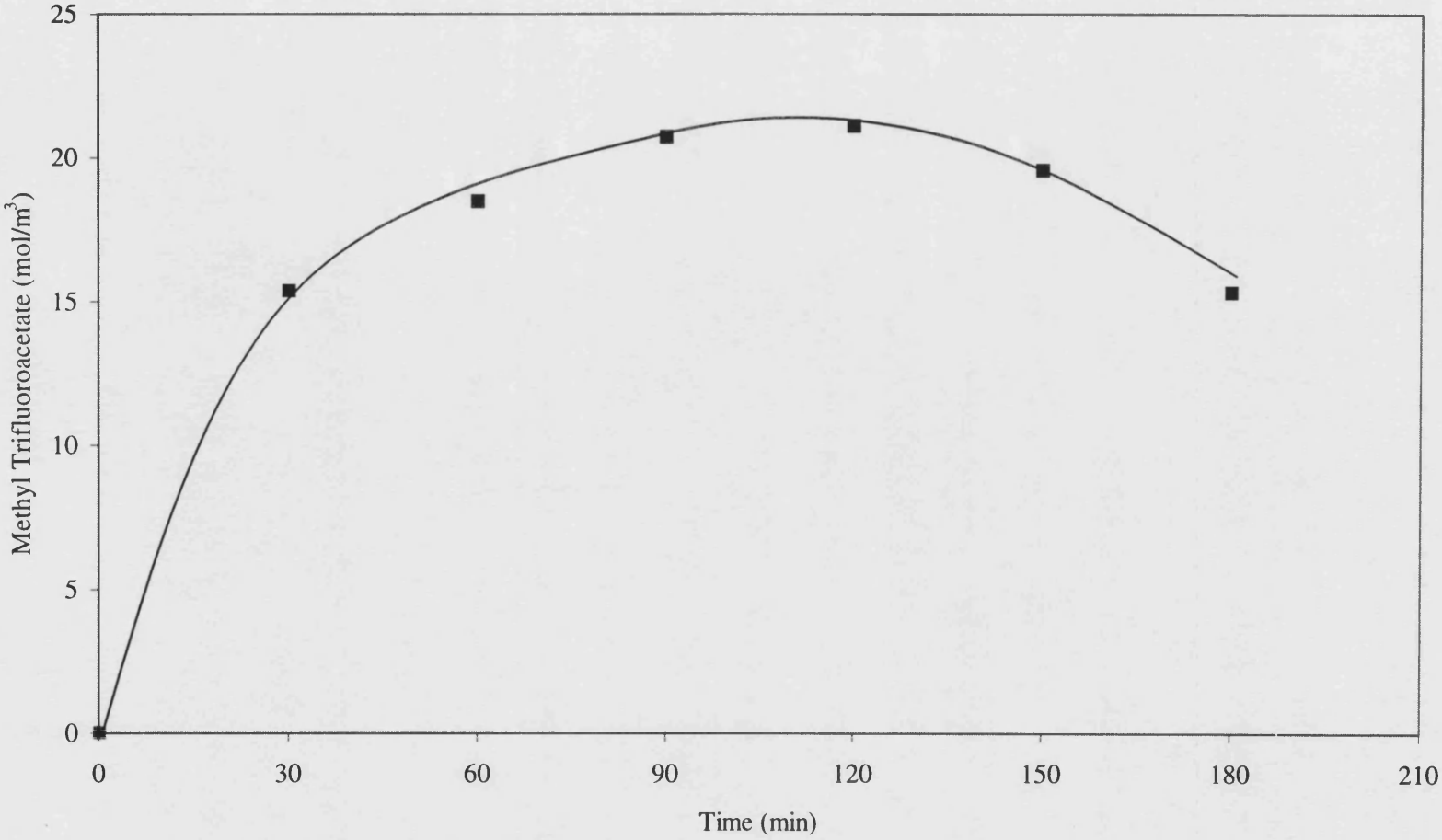

Figure 4.7. Verification of the Use of the Catalyst System with the Porous Tube Reactor

Conditions: $P_{CH4(i)}$ = 62 bar; $P_{CO(i)}$ = 14 bar; $P_{O2(i)}$ = 7 bar; Total Flow = 2 l/min; $[Pd^{2+}]$ = 0.12 mol/m^3; $[CuCl_2]$ = 20 mol/m^3; TFA:H_2O = 3:1 (300 ml); T = 85 °C

4.2.2.2 Effect of Catalyst Concentrations

This parameter was not explored using the batch reactor; the liquid sampling facility of the porous tube reactor lends itself to generating more comprehensive results and so was utilised for observing the effect of varied catalyst concentrations.

Both the works of Lin *et al.* (1995) and Park *et al.* (2000)[a] explored the effect of varying the copper(II) chloride concentration at a fixed palladium (Pd/C) amount in batch reactors. The latter work expressed the parameter as a ratio between copper(II) chloride and palladium. The results reported in the aforementioned citings were plotted as [Methyl Trifluoroacetate] against $CuCl_2$/Pd and are shown in Figure 4.8 and Figure 4.9.

Although the two works are not directly comparable because of differing methane partial pressures, palladium amounts and batch times, it can be seen that an excess of copper chloride was deleterious to ester product formation. Figure 4.9 indicates that for low $CuCl_2$/Pd ratios an increase in $CuCl_2$ promoted product formation.

For this current work using the porous tube reactor, three copper chloride concentrations were selected at a fixed palladium (Pd^{2+}) amount. The reaction time course results are depicted in Figure 4.10. The results indicate a similar trend as that observed by Park *et al.* (2000)[a]; too little copper(II) chloride ($CuCl_2$/Pd = 8) resulted with an impaired reaction performance, whilst an excessive amount ($CuCl_2$/Pd = 168) was also deleterious.

To ascertain whether it was the absolute catalyst ratio that was the important factor or the individual contributions from the two catalyst themselves, experiments were performed with differing amounts of palladium catalyst at a fixed copper(II) chloride amount. The results are shown in Figure 4.11 and data for a varied copper(II) chloride concentration are displayed in Figure 4.12. It can be seen from Figure 4.11, that a 5.5-fold increase in palladium had little influence on product yields, however a 4-fold increase in copper(II) chloride gave a significant detrimental effect (Figure 4.12). Thus it seems that within the catalyst concentration range studied, a variation in the concentration of the copper(II) chloride cocatalyst had a greater influence on product yield than a change in the palladium concentration. Thus it is the role of the individual catalyst that was important, not just the absolute catalyst ratio. This result was further verified by performing an experiment with double the catalyst amount, but keeping the catalyst ratio the same. The results are displayed in Figure 4.13. Thus the effect of doubling the copper(II) chloride concentration (from 4.9 to 9.8 mol/m^3) was dominant over the increase in palladium, in

that less product was formed even though the catalyst ratios were the same and the total amount of catalyst had increased.

According to Park *et al.* (2000)[a], the copper(II) chloride cocatalyst was required not only for the redox chemistry of the Wacker oxidation of CO, but also as a provider of chloride ions which stabilise the palladium(II) oxidation state necessary for effective methane functionalisation. However, if this palladium oxidation state is prevalent in the reaction mixture, because it also catalyses the oxidation of CO, then less of this coreductant is available for generation of the *in situ* oxidant and hence less product would be formed. This could explain why an excess of copper(II) chloride had a detrimental effect on the methyl trifluoroacetete product formation.

From this study, based on the results obtained thus far, a copper(II) chloride concentration of 4.9 mol/m^3 together with a palladium concentration of 0.66 mol/m^3, was selected for use in further experimentation. As well as yielding the more promising results, the selected copper(II) chloride concentration was based on the chloride concentration limit suggested by Oettinger and Fontana (1976), for satisfactory (low corrosion) operation in a 316 stainless steel reactor.

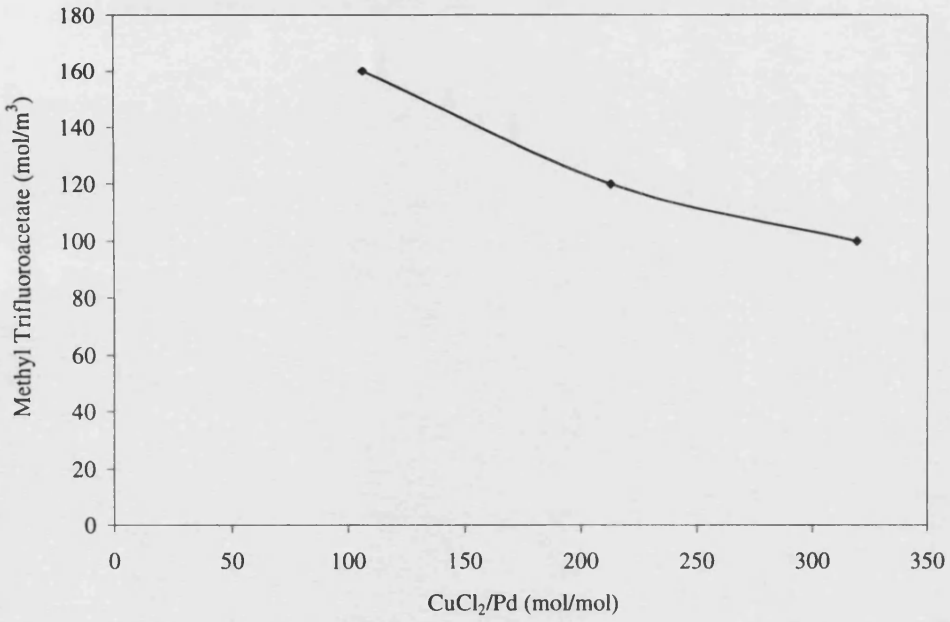

Figure 4.8. Effect of $CuCl_2$ on Product Concentration (Lin *et al.*, 1997)

Conditions: (Batch) P_{CH4} = 62 bar; P_{CO} = 14 bar; P_{O2} = 7 bar;
5 wt.% Pd/C = 1 mg; TFA:H_2O = 3:1 (4 ml);
T = 85 - 95 °C; t = 18 h

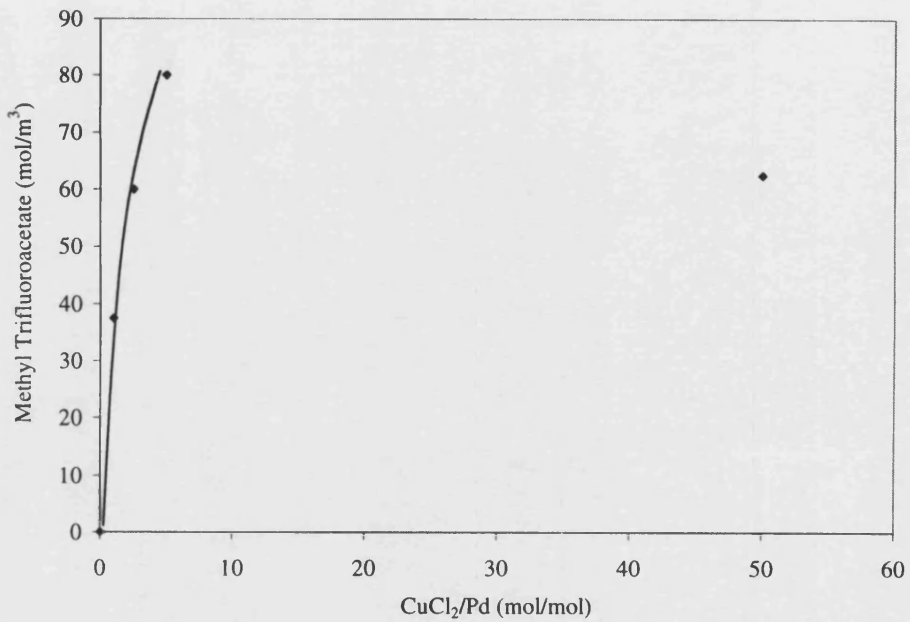

Figure 4.9. Effect of $CuCl_2$ on Product Concentration (Park *et al.*, 2000[a])

Conditions: (Batch) P_{CH4} = 21 bar; P_{CO} = 14 bar; P_{O2} = 7 bar; P_{N2} = 14 bar;
5 wt.% Pd/C = 21.5 mg; TFA:H_2O = 3:1 (4 ml);
T = 80 °C; t = 5 h

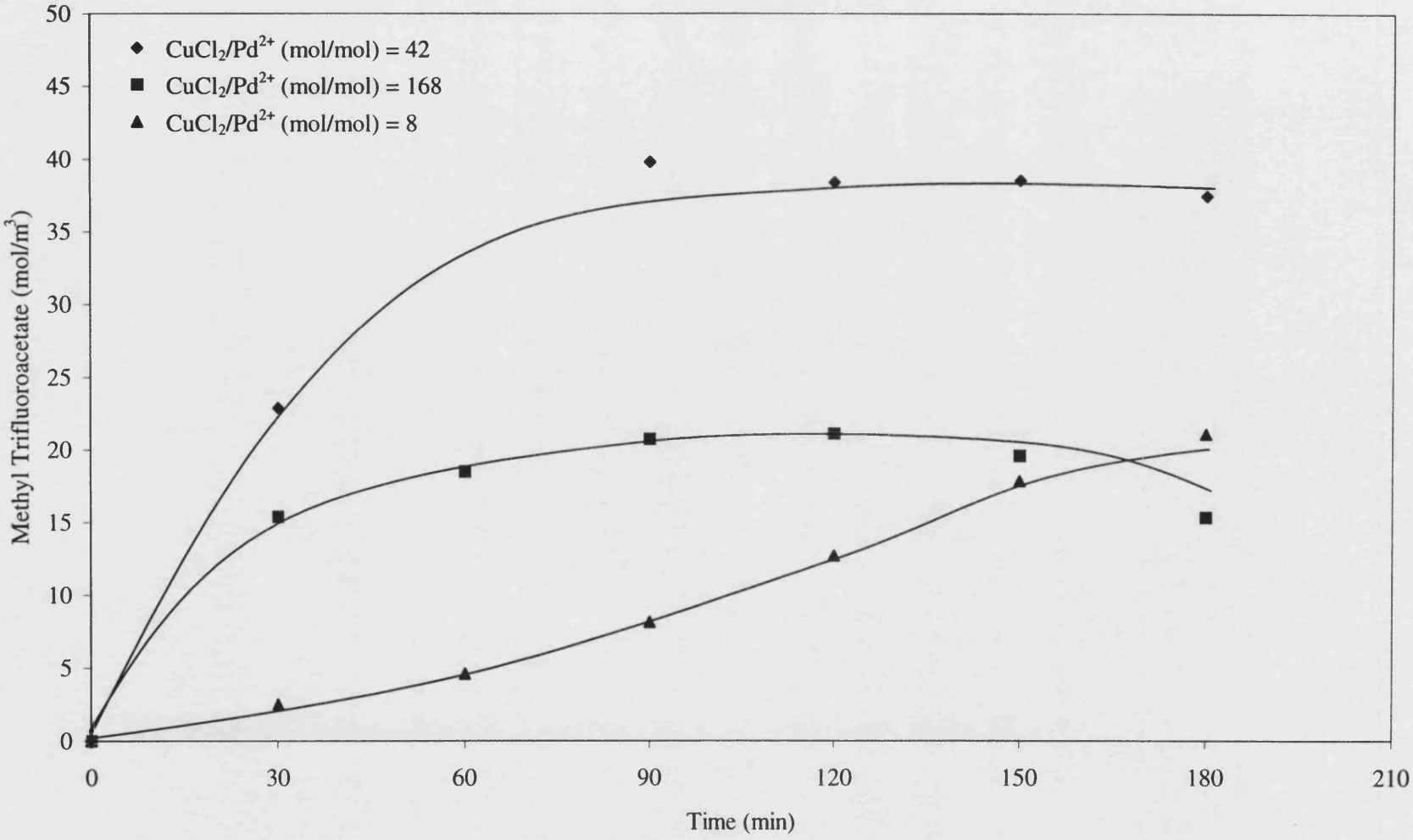

Figure 4.10. Effect of $CuCl_2$ on Product Concentration

Conditions: $P_{CH4(i)}$ = 62 bar; $P_{CO(i)}$ = 14 bar; $P_{O2(i)}$ = 7 bar; Total Flow = 2 l/min; $[Pd^{2+}]$ = 0.12 mol/m^3; TFA:H_2O = 3:1 (300 ml); T = 85 °C

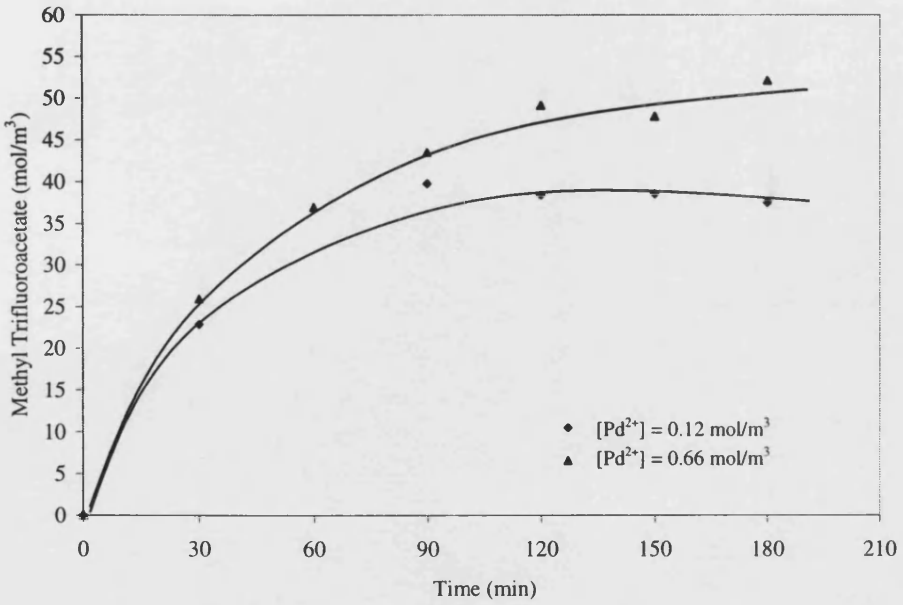

Figure 4.11. Effect of Pd^{2+} on Product Concentration

Conditions: $P_{CH4(i)}$ = 62 bar; $P_{CO(i)}$ = 14 bar; $P_{O2(i)}$ = 7 bar;
Total Flow = 2 l/min; $[CuCl_2]$ = 4.9 mol/m^3;
TFA:H_2O = 3:1 (300 ml); T = 85 °C

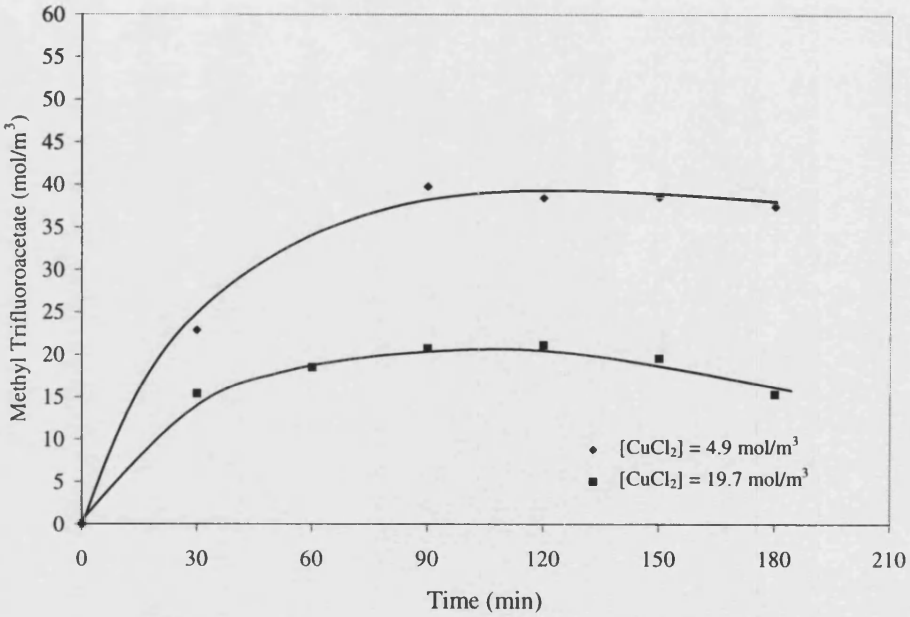

Figure 4.12. Dominant Effect of $CuCl_2$ on Product Concentration

Conditions: $P_{CH4(i)}$ = 62 bar; $P_{CO(i)}$ = 14 bar; $P_{O2(i)}$ = 7 bar;
Total Flow = 2 l/min; $[Pd^{2+}]$ = 0.12 mol/m^3;
TFA:H_2O = 3:1 (300 ml); T = 85 °C

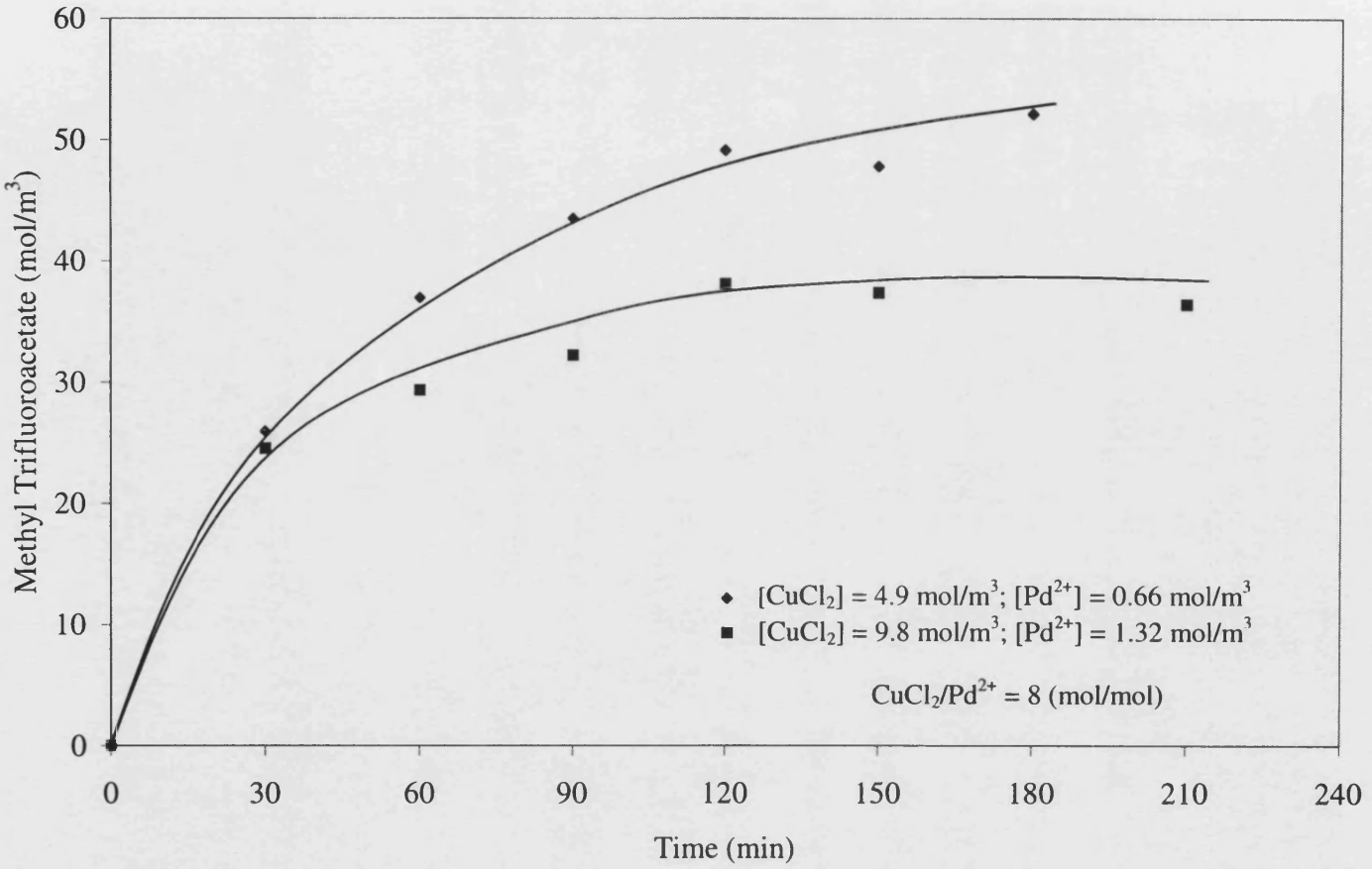

Figure 4.13. Effect of Doubling Catalyst Concentrations on Product Formation

Conditions: $P_{CH4(i)}$ = 62 bar; $P_{CO(i)}$ = 14 bar; $P_{O2(i)}$ = 7 bar; Total Flow = 2 l/min; TFA:H_2O = 3:1 (300 ml); T = 85 °C

4.2.2.3 Influence of Feed Gas Partial Pressures and Flowrates

The effect of varying the initial partial pressure of the gas phase reactants, together with corresponding changes in their flowrates, was studied using the porous tube reactor. The main focus was concentrated on the methane substrate as this was employed at the highest partial pressure out of the three gases. A variation in oxygen partial pressure was not explored due to uncertainties in encountering flammable gas mixtures.

4.2.2.3.1 Influence of Methane Pressure and Flowrate

Three methane pressures and their corresponding flowrates were selected for the experimentation. The results are shown in Figure 4.14. To obtain the observed reaction order with respect to methane, a graph of log([Methyl trifluoroacetate]/h] against log[$P_{CH4(i)}$] was plotted (Figure 4.15). The rate data was obtained for product concentrations after 1 h. Linear regression of the data gave a slope for the methane reaction order of 0.97 ±0.13. Lin *et al.* (1997) obtained a first order methane dependence for pressures up to 700 psi (48 bar), above which a zero order index resumed. In this work an effective first order dependence was seen for methane pressures from 28 - 62 bar. The fact that the former work utilised a pseudo heterogeneous palladium catalyst (K_2PdCl_4 reduced *in situ* by CO to form metallic Pd) in a batch reactor makes the comparison not entirely accurate.

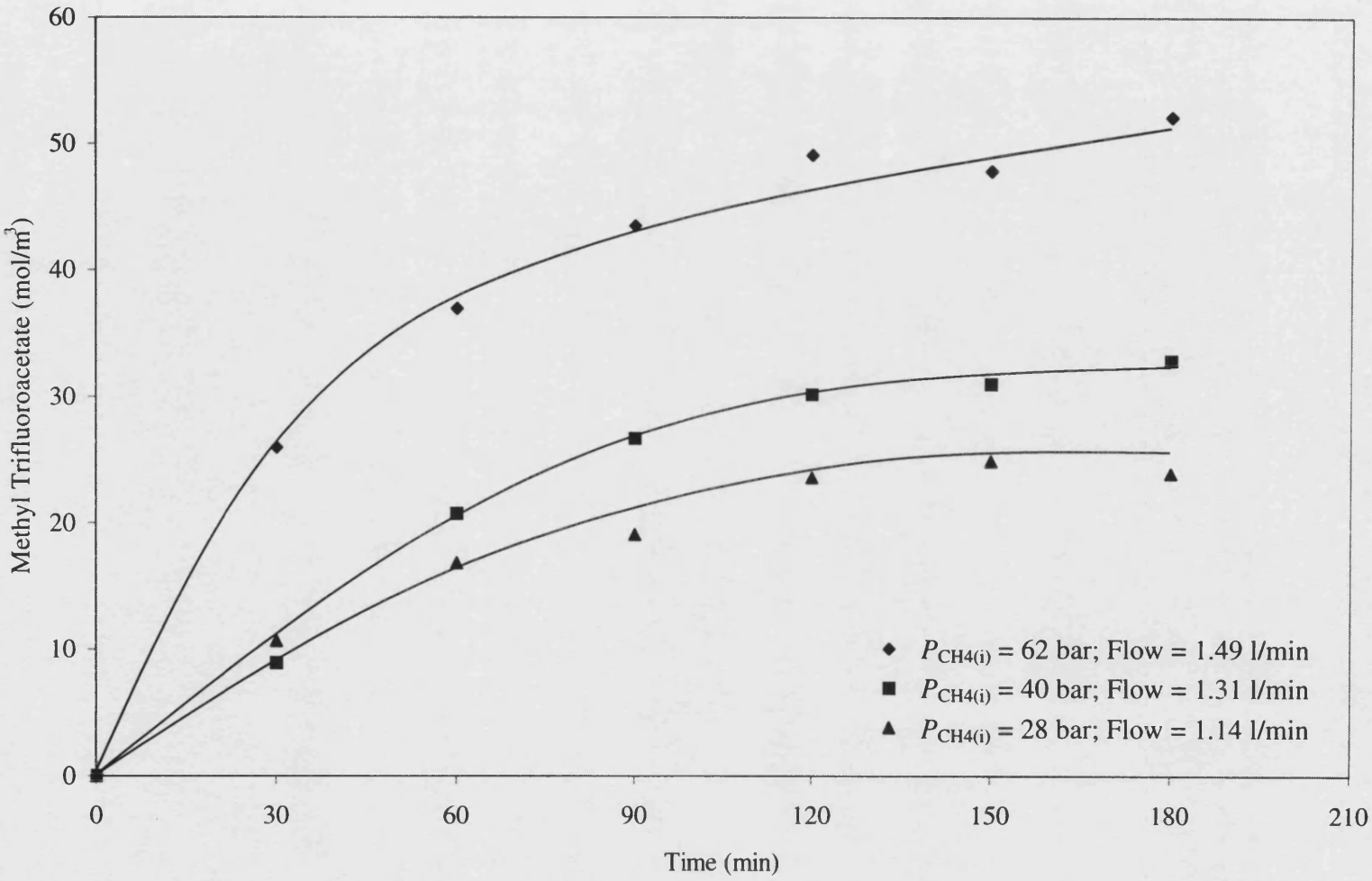

Figure 4.14. Influence of Methane Partial Pressure on Product Formation

Conditions: $P_{CO(i)}$ = 14 bar; $P_{O2(i)}$ = 7 bar; Total Flow = 2 l/min; $[Pd^{2+}]$ = 0.66 mol/m^3; $[CuCl_2]$ = 4.9 mol/m^3; TFA:H_2O = 3:1 (300 ml); T = 85 °C

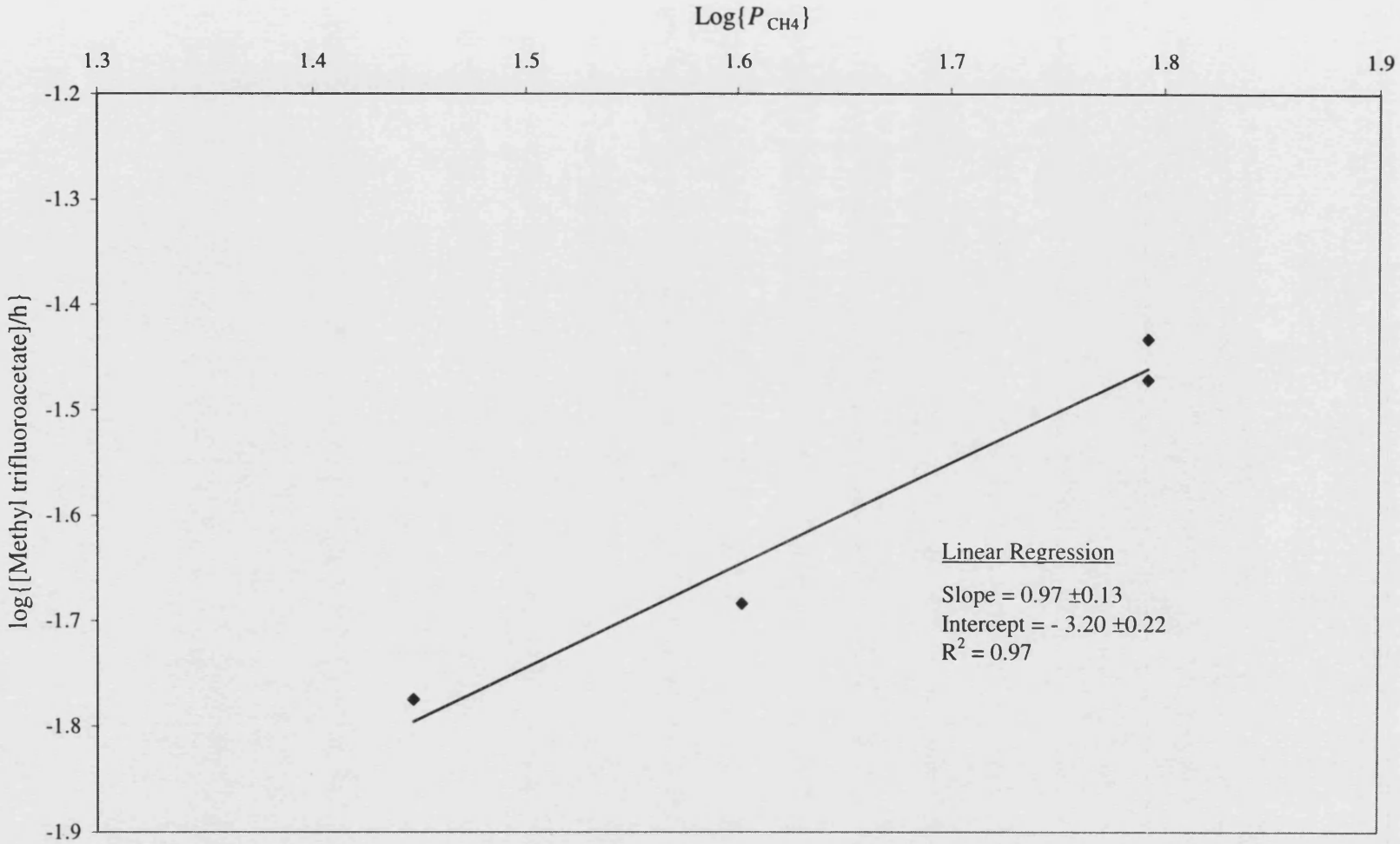

Figure 4.15. Rate Dependence on Methane Partial Pressure

Conditions: $P_{CO(i)}$ = 14 bar; $P_{O2(i)}$ = 7 bar; Total Flow = 2 l/min; $[Pd^{2+}]$ = 0.66 mol/m^3; $[CuCl_2]$ = 4.9 mol/m^3; TFA:H_2O = 3:1 (300 ml); T = 85 °C

4.2.2.3.2 Influence of Carbon Monoxide Pressure and Flowrate

The results of varying the carbon monoxide partial pressure (and flowrate) are shown in Figure 4.16. It can be seen that reducing the carbon monoxide feed had the effect of a reduced rate of product formation. Also, as seen for methane, as the gas partial pressure was reduced, the pseudo end of product formation was observed at a lower concentration. According to the mechanism, CO has two main roles. Firstly, it is involved in the Wacker chemistry for the cyclic generation of metallic palladium, palladium(II), copper(I) and copper(II) oxidation states:

$$Cu^{2+} + Pd(0) \rightarrow Cu^{+} + Pd^{2+} \quad (4.5)$$

$$2Cu^{+} + \frac{1}{2}O_2 + 2H^{+} \rightarrow 2Cu^{2+} + H_2O \quad (4.6)$$

$$Pd^{2+} + CO + H_2O \rightarrow Pd(0) + 2H^{+} + CO_2 \quad (4.7)$$

and secondly for the generation of the *in situ* oxidant, hydrogen peroxide:

$$CO + O_2 + H_2O \rightarrow H_2O_2 + CO_2 \quad (4.8)$$

Thus, due to the aforementioned roles, a reduction in CO would have a detrimental effect on product formation.

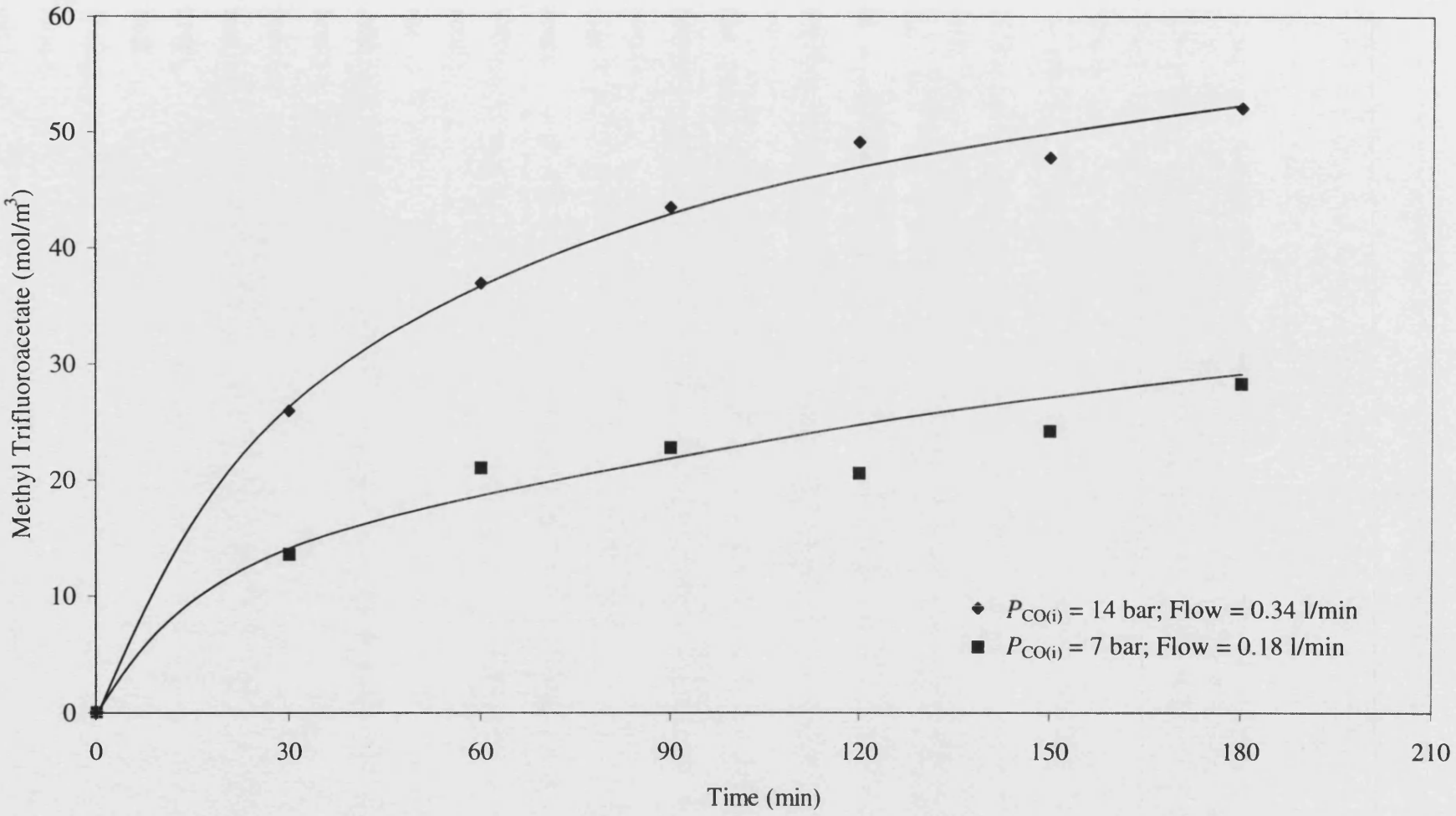

Figure 4.16. Influence of Carbon Monoxide Partial Pressure on Product Formation

Conditions: $P_{CH4(i)}$ = 62 bar; $P_{O2(i)}$ = 7 bar; Total Flow = 2 l/min; $[Pd^{2+}]$ = 0.66 mol/m^3; $[CuCl_2]$ = 4.9 mol/m^3; TFA:H_2O = 3:1 (300 ml); T = 85 °C

4.2.2.4 Operation at a Reduced Pressure

The economics of a hypothetical industrial process would inevitably be impacted on by the pressure requirements. The higher the pressure, the greater the compression costs and the expenses associated with materials required for the fabrication of the reactor and other equipment. Therefore, operation at a lower pressure would be seemingly beneficial. Park *et al.* (2000)[a] employed a pressure of *ca.* 50 bar in their study of this catalytic system. For this current study a similar gas composition (28 bar CH_4; 14 bar CO; 7 bar O_2) at this lower pressure was selected, together with a base composition (62 bar CH_4; 14 bar CO; 7 bar O_2) scaled-down to a total pressure of 50 bar. Because the product concentrations were predicted to be less due to the lower partial pressures of the gases (see Figure 4.14 and Figure 4.16), these experiments were carried out at 120 °C, with the most promising repeated at the normal 85 °C. The results are shown in Figure 4.17. Even at a higher reactor temperature, the product concentrations were lower than those previously performed at the higher pressure of 83 bar at 85 °C using similar catalyst concentrations. An interesting observation with increased temperature operation was that the data obtained was much more "scattered", which may have reflected a decrease in sample condenser efficiency at the elevated temperature. Furthermore, although not mentioned thus far, the differential pressure transducer between the gas inlet and outlet (see Figure 3.3) indicted a significant increase in its value during the course of the reaction. At the base temperature of 85 °C, this pressure was effectively stable throughout the time course. Figure 4.18 depicts this data. On opening the reactor for routine cleaning and maintenance, evidence of liquid foaming was visible on the walls of the hold-up vessel. This was not observed after operation at the lower temperature. Although the exact cause of this increased pressure drop cannot be pinpointed with the limited data obtained, subsequent runs at a lower temperature using the same tube did not indicate a similarly high pressure drop. This observation suggests that internal fouling/plugging of the porous tube was unlikely to have been the cause of the pressure drop, with it therefore being due to a changing composition (chemical or physical) of the bulk liquid at the higher temperature, with potential "blocking" in the liquid-line itself. Unfortunately, these observations indicated limitations of the catalytic system for higher temperature operation and was a reason why temperature kinetic studies were not carried out in any further experimentation using the porous tube reactor.

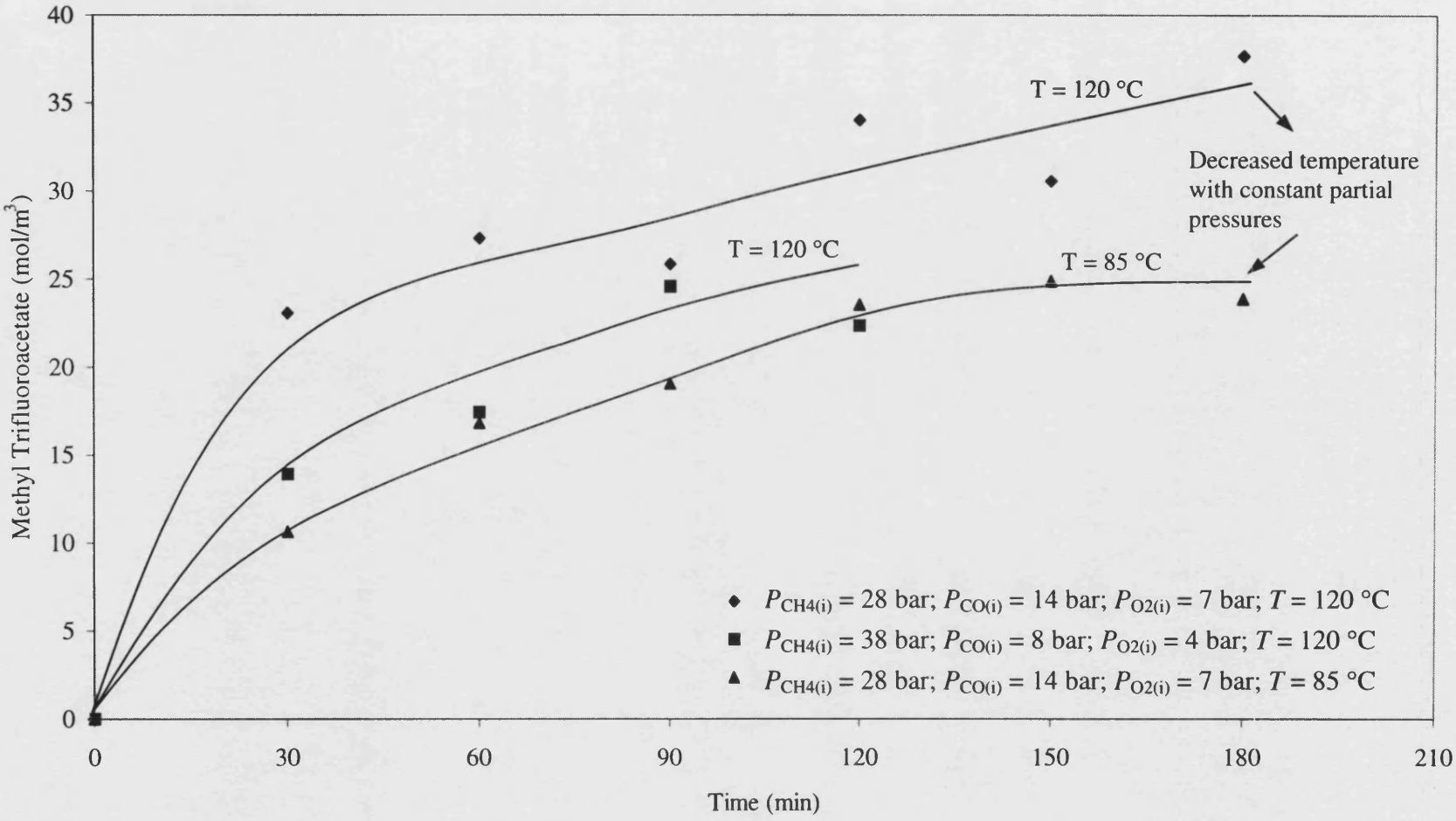

Figure 4.17. Semi-continuous Operation at a Reduced Pressure

Conditions: $P_{Total} \approx 50$ bar (exc. 1 - 3 bar vapour pressure); Total Flow = 2 l/min; $[Pd^{2+}] = 0.66$ mol/m^3; $[CuCl_2] = 4.9$ mol/m^3; TFA:H_2O = 3:1 (300 ml); $T = 85$ °C

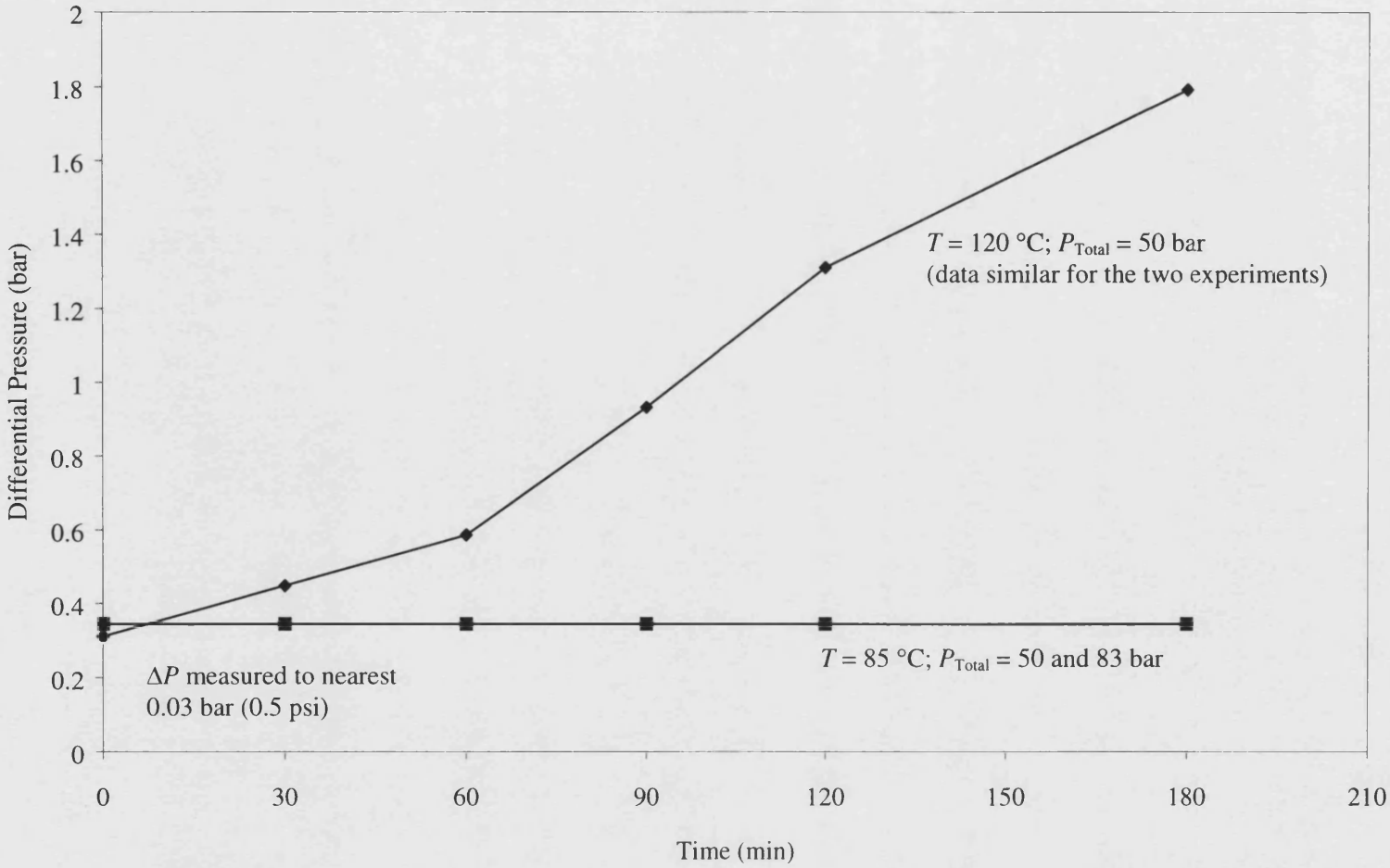

Figure 4.18. Differential Pressure Time Course at Elevated Operating Temperatures

Conditions: Total Flow = 2 l/min; $[Pd^{2+}]$ = 0.66 mol/m^3; $[CuCl_2]$ = 4.9 mol/m^3; TFA:H_2O = 3:1 (300 ml)

4.2.2.5 Increased Reactor Run Time and System Performance

By comparing the batch experimental data in Figure 4.1 with that obtained using the semi-continuous reactor *e.g.* Figure 4.10 and Figure 4.14, it can be seen that in both cases methyl trifluoroacetate product formation effectively stops after *ca.* 1.5 - 2 h. In the case of the batch experiments it was suggested that gas reactant depletion could be responsible for this observation. However, data obtained using the semi-continuous reactor indicated that this was not the case, as the gas phase was continuously supplied to the liquid reactants. To be more certain that this observed pseudo-end was not a temporary phenomenon *e.g.* the reaction rate starts to increase again, an experiment was carried out for a run time of 5 h. The results are shown in Figure 4.19 with the TON and STY depicted in Figure 4.20 and Figure 4.21 respectively.

The data again showed the general trend in that after approximately 2 hours, the product formation was limited. Thus, whilst the increase in TON also depicts a similar format, the STY actually decreases with time in correspondence with the decrease in the rate of product formation. Product degradation was not really evident by the end of the longer batch run (Figure 4.19) although appeared a possibility towards the end of a 3 hour run with a high copper(II) chloride concentration (Figure 4.7). However, product decay was observed, albeit after longer batch times, in other methane oxidation works involving the methyl trifluoroacetate product (*e.g.* Piao *et al.*, 1999; Kao *et al.*, 1991). In the presence of hydrogen peroxide, the overoxidation of methyl trifluoroacetate was shown to have been catalysed by Pd^{2+} (Kao *et al.*, 1991). Indication of product degradation in the presence of the bimetallic catalyst and the *in situ* oxidant (H_2O_2) was also shown in an exemplary batch experiment in this current study (see Section 4.3.3 and Appendix I). Therefore, it appears that reactor run times may be a significant factor to consider, in light of observable product degradation occurring. However, in the batch experiments (see *e.g.* Figure 4.1), no net product degradation was observed after 20 hours and so this factor alone cannot explain the apparent end of the reaction after only 2 hours in both the batch and semi-continuous experiments. One factor inherent in the porous tube reactor, was the possibility of product removal via gaseous stripping. Although condensers were available to "trap" any entrained vapour *e.g.* from the TFA solvent, the condensate would probably not return efficiently to the main reactor liquid phase because of "build-up" on the cold condenser walls. Hence, some formed product would not be analysed in the bulk mixture. The extent of this product stripping forms the topic of the next section.

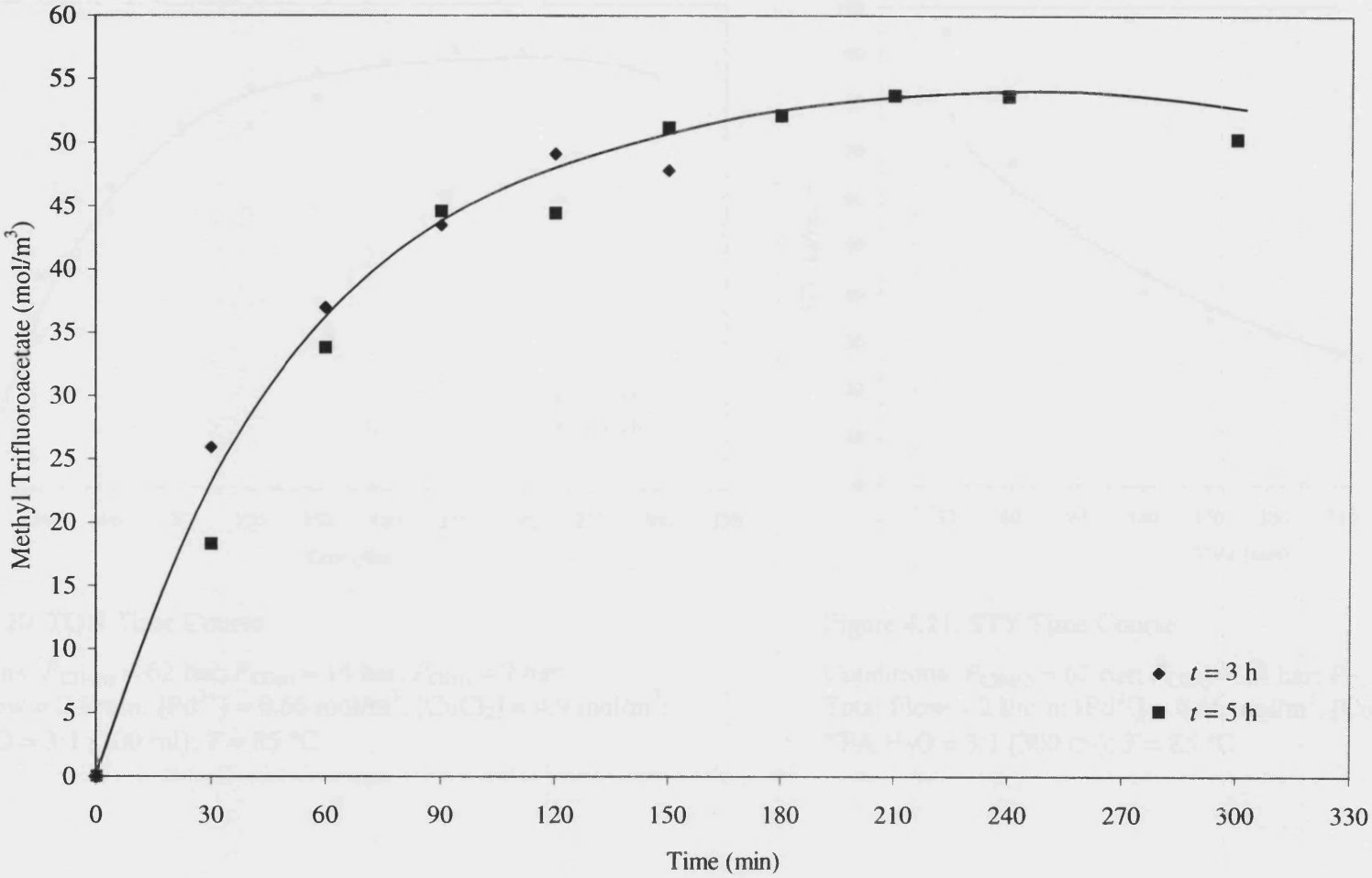

Figure 4.19. Increased Reactor Run Time

Conditions: $P_{CH4(i)}$ = 62 bar; $P_{CO(i)}$ = 14 bar; $P_{O2(i)}$ = 7 bar; Total Flow = 2 l/min; $[Pd^{2+}]$ = 0.66 mol/m^3; $[CuCl_2]$ = 4.9 mol/m^3; TFA:H_2O = 3:1 (300 ml); T = 85 °C

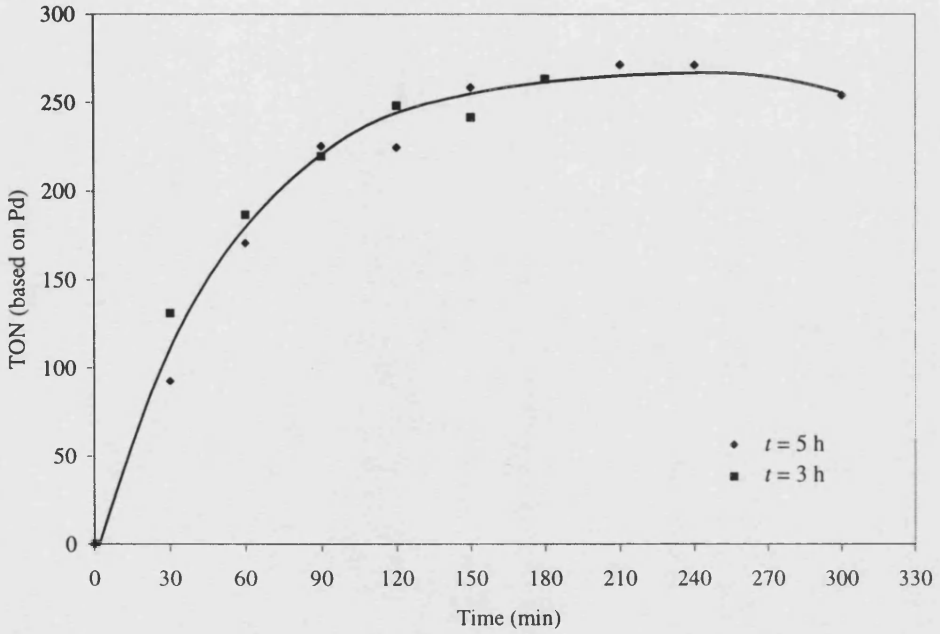

Figure 4.20. TON Time Course

Conditions: $P_{CH4(i)}$ = 62 bar; $P_{CO(i)}$ = 14 bar; $P_{O2(i)}$ = 7 bar;
Total Flow = 2 l/min; $[Pd^{2+}]$ = 0.66 mol/m^3; $[CuCl_2]$ = 4.9 mol/m^3;
TFA:H_2O = 3:1 (300 ml); T = 85 °C

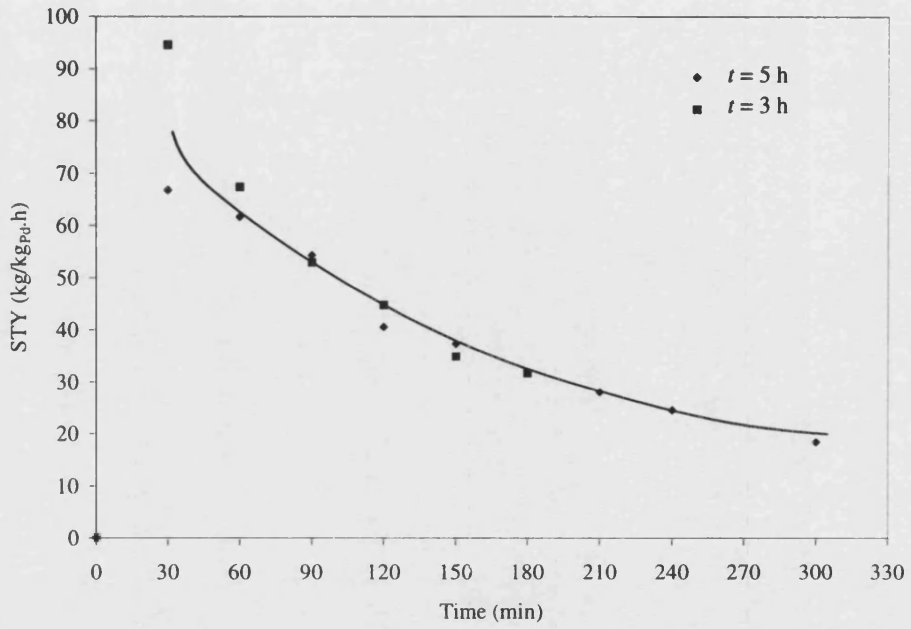

Figure 4.21. STY Time Course

Conditions: $P_{CH4(i)}$ = 62 bar; $P_{CO(i)}$ = 14 bar; $P_{O2(i)}$ = 7 bar;
Total Flow = 2 l/min; $[Pd^{2+}]$ = 0.66 mol/m^3; $[CuCl_2]$ = 4.9 mol/m^3;
TFA:H_2O = 3:1 (300 ml); T = 85 °C

4.2.2.6 Product Removal/Stripping within the Porous Tube Reactor

The removal of methyl trifluoroacetate product via gaseous entrainment in the porous tube reactor is a possible limitation of the reactor's efficient use in methane oxidation experiments. The problem lies in the fact that although two condenser system were located on the gas exit from the hold-up vessel (see Figure 3.3), any "trapped" product would "build-up" on the cold walls of the condensers and not all return to the main re-circulating liquid phase. To ascertain the extent of this happening, experiments were conducted in the absence of the methane substrate, but with an initial quantity of methyl trifluroracetate in the catalyst-containing liquid phase. Runs were carried out in the presence of nitrogen only and also with a mixture of nitrogen and oxygen, the latter effecting a wet-air oxidation environment. The results are displayed in Figure 4.22.

In both cases, product removal was evident, with the effect of added oxygen having only a marginal influence. The rate of this removal appeared reasonably constant throughout the run time, with only an initial lag during the first 30 minutes. Regression of the data obtained from the nitrogen and oxygen run, revealed an estimate for the rate of product "loss" of 11 $mol/m^3.h$.

The data indicates that the pre-described end of product formation is misleading terminology for the porous tube reactor, because product must have been formed to compensate for its removal. Nevertheless, the rate of product formation must have decreased significantly from the start (observed net rate for "best" run (see Figure 4.19) over the first hour was *ca.* 37 $mol/m^3.h$, compared with a removal rate of 11 $mol/m^3.h$), an observation that cannot be attributed to reactant depletion. Furthermore, as a similar phenomenon of product formation was also observed in the batch reactor in which no product stripping would occur, this delimiting effect cannot solely explain the cause of the observed decrease in product formation in both of the reactors.

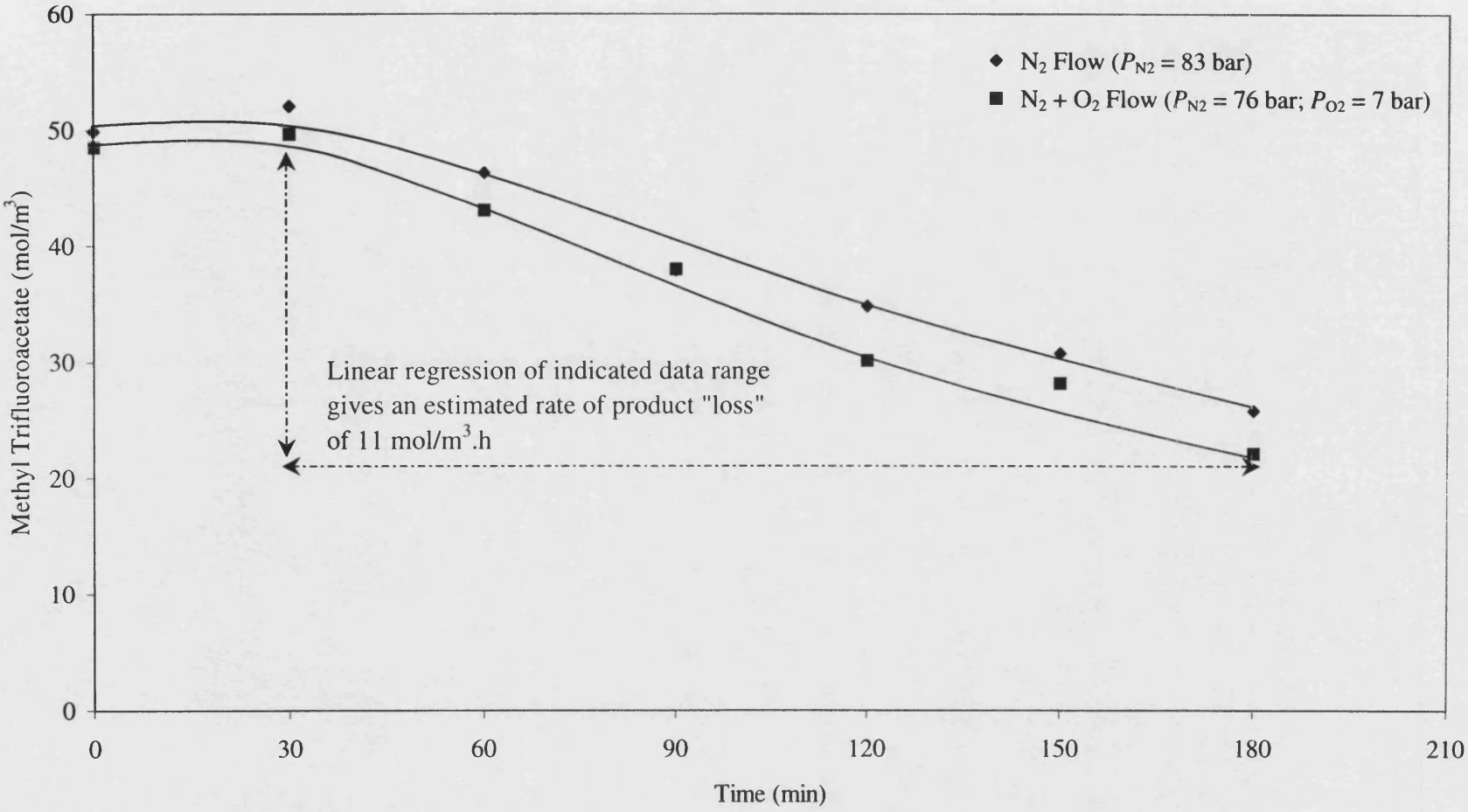

Figure 4.22. Extent of Product Removal within the Porous Tube Reactor

Conditions: Total Flow = 2 l/min; $[Pd^{2+}]$ = 0.66 mol/m^3; $[CuCl_2]$ = 4.9 mol/m^3; TFA:H_2O = 3:1 (300 ml); T = 85 °C

4.2.3 The Use of Heterogeneous Palladium

In Section 4.2.1, the fate of the catalytic porous tube was discussed concluding with its incompatibility with the system. To test whether the use of a heterogeneous palladium catalyst would result in an increased product formation, the commercial Pd/C catalyst powder was used, as in the batch experiments. Although it was uncertain if the natural circulation was sufficient to support a suspension of the particles as in a slurry-type reactor, with also the possibility of blockages in the valve systems occurring, the use of the Pd/C catalyst was nevertheless tried to ascertain whether it had any positive effect. (A ballpark calculation for the settling velocity of a catalyst particle, comparing it with the rising superficial liquid velocity, is detailed in Appendix VII.)

Experiments were conducted with two different catalyst amounts; one based on that used in the batch experiments (Pd/C loading = 0.25 kg/m^3 $\Rightarrow$ [Pd] = 0.12 mol/m^3, $[CuCl_2]$ = 20 mol/m^3), and the other resulting with the "best" product concentrations from this semi-continuous work (Pd/C loading = 1.4 kg/m^3 $\Rightarrow$ [Pd] = 0.66 mol/m^3, $[CuCl_2]$ = 4.9 mol/m^3). The results are displayed in Figure 4.23, together with their equivalent homogenous palladium runs.

With respect to the catalyst amounts, a similar trend to the homogeneous experiments was observed; an excess amount of copper(II) chloride caused less product to be formed with evidence of product degradation. Also, there were still signs of a decreased reaction rate after *ca.* 1.5 hours. However, the product concentrations obtained were less than those from using the homogeneous palladium catalyst. This could be attributed to poor mixing of the catalyst particles or simply the use of a different form of palladium (bulk Pd supported on carbon). Comparing the results with those from the batch work, significantly less product was formed after 3 hours using the porous tube reactor (batch = 45 mol/m^3; semi-continuous = 17 mol/m^3) employing similar catalyst concentrations. Again poor particle mixing in the porous tube reactor, compared to the batch reactor may go someway in explaining this discrepancy.

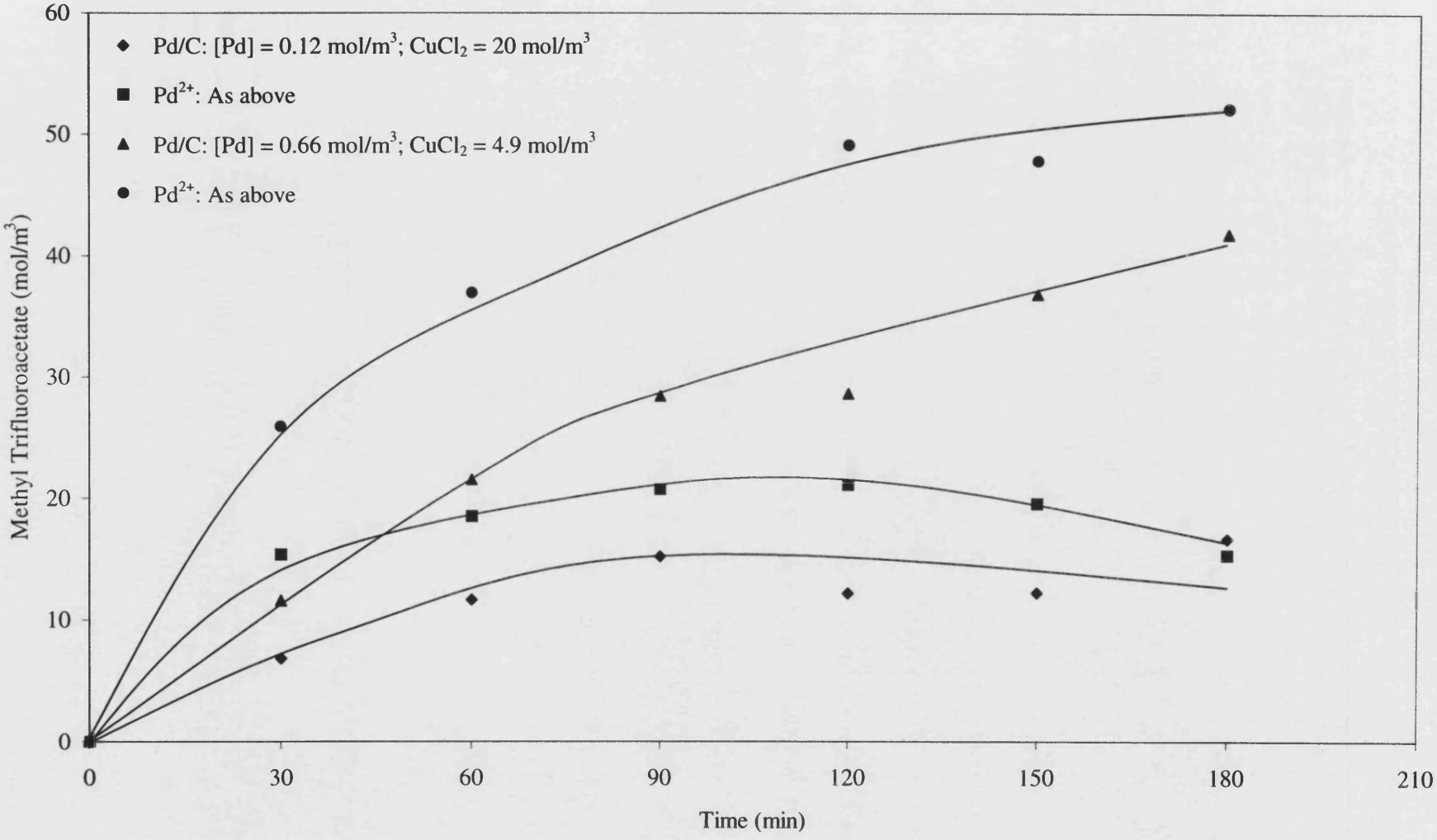

Figure 4.23. Heterogeneous Palladium Versus Homogeneous Palladium Catalysis

Conditions: $P_{CH4(i)}$ = 62 bar; $P_{CO(i)}$ = 14 bar; $P_{O2(i)}$ = 7 bar; Total Flow = 2 l/min; TFA:H_2O = 3:1 (300 ml); T = 85 °C

4.2.4 Relevance of Temperature Indication to Reaction

From the batch experiments, observation of the liquid temperature showed a slight (*ca.* 2 °C) increase at the start of the reaction (see Figure 4.3). Because this increase was relatively small, no firm conclusions could be established whether or not it was due to a reaction exotherm. Although not mentioned until now, a similar observation of increased temperature arose from the experiments performed in the porous tube reactor. Exemplary temperature profiles are shown in Figure 4.24.

It can be seen that there was an increase in liquid temperature during the first 10 minutes of the time course. From the magnitude of this increase (5 to 10 °C), it can be concluded that chemical reaction was responsible and not other sources *e.g.* external heater control. Whilst similar temperature profiles were obtained for both the homogeneous and heterogeneous palladium (0.66 mol/m^3) runs, a much greater increase was observed when the catalyst amounts were doubled. The origin of the chemical heat release can be foreseen by considering the three main reactions of the proposed chemical mechanism:

1) Wacker oxidation of CO (Park *et al.*, 2000[a]):

$$CO + \frac{1}{2}O_2 \rightarrow CO_2 \qquad \Delta H^o_{25°C} = -283.0 \text{ kJ/mol} \qquad ((4.2))$$

2) *In situ* hydrogen peroxide formation

$$CO + O_2 + H_2O \rightarrow H_2O_2 + CO_2 \qquad \Delta H^o_{25°C} = -133.3 \text{ kJ/mol} \qquad ((4.8))$$

3) Methane oxidation

$$CH_4 + H_2O_2 \rightarrow CH_3OH + H_2O \qquad \Delta H^o_{25°C} = -313.4 \text{ kJ/mol} \qquad (4.9)$$

From batch experiments, a similar initial temperature rise was observed both in the presence and in the absence of the methane substrate. Thus, the observed temperature increase was likely to have been derived from the Wacker oxidation of CO and/or the *in situ* formation of hydrogen peroxide. The use of an increased catalyst amount resulted with a higher temperature rise, although no amelioration in ester product formation was

observed (see Figure 4.13). This latter information also supports the origin of the temperature rise not being attributable to methane functionalisation.

A measurable temperature rise was not reported in the literature works, but this could be the result of the increased liquid volumes in the current work facilitating accurate temperature recordings with the continuous flow of gaseous reactants (porous tube reactor) perpetuating the initial heat release.

In light of this information regarding the exothermicity of the reaction, this current work has highlighted a factor that must be taken into account for a larger scale implementation of this system.

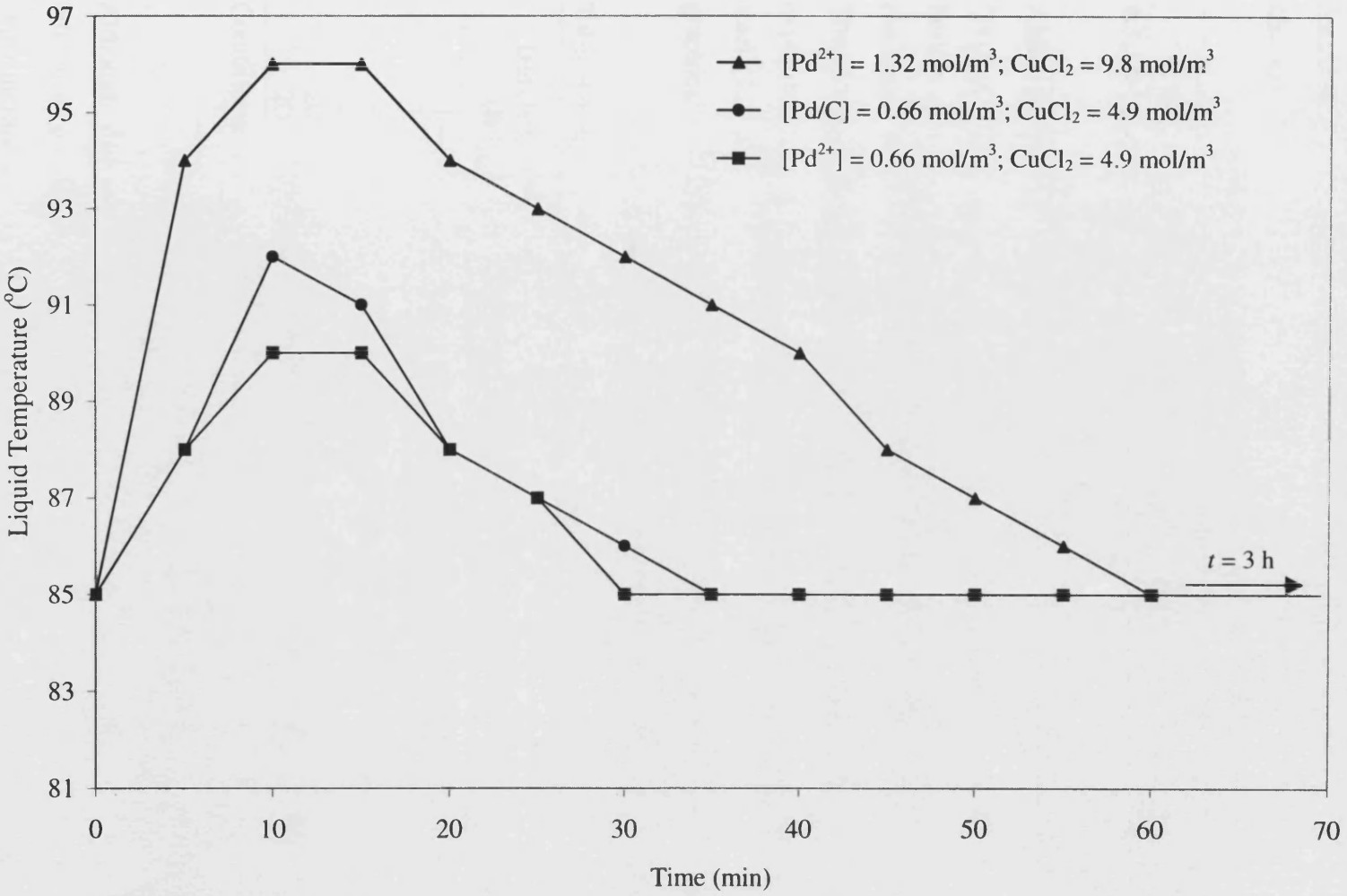

Figure 4.24. Porous Tube Reactor Exemplary Temperature Profiles

Conditions: $P_{CH4(i)}$ = 62 bar; $P_{CO(i)}$ = 14 bar; $P_{O2(i)}$ = 7 bar; Total Flow = 2 l/min; TFA:H_2O = 3:1 (300 ml); T = 85 °C

4.3 Further Exploration for an Improved Catalytic System

This section describes additional experimental work, performed in the batch reactor, focussed on both obtaining a further understanding of the system and incorporating novel changes with an impetus to develop an improved methane oxidation system.

4.3.1 Effect of Reactor Material on Reaction Performance

Although the batch reaction vessel was glass-lined and had PTFE covered internals, a "perfect" exclusion of the core reactor material (316 stainless steel) was not guaranteed. Furthermore, the application of the semi-continuous porous tube reactor meant that the reactants came into unavoidable contact with the stainless steel walls of this reactor. Therefore, in an attempt to gauge the influence of the stainless steel reactor material, experiments were carried out in the presence of a 20 × 20 × 1 mm sample of 316 stainless steel (316 SS) attached to the stirrer body. The key results are shown in Table 4.4 and graphically in Figure 4.25.

Table 4.4. Effect of 316 Stainless Steel on Base Reaction

Batch Time (h)	**316 Stainless Steel (Yes/No)**	**Reaction ΔP (bar)**	**[Methyl trifluoroacetate] (mol/m^3)**
1	Yes	8	38
1	No	7	40
2	Yes	10	49
2	No	9.5	50
20	Yes	11	54
20	No	11	51

Conditions: $P_{CH4(i)}$ = 62 bar; $P_{CO(i)}$ = 14 bar; $P_{O2(i)}$ = 7 bar; 5 wt.% Pd/C = 12.5 mg; [$CuCl_2$] = 20 mol/m^3; TFA:H_2O = 3:1 (50 ml); T = 85 °C; N = 700 rpm

Although this test was by no means exhaustive, the results indicate no significant influence of the stainless steel on the reaction performance under the employed experimental conditions. Perry and Green (1984) gives a composition for 316 stainless steel as: Cr (16-18 %), Ni (10-14 %), Mo (2 - 3 %), C (0.08 %), Si (1 %), Mn (2 %) with the balance being Fe. In the corrosive environment of TFA and chloride ions, some

leaching of metal components from the stainless steel could occur. The effect of other metal ions *e.g.* Fe^{2+}, Mn^{2+}, for the reaction chemistry has been studied by both Lin *et al.* (1997) and Park *et al.* (2000)[a] with the general conclusion that these species were active for the reaction, but not as productive as the intended Cu^{2+} ion. Therefore, because the product yields obtained in both the reactors involved in this current study and in the original work were relatively low, it was not thought necessary to totally exclude any contact with the stainless steel and repeat the experiments. This point is especially poignant with the porous tube reactor whereby replacement of the main stainless steel body with another high pressure, chemically resistant material *e.g.* Hastelloy would be very costly and not justified for these initial feasibility studies.

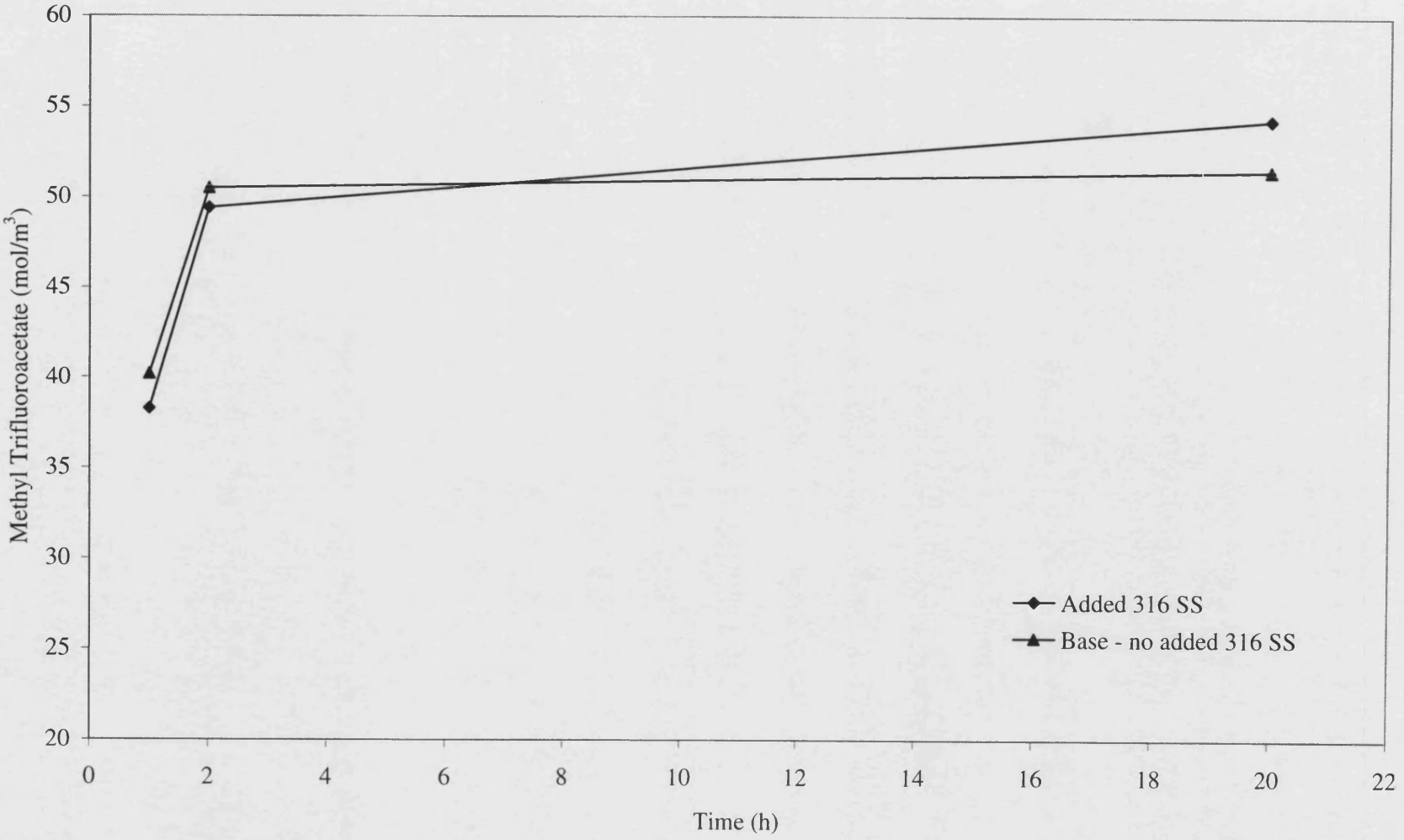

Figure 4.25. Effect of 316 Stainless Steel on Reaction Performance

Conditions: $P_{CH4(i)}$ = 62 bar; $P_{CO(i)}$ = 14 bar; $P_{O2(i)}$ = 7 bar; 5 wt.% Pd/C = 12.5 mg; [$CuCl_2$] = 20 mol/m^3; TFA:H_2O = 3:1 (50 ml); T = 85 °C; N = 700 rpm

4.3.2 Preliminary Study of the Relevance of the Liquid Phase Constitution to Reaction Performance

The focus on the relevance of the gas phase constituents was detailed in Section 4.1.3. This section looks at the contribution of individual species in the liquid phase to the methane oxidation reaction. The approach is only qualitative in that experiments were performed with the omission of a particular species from the liquid reaction mixture and subsequent observations of the reaction pressure drop and final product yield made.

The species present in the liquid phase reactant mixture were 5 wt.% Pd/C (Pd + C), $CuCl_2$ (Cu^{2+} + Cl^-), CF_3COOH (CF_3COO^- + H^+) and H_2O. To allow for segregation of these components the following compounds were used:

$CuSO_4$ ($\rightarrow Cu^{2+}$)
HCl (1M) ($\rightarrow H^+$ and Cl^-)
NaCl ($\rightarrow Cl^-$)
$Cu(CF_3COO)_2$ ($\rightarrow Cu^{2+}$and CF_3COO^-)

The concentrations of the reagents used mimicked the species' concentration in the base mixture that was used in the previous batch experimentation. Substitution of both the H^+ by HCl and CF_3COO^- by $Cu(CF_3COO)_2$ from the TFA was based on the concentration of the chloride ions and the copper(II) ions respectively. The effect of carbon (from Pd/C) was not studied as this was reported to have no influence by Lin *et al.* (1997). Also, the solvent composition of TFA:water was not varied as both Park *et al.* (2000)[a] and Lin *et al.* (1997) concluded that a 3:1 mixture yielded the highest productivity. However some experiments were performed in a sole water solvent.

The results are shown in Table 4.5

Table 4.5. Relevance of Liquid Phase Species to Reaction Performance

Omitted Species (from base mixture)	**Solvent**	**Reaction ΔP (bar)**	**[Methyl trifluoroacetate] (mol/m^3)**	**Methyl trifluoroacetate Yield (%)**	**TON (based on Pd catalyst)**	**STY ($kg/kg_{Pd}.h$)**
None (Base)	TFA/H_2O	11	50	1.5	430	259
5 wt.% Pd/C	TFA/H_2O	3	5	0.2	46	18.4
Cu^{2+}	TFA/H_2O	9	11	0.3	97	39.0
Cl^-	TFA/H_2O	0	0	-	-	-
5wt.% Pd/C and Cu^{2+}	TFA/H_2O	2	4	0.2	33	13.3
CF_3COO^-	H_2O	7.5	N/A	-	-	-
H^+	H_2O	4.5	N/A	-	-	-
None	H_2O	6.5	N/A	-	-	-

Conditions: $P_{CH4(i)}$ = 62 bar; $P_{CO(i)}$ = 14 bar; $P_{O2(i)}$ = 7 bar; T = 85 °C; N = 700 rpm; t = 3 h.
Were relevant $[Cu^{2+}]$ = 20 mol/m^3; $[Cl^-]$ = 40 mol/m^3; 5wt.% Pd/C = 12.5 mg; $TFA:H_2O$ = 3:1 (Total = 50 ml)

The first observation to make is that any change in the catalytic system from the base composition resulted in a significantly lower amount or even absence of a methanol-based product. This was further augmented by a reduced reaction pressure drop. The change in solvent from a 3:1 mixture of TFA:water to only water resulted with no methanol-based products being formed even in the presence of all the ions including those derived from the TFA. This highlights the requirement of a TFA-based solvent. Although not shown, in the absence of water, the ionic solids were insoluble in TFA and furthermore, according to the proposed mechanism (Figure 2.12), water was a reactant. Therefore water was also deemed necessary and experiments in a pure TFA solvent were not performed.

Another key observation is the synergy of the palladium and copper. The absence of either one of them was deleterious. This goes some way in reinforcing the proposed Wacker chemistry for these two species (Park *et al.*, 2000[a]).

The requirement of chloride ions seems paramount as no indication (product formation or pressure drop) of a reaction was observed in their absence. This was also noted by the aforementioned previous authors and also in systems proposed for the generation of H_2O_2 from CO, O_2 and H_2O (*e.g.* Bianchi *et al.*, 1999) and from H_2 and O_2 (*e.g.* Gosser, 1987). As a H_2O_2 *in situ* generated oxidant was proposed for this methane oxidation reaction, the result indicates a possible relevance of the chloride ions for the oxidant formation.

4.3.3 Use of Hydrogen Peroxide as Stoichiometric Oxidant

According to the elucidated mechanism (Figure 2.12) proposed by the original workers (Lin *et al.*, 1997; Lin *et al.*, 1992), hydrogen peroxide was formed *in situ* from carbon monoxide, oxygen and water. Therefore, it was logical to attempt methane oxidation using hydrogen peroxide (H_2O_2), omitting its *in situ* generation step:

$$CH_4 + H_2O_2 + CF_3COOH \rightarrow CF_3COOCH_3 + 2H_2O \qquad ((4.4))$$

In the experiments performed in this current study it was not possible to obtain reliable H_2O_2 concentrations because the necessary redox titration of the sample with potassium permanganate is accompanied by a colour change. As the final product sample was very dark in colour, this colour change would not be observable. Lin *et al.* (1992) performed an experiment in the absence of methane and obtained a concentration for H_2O_2 of 2 mol/m^3. Although possibly only a one-off experiment, they mentioned that their post-reaction solution had been colourless due to some reduction of the $CuCl_2$ to CuCl by the CO. A white precipitate (CuCl) was also seen in this current work in the absence of a methane substrate, although complete precipitation was not observed, with it is easily being re-oxidised back in solution by the oxygen, as in the Wacker chemistry. The differences observed in the two works could be explained by the gas-to-liquid ratios employed, with the cited work having a large excess of carbon monoxide exposed to the 4 ml liquid phase containing the $CuCl_2$. In the more recent work of Park *et al.* (2000) the colour of the solution was not disclosed.

A problem associated with H_2O_2 is its tendency to undergo metal catalysed decomposition:

$$2H_2O_2 \rightarrow 2H_2O + O_2 \qquad (4.9)$$

Therefore, this side-reaction would be catalysed by both the palladium and the copper present in the reaction mixture and hence inferred concentrations would only be estimates.

For the purpose of this work, 2 mol/m^3 was used as the base H_2O_2 concentration, with both a 10-fold and 100-fold increase from this value also studied. Both heterogeneous (Pd/C) and homogeneous (Pd^{2+}) were used with the latter being proposed for the actual methane functionalisation by Park *et al.* (2000)[a]. The catalyst concentrations were the same as those used for the base experiments with the methane partial pressure being 62 bar. Although the reaction was carried out at 85 °C, the methane was added to the cold reactor prior to heating to expose it to the H_2O_2, which would simultaneously be undergoing metal catalysed decomposition that is accelerated by temperature.
The results are highlighted in Table 4.6.

Table 4.6. Use of H_2O_2 as Stoichiometric Oxidant

$[H_2O_2]$ (mol/m^3)	**Catalysts**	**Batch Time (h)**	**[Methyl trifluoroacetate] (mol/m^3)**
2	Pd/C + $CuCl_2$	20	0
20	Pd/C + $CuCl_2$	20	0
200	Pd/C + $CuCl_2$	3	0
200	Pd/C + $CuCl_2$	20	0
200	None	20	5
200	Pd^{2+}	3	0
2	Pd^{2+} + $CuCl_2$	3	0
200	Pd^{2+} + $CuCl_2$	3	0
200	$^*Pd^{2+}$ + $CuCl_2$	3	5
2	$^*Pd^{2+}$ + $CuCl_2$	3	0

Conditions: $P_{CH4(i)}$ = 62 bar; 5 wt.% Pd/C = 12.5 mg; [$CuCl_2$] = 20 mol/m^3; TFA:H_2O = 3:1 (50 ml); T = 85 °C; N = 700 rpm
*These experiments have an added 14 bar of CO

The results indicate that effectively no product was formed with the concentrations of H_2O_2 used. The last two entries in Table 4.6 incorporate the use of CO, which acts as a reducing agent for Pd^{2+} in the Wacker oxidation process (see equations (4.5 - 4.7)).
It was envisaged that the CO would help effect the synergistic relationship between the palladium and copper catalysts such as to favour the methane oxidation reaction, but the small amount of product formed was not conclusive as to its influence.
At first glance the results seem disheartening in that they don't support a hydrogen peroxide intermediate for the studied reaction. Lin *et al.* (1992), effected ethane oxidation to ethanol and other products using H_2O_2. However, they did not report the same reaction using a methane substrate, which is significantly less reactive than the former. To

ascertain whether the methyl trifluoracetate product was overoxidised by H_2O_2 and therefore not being detected by the GC, an experiment was performed in the batch reactor using *in situ* formed H_2O_2 (from CO, O_2 and H_2O) and *ca.* 1 % of the methyl trifluoroacetate product in the catalyst containing TFA-based solvent. After 3 h at 85 °C, approximately 18 % of the product had been converted or oxidised. In a similar experiment involving oxygen and nitrogen in the gas phase, little evidence of ester product degradation was observed. This shows that H_2O_2 was more potent for the product degradation than O_2 but does not explain the total absence of product from the methane oxidation reactions using H_2O_2. Perhaps the key to the effective "difficult" methane oxidation is "fresh" *in situ* generated H_2O_2. Nevertheless, it is a concern as to why the direct use of H_2O_2 for the oxidation of methane in this specific catalyst system has not yet been reported, especially by the pioneers of this system. One explanation given for this was the side reaction of metal decomposition of H_2O_2 limited its use as a reagent for this system. In this current work, an increase in reactor pressure was observed (rather than the normal decrease) which indicated the presence of a possible H_2O_2 decomposition reaction (equation (4.9)). Further work in the understanding of this mechanism is undoubtedly required but is outside the scope of this thesis, which is focussed on a preliminary feasibility study of the already developed catalytic reaction system.

4.3.4 Replacement of TFA with an Acetic Acid Solvent

It has been mentioned that the role of the acidic solvent for methane functionalisation reactions is two-fold. First is the enhancement of an electrophilic mechanism by the weakly co-ordinating acid conjugate base or facilitation of an electron transfer mechanism by altering the relative catalyst metal and alkane substrate redox potentials. Second is the provision of chemical protection *e.g.* esterification. Trifluoroacetic acid (TFA) is an exemplary solvent for such reaction chemistry (Gretz *et al.*, 1987; Vargaftik *et al.*, 1990; Nakata *et al.*, 1994; Yamanaka *et al.*, 1995; Kurioka *et al.*, 1995; Kitamura *et al.*, 1998; Asadullah *et al.*, 2000). However, it is relatively expensive which could have an economic constraint on a full-scale industrial process, although possible regeneration of the acid by methyl trifluoroacetate hydrolysis is envisaged. Also, TFA is very corrosive mandating high material costs. The use of the less corrosive acetic acid would be of interest because it is significantly cheaper, being produced as a bulk chemical and furthermore methanol is the feedstock for acetic acid manufacture *e.g.* the 'Monsanto process', thus providing an incentive for a possible integration of the two processes. As of present, the use of acetic acid in place of TFA has not been reported in the literature.

Preliminary experiments using acetic acid were performed in the batch reactor with the results shown in Table 4.7. Data obtained using TFA is also included for comparison. The pressure time course profile is shown in Figure 4.26.

Table 4.7. The Use of Acetic Acid as Liquid Phase Solvent

Experiment Details	**Reaction ΔP (bar)**	**[Methyl acetate] (mol/m^3)**	**Methyl acetate Yield (%)**	**TON (based on Pd catalyst)**	**STY (kg/kg$_{Pd}$.h)**
(Acetic Acid) BASE Run 1	11	31	0.9	261	60
(Acetic Acid) BASE Run 2	11	27	0.8	226	52
(TFA) BASE	*11*	*50*	*1.5*	*430*	*259*
(Acetic Acid) No CH_4 (replace with N_2)	9	N/A	-	-	-
(TFA) No CH_4 (replace with N_2)	*9*	*N/A*	-	-	-

Conditions: Where included $P_{CH4(i)}/P_{N2}$ = 62 bar; $P_{CO(i)}$ = 174 bar; $P_{O2(i)}$ = 7 bar; 5 wt.% Pd/C = 12.5 mg; [$CuCl_2$] = 20 mol/m^3; Acetic Acid/TFA:H_2O = 3:1 (50ml); T = 85 °C; t = 3 h; N = 700 rpm

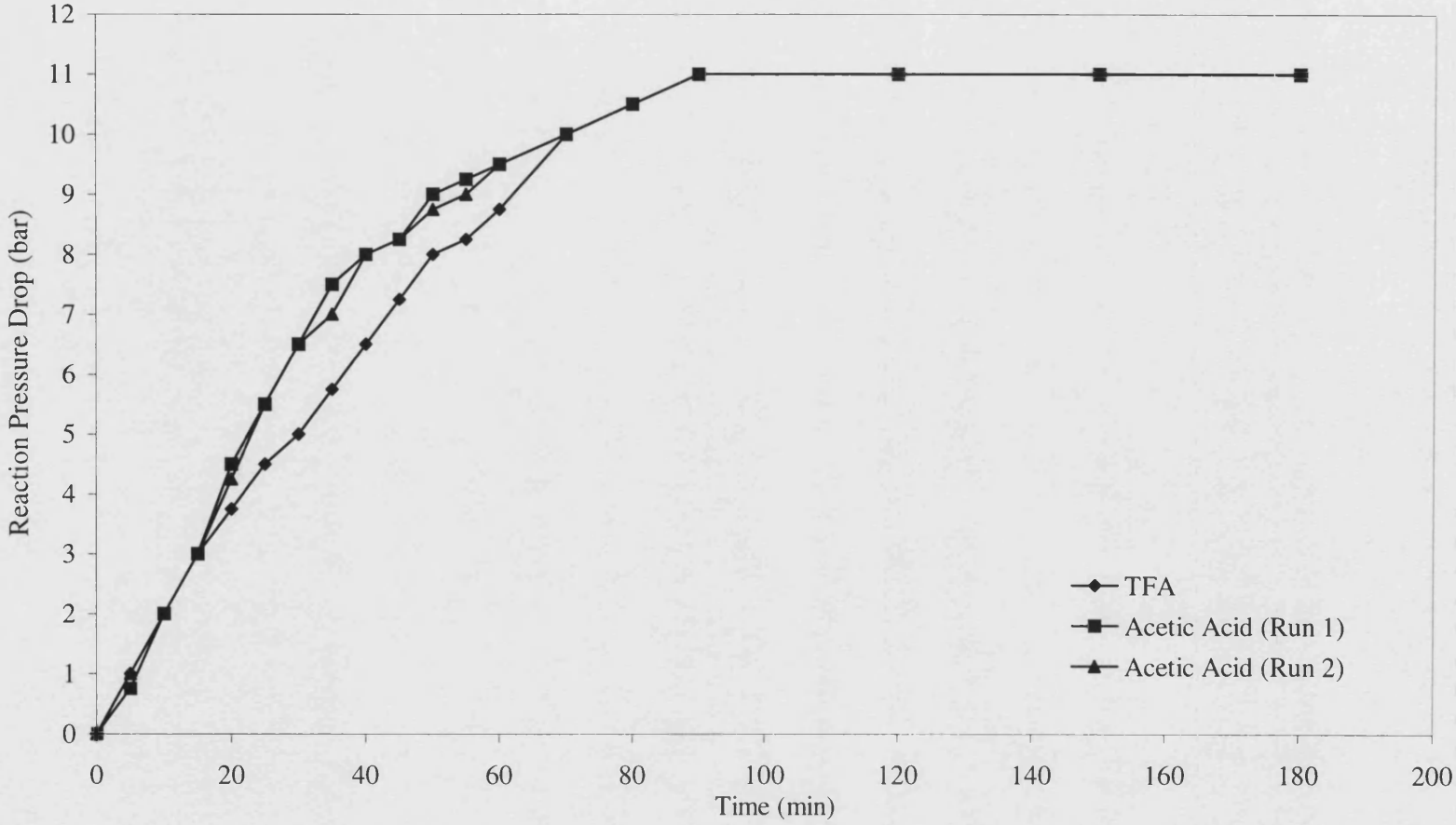

Figure 4.26. Reaction Pressure Drop Profile with Acetic Acid as Liquid Phase Solvent

Conditions: $P_{CH4(i)}$ = 62 bar; $P_{CO(i)}$ = 14 bar; $P_{O2(i)}$ = 7 bar; 5 wt.% Pd/C = 12.5 mg; [$CuCl_2$] = 20 mol/m^3; Acetic Acid:H_2O = 3:1 (50 ml); T = 85 °C; N = 700 rpm

The first positive observation is that a methanol derivative, methyl acetate was formed with this solvent system. However, compared to the use of TFA, the product concentration obtained was lower (*ca.* 40 % less). It should also be noted that the methyl acetate product "loss" during sample preparation prior to GC analysis was estimated to be 16.8 ±5.4 % (Appendix I) which was less than that found with the TFA ester. A possible explanation is that methyl acetate is less volatile than methyl trifluoroacetate. These observations indicate that for the desired product formation, TFA was the better solvent. One point to make is that TFA is a significantly stronger acid than acetic acid ($pK_{a(TFA)} = 0.23$; $pK_{a(Acetic\ acid)} = 4.8$ at 25 °C) and thus as well as enhancing the reaction mechanism, the chemical protective role may be facilitated by the greater availability of H^+ ions which are catalysts for the esterification reaction:

$$\text{Carboxylic Acid} + \text{Alcohol} \xrightarrow{H^+} \text{Ester} + \text{Water} \qquad (4.10)$$

The significance of this last point was tested by carrying out an experiment using acetic acid, together with a few drops 97.5 wt.% H_2SO_4 to increase the H^+ concentration (Appendix I). The result indicated no benefit to product yields with a similar reaction pressure drop being observed. Another explanation could be that the methyl acetate ester itself was more susceptible to degradation (deep oxidation) than the methyl trifluoroacetate ester as in the latter, the CF_3COO group has a greater tendency of deactivating the ester from both electrophilic attack and H-atom abstraction, compared with the CH_3COO group in methyl acetate. This fact, combined with the role of the conjugate base, could form an explanation as to the differing product yields obtained with the two acid solvents, but the intricacies involved in determining the exact cause of the discrepancy were beyond the scope of this thesis.

With respect to the reaction pressure drops, similar rates were observed if not higher, for the acetic acid solvent compared with TFA. This was also true in the absence of methane for the suspected H_2O_2 formation and the Wacker oxidation of CO reactions (results not shown). These results go some way in signifying that the observed pressure drop was not wholly linked with the final product yield.

Although not as effective as TFA, the fact that the use of an acetic acid solvent for methane oxidation reactions had seldom been reported in the literature gave an impetus

for further experimentation. The influence of reaction temperature and the effect of methane partial pressure were both studied. The results are shown in Figures 4.27 - 4.30. A methane partial pressure of 34.5 bar was employed for the study of temperature influence, similar to that used by Lin *et al.* (1997) with the TFA-based solvent. Likewise, a reaction time of 1 h was used as the basis for this study.

It can be seen that the effect of temperature on product concentration was limited (Figure 4.27). However, the influence was more pronounced on the observed reaction pressure drop (Figure 4.28). This indicates that the extent of the pressure drop is not a full indication of the final product yield, and although the *in situ* oxidant formation may be favoured, its catalytic decomposition is also increased with temperature, which could account for the observed behaviour of product concentration. Furthermore, the product itself may undergo degradation, which would be accelerated by an increase in temperature. Thus, product stability with temperature may also be an issue here. Relating to the external mass transfer, the solubility of the three reactant gases, although not calculated, is likely to decrease with temperature over the studied range. This would also have an adverse effect on the observed reaction, although the recorded reaction pressure drops do not show any evidence of this. An Arrhenius plot (Appendix VI) of the average product formation rate over 1 h against the reciprocal of the absolute temperature revealed an activation energy of 7.0 ±0.9 kJ/mol. This value is very low especially compared to that of 15.3 kcal/mol (64 kJ/mol) obtained by Lin *et al.* (1997) using the TFA solvent. However, this latter value was obtained using a pseudo heterogeneous palladium catalyst whereby a homogeneous pre-cursor, K_2PdCl_4, was employed, which was said to have been reduced *in situ* to metallic Pd, although the extent was not verified. A low activation energy could be attributed to intra-particle resistance (*e.g.* Fogler, 1992), however with small Pd/C particle sizes (*ca.* 50 - 100 μm) this would be unlikely and owing to the low temperatures employed, a surface reaction control regime would be more feasible. A ballpark calculation based on the Weisz-Prater parameter revealed little presence of an intra-particle resistance (Appendix VII). If intraphase diffusion limitation was deemed significant the use of a carbon nanofibre palladium support could be an option (*e.g.* Pham-Huu *et al.*, 2000).

The effect of methane partial pressure on product concentration was also an anomaly in that it also had a limited effect (Figure 4.29). Over the range of methane partial pressures studied (14 - 41 bar), an effective zero-order dependence was observed. Using the TFA-

based solvent, a first-order dependence was observed (Lin *et al.*, 1997) over a similar partial pressure range. As mentioned before, the latter work involved a different palladium catalyst and so it is not a genuine comparison. The effect of methane partial pressure on the observed pressure drop was negligible (Figure 4.30), and supports the fact that the pressure drop was mainly due to the consumption of carbon monoxide and oxygen, as for TFA, especially during the early time course of reaction.

In view of these results, interesting phenomena have been observed, although often contrary to what one would predict based on the original work with the TFA-based solvent. For a comprehensive interpretation of the observed behaviour, a more detailed understanding of the reaction chemistry is required, in particular the modelling of the individual transport steps of this slurry-type chemistry. Also the relative stability of the product needs to be assessed because maybe its degradation is in competition with its actual formation. What this work has shown, however, is that the substitution of the TFA-based solvent with acetic acid is feasible (although at first glance not as efficient) and maybe other carboxylic acids including mono- and di-halogenated ones are also possible options with the impetus being the replacement of a relatively expensive solvent (TFA) with a cheaper alternative.

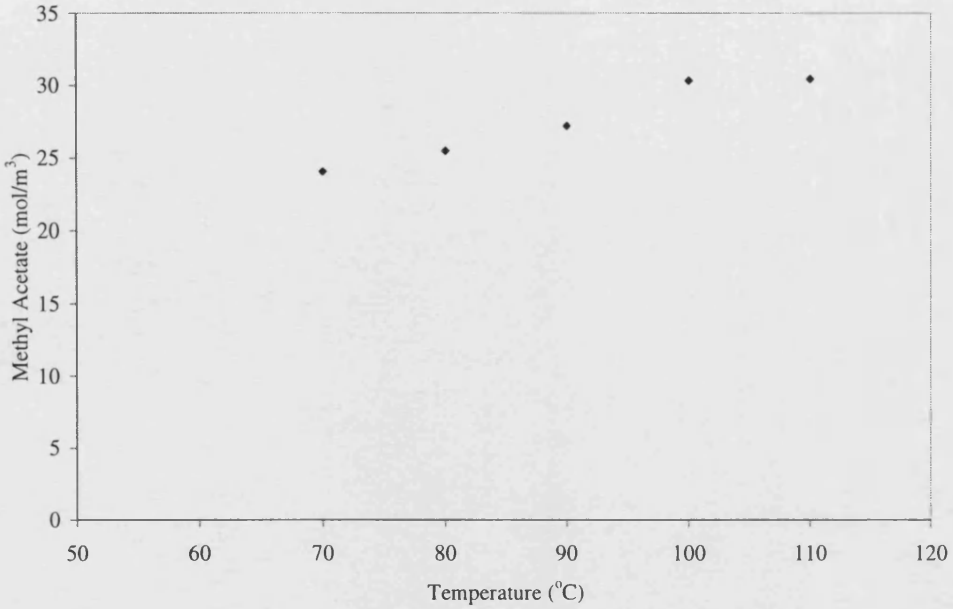

Figure 4.27. Effect of Temperature on Product Concentration

Conditions: P_{CH4} = 34.5 bar; P_{CO} = 14 bar; P_{O2} = 7 bar;
5 wt.% Pd/C = 12.5 mg; $[CuCl_2]$ = 20 mol/m^3;
Acetic Acid:H_2O = 3:1 (50 ml); t = 1 h; N = 700 rpm

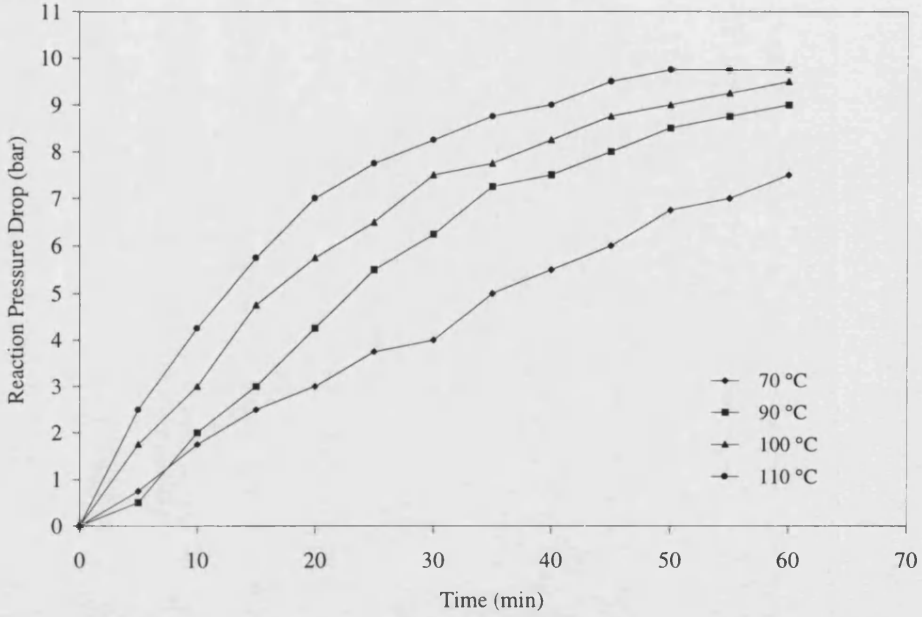

Figure 4.28. Effect of Temperature on Reaction Pressure Drop

Conditions: P_{CH4} = 34.5 bar; P_{CO} = 14 bar; P_{O2} = 7 bar;
5 wt.% Pd/C = 12.5 mg; $[CuCl_2]$ = 20 mol/m^3;
Acetic Acid:H_2O = 3:1 (50 ml); t = 1 h; N = 700 rpm

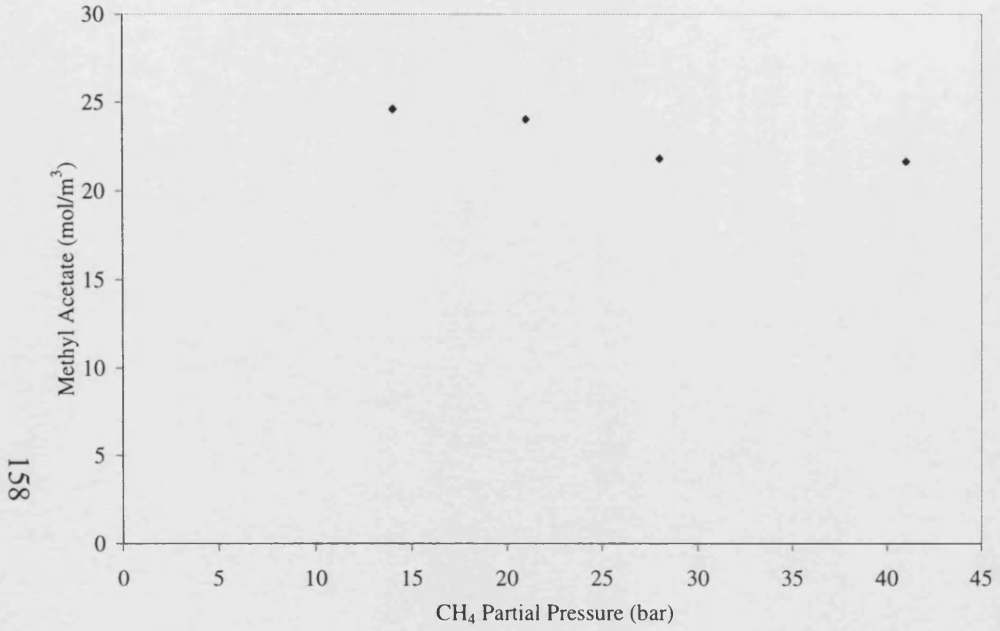

Figure 4.29. Effect of Methane Partial Pressure on Product Concentration

Conditions: $P_{CO(i)}$ = 14 bar; $P_{O2(i)}$ = 7 bar;
5 wt.% Pd/C = 12.5 mg; [$CuCl_2$] = 20 mol/m^3;
Acetic Acid:H_2O = 3:1 (50 ml); T = 90 °C; t = 1 h; N = 700 rpm

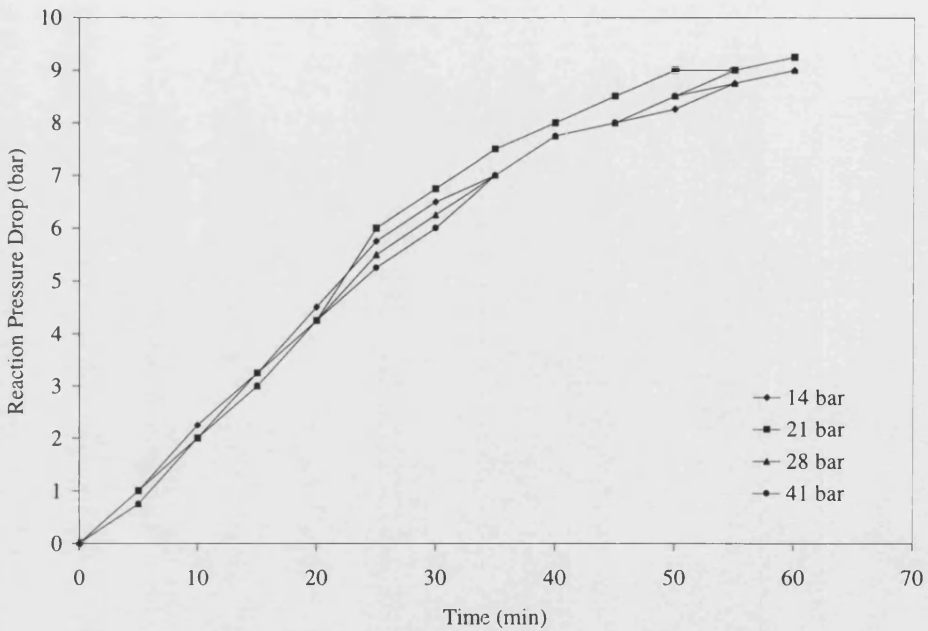

Figure 4.30. Effect of Methane Partial Pressure on Reaction Pressure Drop

Conditions: $P_{CO(i)}$ = 14 bar; $P_{O2(i)}$ = 7 bar;
5 wt.% Pd/C = 12.5 mg; [$CuCl_2$] = 20 mol/m^3;
Acetic Acid:H_2O = 3:1 (50 ml); T = 90 °C; t = 1 h; N = 700 rpm

4.3.5 The Application of a Novel Biphasic System for Methane Oxidation

A system for the efficient generation of hydrogen peroxide from carbon monoxide, water and oxygen was developed by Bianchi and co-workers (Bianchi *et al.*, 1999; see also Thiel, 1999). The current industrial process involves the alternate oxidation and reduction of alkylantraquinone derivatives, which is fairly complex and indirect (*e.g.* Kroschwitz and Howe-Grant, 1995). This novel system was able to directly obtain aqueous H_2O_2 concentrations of up to 8 wt.% employing a biphasic (organic and aqueous) system with a palladium-based catalyst (organic phase) stabilised by nitrogen-based ligands (N-ligands).

$$CO + O_2 + H_2O \rightarrow H_2O_2 + CO_2 \qquad \Delta G^{o}_{25^{o}C} = -134 \text{ kJ/mol} \qquad (4.11)$$

For this current study, it was decided to apply the aforementioned biphasic system for methane oxidation. There were two main reasons for using this system. First, the *in situ* generation of H_2O_2 was a suspected intermediate in the base system of Lin *et al.* (1997) and this novel system maybe a more efficient generator of this oxidant. Secondly, a biphasic system in which the catalyst is more soluble in the organic phase than a methanol-based product (high affinity towards aqueous phase) would present a facile post-reaction separation (*e.g.* Horváth and Rábai, 1994).

The reactants used were based on the most efficient and stable system components found in the original work (Bianchi *et al.*, 1999). Their respective quantities were scaled to a 50 ml reactor volume used in this study.

Organic Phase
Toluene = 17.4 ml
2-methyl-2-butanol = 12.5 ml
Palladium(II) acetate = 0.0047 g
Toluene-4-sulfonic acid = 0.1591 g
2,9-dimethyl-4,7-diphenyl-1,10-phenanthroline (ligand) = 0.0302 g
HCl (0.1 M) = 0.21 ml

The mixture comprised of the following key ratios: ligand/acid/Pd = 4/40/1 (mol/mol/mol), toluene/2-methyl-2-butanol/water = 35/25/40 (v/v/v)

The organic mixture was stirred for approximately 6 hours to produce a homogeneous complex solution. This was then added to 19.9 ml of distilled water to form two distinct phases. Plate 4.2 shows a typical reactant mixture.

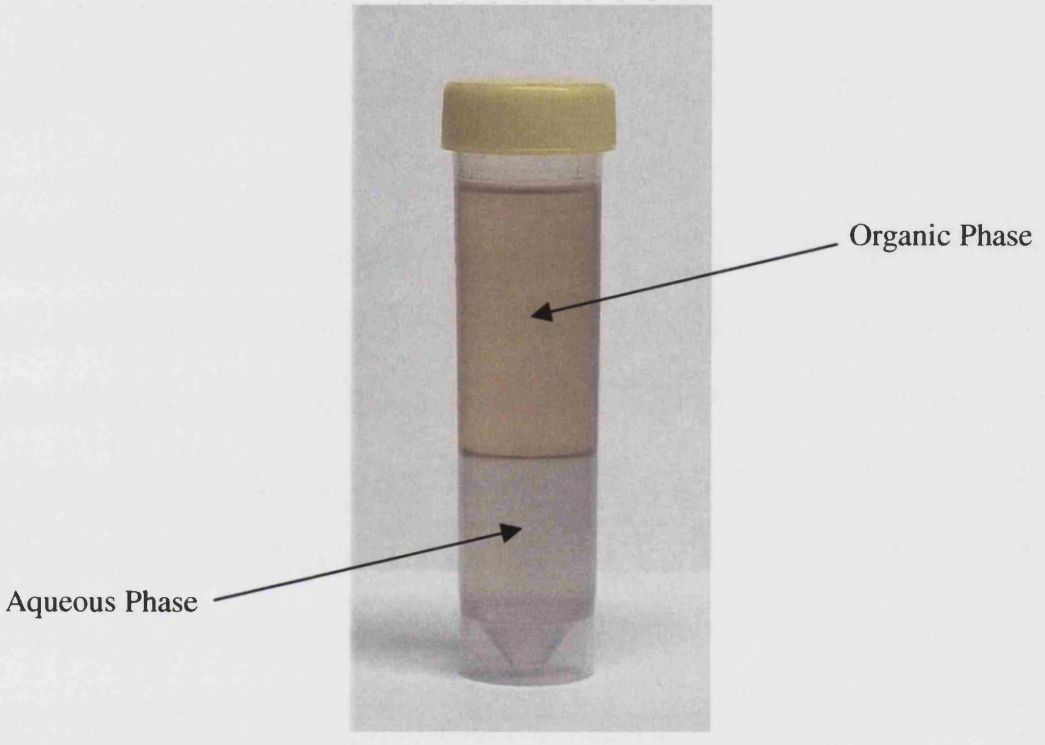

Plate 4.2. The Pre-reaction Biphasic System

Experiments were carried out both in the absence and presence of methane, to observe any pressure drop, which indicated that the system was working. In this system, an oxygen rich environment was used because for CO mole/volume fractions greater than *ca.* 9 % the palladium complex was observed to have become unstable with partial precipitation of the reduced metal being evident (Bianchi *et al.*, 1999).
The results are shown in Table 4.8.

The use of a gas composition akin to that employed in the bimetallic system (Run 1) resulted in no observed reaction (no pressure drop) and the final product contained a black precipitate at the biphasic interface. This highlighted the immediate problems

associated with catalyst stability. Run 2 also showed this problem, even when the CO fraction was less than 9 vol.%. At this stage it was decided to run the reaction for which the system was originally designed *i.e.* in the absence of methane (Runs 3, 4 & 5). A slow pressure drop was observed, with the extent increasing with a higher O_2 partial pressure (Run 4). However, an increase in temperature from 70 °C to 85 °C (Run 5), did not result with an increased reaction pressure drop in the 3 h batch time. The original workers did not increase the reaction temperature beyond 70 °C to prevent any side reactions such as H_2O_2 decomposition and ligand oxidation. These factors may have played a role in the aforementioned observation. The role of palladium was deemed to be paramount as no reaction pressure drop was observed in its absence (Run 6). Qualitative analysis of H_2O_2 was performed by the dropwise addition of 100 mol/m^3 (0.1 mol/dm^3) $KMnO_4$ to the aqueous phase, observing the colour change from purple (Mn^{7+}) to colourless (Mn^{2+}) with a little effervescence (oxygen liberation).

$$2MnO_4^- + 5H_2O_2 + 6H^+ \rightarrow 2Mn^{2+} + 5O_2 + 8H_2O \qquad (4.12)$$

A positive observation of the presence of H_2O_2 was only obtained for the experiments in which a pressure drop had occurred.

The use of a low partial pressure of methane (4 bar) was employed in Runs 7 and 8, with an observation of a reaction pressure drop. However analysis of both the aqueous and organic phases did not reveal the presence of methanol or any obvious methane oxygenate. The peak resolution was made difficult by the fact that several organic components were present even in the aqueous phase, indicating that some partitioning of the organic phase was occurring.

As there was no inherent chemical protection of a possible methanol product, its subsequent oxidation by H_2O_2 could have prevailed accounting for no observed product in the final sample. Therefore, some TFA was added to the system (Runs 9 & 10). In both cases no pressure drop occurred and observation of the pre-reaction mixture indicated that the TFA was interacting with the organic phase, perhaps resulting with the esterification of the 2-methyl-2-butanol co-solvent. Addition of Cu^{2+} ions was used in Run 11 to implicate any synergy between Pd and Cu for methane oxidation as occurring in the bimetallic system. Unfortunately, again no pressure drop was observed.

In conclusion, although the system was proven valid for hydrogen peroxide synthesis, it appeared not so functional for methane oxidation. The constraints placed upon the use of this system include the necessity of an oxygen rich environment to ensure catalyst stability, which mandated the use of a low methane pressure to avoid flammable gas mixtures or the use of very high reaction pressures. These low methane pressures may not have been enough for efficient solubilisation to occur which may help to explain the lack of observed product. Furthermore, the system appeared to be incompatible with a potential methanol chemical protection agent *e.g.* TFA thus exposing any formed oxygenate to an oxidising environment *i.e.* H_2O_2 in the aqueous phase. Therefore, based on these indicative results, further work using this system was not carried out.

Table 4.8. The Application of a Novel Biphasic System for Methane Oxidation

RUN	Temperature (°C)	Batch Time (h)	Initial Gas Composition								Reaction ΔP (bar)
			CO		O_2		CH_4		N_2		
			bar	vol.%	bar	vol.%	bar	vol.%	bar	vol.%	
1	85	2	14	17	7	8	62	75	0	0	0
2	85	2	7	8	14	17	62	75	0	0	1
3	70	3	6	8	65	92	0	0	0	0	2.5
4	70	3	7	8	72	87	0	0	4	5	5
5	85	3	7	8	72	87	0	0	4	5	4
6 (No Catalyst)	85	3	7	8	72	87	4	5	0	0	0
7	70	3	7	8	72	87	4	5	0	0	4
8	85	3	7	8	72	87	4	5	0	0	4
9 (TFA = 27.2 ml)	85	3	7	8	72	87	4	5	0	0	0
10 (TFA = 10 ml)	85	3	7	8	72	87	4	5	0	0	0
11 ($[Cu^{2+}]$ = 20 mM)	85	3	7	8	72	87	4	5	0	0	0

N = 700 rpm

CHAPTER 5 - Discussion

5.1 Batch Operation

The purpose of first utilising the 175 ml batch reactor for the previously discovered methane oxidation system was to obtain some initial data for a scaled-up process. After performing reaction studies in the semi-continuous reactor, the batch reactor was again employed to carry out some experiments focusing on variations of the catalytic system to try to increase productivity.

In this current work, the liquid phase volume was 12.5 times larger than in the original work of Lin *et al.* (1997) and also than that employed in Park *et al.* (2000)[a]. As a result of this increase a pressure drop due to reaction was observed from which a qualitative study of the reaction stoichiometry could be performed to link it to the postulated chemistry. This drop in pressure occurred during the first *ca.* 2 h of the reaction and was attributed mainly (80 %) to reactions consuming both oxygen (H_2O_2 formation and CO Wacker oxidation) and carbon monoxide (CO Wacker oxidation). What is of interest is the fact that the formation of a methanol-based product came to a "pseudo end" after *ca.* 2 h, giving some link with the observed reaction pressure drop. Possible explanations include product degradation and other side reactions, although these were not thought to be significant, with the likely main cause being the depletion of the gaseous reactants.

In terms of the methyl trifluoroacetate product concentrations obtained, these were generally lower than those obtained using similar reactant concentrations in the original work (*e.g.* in 20 h at 85 °C, a concentration of 51 mol/m^3 was obtained for this work compared with 120 mol/m^3 at 85 - 95 °C). Although, the necessary sample preparation in this current work may account for a 20 % "loss" of the ester product and the quoted temperature range from Lin *et al.* (1997) was up to 10 °C higher, nevertheless the product yields were less. Another discrepancy was that Lin and co-workers observed an increase in product with time from 20 to 50 to 90 h, whereas product formation appeared to stop after 2 h in this work. One possible reason is that the ratio of the gas-to-liquid volumes employed in the two reactors was very different. In this current work a gas-to-liquid ratio of 1.6 was used, compared with a significantly larger value of *ca.* 31. The higher value meant that excess gaseous reactants were available which was probably why no observed pressure drop was reported. Furthermore, in this case the reaction would never be limited by the gaseous reactants allowing for a higher build-up of product

concentration. However, the product yield based on methane would consequently be low (not reported). It has been stated (Labinger, 1995) that to achieve higher product yields, the gas phase should be kept to a minimum. This technique was employed by Kitamura *et al.* (1998) who obtained vastly greater product yields, using a heteroployacid/$K_2S_2O_8$/$(CF_3CO)_2O$/CF_3COOH catalyst system, by switching from a 100 ml reaction vessel to a 25 ml vessel. Thus the factor of gas-to-liquid ratio appears to be relatively important, especially when quantifying product yields. Unfortunately, for this current study the value was fixed due to mechanical mixing constraints. Further work is necessary to explore this parameter.

Comparing with other liquid phase methane oxidation systems, although the product yields of *ca.* 1 % percent obtained here were similar (*e.g.* Taylor *et al.*, 1997; Yamanaka *et al.*, 1995), the TON of the methanol-based product on the palladium catalyst was comparable or significantly higher than for catalysts in other systems (*e.g.* Nizova *et al.*, 1997; Yamanaka *et al.*, 1998). This latter observation was partly due to the fact that only a small amount of palladium was required for the catalysis (Lin *et al.*, 1997). This also results with high STY values. Both TON and STY values, based on the larger amount of the copper cocatalyst, would be lower. In commercial processes using Wacker-based oxidations, the concentration of copper far exceeds that of palladium (Masters, 1981); however the former is significantly less expensive.

Regarding the components of the system, it was found that omission of a component or the use of a pure water solvent resulted with a deleterious reaction performance (low pressure drop and product formation). In particular, no reaction was observed in the absence of chloride ions. According to Park *et al.* (2000)[a], chloride ions were necessary to stabilise the palladium(II) oxidation state, which was the elucidated form of palladium for the actual methane oxidation reaction with the *in situ* generated hydrogen peroxide. The solvent was also seen to play a crucial role, both with chemical protection and the reaction mechanism. The role of the acidic solvent could be demonstrated by looking at the actual proposed Wacker chemistry. By considering standard electrode potentials for the oxidation of Pd to Pd^{2+} by Cu^{2+} the reaction is not thermodynamically spontaneous under standard conditions:

$$Pd^{2+} + 2e^- \rightarrow Pd \qquad E^o_{25°C} = +0.92\ V \qquad (5.1)$$

$$Cu^{2+} + e^- \rightarrow Cu^+ \qquad E^o_{25°C} = +0.17\ V \qquad (5.2)$$

$$\Rightarrow \quad Pd + 2Cu^{2+} \rightarrow Pd^{2+} + 2Cu^+ \qquad E^o_{25°C} = -0.58\ V \qquad (5.3)$$

However, the use of a strong acidic solvent alters the redox potentials and coupled with stabilising chloride ions the chemistry becomes favourable (Cornils and Herrmann, 2000).

Further evidence of Wacker chemistry was obtained by a simple experiment. A normal base reactant mixture containing both Pd/C and $CuCl_2$, and one omitting $CuCl_2$ were made up and left to stand in sealed containers at room temperature for several weeks. Analysis of the reactant mixtures using atomic absorption spectrometry (AAS) revealed the presence of a significantly higher concentration of Pd^{2+} ions (the mixture was filtered prior to analysis) for the copper containing mixture compared to without (see Appendix I). Also, analysis of several post-reaction mixtures also revealed the presence of Pd^{2+}. Therefore, it appears that the Cu^{2+} ions were promoting the oxidation of Pd to Pd^{2+} as in the normal Wacker chemistry.

Novel experiments performed with acetic acid replacing the TFA solvent proved that the oxidation was feasible, though less efficient. The anomalous behaviour of the influence of temperature and methane partial pressure called for further mechanistic studies, in particular studying possible side reactions including oxidative degradation of the methyl acetate product. The positive influence of temperature on the reaction pressure drop revealed that this was not wholly indicative of the final product concentration, the latter being hardly affected by temperature. However, the findings showed that replacement of the relatively expensive and corrosive TFA with another solvent (in this case significantly cheaper and less corrosive) was possible.

Considering the proposed mechanism for this methane oxidation (Figure 2.12) it should be possible to oxidise methane starting with a H_2O_2 oxidant. Unfortunately, experimentation based on this theory was not successful and it was concluded that possibly the *in situ* generation of the oxidant was the important factor, with catalytic decomposition of this oxidant appearing as a side reaction. Lin *et al.* (1992) only reported the palladium catalysed oxidation of ethane using H_2O_2; however, this substrate is more reactive than methane. Bearing in mind a possible necessity of an *in situ* generated H_2O_2

oxidant another novel catalyst system was briefly examined for methane oxidation. This had been developed by Bianchi *et al.* (1999) for the generation of H_2O_2 from CO, O_2 and H_2O in a biphasic system containing a ligated palladium catalyst. However, preliminary results indicated the incompatibility of the system for requirements needed for efficient methane oxidation *e.g.* high methane partial pressure, chemical protective solvent.

Focussing back on the initial base reaction studies performed in the batch reactor, it appeared that the product formation was limited which was thought to have been possibly due to the depletion of the gaseous reactants. The use of the porous tube reactor would eliminate this factor, allowing for a constant supply of the gas phase. Furthermore, the facility of liquid sampling from the reactor would be beneficial in obtaining true time course behaviour, not reported in the majority of related methane oxidation works.

5.2 Semi-continuous Operation/Porous Tube Reactor

The use of the porous tube reactor accommodated a further increased liquid phase volume of 300 ml, a continuous supply of gaseous reactants and facilities to allow for liquid sampling. With these added features, more comprehensive information could be obtained for this feasibility study, compared with that resulting from the batch experiments.

The initial use of the catalytic porous tube was found to be not suitable for the reaction system in that the palladium coating was leached into the liquid phase. The nature of the proposed chemical reaction mechanism, with the necessary formation of Pd^{2+} from Pd(0) via Wacker chemistry with the $CuCl_2$ cocatalyst, was thought to have been responsible for this, rather than the mechanical instability of the film coating.
Substitution of the heterogeneous palladium with a homogeneous palladium(II) source, resulted with methyl trifluoroacetate product formation and so was used for subsequent experimentation. In accordance with Park *et al.* (2000)[a], the use of excess copper(II) chloride resulted with a deleterious product formation. Furthermore, evidence of product degradation was apparent. The use of too little copper(II) chloride also resulted with poor product concentrations. Whilst the cocatalyst was shown to have a significant influence,

changes in the amount of the palladium catalyst had a much smaller effect on product formation. By consideration of the Wacker chemistry between palladium and copper, the higher the concentration of copper(II) ions, the more palladium(II) ions are available which in turn are stabilised by an increased concentration of chloride ions:

$$Cu^{2+} + Pd(0) \rightarrow Cu^{+} + Pd^{2+} \qquad ((4.5))$$

$$2Cu^{+} + \frac{1}{2}O_2 + 2H^{+} \rightarrow 2Cu^{2+} + H_2O \qquad ((4.6))$$

$$Pd^{2+} + CO + H_2O \rightarrow Pd(0) + 2H^{+} + CO_2 \qquad ((4.7))$$

These palladium(II) ions were responsible for the Wacker oxidation of carbon monoxide and thus by favouring this side reaction, less carbon monoxide was available for the formation of *in situ* hydrogen peroxide (equation (4.8)) which was deemed necessary for methane functionalisation (equation (4.4)).

$$CO + O_2 + H_2O \rightarrow H_2O_2 + CO_2 \qquad ((4.8))$$

$$CH_4 + H_2O_2 + CF_3COOH \rightarrow CF_3COOCH_3 + 2H_2O \qquad ((4.4))$$

Thus, an excess amount of the cocatalyst would facilitate the Wacker oxidation of CO side-reaction, removing CO, whilst too little would not efficiently effect the Wacker catalytic cycle for generation of key amounts of Pd(0) and stabilised Pd^{2+} required for the main reaction steps involved in methane oxidation. In respect to both palladium species being present in the reaction mixture, X-ray diffraction (XRD) analysis of a filtered post-reaction mixture, from an exemplary semi-continuous run using Pd^{2+} catalysis, revealed the presence of Pd(0) (see Appendix I).

Variation in methane partial pressure was also explored using the porous tube reactor. An effectively first-order dependence (linear regression gave a value of 0.97 ±0.13) for the global reaction was observed in the range of 28 - 62 bar. The effect of changes in carbon monoxide pressure was also briefly examined. Reduction of the carbon monoxide partial pressure from 14 to 7 bar, resulted in less product which could be attributed to its role in both the Wacker chemistry and the *in situ* formation of hydrogen peroxide. The influence

of oxygen partial pressure was not studied due to uncertainties with encountering flammable gas mixtures.

Reducing the total pressure of the system from 83 to 50 bar, resulted in decreased product concentrations and initial rates even at a higher temperature of 120 °C. The impact of reduced partial pressure of the reactant gases was thought to have been the cause of this. Furthermore, operation at the higher temperature of 120 °C resulted with an increased differential pressure drop across the gas inlet and gas outlet. On opening the hold-up vessel for cleaning purposes, there was evidence of liquid foaming. Subsequent use of the same porous ceramic tube at 85 °C did not yield a similarly high pressure drop. Therefore, changes in the liquid composition induced by the higher temperature was believed to have caused the high differential pressure drop, rather than any internal fouling/blocking of the porous tube. If new and/or accelerated reaction chemistry occurred at the higher temperature causing some particulate formation from *e.g* the catalysts, then this could have partially blocked the valves in the liquid-line, which would have also lead to the increased pressure drop. Unfortunately, these findings limited the use of either this catalytic system or at least the use of the porous tube reactor for this methane oxidation at elevated temperatures, and was a reason behind not exploring temperature kinetics for the reaction. More work is necessary to establish the exact cause of this operational constraint.

In all the experiments performed in the semi-continuous reactor the time course profile for product concentration showed a decrease in the observed product formation rate, ending with effectively no further product formation after *ca.* 2 hours. To confer this trend, a longer running time of 5 hours was employed, which also resulted with the same phenomenon. A similar observation was also found from batch experiments using the heterogeneous Pd/C catalyst and also in the porous tube reactor using this same catalyst. Semi-continuous operation indicated that gaseous reactant depletion (prominent in batch operation) cannot be the sole cause of the reduced rate of product formation. One problem associated with the porous tube reactor was the possibility of product removal from the main liquid phase by gaseous stripping. This was tested in independent experiments from which an estimated product removal rate of 11 $mol/m^3.h$ was obtained. These results highlighted the fact that in the porous tube reactor, the product formation must not have ended, but instead was significantly reduced to a value comparable to that of the removal process. In light of this information, the cause behind the noticeable

reduction in product formation in both batch and semi-continuous operations suggests problems associated with catalyst instabilities. One explanation lies with the Wacker catalytic cycle which may, after a short time, become suppressed, due to the inability to reoxidise the Pd(0). It has been observed in other catalytic systems involving the Pd(II)/(0)/(II) cycle that if the palladium(0) is allowed to aggregate, it becomes very difficult to oxidise back to Pd(II) (Sen, 1992; Kesling, 1987). Although it is not possible to conclude the exact cause of the reduced product formation from this current work, data obtained from both batch and semi-continuous operation does suggest that the problem may lie with the intricacies involved in the catalytic cycle.

One observation that arose from the use of the porous tube reactor, was the presence of a temperature rise during the first *ca.* 10 minutes of reaction time. An incline of this was also found in the batch experiments although the rise was too small to speculate any conclusions. It was deduced that the temperature rise was due to chemical reaction, in particular the exothermic reactions of the Wacker oxidation of CO and the *in situ* formation of hydrogen peroxide. The on-set of this initial energy release would need to be a consideration if a further scale-up of the system was conducted.

Relating to the application of the porous tube reactor, the benefits did not proffer in the form of increased product concentrations, but in supplying more comprehensible data in the form of true time course studies with phenomena observed at a level of increased scale with a continuous supply of gaseous reactants. One factor that could not be eliminated with the porous tube reactor was the inherent contact of reactants with the stainless steel reactor walls. In batch works, they had been excluded by use of a glass-liner, although preliminary results indicated that the effect was not significant (see Chapter 4, Figure 4.25). This aspect may play some role, especially in the corrosive environment, but was not thought to be responsible for the diminished production rates.

From the data obtained thus far, the catalytic system has been proved valid in that a methanol-based product was formed, but was shown to lack the productivity and reliability required for commercial implementation. The major bottleneck appears to be the fundamental reaction chemistry, which is not amenable to reactor design.

5.3 General

The review of the available literature (Chapter 2) has revealed a significant interest into the direct conversion of natural gas (chiefly methane) into liquid fuels. An efficient process for achieving this would allow for the on-site conversion of the feedstock, thus facilitating the distribution to a market that is often located far from the reserve. Furthermore, the practical use of the natural gas would prevent the requirement for its venting and/or flaring which has a positive effect for the environment.

This research study has focussed on one potential system for the oxidation of methane to a methanol derivative in the liquid phase (Lin *et al.*, 1997). The current work has taken this promising system and applied it under both batch and semi-continuous operation, employing larger liquid phase volumes than in the original work. In both cases, the feasibility of the reaction chemistry was proven with the generation of a methanol-based product. The maximum Pd/C catalyst loading used in this work was 1.4 kg/m^3. This represents a catalyst charge of 0.1 wt.% with the effect of increased catalyst amount not having a profound effect (Lin *et al.*, 1997). In industry, the catalyst charge in slurry reactors is typically of the order of 1 - 5 wt.% (Fogler, 1992) although, due to the reactor size, mass transfer issues may be more prominent requiring the increased charging.

The product concentrations obtained in this work were less than those obtained in the original and other works (Park *et al.*, 2000[a]). These earlier batch works only operated using small liquid volumes (*ca.* 4 ml) and larger gas-to-liquid ratios (*ca.* 31 - 75) compared with this present work which used 50 ml liquid volume for batch (gas-to-liquid ratio *ca.* 1.6) and 300 ml for semi-continuous operation (continuous gas supply). The inference to the relevance of the gas-to-liquid ratio on productivity (especially with the batch reactor) highlights the need for future work regarding this parameter, in order to maximise product yields.

The benefit of using the porous tube reactor, compared with the batch, has been shown by obtaining true time course reaction studies, not disclosed in both the original work and other related methane oxidation works in the liquid phase. Furthermore, its application for this type of reaction forms a novelty in the field. The concurrent use of both reactor types (batch and semi-continuous) in this current work has revealed some interesting phenomena associated with practical operation such as the reaction pressure drop, initial temperature rise and problems associated with operation at higher temperatures using the porous tube reactor. Furthermore, it has also allowed for the identification of likely

catalyst instabilities causing the limitation for obtainable product yields. These were not observed or at least not commented on in the previous works. Thus, the bottleneck of the catalytic system was shown to involve the fundamental chemistry which would unlikely be amenable to any future reaction engineering studies.

Experiments performed with modifications to the catalyst system have shown that it is possible to replace the relatively expensive TFA solvent with a less expensive one *e.g.* acetic acid, although in this case, further work is necessary to assess product stability and time course reaction behaviour.

For the assessment of industrial feasibility, the product yields obtained both from this and the original work are far from at a level necessary for an economic process. However, further understanding of the chemical mechanism may, in future, ameliorate this potential bimetallic catalytic system for producing more industrially significant yields.

CHAPTER 6 - Conclusions and Recommendations for Future Work

6.1 Conclusions: Batch Operation

- The bimetallic system developed by Lin *et al.* (1997) was verified, in that a methanol derivative was formed, under mild conditions, in a batch system employing 12.5 times greater liquid volume than in the original work.
- Product formation appeared to finish after *ca.* 2 h. A possible explanation of this was gaseous reactant depletion. However, the semi-continuous studies in the porous tube reactor revealed that this was not the sole reason.
- A drop in reactor pressure was observed, which mainly occurred during the first *ca.* 2 h, linking it to product formation.
- The reaction pressure drop was mainly attributed (80 %) to the consumption of both oxygen and carbon monoxide from the previously postulated *in situ* generation of H_2O_2 and the Wacker oxidation of CO.
- The system required all of its chemical components to operate at "best" efficiency. Key constituents in the liquid phase include chloride ions and the acidic solvent (TFA). Carbon monoxide was required in the gas phase.
- The direct use of H_2O_2 as a stoichiometric oxidant yielded no methanol-based reaction products. This mechanism-questioning result may have been influenced by the catalytic decomposition of the oxidant with the functionalisation of the methane substrate being effected only by "fresh" *in situ* formed H_2O_2. Nevertheless, these observations highlight the need for further understanding of the chemical mechanism.
- Replacement of TFA with the less expensive and less corrosive solvent, acetic acid, was shown to be feasible although preliminary experiments revealed that the efficiency was less than that of the original solvent. More understanding of the transport and chemical mechanistic steps was deemed necessary.
- The use of a novel biphasic system developed for direct H_2O_2 generation (Bianchi *et al.*, 1999) was proven to be incompatible with requirements necessary for an efficient methane oxidation process using the *in situ* oxidant.
- The methyl trifluoroacetate concentrations obtained in this work were less than those obtained by the original founders. It was thought that differences in the gas-to-liquid ratio could go some way in accounting for this discrepancy.

6.2 Conclusions: Semi-continuous Operation/Porous Tube Reactor

- The use of the porous tube reactor employing a liquid volume of 300 ml, was proved feasible for obtaining a methanol-based product (more than 50 mol/m^3 in 3 hours) using the previously discovered catalytic system (Lin *et al.*, 1997). However, the use of a palladium coated ceramic tube was not functional due to prominent catalyst leaching, which was attributed to the requirements of the catalytic reaction and not solely to mechanical instabilities of the surface coating.
- The influence of the cocatalyst, copper(II) chloride, on product formation was shown to be more significant than that of palladium; both an excess and too little amount of the cocatalyst resulted in a deleterious reaction performance. The role of copper(II) chloride in the Wacker oxidation of CO was thought to explain these observations.
- An effective first-order dependence on methane partial pressure was observed for the global reaction in the range 28 - 62 bar, using a homogeneous palladium catalyst. Reducing the carbon monoxide partial pressure resulted in a lower product formation, in accordance to its role in the cyclic Wacker chemistry and the generation of *in situ* hydrogen peroxide.
- Operation of the porous tube reactor at a lower pressure of 50 bar gave lower product concentrations even at higher reaction temperatures, probably due to the reduction in the partial pressures of the gaseous reactants.
- The indication of an increased differential pressure drop and visible liquid foaming from operation at 120 °C, imposed a restriction for further experiments being performed at higher temperatures, at least with using the porous tube reactor.
- In all experiments, the rate of product formation significantly decreased as time elapsed. The effect of product removal/stripping from the main liquid phase in the porous tube reactor was deemed not being the reason behind the suppressed production rate. From considering both the batch and semi-continuous works, it was concluded that problems associated with catalyst instabilities were the cause of this phenomenon.
- Although not directly benefiting the observed product yields, the use of the porous tube reactor has provided true time course data enabling key characteristics of the system to be established as well as revealing other interesting observations such as the initial temperature rise which is important for any future scaled-up reactor design.

6.3 Overall Conclusions

- The application of the bimetallic catalytic system (Lin *et al.*, 1997) for the oxidation of methane to methyl trifluoracetate, has been shown valid by use in both the batch and porous tube reactors. These two reactors have employed a significantly larger liquid phase volume than that used in the original batch work, with the porous tube reactor being semi-continuous.

- Product yields obtained in this current study were notably less than those in the original work, with the observation of a "pseudo end" of product formation after *ca.* 2 h, not previously disclosed. One parameter thought to have been associated with the reduced yields is the difference in gas-to-liquid ratios employed in the two works, especially in the batch reactor.

- Use of both the batch and semi-continuous porous tube reactors have identified the possible presence of catalyst instabilities in the system leading to poor production rates and the observed end of reaction. Thus, the major bottleneck of the system appears to be the fundamental reaction chemistry.

- Operational practicalities associated with the reaction pressure drop (batch operation) and temperature rise have also been identified via the use of the two reactors. Furthermore, the application of the porous tube reactor represents a novelty in the liquid phase methane oxidation research field and has shown the operational feasibility of running these systems in larger equipment.

- Novel changes in the original catalyst system have resulted with the initial feasibility of replacing the expensive TFA solvent with a less expensive one such as acetic acid.

- For commercial implementation, the product yields obtained thus far (< 2 % based on methane) are too low for the process to be economically feasible (> 20 % yield). More understanding of the reaction mechanism is required in order to enhance productivity from what is an initially promising, low temperature methane oxidation system.

6.4 Future Work

Although the product yields obtained in this study were far from the requirement of industrial viability, the bimetallic system has been shown to have the potential of producing a methanol-based product from a methane feedstock. Further work is undoubtedly necessary with the focus on achieving a greater understanding of both the fundamental chemistry and some reaction engineering aspects. Some suggestions for the progression of this subject are given below:

- To investigate the effect of gas-to-liquid ratios, especially with the batch reactor. This could be achieved by changing the batch liquid volumes with the necessary adaptation of the agitation/stirrer configuration or the use of a different sized batch reaction vessel.

- To perform analysis of the gas phase composition to establish an accurate mass balance from which methane conversions and product selectivities can be computed. For this, either the use of gas sampling "bombs" or better still, on-line GC analysis, is required together with the necessary modifications to the reactors.

- To employ more thorough analytical techniques with the view of identifying key intermediates and catalyst oxidation states *e.g.* XAFS. The porous tube reactor allows for liquid sampling so, with reliable analysis, the time course of the state of the cyclic Wacker chemistry, with respect to the catalysts, could be obtained. Furthermore, examination of any metallic palladium aggregates is also necessary to identify whether this is a root cause of the instability in the cyclic catalyst chemistry.

- During this study it was not practical to accurately ascertain the *in situ* hydrogen peroxide concentration by titrimetric analysis because the samples were not colourless. Therefore, the development or use of an alternative analytical method that overcomes this would be of benefit towards the understanding of this key intermediate.

- Having a further insight into the chemical mechanism, together with experimental kinetic data for the reaction, would enable a model of the process to be developed. From this model, experimental performance data could be simulated and predicted providing a useful tool for scale-up activities.

- The application of the catalytic system in the porous tube reactor, at a higher temperature of 120 °C, resulted with interesting phenomena regarding the mechanical pressure drop, together with the observation of liquid foaming. As the influence of temperature maybe fundamental to the optimisation of the reaction, especially with the established exotherm that occurred at the beginning of the reaction, then a study of the fluid properties with temperature needs to be performed. The exact cause of the increased pressure drop also needs to be deduced, with this incorporating an understanding of the reaction chemistry at the higher temperatures.

- A heterogeneous based catalyst is more desirable than a homogeneous catalyst in terms of the requirement of post-reaction separation. Therefore, the heterogenisation of the copper(II) and palladium(II) species could prove worthwhile if the stability was shown to be sufficient (*e.g.* Arends and Sheldon, 2001; Park *et al.*, 2000[b]).

- This current work has shown a possible problem related to the catalyst stability. If the bottleneck is associated with the re-oxidation of the palladium species, then maybe a third oxidative catalyst component could be of benefit. With view of the Wacker chemistry involved, previous research has been carried out using heteropolyacids as an example of the added Pd-reoxidant (*e.g.* Weissermel and Arpe, 1997; for a review of the uses of heteropolyacids in liquid phase reactions, the reader is invited to consult the work of Kozhevnikov, 1998).

NOMENCLATURE

A = Arrhenius constant	(1/s)
A_0 = Constant in the BWR equation	(-)
a = Constant in the BWR and RK equations	(-)
B_0 = Constant in the BWR equation	(-)
b = Constant in the BWR and RK equations	(-)
C_0 = Constant in the BWR equation	(-)
c = Constant in the BWR equation	(-)
$C \equiv [\ ]$ = Concentration	(mol/m^3)
C_s = Concentration of reactant on catalyst surface	(mol/cm^3)
C_{WP} = Weisz-Prater parameter	(-)
D = Diameter of orifice	(m)
D_b = Diameter of bubble	(m)
D_{bulk} = Bulk diffusivity	(cm^2/s)
D_e = Effective diffusivity	(cm^2/s)
d_{bm} = Mean bubble diameter	(m)
d = Catalyst particle diameter	(m)
$E^o_{25°C}$ = Standard electrode potential	(V)
E_a = Activation energy	(kJ/mol)
g = Acceleration due to gravity	(m/s^2)
H = Henry's Law constant	(atm/mol/mol solvent)
k_La = Volumetric mass transfer coefficient	(1/s)
k_L = Liquid-side mass transfer coefficient	(m/s)
M = Molar mass	(g/mol)
N = Agitation speed	(rpm)
n = Number of moles	(mol)
P = Pressure or partial pressure with subscript species	(MPa, bar or atm)
P^o = Saturated vapour pressure	(kPa or mmHg)
P_c = Critical pressure	(Pa, bar or atm)
q = Lumped value in Wagner equation	(-)
$-r_{(obs)}$ = Observed rate of reaction	($mol/g._{catalyst}.s$)
r = Catalyst particle average radius	(cm)
R = Molar gas constant	(J/mol/K or litres.atm/mol.K)
T = Temperature	(K or °C)
T_c = Critical temperature	(K)

t = Time (h)

u_b = Bubble rise velocity (m/s)

u_o = Particle terminal velocity (m/s)

V_m = Molar volume (m^3/mol, cm^3/mol or l/mol)

v = Liquid volume fraction (-)

w = Mass (kg)

x = Liquid mole fraction (-)

Z = Compressibility factor (-)

Greek symbols

α = Constant in the BWR equation (-)

γ = Constant in the BWR equation (-)

ε = Gas hold-up (-)

ε_p = Catalyst particle porosity (-)

η_w = Viscosity of water (cp)

μ = Viscosity (kg/m.s)

ρ = Density (kg/m^3 or g/cm^3)

ρ_p = Catalyst particle density (g/cm^3)

σ = Catalyst particle constriction factor (-)

σ_L = Liquid surface tension (N/m)

τ = Catalyst particle tortuosity (-)

Subscripts

A = Refers to species "A"

CH_4 = Refers to methane

CH_3OH = Refers to methanol

CO = Refers to carbon monoxide

f = Final conditions

G = Refers to gas

i = Initial conditions

L = Refers to liquid

$MeTFA$ = Refers to methyl trifluoroacetate

O_2 = Refers to oxygen

Pd = Refers to palladium

S = Refers to solid

$solvent$ = Refers to solvent

w = Refers to water

Abbreviations

AAS = Atomic absorption spectroscopy

BET = Brunauer-Emmerit-Teller

BWR = Benedict/Webb/Rubin

FID = Flame ionisation detector

GC = Gas chromatograph

GCMS = Gas chromatograph mass spectrometer

RK = Redlich/Kwong

SEM = Scanning electron microscopy

STY = Space-time yield

TFA = Trifluoroacetic acid

TON = Turnover number

XAFS = X-ray absorption fine structure

XRD = X-ray diffraction

REFERENCES

Arena, F., Giordano, N. and Parmaliana, A. (1997). Working mechanism of oxide catalysts in the partial oxidation of methane to formaldehyde.
II. Redox properties and reactivity of SiO_2, MoO_3/SiO_2, V_2O_5/SiO_2, TiO_2, and V_2O_5/V_2O_5 systems. *Journal of Catalysis*, **167**, pp. 66-76.

Arends, I.W.C.E. and Sheldon, R.A. (2001). Activities and stabilities of heterogeneous catalysts in selective liquid phase oxidations: recent developments. *Applied Catalysis A: General*, **212**, pp. 175-187.

Asadullah, M., Kitamura, T. and Fujiwara, Y. (2000). Calcium-catalyzed selective and quantitative transformation of CH_4 and CO into acetic acid. *Angew. Chem. Int. Ed.*, **39**(14), pp. 2475-2478.

Barton, D. and Doller, D. (1992). The selective functionalization of saturated hydrocarbons: Gif Chemistry. *Acc. Chem. Res.*, **25**, pp. 504-512.

Barton, D.H.R., Hu, B., Taylor, D.K. and Rojas Wahl, R.U. (1996). The selective functionalization of saturated hydrocarbons. Part 32. Distinction between Fe^{II}-Fe^{IV} and Fe^{III}-Fe^{V} manifolds in Gif chemistry. The importance of carboxylic acids for alkane activation. Evidence for a dimeric iron species involved in Gif-type chemistry. *J. Chem. Soc., Perkin Trans. 2*, pp. 1031-1041.

Bianchi, D., Rossella, B., D'aloisio, R.D. and Ricci, M. (1999). A novel palladium catalyst for the synthesis of hydrogen peroxide from carbon monoxide, water and oxygen. *Journal of Molecular Catalysis A: Chemical*, **150**, pp. 87-94.

Burch, R., Squire, G.D. and Tsang, S.C. (1989). Direct conversion of methane into methanol. *J. Chem. Soc., Faraday Trans. 1*, **85**, pp. 3561-3568.

Campbell, F.T., Pfefferkorn, R. and Rounsaville, J.F., Eds. (1985). *Ullmann's encyclopedia of industrial chemistry.* 5th ed. Weinheim: VCH Verlagsgesellschaft mbH.

Chepaikin, E.G., Bezruchenko, A.P., Leshcheva, A.A., Boyko, G.N., Kuzmenkov, I.V., Grigoryan, E.H. and Shilov, A.E. (2001). Functionalisation of methane under dioxygen and carbon monoxide catalyzed by rhodium complexes. Oxidation and oxidative carbonylation. *Journal of Molecular Catalysis A: Chemical*, **169**, pp. 89-98.

Choi, K.H. and Lee, W.K. (1993). Circulation liquid velocity, gas holdup and volumetric oxygen transfer coefficient in external-loop airlift reactors. *J. Chem. Tech. Biotechnol.*, **56**, pp. 51-58.

Cini, P., Blaha, S.R. and Harold, M.P. (1991). Preparation and characterization of modified tubular ceramic membranes for use as catalyst supports. *Journal of Membrane Science*, **55**, pp. 199-225.

Cini, P. and Harold, M.P. (1991). Experimental study of the tubular multiphase catalyst. *AIChE Journal*, **37**(7), pp. 997-1008.

Clerici, M.G. and Ingallina, P. (1998). Oxidation reactions with in situ generated oxidants. *Catalysis Today*, **41**, pp. 351-364.

Corder, R.E., Johnson, E.R., Vega, J.L., Clausen, E.C. and Gaddy, J.L. (1988). Biological production of methanol from methane. *Am. Chem. Soc., Div. Fuel. Chem.*, **33**, pp. 469-478.

Cornils, B. and Herrmann, W.A., Eds. (2000). *Applied homogeneous catalysis.* Weinheim: Wiley-VCH.

Couslon, J.M. and Richardson, J.F. (1991). *Chemical engineering volume 2.* 4th ed. Oxford: Pergamon Press Ltd.

Crabtree, R.H. (1995). Aspects of methane chemistry. *Chem. Rev.*, **95**, pp. 987-1007.

Dowden, D.A., Schnell, C.R. and Walker, G.T. (1968). The design of complex catalysts. *Proceedings of the 4th International Congress on Catalysts*, Moscow, pp. 201-215.

Edwards, J.H. and Foster, N.R. (1986). The potential for methanol production from natural gas by direct catalytic partial oxidation. *Fuel Science & Technology International*, **4**(4), pp. 365-390.

Felder, R.M. and Rousseau, R.E. (1986). *Elementary principles of chemical processes.* 2nd ed. Singapore: John Wiley & Sons, Inc.

Fogler, H.S. (1992). *Elements of chemical reaction engineering.* 2nd ed. Englewood Cliffs: Prentice-Hall, Inc.

Foral, M.J. (1992). The noncatalytic partial oxidation of natural gas to methanol. *Symposium on Natural Gas Upgrading II*, San Francisco, April 5-10, pp. 34-40.

Frusteri, F., Arena, F., Bellitto, S. and Parmaliana, A. (1999). Partial oxidation of light paraffins on supported catalytic membranes. *Applied Catalysis A: General*, **180**, pp. 325-333.

Frusteri, F., Parmaliana, A., Arena, F. and Giordano, N. (1991). Thin-layer supported Nafion catalysts for the partial oxidation of light alkanes. *J. Chem. Soc., Chem. Commun.*, pp. 1332-1334.

Gang, X., Birch, H., Zhu, Y., Hjuler, H.A. and Bjerrum, N.J. (2000). Direct oxidation of methane to methanol by mercuric sulfate catalyst. *Journal of Catalysis*, **196**, pp. 287-292.

Geerts, J.W.M.H., Hoebink, J.H.B.J. and van der Wiele, K. (1990). Methanol from natural gas. Proven and new technologies. *Catalysis Today*, **6**, pp. 613-620.

Gesser, H.D., Hunter, N.R. and Morton, L. (1986). *Direct conversion of natural gas to methanol by controlled oxidation.* US Patent 4,618,732.

Gesser, H.D., Hunter, N.R. and Prakash, C.B. (1985). The direct conversion of methane to methanol by controlled oxidation. *Chem. Rev.*, **85**(4), pp. 235-244.

Glassman, I. (1987). *Combustion.* 2nd ed. London: Academic Press Inc.

Gosser, L.W. (1987). *Catalytic process for making H_2O_2 from hydrogen and oxygen.* US Patent 4,681,751.

Gradassi, M.J. and Green, N.W. (1995). Economics of natural gas conversion processes. *Fuel Processing Technology*, **42**, pp. 65-83.

Gretz, E., Oliver, T.F. and Sen, A. (1987). Carbon-hydrogen bond activation by electrophilic transition-metal compounds. Palladium(II)-mediated oxidation of arenes and alkanes including methane. *J. Am. Chem. Soc.*, **109**, pp. 8109-8111.

Hall, T.J., Hargreaves, S.J., Hutchings, G.J., Joyner, R.W. and Taylor, S.H. (1995). Catalytic synthesis of methanol and formaldehyde by the partial oxidation of methane. *Fuel Processing Technology*, **42**, pp. 151-178.

Holtcamp, M.W., Labinger, J.A. and Bercaw, J.E. (1997). C-H activation at cationic platinum(II) centers. *J. Am. Chem. Soc.*, **119**, pp. 848-849.

Horváth, I.T. and Rábai, J. (1994). Facile catalyst separation without water: fluorous biphase hydroformylation of olefins. *Science*, **266**, pp. 72-75.

Hunter, N.R., Gesser, H.D., Morton, L.A., Yarlagadda, P.S. and Fung, D.P.C. (1990). Methanol formation at high-pressure by the catalysed oxidation of natural-gas and by the sensitized oxidation of methane. *Applied Catalysis*, **57**(1), pp. 45-54.

Hutchings, G.J. and Taylor, S.H. (1999). Designing oxidation catalysts. *Catalysis Today*, **49**, pp. 105-113.

Jenzer, G., Mallat, T., Maciejewski, M., Eigenmann, F. and Baiker, A. (2001). Continuous epoxidation of propylene with oxygen and hydrogen on a Pd-Pt/TS-1 catalyst. *Applied Catalysis A: General*, **208**, pp. 125-133.

Kao, L.C., Hutson, A.C. and Sen, A. (1991). Low-temperature, palladium(II)-catalyzed, solution-phase oxidation of methane to a methanol derivative. *J. Am. Chem. Soc.*, **113**, pp. 700-701.

Kaštánek, F., Zahradník, J., Kratochvíl, J. and Cermák, J. (1993). *Chemical reactors for gas-liquid systems.* New York: Ellis Horwood.

Kesling, H.S. (1987). Oxidative carbonylation. A new synthesis gas route to adipic and sebacic acids. **In**: *Industrial chemicals via C_1 processes.* (F. R. Fahey, ed.), **328**, pp. 77-95. Washington, DC: American Chemical Society.

Kim, S. (2000). *Measurement of the effective diffusivity of gasoline compounds in coated monoliths and associated factors.* Ph.D thesis, University of Bath, Bath.

Kitamura, T., Piao, D., Taniguchi, Y. and Fujiwara, Y. (1998). Heteropolyacid-catalyzed partial oxidation of methane in trifluoroacetic acid. *Studies in Surface Science and Catalysis*, **119**, pp. 301-305.

Konno, M., Shindo, M., Sugawara, S. and Saito, S. (1988). A composite palladium and porous aluminium oxide membrane for hydrogen gas separation. *Journal of Membrane Science*, **37**, pp. 193-197.

Kozhevnikov, I.V. (1998). Catalysis by heteropoly acids and multicomponent polyoxometalates in liquid-phase reactions. *Chem. Rev.*, **98**, pp. 171-198.

Kroschwitz, J.I. and Howe-Grant, M., Eds. (1995). 4th ed. *Kirk-Othmer encyclopedia of chemical technology.* New York: John Wiley & Sons, Inc.

Kurioka, M., Nakata, K., jintoku, T., Taniguchi, Y., Takaki, K. and Fujiwara, Y. (1995). Palladium-catalyzed acetic acid synthesis from methane and carbon monoxide or dioxide. *Chemistry Letters*, pp. 244.

Labinger, J.A. (1995). Methane activation in homogeneous systems. *Fuel Processing Technology*, **42**, pp. 325-338.

Labinger, J.A., Herring, A.M. and Bercaw, J.E. (1990). Selective hydroxylation of methyl groups by platinum salts in aqueous medium. Direct conversion of ethanol to ethylene glycol. *J. Am. Chem. Soc.*, **112**(14), pp. 5628-5629.

Labinger, J.A., Herring, A.M., Lyon, D.K., Luinstra, G.A. and Bercaw, J.E. (1993). Oxidation of hydrocarbons by aqueous platinum salts: mechanism and selectivity. *Organometallics*, **12**, pp. 895-905.

Lance, D. and Elworthy, E.G. (1906). *Process for the manufacture of methyl alcohol from methane*. UK Patent 7,297.

Lambert, C.K. and Gonzalez, R.D. (1999). Sol-gel preparation and thermal stability of Pd/γ-Al_2O_3 catalysts. *Journal of Materials Science*, **34**, pp. 3109-3116.

Laufer, W. and Hoelderich, W.F. (2001). Direct oxidation of propylene and other olefins on precious metal containing Ti-catalysts. *Applied Catalysis A: General*, **213**(2), pp. 163-171.

Lee, J.H. and Foster, N.R. (1996). Direct partial oxidation of methane to methanol in supercritical water. *The Journal of Supercritical Fluids*, **9**, pp. 99-105.

Lee, S., Yang, S. and Park, S.B. (1994). Synthesis of palladium impregnated alumina membrane for hydrogen separation. *Journal of Membrane Science*, **96**, pp. 223-232.

Lide, D.R., Ed. (1991). *CRC handbook of chemistry and physics*. Boca Raton: CRC Press.

Lin, A., Hogan, T. and Sen, A. (1997). A highly catalytic bimetallic system for the low-temperature selective oxidation of methane and lower alkanes with dioxygen as the oxidant. *J. Am. Chem. Soc.*, **119**, pp. 6048-6053.

Lin, M., Hogan, T. and Sen, A. (1996). Catalytic carbon-carbon and carbon-hydrogen bond cleavage in lower alkanes. Low-temperature hydroxylations and hydroxycarbonylations with dioxygen as the oxidant. *J. Am. Chem. Soc.*, **118**, pp. 4574-4580.

Lin, M. and Sen, A. (1992). A highly catalytic system for the direct oxidation of lower alkanes by dioxygen in aqueous medium. A normal heterogeneous analog of alkane monooxygenases. *J. Am. Chem. Soc.*, **114**, pp. 7307-7308.

Luinstra, G.A., Wang, L., Stahl, S.S., Labinger, J.A. and Bercaw, J.E. (1995). C-H activation by aqueous platinum complexes: a mechanistic study. *Journal of Organometallic Chemistry*, **504**, pp. 75-91.

Lunsford, J.H. (2000). Catalytic conversion of methane to more useful chemicals and fuels: a challenge for the 21st century. *Catalysis Today*, **63**, pp. 165-174.

Mantegazza, M.A., Petrini, G., Spanò, G., Bagatin, R. and Rivetti, F. (1999). Selective oxidations with hydrogen peroxide and titanium silicate catalyst. *Journal of Molecular Catalysis A: Chemical*, **146**, pp. 223-228.

Masters, C. (1981). *Homogeneous transition-metal catalysis.* Cambridge: University Press.

McLurgh, D.B. (1997). *Study of a porous tube reactor for the wet air oxidation of aqueous wastes.* Ph.D thesis, University of Bath, Bath.

Mehta, P.K., Mishra, S. and Ghose, T.K. (1991). Methanol biosynthesis by covalently immobilized cells of Methylosinus trichosporium: batch and continuous studies. *Biotech. Bioeng.*, **37**, pp. 551-556.

Mills, P.L., Ramachandran, P.A. and Chaudhari, R.V. (1992). Multiphase reaction engineering for fine chemicals and pharmaceuticals. *Reviews in Chemical Engineering*, **8**(1-2), pp. 1-176.

Minkoff, C.J. and Tipper, C.F.H. (1962). *Chemistry of combustion reactions.* London: Butterworths.

Nakata, K., Yamaoka, Y., Miyata, T., Taniguchi, Y., Takaki, K. and Fujiwara, Y. (1994). Palladium(II) and/or copper(II)-catalyzed carboxylation of small alkanes such as methane and ethane with carbon monoxide. *Journal of Organometallic Chemistry*, **473**, pp. 329-334.

Nizova, G.V., Süss-Fink, G. and Shul'pin, G.B. (1997)[a]. Catalytic oxidation of methane to methyl hydroperoxide and other oxygenates under mild conditions. *Chem. Commun.*, pp. 397-398.

Nizova, G.V., Süss-Fink, G. and Shul'pin, G.B. (1997)[b]. Oxidations by the reagent <<O_2 - H_2O_2 - vanadium complex - pyrazine-2-carboxylic acid>> - 8. Efficient oxygenation of methane and other lower alkanes in acetonitrile. *Tetrahedron*, **53**(10), pp. 3603-3614.

Noceti, R.P., Taylor, C.E. and D'Este, J.R. (1997). Photocatalytic conversion of methane. *Catalysis Today*, **33**, pp. 199-204.

Oettinger, T.P. and Fontana, M.G. (1976). Austenitic stainless steels and titanium for wet air oxidation of sewage sludge. *Materials Performance*, **15**(11), November, pp. 29-35.

Park, E.D., Choi, S.H. and Lee, J.S. (2000)[a]. Characterization of Pd/C and Cu catalysts for the oxidation of methane to a methanol derivative. *Journal of Catalysis*, **194**, pp. 33-44.

Park, E.D., Lee, K.H. and Lee, J.S. (2000)[b]. Easily separable molecular catalysis. *Catalysis Today*, **63**, pp. 147-157.

Parmaliana, A. and Arena, F. (1997). Working mechanism of oxide catalysts in the partial oxidation of methane to formaldehyde.
I. Catalytic behaviour of SiO_2, MoO_3/SiO_2, V_2O_5/SiO_2, TiO_2, and V_2O_5/TiO_2 systems. *Journal of Catalysis*, **167**, pp. 57-65.

Parmaliana, A., Frusteri, F., Arena, F. and Giordano, N. (1992). Selective partial oxidation of light paraffins with hydrogen peroxide on thin-layer supported Nafion-H catalysts. *Catalysis Letters*, **12**, pp. 353-359.

Parmaliana, A., Frusteri, F., Mezzapica, A., Miceli, D., Scurrell, M.S. and Giordano, N. (1993). A basic approach to evaluate methane partial oxidation catalysts. *Journal of Catalysis*, **143**, pp. 262-174.

Periana, R.A. (1997). A novel, high-yield system for the oxidation of methane to methanol. *Advances in Chemistry Series*, **253**, pp. 61-78.

Periana, R.A., Taube, D.J., Evitt, E.R., Löffler, D.G., Wentrcek, P.R., Voss, G. and Masuda, T. (1993). A mercury-catalyzed, high-yield system for the oxidation of methane to methanol. *Science*, **259**, pp. 340-342.

Periana, R.A., Taube, D.J., Gamble, S., Taube, H., Satoh, T. and Fuji, H. (1998). Platinum catalysts for the high-yield oxidation of methane to a methanol derivative. *Science*, **280**, pp. 560-564.

Perry, R.H. and Green, D. (1984). *Perry's chemical engineers' handbook.* 6th ed. New York: McGraw-Hill, Inc.

Pham-Huu, C., Keller, N., Charbonniere, L.J., Ziessel, R. and Ledoux, M.J. (2000). Carbon nanofiber supported palladium catalyst for liquid-phase reactions. An active and selective catalyst for hydrogenation of C=C bonds. *Chem. Commun.*, pp. 1871-1872.

Piao, D., Inoue, K., Shibasaki, H., Taniguchi, Y., Kitamura, T. and Fujiwara, Y. (1999). An efficient partial oxidation of methane in trifluoroacetic acid using vanadium-containing heteropolyacid catalysts. *Journal of Organometallic Chemistry*, **574**, pp. 116-120.

Pitchai, R. and Klier, K. (1986). Partial oxidation of methane. *Catal. Rev-Sci. Eng.*, **13**, pp. 13-88.

Ramachandran, P.A. and Chaudhari, R.V. (1983). *Three-phase catalytic reactors.* New York: Gordon and Breach, Science Publishers, Inc.

Reid, R.C., Prausnitz, J.M. and Poling, B.E. (1987). *The properties of gases and liquids.* 4th ed. New York: McGraw-Hill, Inc.

Retallick, W.B. (1988). W. R. Grace & Co. *Washcoat for a catalyst support.* US Patent 4,762,567.

Rostovtsev, V.V., Labinger, J.A., Bercaw, J.E., Lasseter, T.L. and Goldberg, K.I. (1998). Oxidation of dimethylplatinum(II) complexes with dioxygen. *Organometallics*, **17**, pp. 4530-4531.

Savage, P.E., Li, R. and Santini, J.T. (1994). Methane to methanol in supercritical water. *The Journal of Supercritical Fluids*, **7**, pp. 135-144.

Sen, A. (1998). Catalytic functionalization of carbon-hydrogen and carbon-carbon bonds in protic media. *Acc. Chem. Res*,, **31**, pp. 550-557.

Sen, A., Benvenuto, M.A., Lin, M., Hutson, A.C. and Basickes, N. (1994). Activation of methane and ethane and their selective oxidation to the alcohols in protic media. *J. Am. Chem. Soc*,, **116**, pp. 998-1003.

Sen, A., Lin, M., Kao, L.C. and Hutson, A.C. (1992). C-H activation in aqueous medium. The diverse roles of platinum(II) and metallic platinum in the catalytic and stoichiometric oxidative functionalization of organic substrates including alkanes. *J. Am. Chem. Soc.*, **114**, pp. 6385-6392.

Shah, Y.T. (1979). *Gas-liquid-solid reactor design.* New York: McGraw-Hill Inc.

Shilov, A.E. (1984). Activation of alkanes by metal complexes of medium and low oxidation state. *Activation of Saturated Hydrocarbons by Transition Metal Complexes.* Dordrecht: D. Reidel Publishing Company.

Shilov, A.E. and Shul'pin, G.B. (1997). Activation of C-H bonds by metal complexes. *Chem. Rev.*, **97**, pp. 2879-2932.

Shu, J., Grandjean, B.P.A. and Kaliaguine, S. (1997). Gas permeation and isobutane dehydrogenation over very thin Pd/ceramic membranes. *The Canadian Journal of Chemical Engineering*, **75**, pp. 712-720.

Sinnott, R.K. (1993). *Coulson & Richardson's chemical engineering.* 2nd ed. Oxford: Pergamon Press Ltd.

Smith, J.M. (1981). *Chemical engineering kinetics.* Singapore: McGraw-Hill, Inc.

Smith, J.M. and Van Ness, H.C. (1987). *Introduction to chemical engineering thermodynamics.* 4th ed. Singapore: McGraw-Hill, Inc.

Spencer, N.D., Pereira, C.J. and Grasselli, R.K. (1990). The effect of sodium on the MoO_3-SiO_2-catalyzed partial oxidation of methane. *Journal of Catalysis*, **126**, pp. 546-554.

Srivastava, R.D., Zhou, P., Stiegel, G.J., Rao, V.U.S. and Cinquegrane, G. (1992). Direct conversion of methane to liquid fuels and chemicals. *Catalysis(London)*, **9**, pp. 183-228.

Stahl, S.S., Labinger, J.A. and Bercaw, J.E. (1995). Formation and reductive elimination of a hydridoalkylplatinum(IV) intermediate upon protonolysis of an alkylplatinum(II) complex. *J. Am. Chem. Soc.*, **117**, pp. 9371-9372.

Stahl, S.S., Labinger, J.A. and Bercaw, J.E. (1996). Exploring the mechanism of aqueous C-H activation by Pt(II) through model chemistry: evidence for the intermediacy of alkylhydridoplatinum(IV) and alkane σ-adducts. *J. Am. Chem. Soc.*, **118**, pp. 5961-5976.

Stahl, S.S., Labinger, J.A. and Bercaw, J.E. (1998). Homogeneous oxidation of alkanes by electrophilic late transition metals. *Angew. Chem. Int. Ed.*, **37**, pp. 2180-2192.

Süss-Fink, G., Nizova, G.V., Stanislas, S. and Shul'pin, G.B. (1998). Oxidations by the reagent 'O_2 - H_2O_2 - vanadate anion - pyrazine-2-carboxylic acid'. Part 10. Oxygenation of methane in acetonitrile and water. *Journal of Molecular Catalysis A: Chemical*, **130**, pp. 163-170.

Taylor, C.E., Anderson, R.R. and Noceti, R.P. (1997). Activation of methane with organopalladium complexes. *Catalysis Today*, **35**, pp. 407-413.

Taylor, C.E. and Noceti, R.P. (2000). New developments in the photocatalytic conversion of methane to methanol. *Catalysis Today*, **55**, pp. 259-267.

Thiel, W.R. (1999). New routes to hydrogen peroxide: alternatives for established processes? *Angew. Chem. Int. Ed.*, **38**(21), pp. 3157-3158.

Vargaftik, M.N., Stolarov, I.P. and Moiseev, I.I. (1990). Highly selective partial oxidation of methane to methyl trifluoroacetate. *J. Chem. Soc., Chem. Commun.*, pp. 1049-1050.

Weissermel, K. and Arpe, H. (1997). *Industrial Organic Chemistry.* 3rd ed. Weinheim: VCH Verlagsgesellschaft mbH.

Williams, G.R., Alvarez, P., Kolaczkowski, S.T. and Plucinski, P. (2001). Development of a continuous process for the direct liquid-phase partial oxidation of natural gas to methanol. *6th World Congress of Chemical Engineering,* Melbourne, September 23-27.

Wolf, D. (1998). High yields of methanol from methane by C-H bond activation at low temperatures. *Angew. Chem. Int. Ed.*, **37**(24), pp. 3351-3353.

Wolf, E.E. (1992). *Methane conversion by oxidative processes, fundamental and engineering aspects.* New York: Van Norstrand Reinhold.

Yamanaka, I., Morimoto, K., Soma, M. and Otsuka, K. (1998). Oxidation of methane and benzene with oxygen catalyzed by reduced vanadium species at 40 °C. *Journal of Molecular Catalysis A: Chemical*, **133**, pp. 251-254.

Yamanaka, I., Soma, M. and Otsuka, K. (1995). Oxidation of methane to methanol with oxygen catalysed by europium trichloride at room temperature. *J. Chem. Soc., Chem. Commun.*, **21**, pp. 2235-2236.

Yamanaka, I., Soma, M. and Otsuka, K. (1996). Enhancing effect of titanium(II) for the oxidation of methane with O_2 by an $EuCl_3$-Zn-CF_3CO_2H-catalytic system at 40 °C. *Chemistry Letters*, **7**, pp. 565-566.

Yarlagadda, P.S., Morton, L.A., Hunter, N.R. and Gesser, H.D. (1988). Direct conversion of methane to methanol in a flow reactor. *Industrial & Engineering Chemistry Research*, **27**(2), pp. 252-256.

Yoldas, B.E. (1975). Alumina sol preparation from alkoxides. *Amer. Ceram. Soc. Bull.*, **54**(3), pp. 289-290.

Electronic Sources:

Energy Information Administration: [WWW] http://www.eia.doe.gov/iea (August 5 2001)

American Methanol Institute: [WWW]: http://www.methanol.org (August 5 2001)

APPENDICES

APPENDIX I - Miscellaneous Experiments and Analysis

APPENDIX II - Gas Chromatograph Settings and Example Traces

APPENDIX III - Tables of Experimental Data Obtained for the Batch Reactor (Chapter 4)

APPENDIX IV - Tables of Experimental Data Obtained for the Porous Tube Reactor (Chapter 4)

APPENDIX V - Miscellaneous Tables of Data

APPENDIX VI - Calculation of Global Arrhenius Parameters for Acetic Acid Based Solvent

APPENDIX VII - Example Calculations, Bubble Diameter and Rise Velocity, Catalyst Particle Settling Velocity and Weisz-Prater Parameter

APPENDIX VIII - Conference Publication by Williams *et al.* (2001)

APPENDIX I - Miscellaneous Experiments and Analysis

1) Methyl trifluoroacetate degradation (as mentioned in Chapter 4)

Degradation Process	INITIAL [Methyl Trifluoroacetate] (mol/m^3)	FINAL [Methyl Trifluoroacetate] (mol/m^3)	Apparent Product "Loss" (% of initial)
Wet-Air Oxidation (use O_2 and N_2)	96	95	1
In situ H_2O_2 (use CO and O_2 and N_2)	96	79	18

Conditions: Where included P_{N2} = 62 bar; P_{CO} = 14 bar; P_{O2} = 7 bar;
5 wt.% Pd/C = 12.5 mg; $[CuCl_2]$ = 20 mol/m^3;
TFA:H_2O = 3:1 (50ml); T = 85 °C; t = 3 h; N = 700 rpm

2) Effect of mineral acid addition to an acetic acid based solvent (as mentioned in Chapter 4)

Experiment Details	Reaction ΔP (bar)	[Methyl acetate] (mol/m^3)	Methyl acetate Yield (%)	TON (based on Pd catalyst)	STY ($kg/kg_{Pdcat}.h$)
BASE	11	31	0.9	261	60.4
BASE + added H_2SO_4	11	27	0.8	226	52.4

Conditions: P_{CH4} = 62 bar; P_{CO} = 14 bar; P_{O2} = 7 bar;
5 wt.% Pd/C = 12.5 mg; $[CuCl_2]$ = 20 mol/m^3;
Acetic Acid/TFA:H_2O = 3:1 (50ml); T = 85 °C; t = 3 h; N = 700 rpm

3) Atomic Absorption Spectrometry (AAS)

i) Effect of $CuCl_2$ on Pd oxidation (as mentioned in Chapter 4)

Experiment Description	$[Pd^{2+}]$ (ppm)	$[Pd^{2+}]$ (mol/m^3)
Pd/C = 12.5 mg; TFA:H_2O = 3:1 (50 ml); T = 20 °C; t = 4 weeks	0.7	0.0066
Pd/C = 12.5 mg; [$CuCl_2$] = 20 mol/m^3; TFA:H_2O = 3:1 (50 ml); T = 20 °C; t = 4 weeks	1.9	0.0179

ii) Evidence of catalyst leaching from catalytic porous tube (as mentioned in Chapter 4)

	$[Pd^{2+}]$ (ppm)	$[Pd^{2+}]$ (mol/m^3)
RUN 1	4.5	0.0423
RUN 2	1.1	0.0103
RUN 3	0.7	0.0066

Conditions: Where included P_{CH4} = 62 bar; P_{O2} = 7 bar; [$CuCl_2$] = 20 mol/m^3; TFA:H_2O = 3:1 (300 ml); T = 85 °C; t = 3 h

4) Efficiency of the Sample Preparation Procedure for Methyl Acetate Product (Acetic Acid Reaction Solvent)

Sample Ester Concentration BEFORE Distillation (mol/m^3)	Sample Ester Concentration AFTER Distillation (mol/m^3)			Apparent Sample Ester "Loss" (%)					Maximum Ester "Loss" (%)	Minimum Ester "Loss" (%)
	1	2	3	1	2	3	Mean	Standard Deviation		
59.63	46.66	51.82	46.00	21.75	13.10	22.86	19.24	5.34	24.58	13.9
104.49	93.42	88.08	-	10.60	15.71	-	13.15	3.61	16.76	9.54
Overall Estimate for Ester "Loss" = 16.8 ±5.4 %										

5) X-ray Diffraction (XRD) Characterisation of Exemplary Semi-continuous Experimental Run

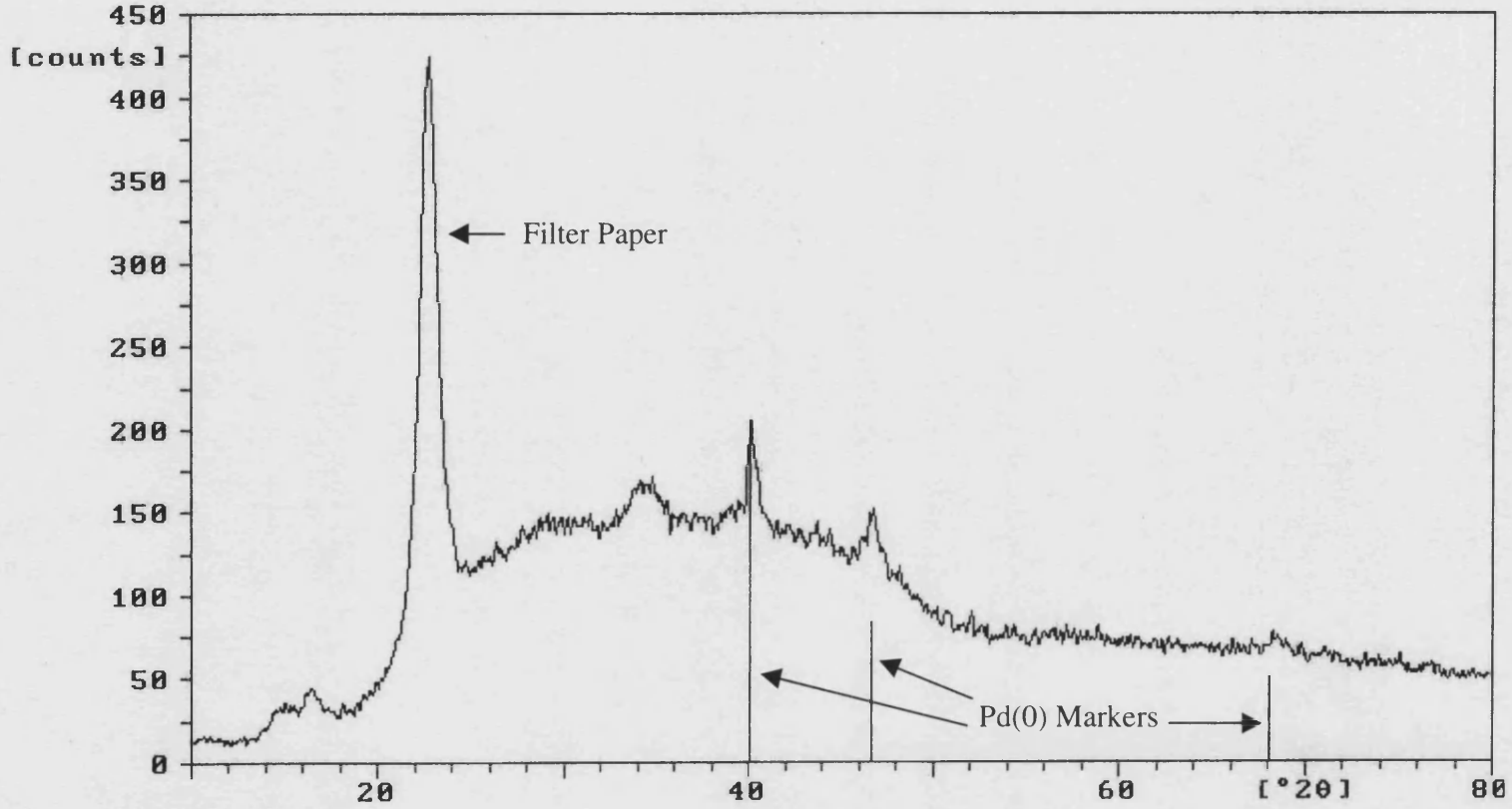

Conditions: $P_{CH4(i)}$ = 62 bar; $P_{CO(i)}$ = 14 bar; $P_{O2(i)}$ = 7 bar; Total Flow = 2 l/min;

$[Pd^{2+}]$ = 1.32 mol/m^3; $[CuCl_2]$ = 9.8 mol/m^3; TFA:H_2O = 3:1 (300 ml); T = 85 °C; t = 3 h

Prior to XRD, the final reactor effluent was filtered then washed *in situ* to remove soluble copper salts

APPENDIX II - Gas Chromatograph Settings and Example Traces

Equipment: HP5890 Series II GC, with a HP7673 automatic sampler and a HP3396 Series II integrator (Agilent Technologies (UK), Queensferry, UK).

Detector: Flame ionisation (FI) using hydrogen and air.

Column: Capillary type, model = BP20 (SGE Europe Ltd., Milton Keynes, UK); length = 50 m; ID = 0.32 mm; stationary phase thickness = 1μm

GC Run Set-up:

i) TFA based Solvent

GC Setting		Value
Carrier Gas Flowrate	(ml/min)	1.5
Injection Temperature	(°C)	130
Initial Temperature	(°C)	35
Initial Time	(min)	2
Temperature Ramp	(°C/min)	30
Final Temperature	(°C)	170
Final Time	(min)	23.5
Total Run Time	(min)	30

ii) Acetic Acid based Solvent

GC Setting		Value
Carrier Gas Flowrate	(ml/min)	1.5
Injection Temperature	(°C)	130
Initial Temperature	(°C)	35
Initial Time	(min)	2
Temperature Ramp	(°C/min)	30
Final Temperature	(°C)	170
Final Time	(min)	18.5
Total Run Time	(min)	25

iii) Biphasic Solvent

GC Setting		Value
Carrier Gas Flowrate	(ml/min)	1.5
Injection Temperature	(°C)	150
Initial Temperature	(°C)	35
Initial Time	(min)	2
Temperature Ramp	(°C/min)	10
Final Temperature	(°C)	170
Final Time	(min)	9.5
Total Run Time	(min)	25

EXAMPLE GC TRACE - TFA BASED SOLVENT

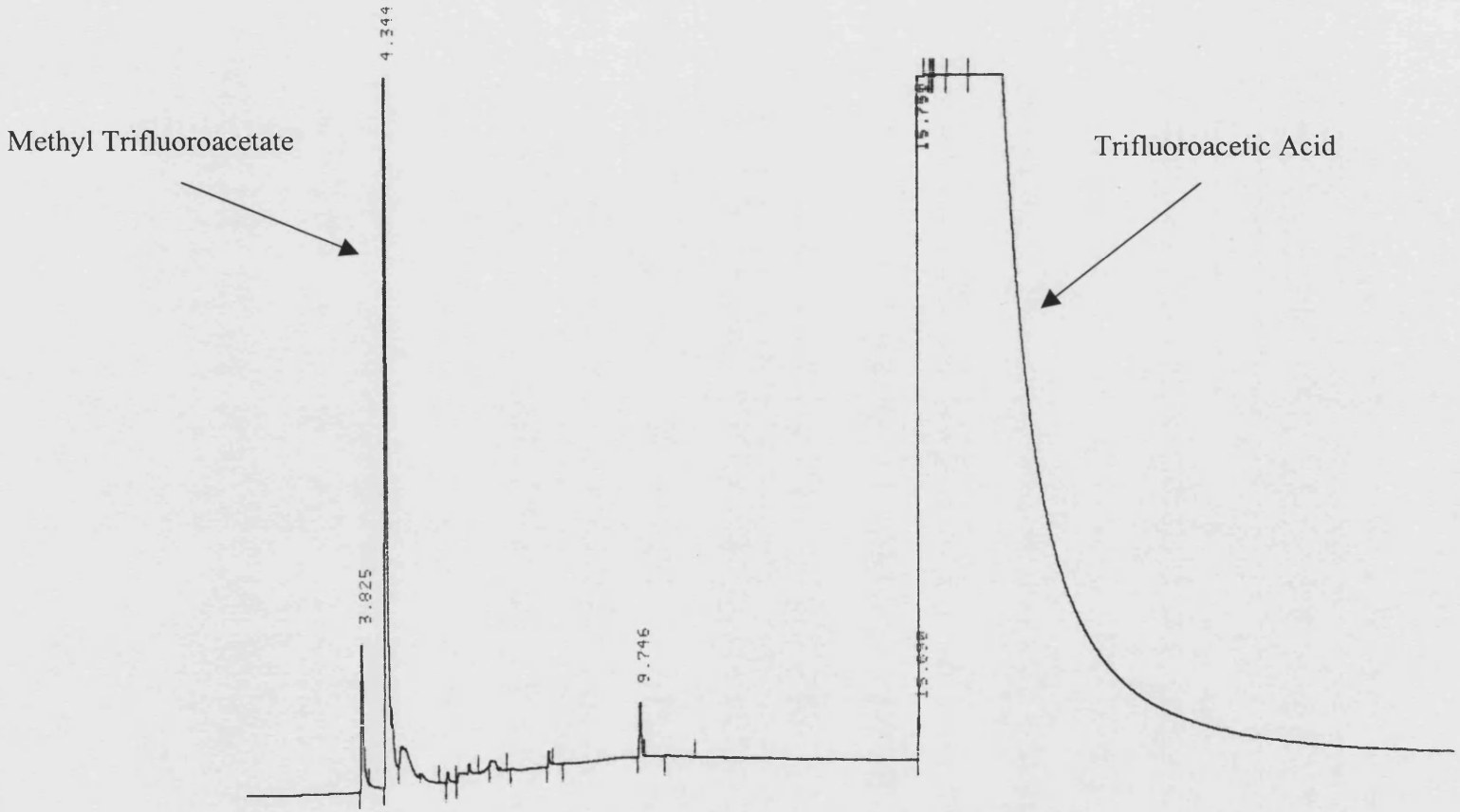

Conditions: $P_{CH4(i)}$ = 62 bar; $P_{CO(i)}$ = 14 bar; $P_{O2(i)}$ = 7 bar; Total Flow = 2 l/min; $[Pd^{2+}]$ = 0.12 mol/m^3; $[CuCl_2]$ = 4.9 mol/m^3; TFA:H_2O = 3:1 (300 ml); T = 85 °C; t = 3 h

EXAMPLE GC TRACE - ACETIC ACID BASED SOLVENT

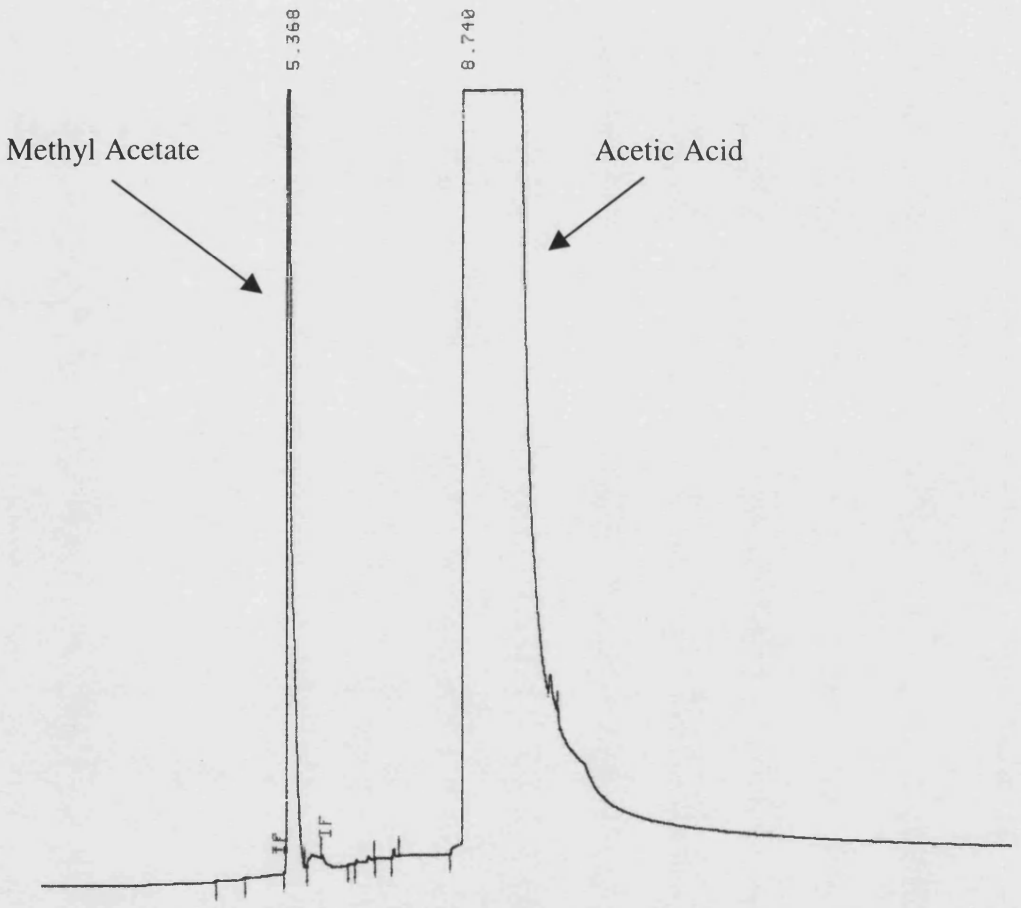

Conditions: P_{CH4} = 34.5 bar; P_{CO} = 14 bar; P_{O2} = 7 bar; 5 wt.% Pd/C = 12.5 mg; [$CuCl_2$] = 20 mol/m^3; Acetic Acid:H_2O = 3:1 (50 ml); N = 700 rpm; t = 1 h

APPENDIX III - Tables of Experimental Data Obtained for the Batch Reactor (Chapter 4)

Figure 4.1. Time Course of Methanol-based Product

Time (h)	Methyl Trifluoroacetate (mol/m^3)
0	0
1	40
2	50
3	50
20	51

Figure 4.2. Batch Reaction Pressure Drop Profile

Time (min)	Reaction Pressure Drop (bar)			
	$t = 1$ h	$t = 2$ h	$t = 3$ h	$t = 20$ h
0	0	0	0	0
5	0.75	0.75	0.75	0.5
10	1.5	1.5	1.5	1
15	2	2	2	1.75
20	2.75	2.5	2.75	2
25	3	2.75	3	2.75
30	3.5	3	3.75	3
35	4.25	3.25	4.25	3
40	5	3.5	4.75	3.25
45	5.5	4	5.25	3.5
50	6	4.5	5.75	4
55	6.5	5	6.25	4.5
60	6.75	5.5	6.75	5
70	-	6.25	8	5.75
80	-	6.75	8.5	6
90	-	8	9	7
120	-	9.25	10.25	8.5
150	-	-	10.5	10
180	-	-	11	11

Figure 4.3. Batch Liquid Temperature Profile

Time (min)	Liquid Temperature (°C)			
	$t = 1$ h	$t = 2$ h	$t = 3$ h	$t = 20$ h
0	85	85	85	85
5	86	86	87	86
10	86	86	86	86
15	85	85	85	85
20	85	84	84	84
25	84	84	84	84
30	84	85	84	85
35	85	85	85	85
40	85	85	85	85
45	85	85	85	85
50	85	85	85	85
55	85	85	85	85
60	85	85	85	85
70	-	85	85	85
80	-	85	85	85
90	-	85	85	85
120	-	85	85	85
150	-	-	85	85
180	-	-	85	85

Figure 4.4. Effect of Agitation Speed on Product Formation

N (rpm)	Methyl Trifluoroacetate (mol/m^3)
500	50
700	46
900	45

Figure 4.5. Effect of Agitation Speed on Reaction Pressure Drop

Time (min)	Reaction Pressure Drop (bar)		
	N = 500 rpm	N = 700 rpm	N = 900 rpm
0	0	0	0
5	0.75	0.5	1
10	1.5	1.25	2
15	2	2	3
20	2.75	2.75	3.75
25	3	3.25	4.5
30	3.75	4.25	5
35	4.25	5.25	5.75
40	4.75	5.75	6.5
45	5.25	6.5	7.25
50	5.75	7	8
55	6.25	7.75	8.25
60	6.75	8.25	8.75
70	8	9	10
80	8.5	9.75	10.5
90	9	10.5	11
120	10.25	11.25	11
150	10.5	11.5	11
180	11	11.5	11

Figure 4.6. Influence of Methane Presence on Reaction Pressure Drop

Time (min)	Reaction Pressure Drop (bar)			
	$CH_4 + O_2 + CO$ (Run 1)	$CH_4 + O_2 + CO$ (Run 2)	$O_2 + CO$ (Run 1)	$O_2 + CO$ (Run 2)
0	0	0	0	0
5	1	0.5	1	1
10	2	1.25	2	1.75
15	3	2	3	2.75
20	3.75	2.75	3.75	3.75
25	4.5	3.25	4.75	4.75
30	5	4.25	5.5	5.5
40	6.5	5.75	6.5	6.5
50	8	7	7.5	7.5
60	8.75	8.25	8	8
70	10	9	8.25	8.25
90	11	10.5	9	9
120	11	11.25	9	9
180	11	11.5	9	9

Figure 4.25. Effect of 316 Stainless Steel on Reaction Performance

Time (h)	316 Stainless Steel (Yes/No)	Methyl Trifluoroacetate (mol/m^3)
1	Yes	38
2	Yes	49
20	Yes	54
1	No	40
2	No	50
20	No	51

Figure 4.26. Reaction Pressure Drop Profile with Acetic Acid as Liquid Phase Solvent

Time (min)	Reaction Pressure Drop (bar)		
	TFA	Acetic Acid (Run 1)	Acetic Acid (Run2)
0	0	0	0
5	1	0.75	1
10	2	2	2
15	3	3	3
20	3.75	4.5	4.25
25	4.5	5.5	5.5
30	5	6.5	6.5
35	5.75	7.5	7
40	6.5	8	8
45	7.25	8.25	8.25
50	8	9	8.75
55	8.25	9.25	9
60	8.75	9.5	9.5
70	10	10	10
80	10.5	10.5	10.5
90	11	11	11
120	11	11	11
150	11	11	11
180	11	11	11

Figure 4.27. Effect of Temperature on Product Concentration

Temperature (°C)	Methyl Trifluoroacetate (mol/m^3)
70	24
80	25
90	27
100	30
110	30

Figure 4.28. Effect of Temperature on Reaction Pressure Drop

Time (min)	Reaction Pressure Drop (bar)			
	$T = 70$ °C	$T = 90$ °C	$T = 100$ °C	$T = 110$ °C
0	0	0	0	0
5	0.75	0.5	1.75	2.5
10	1.75	2	3	4.25
15	2.5	3	4.75	5.75
20	3	4.25	5.75	7
25	3.75	5.5	6.5	7.75
30	4	6.25	7.5	8.25
35	5	7.25	7.75	8.75
40	5.5	7.5	8.25	9
45	6	8	8.75	9.5
50	6.75	8.5	9	9.75
55	7	8.75	9.25	9.75
60	7.5	9	9.5	9.75

Figure 4.29. Effect of Methane Partial Pressure on Product Concentration

$P_{CH4(i)}$ (bar)	Methyl Trifluoroacetate (mol/m^3)
14	25
21	24
28	22
41	22

Figure 4.30. Effect of Methane Partial Pressure on Reaction Pressure Drop

Time (min)	Reaction Pressure Drop (bar)			
	P_{CH4} = 14 bar	P_{CH4} = 21 bar	P_{CH4} = 28 bar	P_{CH4} = 41 bar
0	0	0	0	0
5	1	1	0.75	0.75
10	2.25	2	2	2
15	3.25	3.25	3	3
20	4.5	4.25	4.25	4.25
25	5.75	6	5.5	5.25
30	6.5	6.75	6.25	6
35	7	7.5	7	7
40	7.75	8	7.75	7.75
45	8	8.5	8	8
50	8.25	9	8.5	8.5
55	8.75	9	8.75	9
60	9	9.25	9	9.25

APPENDIX IV - Tables of Experimental Data Obtained for the Porous Tube Reactor (Chapter 4)

Figure 4.7. Verification of the Use of the Catalyst System with the Porous Tube Reactor

Time (min)	Methyl Trifluoroacetate (mol/m^3)
0	0
30	15
60	18
90	21
120	21
150	20
180	15

Figure 4.10. Effect of $CuCl_2$ on Product Formation

Time (min)	Methyl Trifluoroacetate (mol/m^3)		
	$CuCl_2/Pd^{2+} = 42$	$CuCl_2/Pd^{2+} = 168$	$CuCl_2/Pd^{2+} = 8$
0	0	0	0
30	23	15	2
60	n/a	18	5
90	40	21	8
120	38	21	13
150	40	20	18
180	37	15	21

Figure 4.11. Effect of Pd^{2+} on Product Concentration

Time (min)	Methyl Trifluoroacetate (mol/m^3)	
	$[Pd^{2+}] = 0.12\ mol/m^3$	$[Pd^{2+}] = 0.66\ mol/m^3$
0	0	0
30	23	26
60	n/a	37
90	40	44
120	39	49
150	39	48
180	38	52

Figure 4.12. Dominant Effect of $[CuCl_2]$ on Product Concentration

Time (min)	Methyl Trifluoroacetate (mol/m^3)	
	$[CuCl_2] = 4.9\ mol/m^3$	$[CuCl_2] = 19.7\ mol/m^3$
0	0	0
30	23	15
60	n/a	18
90	40	21
120	39	21
150	39	20
180	38	15

Figure 4.13. Effect of Doubling Catalyst Concentrations on Product Formation

Time (min)	Methyl Trifluoroacetate (mol/m^3)	
	$[CuCl_2] = 4.9\ mol/m^3$; $[Pd^{2+}] = 0.66\ mol/m^3$	$[CuCl_2] = 9.8\ mol/m^3$ $[Pd^{2+}] = 1.32\ mol/m^3$
0	0	0
30	26	25
60	37	29
90	44	32
120	49	38
150	48	37
180	52	-
210	-	36

Figure 4.14. Influence of Methane Partial Pressure on Product Formation

Time (min)	Methyl Trifluoroacetate (mol/m^3)		
	$P_{CH4} = 62$ bar	$P_{CH4} = 40$ bar	$P_{CH4} = 28$ bar
0	0	0	0
30	26	9	11
60	37	21	17
90	44	27	19
120	49	30	24
150	48	31	25
180	52	33	24

Figure 4.15. Rate Dependence on Methane Partial Pressure

log [P_{CH4}]	log {[Methyl Trifluoroacetate]/h}
1.45	- 1.77
1.60	- 1.68
1.79	- 1.43
1.79	- 1.47

Figure 4.16. Influence of Carbon Monoxide Partial Pressure on Product Formation

Time (min)	Methyl Trifluoroacetate (mol/m^3)	
	P_{CO} = 14 bar	P_{CO} = 7 bar
0	0	0
30	26	14
60	37	21
90	44	23
120	49	21
150	48	24
180	52	28

Figure 4.17. Semi- Continuous Operation at a Reduced Pressure

Time (min)	Methyl Trifluoroacetate (mol/m^3)		
	P_{CH4} = 28 bar; P_{CO} = 14 bar; P_{O2} = 7 bar T = 120 °C	P_{CH4} = 38 bar; P_{CO} = 8 bar; P_{O2} = 4 bar T = 120 °C	P_{CH4} = 28 bar; P_{CO} = 14 bar; P_{O2} = 7 bar T = 85 °C
0	0	0	0
30	23	14	11
60	27	17	17
90	26	25	19
120	34	22	24
150	31	-	25
180	38	-	24

Figure 4.18. Differential Pressure Time Course at Elevated Operating Temperatures

Time (min)	Differential Pressure (bar)		
	T = 120 °C; P_{Total} = 50 bar	T = 85 °C; P_{Total} = 50 bar	T = 85 °C; P_{Total} = 50 bar
0	0.31	0.34	0.34
30	0.45	0.34	0.34
60	0.59	0.34	0.34
90	0.93	0.34	0.34
120	1.31	0.34	0.34
180	1.79	0.34	0.34

Figure 4.19. Increased Reactor Run Time

Time (min)	Methyl Trifluoroacetate (mol/m^3)	
	t = 3 h	t = 5 h
0	0	0
30	26	18
60	37	34
90	44	45
120	49	44
150	48	51
180	52	52
210	-	54
240	-	54
300	-	50

Figure 4.20. TON Time Course

Time (min)	TON (based on Pd)	
	t = 3 h	t = 5 h
0	0	0
30	140	93
60	187	171
90	220	225
120	248	225
150	242	258
180	263	263
210	-	271
240	-	271
300	-	254

Figure 4.21. STY Time Course

Time (min)	STY ($kg/kg_{Pdcat.}.h$)	
	t = 3 h	t = 5 h
0	0	0
30	95	67
60	67	62
90	53	54
120	45	41
150	35	37
180	32	32
210	-	28
240	-	24
300	-	18

Figure 4.22. Extent of Product Removal within the Porous Tube Reactor

Time (min)	Methyl Trifluoroacetate (mol/m^3)	
	N_2 Flow	N_2 + O_2 Flow
0	50	49
30	52	50
60	46	43
90	38	38
120	35	30
150	31	28
180	26	22

Figure 4.23. Heterogeneous Palladium Versus Homogeneous Palladium Catalysis

Time (min)	Methyl Trifluoroacetate (mol/m^3)			
	[Pd] = 0.12 mol/m^3 [$CuCl_2$] = 20 mol/m^3	[Pd^{2+}] = 0.12 mol/m^3 [$CuCl_2$] = 20 mol/m^3	[Pd] = 0.66 mol/m^3 [$CuCl_2$] = 4.9 mol/m^3	[Pd^{2+}] = 0.66 mol/m^3 [$CuCl_2$] = 4.9 mol/m^3
0	0	0	0	0
30	7	15	12	26
60	12	18	22	37
90	15	21	28	44
120	12	21	29	49
150	12	20	37	48
180	17	15	42	52

Figure 4.24. Porous Tube Reactor Exemplary Temperature Profiles

Time (min)	Liquid Temperature (°C)		
	$[Pd^{2+}] = 0.66$ mol/m^3 $[CuCl_2] = 4.9$ mol/m^3	$[Pd/C] = 0.66$ mol/m^3 $[CuCl_2] = 4.9$ mol/m^3	$[Pd^{2+}] = 1.32$ mol/m^3 $[CuCl_2] = 9.8$ mol/m^3
0	85	85	85
5	88	88	94
10	90	92	96
15	90	91	96
20	88	88	94
25	87	87	93
30	85	86	92
35	85	85	91
40	85	85	90
45	85	85	88
50	85	85	87
55	85	85	86
60	85	85	85

APPENDIX V - Miscellaneous Tables of Data

Figure 3.5. Liquid Circulation Rates in the Porous Tube Reactor

Nitrogen Flowrate (l/min @ 15 °C, 0.1 MPa)	Water Circulation Rate (ml/min @ 20 °C)	
	Liquid Volume = 200 ml	Liquid Volume = 350 ml
0.2	140	-
0.25	-	160
0.5	190	195
1	210	210
1.5	225	225
2	235	235

Figure 3.6. Prediction of Experimental Methane *P-T* Behaviour

Temperature (°C)	Experimental (bar(a))	Ideal Gas (bar)	Redlich/Kwong (bar)	Benedict/Webb/Rubin (bar)
17	70.8	70.8	70.8	70.8
30	74.3	73.9	75.2	75.2
40	77.0	76.4	78.6	78.6
50	79.8	78.8	82.0	82.0
60	82.3	81.3	85.4	85.4
70	84.8	83.7	88.8	88.8
80	87.5	86.1	92.2	92.2
90	90.3	88.6	95.5	95.6
100	92.8	91.0	98.9	98.9
110	95.3	93.4	102.2	102.3
120	97.5	95.9	105.5	105.6
130	100.3	98.3	108.8	109.0

Figure 3.7. Vapour Pressure Predictions for TFA and Water

Temperature (°C)	Liquid Vapour Pressure (bar)	
	Water	TFA
10	0.012	0.069
20	0.023	0.117
30	0.042	0.191
40	0.074	0.298
50	0.123	0.452
60	0.199	0.665
70	0.312	0.952
80	0.474	1.332
90	0.701	1.824
100	1.013	2.452
110	1.432	3.240
120	1.985	4.217
130	2.702	5.412
140	3.615	6.861
150	4.763	8.601

Figure 3.8. Application of Raoult's Law to a 3:1 (v/v) mixture of TFA:Water

Temperature (°C)	Partial Pressure (bar)
10	0.036
20	0.063
30	0.105
40	0.168
50	0.262
60	0.395
70	0.582
80	0.835
90	1.175
100	1.620
110	2.194
120	2.926
130	3.844
140	4.983
150	6.381

APPENDIX VI - Calculation of Global Arrhenius Parameters for Acetic Acid Based Solvent

Temperature		[Methyl acetate]		[Methyl acetate]/time	ln{[Methyl acetate]/time}	1/T
°C	K	mol/m^3	mol/dm^3	(×10^6 mol/dm^3.s)		(× 10^3 K^{-1})
70	343	24.0	0.0240	6.68	**- 11.9(2)**	**2.92**
80	353	25.5	0.0255	7.07	**- 11.8(6)**	**2.83**
90	363	27.2	0.0272	7.55	**- 11.7(9)**	**2.75**
100	373	30.3	0.0303	8.42	**- 11.6(8)**	**2.68**
110	383	30.4	0.0304	8.46	**- 11.6(8)**	**2.61**

Conditions: P_{CH4} = 34.5 bar; P_{CO} = 14 bar; P_{O2} = 7 bar;
5 wt.% Pd/C = 12.5 mg; [$CuCl_2$] = 20 mol/m^3;
Acetic Acid:H_2O = 3:1 (50 ml); t = 1 h; N = 700 rpm

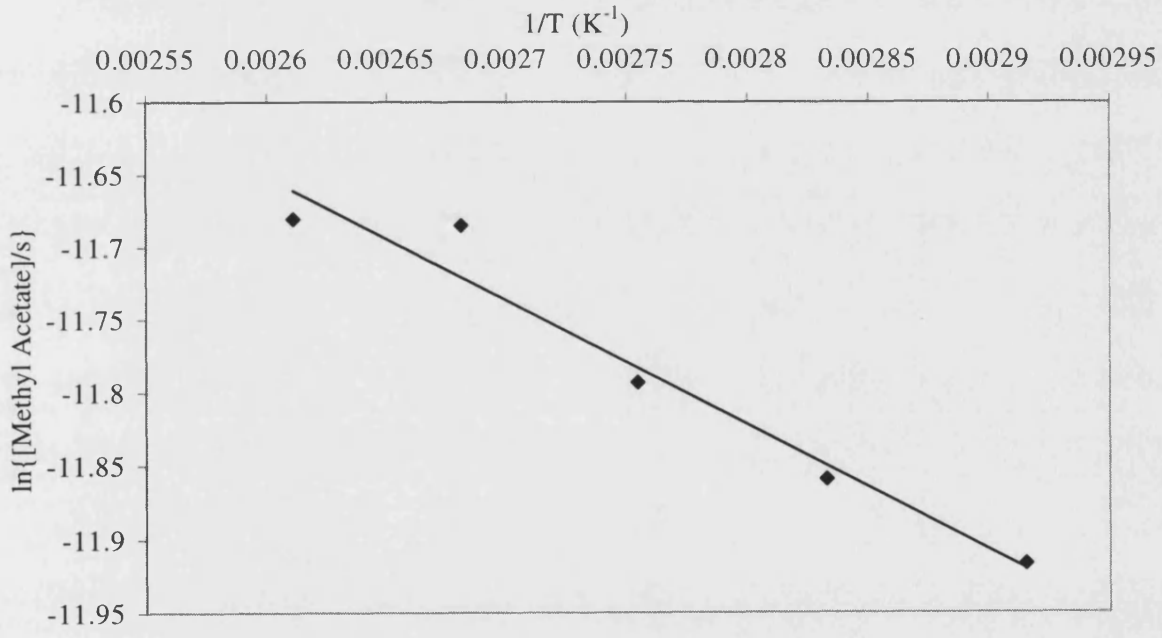

Non-linear regression on the data to fit an Arrhenius form of equation *i.e.*

Rate = $A \exp\left(\frac{-E_a}{RT}\right)$, yields the kinetic constants, A = 7.8 × 10^{-5} ±2.4 × 10^{-5} s^{-1} and

E_a = 7.0 ±0.9 kJ/mol.

APPENDIX VII - Example Calculations, Bubble Diameter and Rise Velocity, Catalyst Particle Settling Velocity and Weisz-Prater Parameter

1) Calculation of Methyl Trifluoroacetate Concentration

- First obtain the volume fraction of methyl trifluoroacetate in the post-reaction mixture of 3:1 TFA:H_2O from the calibrated GC. To convert to a concentration the following equation is used:

$$C_{MeTFA} = \frac{v_{MeTFA}\,\rho_{MeTFA} \times 10^3}{M_{MeTFA}} \qquad \text{(AVII-1)}$$

Where: C_{MeTFA} = Concentration of methyl trifluoroacetate (mol/m^3)

v_{MeTFA} = Volume fraction of methyl trifluoroacetate (vol/vol)

ρ_{MeTFA} = Density of methyl trifluoroacetate (= 1282 kg/m^3 at 20 °C)

M_{MeTFA} = Molar mass of methyl trifluoroacetate (= 128.0 g/mol)

e.g. for a volume fraction of methyl trifluoroacetate = 0.0049 vol/vol

$$C_{MeTFA} = \frac{0.0049 \times 1282 \times 10^3}{128.0} = 49 \text{ mol/m}^3$$

2) Calculation of Methyl Trifluoroacetate Yield

$$\text{MeTFA Yield} = \frac{n_{MeTFA}}{n_{CH_4(i)}} \times 100 \qquad \text{(AVII-2)}$$

To obtain the initial number of moles of CH_4, the ideal gas equation of state is used:

$$n = \frac{PV}{RT} \qquad \text{(AVII-3)}$$

e.g. for an initial CH_4 partial pressure of 62 bar at 85 °C with a gaseous volume of 80 ml, and a product concentration of 49 mol/m^3 in a liquid volume of 50 ml:

$$n_{MeTFA} = 49 \times 50 \times 10^{-6} = 2.5 \times 10^{-3}\ moles$$

$$n_{CH_4(i)} = \frac{(62/1.013) \times 10^5 \times 80 \times 10^{-6}}{8.314 \times (85 + 273)} = 0.16\ moles$$

$$\Rightarrow \qquad \text{MeTFA Yield} = \frac{2.5 \times 10^{-3}}{0.16} \times 100 = 1.6\ \%$$

3) Calculation of TON based on Palladium

$$\text{TON} = \frac{n_{MeTFA}}{n_{Pd}} \qquad \text{(AVII-4)}$$

e.g. for 2.5×10^{-3} moles of product and 0.0125 g of 5 wt.% Pd/C catalyst:

$M_{Pd} = 106.7$ g/mol

$$\text{TON} = \frac{2.5 \times 10^{-3}}{0.05 \times (0.0125/106.7)} = 427$$

4) Calculation of STY based on Palladium

$$\text{STY} = \frac{w_{MeTFA}}{w_{Pd} \times t} \qquad \text{(AVII-5)}$$

e.g. for 2.5×10^{-3} moles of product formed in 1h and 0.0125 g of 5 wt.% Pd/C catalyst:

$$\text{STY} = \frac{2.5 \times 10^{-3} \times 128.0}{0.05 \times 0.0125 \times 2} = 256\ \text{kg/kg}_{\text{Pd}}\text{.h}$$

5) Bubble Diameter (produced from porous tube) and Rise Velocity

To get an idea as to the velocity of the rising bubbles being carried by the circulating liquid, the following calculation is performed assuming nitrogen/water being the fluid phases:

To establish a ballpark figure for the bubble diameter produced from the porous tube, the following equation is used, based on single-bubble development from an orifice (Perry and Green, 1984):

$$\frac{D_b}{D} = \left[\frac{6\sigma_L}{D^2(\rho_L - \rho_G)g}\right]^{\frac{1}{3}} \qquad \text{(AVII-6)}$$

Where:
D_b = Diameter of bubble (m)
D = Diameter of orifice (= 1×10^{-6} m)
σ_L = Liquid surface tension (= 0.0728 N/m for water at 20 °C)
ρ_L = Liquid density (= 998 kg/m^3 for water at 20 °C)
ρ_G = Gas density (= 1.2 kg/m^3 for N_2 at 20 °C, 0.1 MPa)
g = Acceleration due to gravity (= 9.81 m/s^2)

Inserting the values gives $D = 3.5 \times 10^{-4}$ m or 0.35 mm
This value represents a tiny bubble (D < 2 mm) for design purposes (Kaštánek *et al.*, 1993).

An empirical relation for the bubble rise velocity in air-lift reactors is as follows (Kaštánek *et al.*, 1993):

$$u_b = 1.5\left[\frac{\sigma_L\, g(\rho_L - \rho_G)}{\rho_L^2}\right]^{\frac{1}{4}} \qquad \text{where } u_b = \text{bubble rise velocity (m/s)} \qquad \text{(AVII-7)}$$

Inserting the values results with u_b = 0.25 m/s. For a wide range of operating conditions the vertical velocity of bubbles rising through a liquid is about 0.2 m/s (Smith, 1981).

The selected water circulation rate = 235 ml/min at 15 °C, 0.1 MPa (Section 3.2.5). With a maximum reactor I.D of 15 mm, this computes to a superficial liquid velocity of at least 0.02 m/s. This velocity component would tend to increase the bubble rise velocity in the riser section with a possibility of bubble carry over into the downcomer section causing additional gas hold-up which increases the mass transfer interfacial area.

6) Calculation of particle settling velocity to estimate whether the natural liquid circulation in the porous tube reactor is sufficient to circulate the Pd/C catalyst particles (taken from methods described in Coulson and Richardson, 1991)

As the maximum catalyst loading employed is 1.4 kg/m^3, particles are assumed to settle freely and not influenced by others (non-hindered). For simplification, water is assumed to constitute the liquid phase as that was used for the circulation rate experiments (see Chapter 3).

Define dimensionless Galileo number, *Ga*:

$$Ga = \frac{d^3 \rho_L (\rho_S - \rho_L) g}{\mu_L^{\,2}} \qquad \text{(AVII-8)}$$

Where: d = Catalyst particle (spherical) diameter (= 75 × 10^{-6} m)

ρ_L = Liquid density (= 998 kg/m^3 for water at 20 °C)

ρ_S = Particle density (= 2100 kg/m^3)

g = Acceleration due to gravity (= 9.81 m/s)

μ_L = Liquid viscosity (= 1002 × 10^{-6} kg/m.s)

Inserting the numerical values computes Ga = 0.0045

For this value, the following approximation exists:

$$Ga = 18\ Re'_o \qquad \text{valid for } Ga < 3.6 \qquad \text{(AVII-9)}$$

Where: $Re'_o = \frac{u_o d \rho_L}{\mu_L}$ with u_o = particle terminal velocity (m/s)

Use of equations (AVII-6 and AVII-7) results with $u_0 = 3.4 \times 10^{-6}$ m/s

The selected water circulation rate = 235 ml/min at 15 °C, 0.1 MPa (Section 3.2.5). With a maximum reactor I.D of 15 mm, this computes to a superficial liquid velocity of at least 0.02 m/s. Therefore, the approximate velocity values suggest that the catalyst particles would probably be carried around the reactor as desired.

7) Weisz-Prater parameter for internal diffusion (see *e.g.* Fogler, 1992):

$$C_{WP} = \frac{-r_{(obs)}\,\rho_p\,r^2}{D_e\,C_s} \qquad \text{(AVII-10)}$$

Where: C_{WP} = Weisz-Prater parameter (-)

$-r_{(obs)}$ = Observed rate of reaction (mol/g$_{\cdot catalyst}$·s)

ρ_p = Catalyst particle density (g/cm^3)

r = Catalyst particle average radius (cm)

D_e = Effective diffusivity (cm^2/s)

C_s = Concentration of reactant on catalyst surface (mol/cm^3)

Although the actual methane oxidation reaction comprises of three gaseous reactants, and a TFA/H_2O liquid solution containing dissolved copper(II) chloride, for simplicity the calculation of the Weisz-Prater is based on a methane substrate with a water liquid phase into which the Pd/C catalyst is distributed. The Weisz-Prater parameter value is only meant to be an indication of intra-particle resistance and thus no rigour is attached to the calculation for what is, in reality, a complex reaction system.

Estimation of reactant surface concentration:

For negligible external resistance the surface reactant concentration is comparable to that in the bulk phase *i.e.* $C_s \approx C_{bulk}$

For a low solubility methane substrate in water, Henry's Law may apply:

$$P_A = H\,x_A \qquad \text{(AVII-11)}$$

Where: P_A = Partial pressure of species "A" (atm)

H = Henry's Law constant (atm/mol/mol solvent)

x_A = Liquid mole fraction of species "A" (-)

then to obtain C_{bulk}:

$$C_{bulk} = \frac{x_A \rho_{solvent}}{M_{solvent}} \qquad \text{(AVII-12)}$$

where: $\rho_{solvent}$ = Density of solvent (g/cm^3)

$M_{solvent}$ = Molar mass of solvent (g/mol)

Estimation of reactant effective diffusivity:

The two main types of diffusion of the solute reactant in the porous catalyst are molecular diffusion and Knudsen diffusion, whilst surface diffusion is generally very small. Because the mean free path in a liquid medium is small, usually Knudsen diffusion in the liquid-filled catalyst pores can be neglected (Smith, 1981). An expression to calculate the effective diffusivity in this case is given in Fogler, 1992.

$$D_e = \frac{D_{bulk}\, \varepsilon_p \sigma}{\tau} \qquad \text{(AVII-13)}$$

Where: D_{bulk} = Bulk diffusivity of species (cm^2/s)

ε_p = Catalyst particle porosity (-)

σ = Catalyst particle constriction factor

τ = Catalyst particle tortuosity (-)

For bulk diffusion of a solute of low solubility in water, Hayduk and Minas (see Reid *et al.*, 1987) obtained the following correlation:

$$D_{bulk} = 1.25 \times 10^{-8} (V_A^{-0.19} - 0.292) T^{1.52} \eta_w^{\left(\frac{9.58}{V_A} - 1.12\right)} \qquad \text{(AVII-14)}$$

Where: V_A = Molar liquid volume of solute "A" at normal boiling point (cm^3/mol)

T = Temperature (K)

η_w = Viscosity of water (cp)

For the calculation of the Weisz-Prater parameter, the following values were used for the 5 wt.% Pd/C catalyst, a methane substrate and a water liquid phase, as shown in the table below:

Quantity	Value	Comment
ρ_p	2.1 g/cm^3	Measured using a pycnometer (AccuPyc 1330, Micrometrics Instrument Co., USA) assuming a negligible interparticle voidage
r	37.5×10^{-4} cm	From SEM measurements
ε_p	0.81	Estimated from nitrogen adsorption experiments and particle density
τ	3	General value taken from Fogler, 1992
σ	0.8	As above
T	358 K	-
H	6.87×10^4 at 358 K atm/mol/mol solvent	Obtained from Perry and Green (1984)
V_{CH4}	37.92 cm^3/mol at 112 K	As above
M_{CH4}	16 g/mol	-
η_w	0.33 cp at 358 K	Obtained from Perry and Green (1984)
ρ_w	0.969 g/cm^3 at 358 K	As above
$P_{(CH4)}$	61.2 atm	-
$-r_{(obs)}$	4.44×10^{-5} moles/$g_{catalyst}$.s	Based on 1 h product formation rate (see Chapter 4, Figure. 4.1)
$C_s \approx C_{bulk}$	4.86×10^{-5} mol/cm^3	Calculated using equations (AVII-11) and (AVII-12)
D_{bulk}	5.21×10^{-5} cm^2/s	Calculated using equation (AVII-14)
D_e	1.14×10^{-5} cm^2/s	Calculated using equation (AVII-13)

Using the data in the table above and equation (AVII-6), a value for the Weisz-Prater parameter,C_{WP}, of 2.4 is obtained. Values of $C_{WP} >> 1$ indicates the presence of a significant pore resistance (the opposite is true for values << 1) (Fogler, 1992), so the calculated value being close to 1, although inconclusive, hints at only minimal intra-particle resistance. It should not be forgotten, however, that the calculation is only ballpark and includes some estimated constants (*e.g.* τ and σ) with the actual system modelled being much more complex than that assumed for the calculation.

Applying the same calculation procedure for the acetic acid based solvent (assumed to be water) with $-r_{(obs)}$ equal to 3.02×10^{-5} moles/$g_{catalyst}$.s based on a 1 h product formation rate at 90 °C (363 K) and η_w = 0.31, ρ_w = 965.3 kg/m^3, H = 6.92×10^4 atm/mol/mol.solvent all at 363 K, a value for C_{WP} of 1.5 is obtained. Again this value signifies little pore resistance.

APPENDIX VIII - Conference Publication by Williams *et al.* (2001)

Williams, G.R., Alvarez, P., Kolaczkowski, S.T. and Plucinski, P. (2001). Development of a continuous process for the direct liquid-phase partial oxidation of natural gas to methanol. *6th World Congress of Chemical Engineering,* Melbourne, September 23-27.

Development of a continuous process for the direct liquid-phase partial oxidation of natural gas to methanol

Gareth R. Williams, Pedro Alvarez,
Stan T. Kolaczkowski and Pawel Plucinski

University of Bath, Department of Chemical Engineering,
Claverton Down, Bath BA2 7AY, UK

In this work the catalytic bimetallic (Pd/C (or Pd^{2+}) + $CuCl_2$) system for the direct liquid phase oxidation of methane and lower alkanes to methanol, using dioxygen as the stoichiometric oxidant has been selected for reaction engineering studies. The process typically operates in a mixture of trifluoroacetic acid and water in the presence of oxygen and carbon monoxide as a co-reductant. Compared to the other systems of methane functionalisation described in the literature, the ability to induce C-C cleavage (i.e. production of methanol from higher alkanes) as well as C-H cleavage makes the system flexible for a varying natural gas feedstock. The main focus of the work is the development of semi-continuous operation using a three-phase porous tube reactor. The application of trifluoroacetic acid as a solvent leads to the esterification of formed methanol, which intentionally affects chemical protection against further oxidation. Kinetic studies of ester (methyl trifluoroacetate) hydrolysis, using solid acids (Amberlyst 15), resulted in kinetic expressions which can be used to design a reactive distillation process for final separation of the product.

INTRODUCTION

Natural gas is a growing factor in the world production of primary energy [1]. However, a large portion of natural gas reserves are found in remote locations, where the transport to the market, either as liquefied natural gas (LNG) or using pipelines, is associated with logistic and economic drawbacks. Both transport methods exhibit inherent cost limitations e.g. due to the necessity of refrigeration of pressurised gas to obtain LNG or compression to ca. 80 bars for pipeline distribution. Therefore, in contrast to oil, where the cost of transport is a minor factor, the expenditure associated with gas transport is high dictating that most of the gas be consumed in the region of its production [2]. Transport would be facilitated if it were possible to transform natural gas, largely methane, into a liquid fuel (e.g. methanol) that would not need refrigeration or compression. However, the selective oxidation of methane to methanol or other efficiently transportable materials is one of the greatest challenges posed to the scientists and engineers.

The on-site conversion of associated natural gas to a liquid fuel can also be regarded as an alternative to the environmentally detrimental flaring and venting. As well as eliminating greenhouse gas emission (flaring and venting) the conversion of natural gas to high energy oxygenates preserves this non-renewable energy resource.

There have been several reported catalyst systems that have the potential to serve the purpose in the gas phase and/or in the liquid phase but few have generated product yields attractive to an economic viewpoint for commercial application. Recently, metal catalysed systems in protic media have attracted much attention because highly selective and productive functionalisation of methane has been accomplished [3, 4]. A promising system in terms of methane conversion, product selectivity and yield, is that developed by Catalytica Inc. [5, 6]. However the major disadvantage is the use of pure sulphuric acid as both the solvent and oxidising agent (which must be then re-oxidised) and in several cases mercuric sulphate as the catalyst (high toxicity of mercury compounds). For practical implementation of the partial oxidation of methane to methanol, the use of dioxygen is a preferred terminal oxidant. Another system developed by Yamanaka et al. [7] (using oxygen) is characterised by a very low reaction temperature (< 40°C) but is plagued by low product yield, expensive europium catalyst and unavoidable solvent degradation. Sen and co-workers [4, 8, 9] have reported the activation of small hydrocarbons over Pd-based catalyst systems in the presence of CO and O_2. They employed 5% Pd/C and soluble copper salts (mainly chloride) in a mixture of trifluoroacetic acid (TFA) and water. In this system, carbon monoxide must be present (as co-reductant) in the reaction mixture in order to facilitate this "difficult" methane oxidation with the copper salt acting as a selectivity

agent (virtually only methanol is formed in its presence [9]). The investigated system has the unprecedented advantage of simultaneous cleavage of C-H and C-C bonds, thus producing methanol from both methane and other lower alkanes and so could be applicable to natural gas feedstocks. The presence of a strong acid (pK_{TFA} = 0.23) enhances both the electrophilicity of the metal ion (the conjugate bases of strong acids are poorly co-ordinating) as well as providing chemical protection, by esterification, of the reaction product methanol from its over oxidation. Therefore, in the process, methyl trifluoroacetate (MeTFA) is formed and thus an additional step of hydrolysis is needed to obtain pure methanol as the product of this partial oxidation of methane. This can be done by applying reactive distillation [10], which offers distinct advantages over the conventional approach of performing the hydrolysis reaction and separation sequentially. The design of reactive distillation columns requires reliable kinetic data besides other information, like phase equilibrium data, chemical equilibrium data, transport property data, or the various pure component properties [10]. Hydrolysis of an ester is a reversible liquid-phase reaction generally catalysed by acids such as hydrochloric acid, sulphuric acid or solid acids (e.g. acidic ion exchange resins). Solid ion exchange resins offer advantages over homogeneous mineral acids because of the easier recovery of catalyst and less reactor corrosion. In the last few years a number of ester hydrolysis reactions have been successfully developed by using Amberlyst 15 as an acid resin catalyst.

The aim of this work is to asses the feasibility of the low temperature (< 100°C) liquid phase partial oxidation of methane to methanol in a continuous porous tube reactor, applying the catalyst system developed by Sen and co. [4, 8, 9]. As mentioned previously, inherent within the catalytic system is the formation of methyl ester as the primary product. Additional studies also focus on the kinetics of ester hydrolysis to obtain the desired methanol.

EXPERIMENTS

The experimental set-ups (semi-continuous porous tube and batch slurry reactors) are schematically shown in Figure 1. Continuous apparatus comprises of two 316 stainless steel pressure vessels (reactor and separator) fabricated by Baskerville Reactors and Autoclaves Ltd. (UK) and rated for maximum operating conditions of 20.0 MPa and 573 K. The details of the reactor design can be found elsewhere [11]. Mass flow controllers (5850S, Brooks) were used to regulate the flow of the three reactant gases (CO, O_2 and CH_4). A porous alumina tube (Multilab, UK) in the reactor section (182 mm long, with 20 mm O.D, and 15 mm I.D) is utilised foremost as a gas distributor to the liquid phase but also lends itself to a catalyst support. For this secondary role the tube was first coated on its inside wall with a gamma-alumina washcoat derived from a 20 wt.% alumina sol (CONDEA Vista Co.). The palladium catalyst was then added via an ammonium hexachloropalladate (IV) precursor (Sigma-Aldrich) reduced in-situ on the tube wall by hydrazine solution. The palladium phase typically represented 5 wt.% of the washcoat.

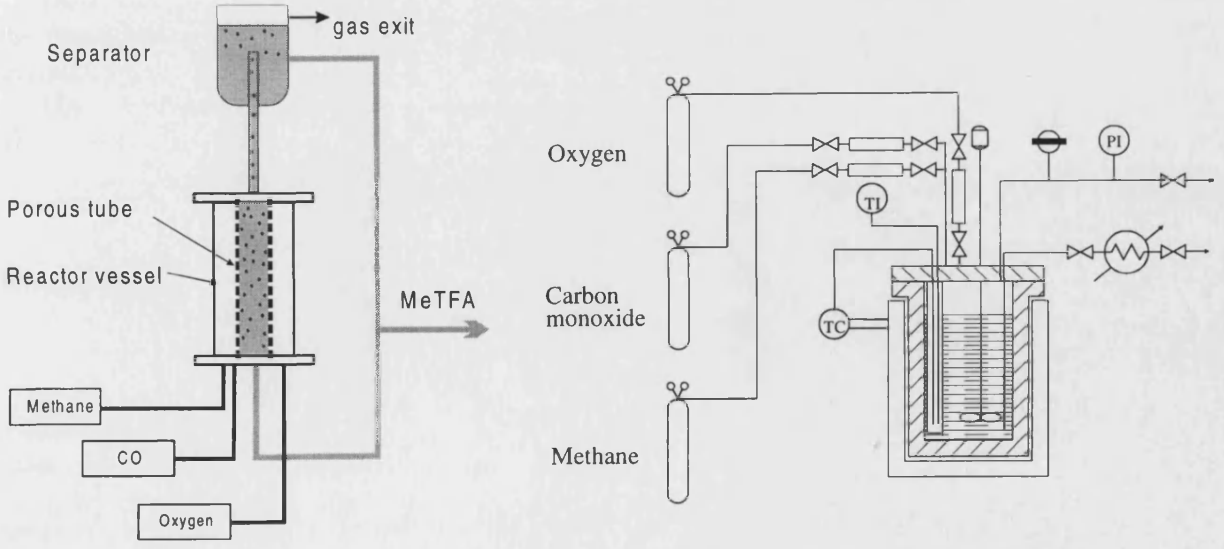

Figure 1. Schematic views of semi-continuous porous tube and batch slurry reactors

Additional studies of methane oxidation in batch slurry reactor have been performed in a 175 cm^3 high pressure autoclave (Baskerville, UK). The reactor is equipped with a heating jacket connected to a control

box, which regulates the temperature and allows manual variation in the agitation speed of the stirrer in the reactor.

A low temperature glass batch slurry reactor was used for the kinetics experiments (hydrolysis) of methyltrifluoroacetate, similar to that described by Xu and Chaung [12]. The experimental set-up consisted of a 250 cm^3 glass-made vessel fitted with stirring, heating, sampling and temperature control devices. From preliminary studies the agitation speed chosen was 300 rpm, so as to avoid diffusional limitations. Samples were withdrawn periodically and analysed by gas chromatography.

Trifluoroacetic acid (TFA), methyltrifluoroacetate (MeTFA), and methanol (MeOH) were supplied by Sigma-Aldrich Company Ltd. All chemicals were used without further purification. Acid resin Amberlyst 15 was also obtained from Sigma-Aldrich and it was used as catalyst without any pre-treatment.

The concentrations of MeTFA and reaction products (methanol and trifluoroacetic acid) were measured using a gas chromatograph (GC 5890, Hewlett Packard) equipped with a FI detector.

MODELLING OF HYDROLYSIS REACTION

The pseudo-homogeneous model of resin (Amberlyst 15) catalysed hydrolysis has been applied to describe the kinetic data. The model is based on Hellferich approach [13], which treats catalysis by ion exchange resin as a homogeneous one confined within the internal catalyst mass, wherein the reactants, products, and solvents are in distribution equilibrium with the bulk solution. The hydrated protons, from fully swollen resin in the aqueous phase, are the catalytic agent for the hydrolysis reaction. The swelling of resin particles leads to easy accessibility of the acid groups to the reaction and free mobility of all the components [14]. In order to shift the reaction of hydrolysis towards product formation, an excess of water has to be used; therefore the modelling of the kinetics is based on the activities rather than on concentrations.

The reaction of hydrolysis:

$$MeTFA + Water \overset{K}{\leftrightarrow} TFA + MeOH \tag{1}$$

is characterised by an equilibrium constant K_a defined as:

$$K_a = \frac{a_{TFA}\, a_{MeOH}}{a_{MeTFA}\, a_w} \tag{2}$$

It should be noted that from the unequal characteristics of the components in the mixture, the modelling of the equilibria and kinetics should be based on activities rather than on concentration.

From the temperature dependency of the equilibrium constant the standard Gibbs energy of the reaction and the standard enthalpy of reaction can be evaluated. The activity coefficients, γ_i, necessary to account for the real behaviour of the liquid phase were calculated using UNIQUAC equation [15].

The kinetics of hydrolysis was investigated for two cases: homogeneous and heterogeneous catalysis. In the first case the reaction has been catalysed by free non-reacted TFA (present in the solution leaving the porous tube reactor), in the second case by the solid ion exchanger, Amberlyst 15.

The resulting reaction rates can be expresses as follow:

a) homogeneous catalysis

$$r = n_T \cdot \frac{dx_{MeOH}}{dt} = a^{\alpha}\left(k_1 a_{MeTFA}\, a_w - k_{-1} a_{TFA}\, a_{MeOH}\right) \tag{3}$$

b) heterogeneous catalysis (as pseudo-homogeneous model)

$$r = \frac{n_T}{m_{cat}} \cdot \frac{dx_{MeOH}}{dt} = k_1 a_{MeTFA}\, a_w - k_{-1} a_{TFA}\, a_{MeOH} \tag{4}$$

The concentration profiles were calculated by integrating relevant rate expressions. The calculations were made using a Runge-Kutta-Merson integration routine from the NAG Fortran library. Values of the reaction constant were varied to give calculated concentrations close to the experimental data. The accuracy of the predicted values was represented by the root mean square difference between the predicted and experimental values.

The Arrhenius law was then applied for calculation of activation energies from temperature dependent rate constants:

$$k_1 = k_1^0 \exp\left(\frac{-\Delta E_A}{RT}\right) \tag{5}$$

the amount of Cl^- added as NaCl [9, 16]. However, an excessive amount of NaCl (as $[Cl^-]/[Pd] > 100$) had an adverse effect on the yield of MeTFA [16]. A similar tendency was also observed in the porous tube reactor (Figure 3). However, similar to that observed in the batch reactor with limited amount of gas reactants, also in the continuous reactor the formation of methyl ester either was strongly reduced ($[Cl^-]/[Pd] = 15$) or came to a stagnation or even decreased ($[Cl^-]/[Pd] = 83$ or 333) after 2 hours. In the case of the semi-continuous reactor the gaseous reactant were supplied in excess, therefore the consumption of the oxygen and co-reductant CO cannot be responsible for the observed behaviour. It might be that either formed hydrogen peroxide is decomposed in stainless steel tubes or catalyst system became unstable. Bearing in mind that in-situ formed H_2O_2 does not have any contact with steel in the porous tube it seems that catalyst deactivation is the main reason for the observed behaviour.

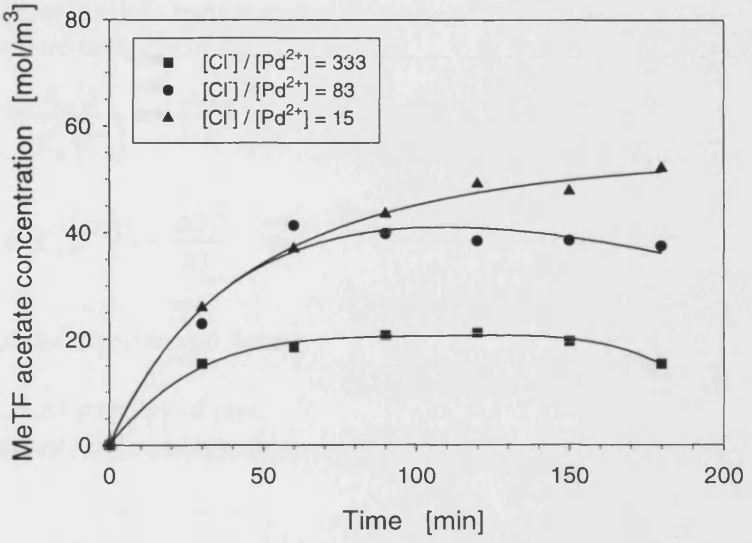

Figure 3. The results of the partial oxidation of methane in a semi-continuous porous tube reactor. T = 358 K, p_T = 84 bar, volume of liquid phase = 300 cm^3 (TFA:water 3:1), total flow 2.0 dm^3/min, flow rates of individual gases corresponded to their fractions in the batch reactor.

The initial rate of MeTFA formation was equal to 1.4×10^{-5} kmol/m^3 s and was comparable to that measured in batch experiments by Sen et al. [9] (also for homogeneous catalysis ca. 1.5×10^{-5} kmol/m^3 s).

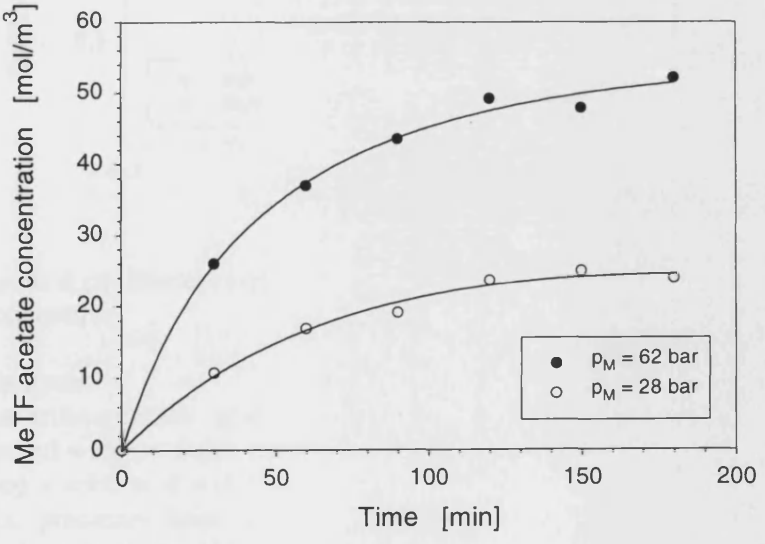

Figure 4. The influence of methane partial pressure. T = 358 K, total flow 2.0 dm^3/min.

The rate of formation of MeTFA depends strongly on the partial pressure of methane (Figure 4). The increase of partial pressure of methane resulted with a higher rate of ester formation i.e. 5.9×10^{-6} kmol/m^3 s and 1.45×10^{-5} kmol/m^3 s for 28 bar and 62 bar respectively.

The semi-continuous porous tube reactor has the advantage over the standard batch slurry reactor in that it allows liquid sampling to monitor time-dependency of the reaction. This was not possible using our batch reactor and indeed not reported from those utilised in the other works [9, 16]. The presented preliminary experimental results suggest the problems of catalyst stability. Nevertheless, because of high oxidation selectivity (no acids were detected in GC analysis) and additional possibility of C-C cleavage (see Sen et al. [9]) this system demands further investigation to clarify its industrial feasibility.

Hydrolysis of methyltrifluoroacetate

Chemical equilibrium

Figure 5 shows the calculated equilibrium constants (based on activities and concentrations) as a function of the reciprocal of the absolute temperature. The slope and intercept of the linear regression of the data are related to the standard enthalpy of the reaction and standard Gibbs energy according to:

$$ln\frac{K_a(T)}{K_a(T^0)} = -\frac{\Delta H_r^0}{R}\left(\frac{1}{T} - \frac{1}{T^0}\right) \tag{6}$$

$$ln\,K_a(T^0) = -\frac{\Delta G_r^0}{RT} \tag{7}$$

The evaluation of the experimental data resulted with the following values:

Standard enthalpy of reaction	$\Delta H_r^0 = 10.42 \pm 0.39$ kJ/mol
Standard Gibbs energy of reaction	$\Delta G_r^0 = 5.69 \pm 0.41$ kJ/mol

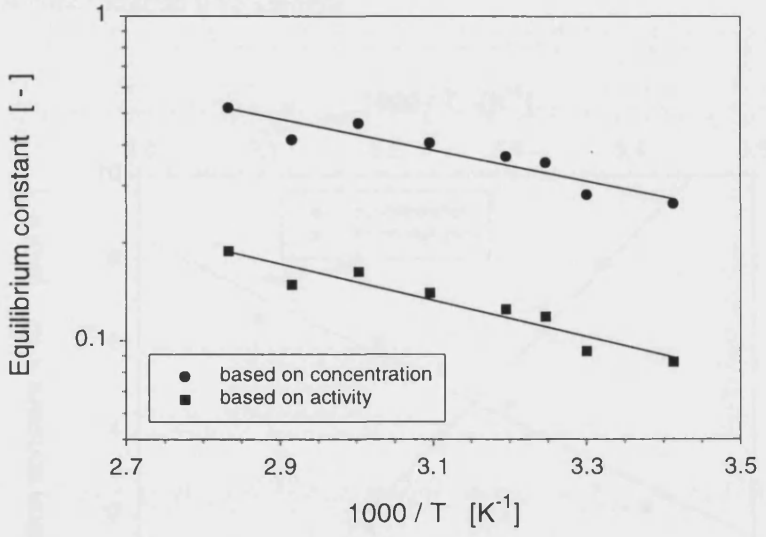

Figure 5. Chemical equilibrium constants (mean values from 3 experiments) as a function of temperature.

Kinetics of hydrolysis

The presence of trifluoroacetic acid in the process of methanol recovery (i.e. reactive distillation) is inevitably connected with the entire process of partial oxidation of methane. Therefore, even heterogeneous catalysis applying a solid acid will be coupled with homogeneous hydrolysis catalysed by TFA. Thus all possible catalytic processes have to be described separately. Figure 6 shows concentration profiles of methanol (desired product) and MeTFA (reactant) for heterogeneous (Amberlyst 15), homogeneous (TFA) and combined hydrolysis. As one can see the combination of both catalysts leads to a synergistic effect (the rate of reaction is higher).

In the first step the homogeneous reaction of hydrolysis was investigated. The results of these studies are shown in Figure 7. For TFA concentration $c_{TFA} \leq 0.25$ kmol/m^3 a very slow reaction was observed. In the concentration region ($0.5 \leq c_{TFA} \leq 1.5$ kmol/m^3) the dependency of the forward reaction constant on the acid

Table 1. Kinetic parameters for homogeneously catalysed hydrolysis

Method	k_1^0 [mol s^{-1}]	$\Delta E_{A,1}$ kJ mol^{-1}	k_{-1}^0 [mol s^{-1}]	$\Delta E_{A,-1}$ kJ mol^{-1}
H^+ as catalyst	7.15×10^5	54.9	1.72×10^4	39.8
TFA as catalyst	5.60×10^5	54.4	1.35×10^4	39.2

Heterogeneously catalysed hydrolysis

Preliminary experiments were used to determine a sufficient stirrer speed to insure the absence of external mass transfer limitations. An agitation speed of 300 rpm was found to be sufficient to assume the absence of external mass transfer.

In the next series of experiments, the influence of catalyst loading and temperature on the concentration changes of reactant (MeTFA) and products (MeOH, TFA) with time was investigated and the resulting kinetic constants are shown in Figure 8. A straight-line dependency of the reaction constant ($k_1 \times m_{cat}$) was observed validating the assumed pseudo-homogeneous model. In the investigated concentration range of MeTFA, its adsorption on the surface of Amberslyst 15 did not play a significant role. The temperature dependency allowed for the calculation of the activation energy for heterogeneous catalysed hydrolysis. The mathematical analysis of these results led to the kinetic parameters summarised in Table 2.

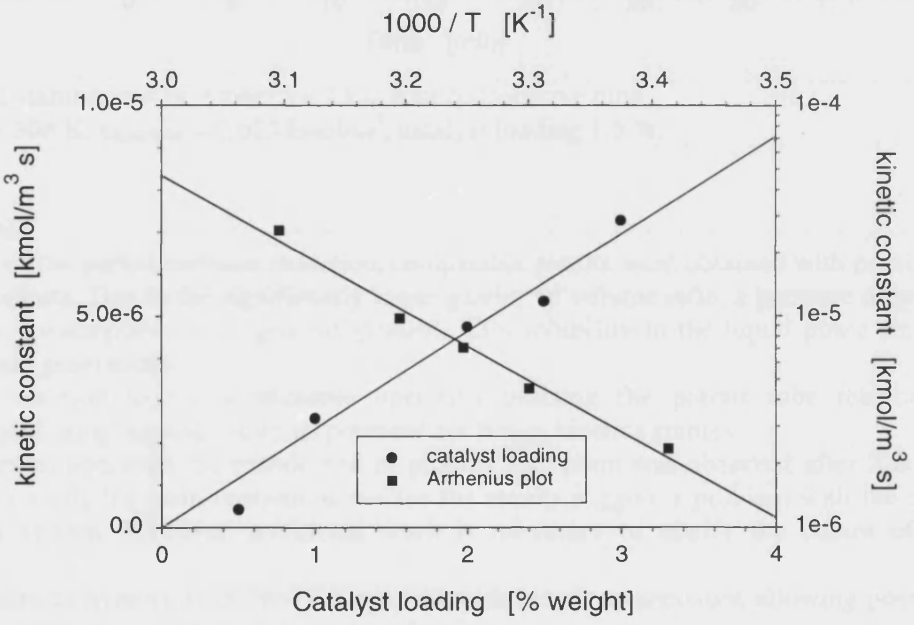

Figure 8. The influence of catalyst loading and temperature on the heterogeneous reaction constant.
Catalyst loading: T = 308 K, $c_{0,MeTFA} = 0.025$ kmol/m^3,
Arrhenius plot: $c_{0,MeTFA} = 0.025$ kmol/m^3, catalyst loading 1.5 %

Table 2. Kinetic parameters for heterogeneously calatysed hydrolysis

Model	k_1^0 mol g_{cat}^{-1} s^{-1}	$\Delta E_{A,1}$ kJ mol^{-1}	k_{-1}^0 mol g_{cat}^{-1} s^{-1}	$\Delta E_{A,-1}$ kJ mol^{-1}
Pseudo-homogeneous	1.75×10^4	62.2	6.85×10^3	48.3

The kinetic constants summarised in Tables 1 and 3 were then used for the calculation of concentration profiles in experiments using both catalysts: heterogeneous Amberlyst 15 and homogeneous TFA. A good prediction of experimental results was obtained for all experimental conditions.

Indices

a	activity
α	coefficient depending on the assumption on catalytic mechanism; catalysis via solvated protons (α = 0.5) or via undissociated TFA (α = 1.0) [17]
cat	catalyst
CM	carbon monoxide
i	component
M	methane
MeTFA	methyltrifluoroacetate
O	oxygen
r	reaction
T	total
TFA	trifluoroacetic acid
w	water
0	standard
1	forward
-1	backward

REFERENCES

1. Crabtree, R.H., (1995), Aspects of methane chemistry, *Chem. Rev.*, **95**, 987.
2. Julius D., Mashayekhi, A., *The Economics of Natural Gas*, Oxford University Press, Oxford, 1990.
3. Stahl, S.S., Labinger, J.A., Bercaw, J.E., (1998), Homogeneous Oxidation of Alkanes by Electrophilic Late Transition Metals, *Angew. Chem. Int. Ed.* **37**, 2180.
4. Sen, A., (1998), Catalytic Functionalization of Carbon-Hydrogen and Carbon-Carbon Bonds in Protic media, *Acc. Chem. Res.*, **31**, 550.
5. Periana, R.A. (1997), A novel, high-yield system for the oxidation of methane to methanol. *Adv. Chem. Ser.*, **253**, 61.
6. Periana, R.A., Taube, D.J., Gamble, S., Taube, H., Satoh, T., Fuji, H., (1998) Platinum catalysts for the high-yield oxidation of methane to a methanol derivative, *Science*, **280**, 560.
7. Yamanaka, I., Soma, M., Otsuka, K., (1995), Oxidation of methane to methanol with oxygen catalysed by europium trichloride at room temperature, *J. Chem. Soc., Chem. Commun*, 2235.
8. Lin, M., Sen, A., (1992), Highly Catalytic System for the Direct Oxidation of Lower Alkanes by Dioxygen in Aqueous Medium. A normal Heterogeneous Analog of Alkane Monooxygenases, *J. Am. Chem. Soc.*, **114**, 7307.
9. Lin, M., Hogan, T., Sen, A., (1997), Highly Catalytic Bimetallic System for the Low-Temperature Selective Oxidation of Methane and Lower Alkanes with Dioxygen as the Oxidant, *J. Am. Chem. Soc.*, **119**, 6048.
10. Malone, M. F., Doherty, M.F., (2000), Reactive Distillation, *Ind. Eng. Chem. Res.*, **39**, 3953 and literature cited therein.
11. McLurgh, D.B. (1997) Study of a porous tube reactor for the wet air oxidation of aqueous wastes, PhD Thesis, University of Bath, UK.
12. Xu, Z.P., Chuang, K.T. (1996). Kinetics of acetic acid esterification over ion exchange catalysts, *Can. J. Chem. Eng.* **74**, 493.
13. Helfferich, F. (1962). *Ion Exchange*, McGraw Hill, New York.
14. Chakrabarti, A., Sharma, M.M. (1993). Cationic ion exchange resins as catalyst, *React. Polymers*, **20**, 1.
15. Reid, R.C., Prausnitz, J.M., Poling, B.E. (1987) The properties of gases and liquids, McGraw Hill, Inc., New York
16. Park, E.D., Sun, H.C., Lee, J.S. (2000), Characterization of Pd/C and Cu Catalyst for the Oxidation of Methane to Methanol Derivative, J. Catalysis, **194**, 33-44.
17. Pöpken, T., Götze L., Gmehling J. (2000). Reaction kinetics and chemical equilibrium of homogeneously and heterogeneously catalyzed acetic acid esterification with methanol and methyl acetate hydrolysis. *Ind. Eng. Chem. Res.* **39**, 2601-2611.